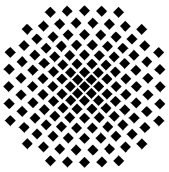

Universität Stuttgart *IER*

Sixth Framework Programme

Rainer Friedrich and Alexandra Kuhn (eds.)
University of Stuttgart

Integrated Environmental Health Impact Assessment for Europe

Methods and results of the HEIMTSA/INTARESE Common Case Study

FP6 Project GOCE-CT-2006-036913-2
HEIMTSA
Health and Environment Integrated Methodology and Toolbox for Scenario Development

FP6 Project No. 018385
INTARESE
Integrated Assessment of Health Risks of Environmental Stressors in Europe

Participating Institutions: University of Stuttgart, Institute of Occupational Medicine Edinburgh, Imperial College London, Aristotle University of Thessaloniki, Centre for Research and Technology Hellas, Danmarks Tekniske Universitet, Ecole Nationale des Ponts et Chausses Paris, Eidgenössische Technische Hochschule Zürich, University of Exeter, Institut National de l'Environnement Industriel et des Risques, Joint Research Centre Ispra, Kuratorium für Technik und Bauwesen in der Landwirtschaft Darmstadt, Meteorological Synthesizing Centre – East Moscow, Meteorologisk Institutt Oslo, Norsk Institutt for Luftforskning Kjeller, NILU Polska LtD. Katowice, Rijksinstituut voor Volksgezondheid en Milieu Bilthoven, Terveyden Ja Hyvinvoinnin Laitos Helsinki, TNO Delft, University of Bath, University of Maastricht, University of Manchester.

Forschungsbericht des Instituts für Energiewirtschaft und Rationelle Energieanwendung der Universität Stuttgart
2011

SUMMARY

One of the objectives of the HEIMTSA and INTARESE projects is to test the integrated environmental health impact assessment system (IEHIAS) developed in INTARESE WP 4.2 and HEIMTSA WP 5.2 and to apply the INTARESE/HEIMTSA methodology to a realistic policy scenario, in order to (i) test the usability of the full chain methodology of IEHIAS as a whole; (ii) provide necessary parameter values and functions (e.g. concentration-impact functions, monetary values); (iii) demonstrate the use of the methodology and provide results; and (iv) discuss and evaluate both the methodology (for its reliability and completeness) and the results (for their plausibility and practical use).

The so-called Common Case Study described in this report is the means to fulfil these objectives. Its aims are to assess environmental health impacts of a high-level, cross-cutting policy issue at EU level and thus to provide a full example of an integrated environmental health impact assessment according to INTARESE and HEIMTSA recommendations.

The following problem is addressed in the Common Case Study:

Policies and measures for mitigation of and adaption to climate change are nearly always chosen with a focus on the reduction of CO_2-eq and the cost of the measures. However, there may be relevant side benefits or damages, e.g. decreases or increases in health impacts. Those should also be taken into account during the decision process.

To inform decision makers about these side effects, the Common Case Study answered the following questions:

What are the (negative or positive) health impacts of climate change policies in Europe for the years 2020, 2030, and 2050? Specifically,

a) How do EU climate mitigation policies, i.e. policies with the primary purpose of reducing the emissions of greenhouse gases (policies and resulting measures), affect environmental health impacts in Europe, e.g. increased use of biomass as energy source?

b) How do EU climate adaptation options and policies, i.e. policies that reduce negative climate change impacts, affect environmental health impacts in Europe?

This study follows the approach of integrated environmental health impact assessment (IEHIA) developed in the projects INTARESE and HEIMTSA. An IEHIA is an inclusive and, as far as feasible, comprehensive assessment of the risks to, and impacts on, human health as a result either of exposures to a defined set of environmental hazards or of the effects of policies or other interventions that operate via the ambient or living environment (Briggs 2008).

The approach taken in this case study is to develop scenarios for a baseline year (2005) and several future years (2020, 2030 and 2050). Within these years a business as usual scenario is generated (activities follow the current trend, furthermore all policies and measures that are already in place and implemented, are taken into account; however after 2012 no additional policies for climate protection are assumed to take place). Furthermore, a policy scenario is analysed, that includes the climate change policies of interest. As a final step and main result the difference between the two scenarios in each year is explored.

The policy scenario includes all the policies that might be needed to be implemented by the EU to achieve the 2°C aim (average world surface temperature should not exceed an increase of 2° compared to preindustrial times). This includes the climate and energy package (EC 2008, COM 2008) and in addition further policies up to 2050. To assess the importance of single measures within this bundle of all measures, not only the full bundle of measures, but also selected single measures have been analysed.

Results show that the impact of most climate change mitigation policies on environmental human health is nearly as important as the climate change effects themselves. Taking health impacts into account when making decisions about climate protection will change the cost benefit ratio and the ranking of policies considerably. It is thus obvious that any decision support in the field of climate protection should be accompanied by an integrated health impact assessment. The methodology developed in INTARESE and HEIMTSA should be applied, as it is an integrated approach that is capable of taking all relevant aspects of a question into account and uses information and methods according to the current state of knowledge.

Quite some climate protection policies have important positive effects, i.e. they reduce health effects considerably (e.g. the use of wind or solar energy replacing oil and coal). However some policies, especially biomass burning and reducing air exchange rates in houses, cause quite high additional health impacts. Thus, a recommendation here would be to use wood in small furnaces only when equipped with an appropriate filter and to install mechanical venting systems in all new buildings.

The analysis also allows a ranking of stressors in environmental media with regard to overall health impacts in the EU:

The highest overall damage stems from primary and secondary fine particles, followed by noise and radon. Less damage is caused by ozone, then mould followed by dioxins and heat waves. Pesticides and especially PCBs cause relatively low health impacts if only cancer endpoints are considered. This hierarchy does not change if different indicators like DALYs or monetary values are applied. Sensitivity analyses furthermore show that the pattern of importance does not change, either, if different toxicity of PM components is assumed. This information is useful to identify priorities when planning health protection policies.

For uncertainty assessment quantitative and qualitative methods have been used in all parts of the CCS. In summary the overall assessment of the health impact and valuation estimates of the CCS tends to be characterized by low to moderate uncertainty levels. The estimates tend to over-estimate the final health impact and are thus conservative. Finally, the overall knowledge base of this study has a moderate uncertainty when all parts of the integrated assessment chain are taken into account.

A general conclusion is that taking relevant ‘environmental health effects’ into account will change policy recommendations in many fields substantially.

TABLE OF CONTENTS

LIST OF FIGURES

LIST OF TABLES

1 INTRODUCTION

1.1 AIM OF THE COMMON CASE STUDY

One of the objectives of HEIMTSA/INTARESE is to test the integrated environmental health impact assessment system (IEHIAS) developed in INTARESE WP 4.2 and HEIMTSA WP 5.2 and to apply the INTARESE/HEIMTSA methodology to a realistic policy scenario, in order to (i) test the usability of the full chain methodology of IEHIA and the IEHIAS as a whole; (ii) identify any important gaps; (iii) generate results; and (iv) discuss and evaluate both the methodology (for its reliability and completeness) and the results (for their plausibility and practical use).

The so-called Common Case Study is the means to fulfil these objectives. Its aims are to assess environmental health impacts of a high-level, cross-cutting policy issue at EU level and thus to provide a full example of an integrated environmental health impact assessment according to INTARESE and HEIMTSA recommendations.

The Common Case Study draws on the methodology developed and enhanced in INTARESE and HEIMTSA, including the issues framing and scoping phase of an assessment, the execution and the reporting of results. In this sense, the present report describes the methodology used (with references to more detailed methodology reports) and presents the results and insights gained. As scoping and issue framing formed a very important basis of the final case study design, this process and its outcomes are described in a separate report: HEIMTSA D 5.3.3 selection of priority pathways = INTARESE D 93 Common Case Study Protocol.

1.2 THE QUESTION ADRESSED IN THE COMMON CASE STUDY

An important first step of the IEHIA methodology is the clear definition of the question that should be answered in the analysis. Within several discussion as well within the project team as with the advisory board it was decided to answer the following question, as it is as well highly policy relevant as well suited to demonstrate the integration of many different elements from different areas into the assessment:

Policies and measures for mitigation of and adaption to climate change are nearly always chosen with a focus on the reduction of CO_2-eq and the cost of the measures. However, there may be relevant side benefits or damages, e.g. decreases or increases in health impacts. Those should also be taken into account during the decision process.

To inform decision makers about these side effects, the Common Case Study answered the following questions:

What are the (negative or positive) health impacts of climate change policies in Europe for the years 2020, 2030, and 2050? Specifically,

a How do EU climate mitigation policies, i.e. policies with the primary purpose of reducing the emissions of greenhouse gases (policies and resulting measures), affect environmental health impacts in Europe, e.g. increased use of biomass as energy source?

b How do EU climate adaptation options and policies, i.e. policies that reduce negative climate change impacts, affect environmental health impacts in Europe?

In INTARESE/HEIMTSA the integrated environmental health impact assessment in its scope was defined narrowly, meaning that only health effects were considered that were mediated via environmental media. In effect, most effects quantified were pollutant based; however, also noise and heat were taken into account as stressors. In future projects it would be good to investigate in how far also health benefits not attributed to environmental pollution (e.g. via cycling) could be included in the scope of the question.

1.3 SCOPE

Within the scoping process, the main elements of the issue addressed have to be specified. This is described in the following:

Environmental health effects:

Environmental health effects are defined here as health effects, that are caused by substances or energy, that are released during a human activity into the environmental media (air, soil, water, indoor air).

Spatial boundaries:

The case study looked at the European scale (EU29). Measures were implemented in the EU member states, the health impacts were estimated for the whole of Europe. The spatial resolution differed for sectors and pollutants as appropriate. For air pollutants, it was based on 50x50 km^2 EMEP[1] grid cells for regional effects and on a smaller grid for local effects (e.g. traffic in cities). For indoor air parameters were used on a country level including probability distributions.

Temporal boundaries:

The case study looked at a base year (for emission scenario modelling, 2005) and developed scenarios for the future years 2020, 2030 and 2050, i.e. described the state of the system (policies, activities, emission factors…) and emissions of pollutants in these years. While scenarios for 2020 and 2030 could be developed with a higher degree of certainty, i.e. the possible ranges of parameters were large but still limited; scenarios for 2050 had to be based on less certain assumptions and, thus, bear higher

[1] http://www.eea.europa.eu/data-and-maps/data/emep-grids-reprojected-by-eea

uncertainty. Nevertheless, a quantitative scenario description proved to be helpful in exploring the possible effects of policies including emission mitigation measures.

Effects of emissions might be observed only later than the time of emissions (e.g. eposure is delayed due to a slow dispersion of stressors in the environment; or health impacts may occur only years after exposure) but are attributed to the year of emission, i.e. the impacts caused by an activity in a certain year are allocated to this year, even if they are occurring in future years.

Population:

Receptor for the exposure was the European population. As exposure models and exposure-response relationships differentiate between age groups and gender, population data had to be provided differentiated into gender and age groups for each 50x50 km^2 Emep grid cell. Its growth was also projected to the years 2020, 2030, and 2050 separately for each age group.

Age/sub groups in the $PM_{2.5}$ exposure modelling were: 0-14, 15-64 and 65+ years of age. The group 15-64 was split by working and non-working people. All groups were stratified by gender.

Age groups for health effect estimation (impact functions) differed from the personal exposure modelling groups. They were 0-1, 0-3, 5-14, 5-16, 0-16, 0-18, 15-64, 18-64, 20+, 25+, 27+, 30+, 65+, 18+ and all ages.

The reason of working with different age groups during the application of impact functions is that the impact functions were either derived in studies looking at those subgroups (e.g. when looking especially on children) or are only applicable to those subgroups (e.g. susceptibility to ozone for elderly, or infant mortality for infants).

The reason of working with different sub groups during the personal exposure modelling to $PM_{2.5}$ is to facilitate the comparison of different sub groups, i.e. to explore the impact of different mitigation measures and scenarios on the sub groups.

Stressors:

The stressors, which might be relevant for answering the case study question and thus have been included in the analysis, have been identified within a screening process (see chapter 1.5). Please note that in this list the stressors released to the environment are listed. These may be transformed in the environment to by chemical or physical processes to other pollutants.

- Outdoor air pollutants: emissions of primary PM_{10} and primary $PM_{2.5}$ including compounds, NO_x, SO_2, NMVOCs, NH_3
- Indoor air pollutants: $PM_{2.5}$ and PM_{10}, mould/dampness, CH_2O (formaldehyde), environmental tobacco smoke (ETS), radon
- Persistent organic pollutants (POPs): PCB-153 and 2,3,4,7,8-PeCDF

- Noise due to road traffic/transport
- Pesticides: 14 fungicides, 49 herbicides, 7 insecticides, 3 plant growth regulators
- Greenhouse gases (GHGs): CO_2, CH_4, N_2O. They are only taken into account for assessing the reduction of GHGs, i.e. how many CO2-equivalents a policy scenario or mitigation measure reduces. No health effects are implied by GHGs, as the health impacts of mitigation measures, but not of climate change itself has been assessed.
- Heat: It was explored how measures in urban development like shading impacts on heat stress.

To our knowledge this is the first time that a study has taken all these stressors into account in an integrated way.

The following stressors have been discussed, but not included into the analysis:

Heavy metals, radioactive substances, nitrates in drinking water, disinfection byproducts (expected health impact several orders of magnitude lower than that of e.g. air pollution), nanoparticles (not enough information available)

Health effects:

Impact functions were given as European average. For some functions, due to differences in background rates of disease, impact functions were additionally given for the regions Western, Eastern, Northern and Southern Europe. For the following health endpoints exposure-response-relationships, that have been assessed as reliable, could be identified and used:

- PM_{10}: cardiovascular hospital admissions, respiratory hospital admissions, asthma medication usage (children and adults), lower respiratory symptoms including cough (children and adults)
- $PM_{2.5}$: reduction of life expectancy, work loss days, minor restricted activity days, restricted activity days
- Ozone: mortality, respiratory hospital admissions, asthma medication usage (children and adults), lower respiratory symptoms excluding cough (children), cough (children), minor restricted activity days
- Environmental tobacco smoke (ETS): coronary heart disease hospitalisation, lung cancer, sudden infant deaths (SIDs), lower respiratory illness symptom days and hospitalisation (children), cough (children), wheeze (children), asthma induction
- Radon: lung cancer
- Formaldehyde: asthma

- Naphthalene: cancer
- Mould/dampness: wheeze (children and adults), asthma development (children and adults)
- Noise: % highly annoyed, % annoyed, % highly sleep disturbed, myocardial infarction
- Pesticides: generic cancer (it is acknowledged that it is likely that other health effects like neurotoxic effects occur, however, no dose response functions could be found.)
- POPs: generic cancer
- Heat: summer mortality due to heat stress

1.4 OVERALL METHODOLOGY

This study follows the approach of integrated environmental health impact assessment (IEHIA) developed in the projects INTARESE and HEIMTSA. An IEHIA is an inclusive and, as far as feasible, comprehensive assessment of the risks to, and impacts on, human health as a result either of exposures to a defined set of environmental hazards or of the effects of policies or other interventions that operate via the ambient or living environment (Briggs 2008).

The approach taken in this case study is to develop scenarios for a baseline year (2005) and several future years (2020, 2030 and 2050). Within these years a business as usual scenario is generated (activities follow the current trend, furthermore all policies and measures that are already in place and implemented, are taken into account; however after 2012 no additional policies for climate protection are assumed to take place). Furthermore, a policy scenario is analysed, that includes the climate change policies of interest. As a final step and main result the difference between the two scenarios in each year is explored.

The policy scenario includes all the policies that might be needed to be implemented by the EU to achieve the 2°C aim (average world surface temperature should not exceed an increase of 2° compared to preindustrial times. This includes the climate and energy package (EC 2008, COM 2008) and in addition further policies up to 2050. To assess the importance of single measures within this bundle of all measures, not only the full bundle of measures, but also selected single measures have been analysed.

Within this report we will in each chapter first explain the methodology, followed by a presentation of the results of each step.

1.5 SCREENING

During the issue framing and scoping phase of the common case study emission mitigation measures in different sectors were coarsely investigated to assess if they should be included into the detailed analysis. During the screening simplified and rough methods were used to estimate the order of magnitude of the health effects avoided or induced by these measures.

For some mitigation measures, the change in health impacts (DALYs) per ton avoided CO_2-eq was calculated. A negative figures means, that a policy reduces greenhouse gas emissions as well as health impacts. In monetary terms, a mDALY can be roughly translated into around 40 €, future marginal avoidance costs for CO_2 in 2020 could be in the range of about 30-40 € per ton. Thus, a value of 1 mDALY per avoided ton of CO_2-eq would mean that the impacts of the mitigation measure on health effects are about as important as their climate change mitigation effects. For other policies, not the absolute damage costs but the changes in health effects between two example scenarios have been estimated (answering the question how would the health effects change if the exposure changed by xy%).

For a smaller number of other measures, a qualitative analysis was conducted, i.e. it was discussed qualitatively, why it is plausible that the use of a measure has a non-negligible health impact.

Some policies could not be quantitatively assessed in the screening process but were identified as less relevant for the detailed assessment and, thus, not further investigated.

Examples for screened mitigation measures in the transport sector are increased energy efficiency, shifts in transport modes, alternative fuels and drive trains, and economic policies like increased fuel tax and city tolls. Screening indicated that the avoided health effects due to these climate mitigation measures range between 0.1 and 1.5 mDALYs per ton avoided CO_2-eq. Different stressors like air pollutants (main influence) and persistent organic pollutants were included.

Examples for screened mitigation measures in the energy sector are increased energy efficiency (e.g. insulating buildings to reduce heating demand), and changes in electricity supply mix including larger share of bio mass burning, larger share of bio fuels, larger share of renewable energies, and heat and combined heat and power. Screening indicated that the avoided health effects due to these climate mitigation measures range between 0.54 and 1.23 mDALYs per ton avoided CO_2-eq.

The main screened mitigation measure for indoor air quality was change in housing quality, leading to ca. 30% less health effects under certain assumptions like reduced exposure to dampness/mould. Radon was identified as further pollutant to be considered in the detailed analysis.

Health effects due to pesticides via direct application onto plants and further following the food chain were qualitatively assessed as potentially important and thus included in the detailed analysis.

Health effects due to pesticides present in drinking water were also investigated in the screening process. Due to a lack of continuous exposure data, a very large number of individual chemicals with different properties, and the lack of epidemiological data forcing the application of a highly conservative methodology using toxicologically-derived cancer slope factors, the results were very uncertain and probably represented a considerable overestimate of health impacts. The actual risks at these levels of exposure could be very low or even zero. The main finding of this screening, therefore, has been to highlight the problems in developing such a model at the European level for drinking water, and to recommend that this particular area of assessment be excluded from the common case study

Disinfection by-products (DBPs) in drinking water were also considered in the screening process. One of the findings was that the changes in levels of DBPs in drinking water were more related to direct effects of climate change than to climate mitigation and adaptation measures. It was acknowledged that the water sector was not well adapted to the pre-determined methodology developed for assessing the main stressors (like air pollution) under the case study framework. Thus, it was decided to exclude DBPs from the detailed analysis but to investigate them separately.

Health effects due to road traffic noise were identified as important (e.g. based on the reported number of highly annoyed persons due to traffic noise in europe) and included in the detailed analysis.

Changes in meat demand were investigated as climate mitigation measure in the agricultural sector.

Health effects due to reduction of heat in urban areas (heat island effects), as an example of a climate mitigation measure, has been identified as important within a qualitative analysis.

For heavy metals, results of the EC project ESPREME have been used (http://espreme.ier.uni-stuttgart.de/). Heavy metals are usually included in particulate matter. Results show that the health impacts of heavy metals are several orders of magnitude lower than the health impacts of the PM_{10}, where they are contained.

2 GENERATION OF ACTIVITY AND EMISSION SCENARIOS

2.1 SCENARIO APPROACH

A scenario is defined as a possible consistent future development of a system. In this study the effects of climate change mitigation policies and adaptation policies on human health are assessed by simulating the implementation of single policies and measures embedded in scenarios of the future development of the relevant parameters and systems.

For each of the years 2020, 2030 and 2050 two scenarios were defined:

a The business as usual scenario (BAU), also named reference scenario (REF), describes the development of an energy/transport/agriculture system without any additional energy or climate policies implemented after the year 2012.

b The Climate Policy Scenario describes a prosperous world, where the world together manages to reduce greenhouse gas emissions to an amount that leads to an average temperature increase of not more than 2°C (with a 50% propability) compared to preindustrial times. This means that the CO_2 concentration has to stabilise on a level of 450 ppm. Consequently, annual reductions of GHG emissions of 71% in 2050 compared to the year 1990 need to be achieved for the EU. This reduction includes the 20% GHG reduction target for 2020 compared to 1990 set by the EU.

Overall, two scenarios (BAU and climate protection policy) have been generated for 4 years (2005, 2020, 2030, 2050). Furthermore a larger number of scenarios where single policies and measures have been removed from the climate policy scenario to show the contribution of this policy to the overall change in health impacts and greenhouse gas emissions have been generated and analysed.

In the following, authors have partly used different terms when referring to these two scenarios. The business as usual (BAU) scenario is also named as reference scenario (REF), the climate policy scenario as climate protection scenario or 450ppm scenario.

2.1.1 Political frame

In 2007, the EU agreed on an independent commitment to achieve energy and climate targets for (EC 2008)

- a at least 20% reduction of green house gases by 2020 compared to 1990 levels and
- a 20% mandatory use of renewable energy by 2020 including a 10% share of bio fuels in petrol and diesel.

Along with that, the “Climate action and renewable energy package” describes the contribution expected from each Member State and proposes policies to achieve them (COM 2008):

- strengthening and expanding the EU Emission Trading System (ETS)
- setting emission targets per Member State for non-ETS sectors (transport except aviation (included in ETS from 2012 on), housing, agriculture and waste) ranging from -20% to +20%
- national renewable energy targets with a minimum share of 10% bio fuels in petrol and diesel by 2020
- development and safe use of Carbon Capture and Storage (CCS) and
- increasing energy efficiency to save 20% of energy consumption by 2020.

2.1.2 Consistency and interrelation of policies in different sectors

During the development of the scenarios consistency of assumptions from different sectors and models was striven for as far as possible. The interrelation of the different policies in the different sectors was especially challenging, the following examples show this:

Increased use of biomass and biofuels in the transport and energy sector leads to increased cultivation of energy crops, which again leads to a competition of demand between agricultural land for energy crop cultivation and cultivation of crops for food consumption. Increased biomass burning in houses might lead to higher exposure to combustion products.

Further changes in drive trains of vehicles like electric cars lead to changes in the energy demand and, thus, energy supply, which again impacts on outdoor air pollutant emissions.

Insulation of buildings leads on the one hand to energy efficiency and reduced heating demand. This reduces emissions of outdoor air pollutants from power generation. Secondly, however, it may lead to a reduced air exchange rate if the building envelopes are made tighter but a hygienic air exchange rate is not ensured. In this case pollutants can accumulate indoors causing a antagonistic effect to the one intended.

2.2 SCENARIOS OF ACTIVITIES AS DRIVERS FOR EMISSIONS

2.2.1 Overview of models used for determining activities

Anthropogenic greenhouse gas emissions mainly stem from three sectors: energy (supply of energy and energy conversion according to the demand of energy services is associated with the burning of fossil fuels), transport (as well burning of liquid fuels as producing electricity for transport causes CO_2 emissions) and agriculture (cattle produces methane, using fertilizer and manure cause N_2O emissions).

Thus policies to reduce GHG emissions also have to focus on these sectors. So, for simulating the impacts of climate policies, we need models, that model activities in these areas. The scenarios of activities in the CCS study have been compiled on base of consistent European models, that are linked with each other to generate consistent models.

Figure 2-1: Integrated Model System for emission scenario modelling.

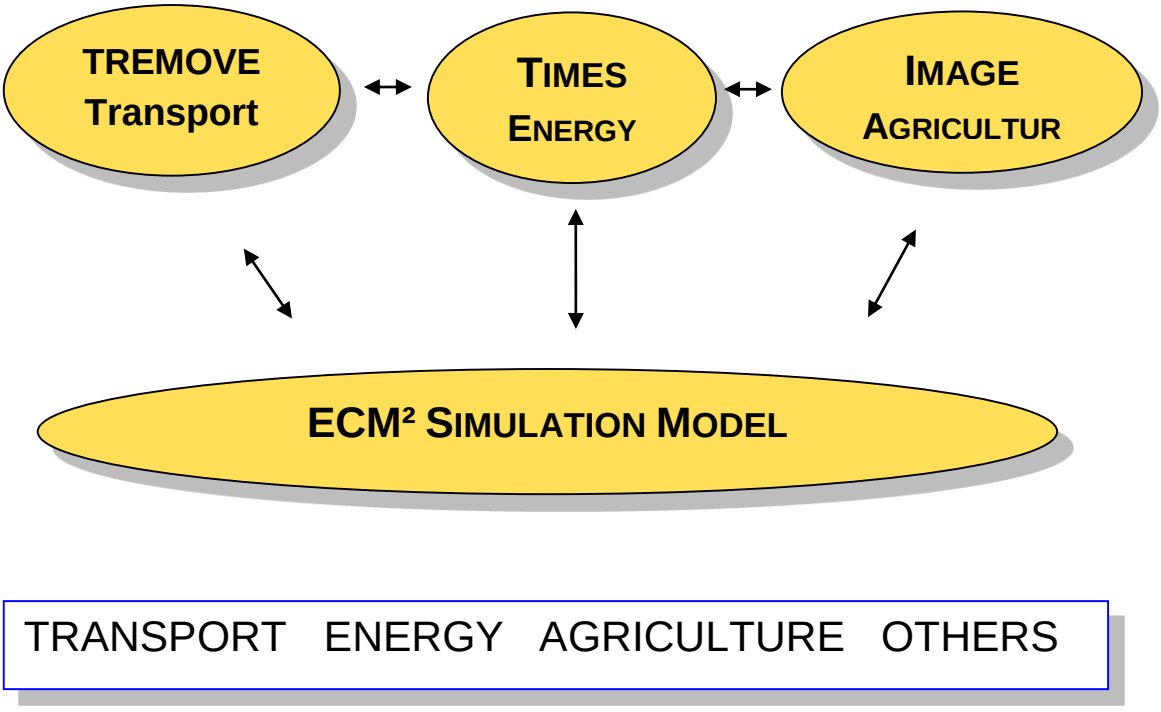

Figure 2-1 depicts the model system (models described above). To be able to develop consistent scenarios which allow for simultaneous changes in all sectors, interfaces between the models have been established. Transport demand is transferred from TREMOVE to TIMES, where energy demand and supply for meeting transport results is estimated. The demand for biomass is transferred to the agricultural model, where additional areas for biomass production are foreseen. Please note that for TREMOVE and IMAGE existing model runs are used – and results are adjusted to fit to the

scenarios generated here, whereas for the most important drivers of emissions, i.e. energy conversion, new TIMES runs are made.

The demand of energy was determined by application of the Pan-European TIMES energy system model (Blesl et al. 2011). The Pan-European TIMES energy system model (short TIMES PanEU) is an energy model of 30 regions which contains all countries of EU-27 as well as Switzerland, Norway and Iceland. The model minimizes an objective function representing the total discounted system cost over the time horizon from 2000 to 2050. A perfect competition among different technologies and pathways of energy conversion is assumed in the model. TIMES PanEU covers at country level all sectors connected to energy supply and demand, namely the supply of resources, the public and industrial generation of electricity and heat, as well as the sectors industry, commercial, households and transport. The TIMES-PanEU model results about the development of the total final energy consumption for EU30 in the different scenarios are shown in Section 2.2.3.

In the next step, the pressures to the environment resulting from the activities are calculated. Thus the solution variables from the sectoral models, especially the activities and their intensities (e.g. km driven in urban areas with EURO 4 diesel car, ha of wheat production and wheat yield per ha) would feed into the ECM² model in order to assess their environmental impacts.

Emissions stem from processes/activities like burning oil, driving a car or farming cattle. To be able to analyse the impacts of policies ECM² is used, which is a model that is able to simulate the impact of policies on activities (like km driven with a certain car type or fuel oil burnt per year in heatings in houses of a certain type) and the pressures to the environment caused by these activities. The central element of this model system is a stock-activity-emission factor data base. This data base contains the stock (e.g. number EURO 6 diesel passenger cars) – the activity (km of this car type driven in urban areas) – and the emission factors (e.g. g CO2 per km) for all activities that cause greenhouse gases in all sectors. GHG Emissions are then estimated by multiplying the three parameters. Emission factors for pollutants are also added, thus being able to estimate the effect of GHG mitigation measures on the emissions of pollutants. Technical and non-technical measures to reduce greenhouse gases will reduce stock, activity and/or emission factor. The measure can thus be expressed as an operator that changes the data in the stock-activity-emission factor data base. The advantage of this is that the effect of applying two measures can be simulated by applying one after the other operator and get consistent results for the combination.

The emission factors are based on assumptions from several sector specific data bases and models (TREMOVE (http://www.tremove.org/, GAINS (http://gains.iiasa.ac.at/index.php/home-page/241-on-line-access-to-gains) and own assumptions. The development of the emission factors is mainly driven by technical developments and air quality policies. The emission factors for 2050 have been mainly projected from 2030 to 2050 assuming them as constant or taking into account a technological or/and efficiency development.

The used emission factors are disaggregated according to different technologies and different sizes of processes, e.g. for the sectors 'public electricity and heat production' small and medium combustion plants are treated separately. For the on-road traffic activities emission factors on base of a very detailed technology split (e.g. Euro6, diesel, passenger cars, etc.) have been applied. The analysis is thus process-specific and not only sector-specific.

2.2.2 Definition of scenario drivers

In the following table, the main drivers for the activities in energy, transport and agriculture are described.

Table 2-1: Scenario description as used in the common case study.

REF = BAU	In the REF scenario (reference or business as usual scenario) it is assumed that all efforts for climate protection are stopped after 2012. This also implies that already decided targets and measures affecting the time beyond 2012 like for example the agreed emission reduction in the sectors covered by the European emissions trading scheme (ETS) (-21 % until 2020 compared to 2005) are offset. However national programs for support of renewable continue.
Climate policy scenario	• Reduction of EU greenhouse gas emissions by 20 % until 2020 and 71 % until 2050 compared to 1990 • Reduction of emissions in the ETS sector by 21 % until 2020 compared to 2005 • Minimum share of renewable energy in total final energy consumption (20 % in 2020, 40 % in 2050) • Increased minimum production of electricity from renewables • Lower demand for space heating due to improved building isolation • Faster and stronger improvement of conventional vehicle efficiencies compared to REF • Minimum market shares for hybrid electric, battery electric and plug-in hybrid electric vehicles based on national targets • Implementation of EU directive 2009/28/EC requesting a minimum quota of renewable transport fuels in transport final energy consumption (10 % in 2020) • Stronger modal shift from motorized individual transport to public transport

Table 2-2: Key model assumptions for the EU-27 as applied in the common case study.

		2005	2020	2030	2040	2050
Development of economy and population in the EU-27						
Population	Mill.	488	496	495	487	472
Av. annual growth	%		0.01	0.00	-0.2	-0.3
GDP	10^{12} EUR_{2007}	11.7	15.0	17.8	20.8	24.4
Energy prices (free boarder)						
Crude oil	USD_{2007}/bbl		88	100	106	109
Natural gas	EUR_{2007}/GJ	4.3	7.1	7.9	8.3	8.5
Coal	EUR_{2007}/GJ					
Households and living space						
Number of dwellings	Mill.	197.9	260.2	273.6	267.9	259.8
Number of buildings	Mill.	114.9	147.2	154.4	156.1	152.0
Living space of dwellings	Mill. m^2	15856	20502	22041	22619	22320
Percent houses with very good insulation standards	%					BAU: 58 Policy: 81
Transport demand (REF)						
Passenger transport (excl. aviation)	Bill. pkm	5826	6451	6742	6884	6914
Aviation	PJ	2066	2947	3399	3634	3786
Freight transport	Bill. tkm	2538	3263	3745	3992	4117
Renewable electricity						
Min. electricity quantities according to national policies in the EU-27	BAU [TWh]	455	770	835	855	895
	Policy [TWh]	455	995	1330	1510	1785
Potentials of renewable electricity generation in the EU-27	TWh	455	1700	2460	2880	3310

The emissions from waste incineration plants were provided by Swiss Federal Institute of Technology Zurich (ETH) for the whole period until 2050, see Deliverable 5.1.1 and Deliverable 5.1.2 (ETHZ 2009a), (ETHZ 2009b). The emissions from landfills were estimated by Department of Environmental Engineering, Technical University of Denmark (DTU) for the time period until 2050; see Deliverable 5.1.3, Part 2 (DTU 2010).

2.2.3 Activities in energy and transport

The detailed report of results of TIMES PanEU Energy model runs can be found in: "Energy model runs with TIMES PanEU for the Common Case Study- Scenario analysis of the 2°C target with and without external costs" in Blesl et al. (2011). A summary of the results is described in the following:

Three scenarios have been generated. 'REF' describes the BAU scenario based on the assumptions described above, i.e. a trend scenario without further climate protection measures. '450ppm' is the climate policy scenario as defined above, which sets strong reductions of greenhouse gases. '450ppm_DAM' is a scenario with the same reduction of greenhouse gases than in the 450ppm scenario. However while in the 450ppm scenario the energy system is determined by minimising the costs, in the 450_ppm DAM scenario (DAM stands for 'damage costs') external costs due to pressures to the environment are taken into account and social costs (= sum of private and external costs) are minimised. External costs do not include impacts due to climate change, as these are considered by the constraints on greenhouse gas emissions. Thus the external costs considered mainly consist of environmental health effects. Thus the differences between '450ppm' and '450ppm_DAM' directly indicate the changes, that will occur, if environmental health impacts are taken into account when making decisions for the energy system.

Concerning the development of primary energy consumption until 2050 (Figure 2-2), a continuous growth can be observed in case of the REF scenario. Fossil fuels like coal, lignite, oil and gas are the dominant primary energy carriers and account constantly for about 78 % of total primary energy consumption between 2010 and 2050. Due to the absence of a GHG reduction target the share of coal among the fossil fuels increases steadily from 18 % in 2010 to 33 % in 2050. Coal is mainly used for electricity production and for the production of CtL-(coal-to-liquids) fuels that are increasingly employed instead of oil based fuels in the transport sector. By contrast, primary energy consumption in the scenarios with intensified actions for climate protection (scenarios 450ppm and 450ppm_DAM) is characterized by a decrease between 2010 and 2050. The reductions add up to 10 % until 2050 and are the result of efficiency improvements and the implementation of energy saving measures. While the consumption of fossil fuels diminishes strongly in the climate scenarios, the consumption of renewable energy rises considerably. Renewable energy sources are either employed in the conversion sector for the production or electricity or biofuels or they are used directly as final energy carriers in the end use sectors. Additionally, electricity imports from

outside Europe (North Africa) contribute to primary energy consumption (up to 649 TWh in scenario 450ppm_DAM in 2050).

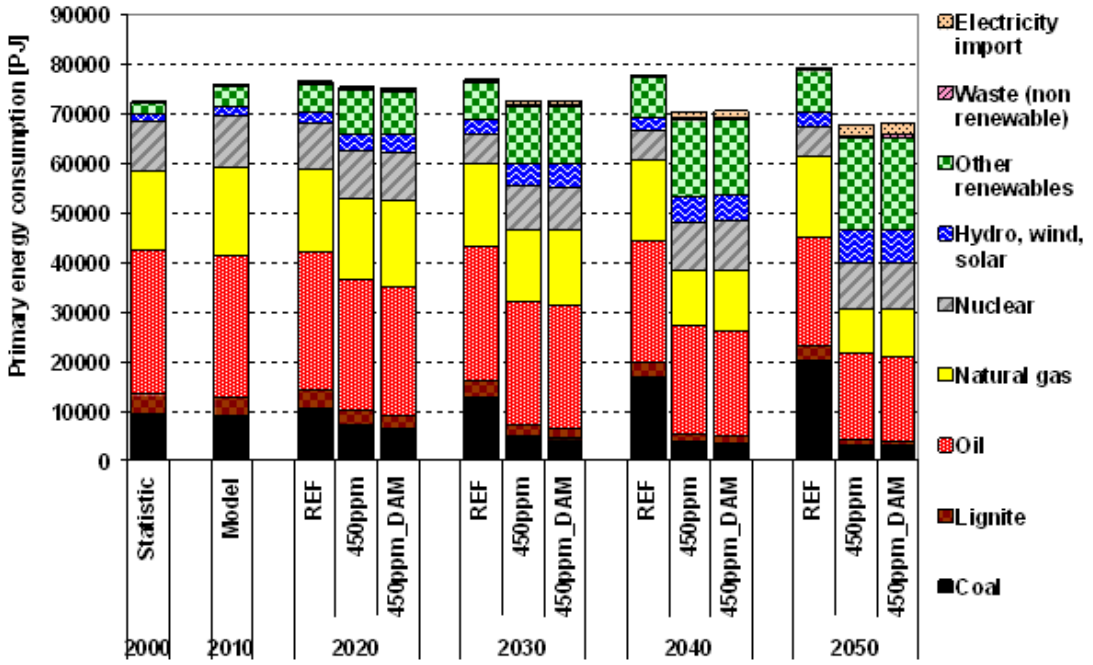

Figure 2-2: Primary energy consumption (EU-27).

Figure 2-3 gives an overview of the utilization of biomass by application in the different scenarios. The overall utilization grows in all scenarios and even in the REF scenario leads to more than a doubling of biomass consumption between 2010 and 2050. The main field of biomass application in the reference case is heat production in households and industry. But also public electricity and heat production as well as biogas production show a significant increase of biomass consumption. Due to the non-consideration of the EU directive on the minimum use of renewable transport fuels in the REF scenario, the use of biomass for the production of biofuels is negligible.

In the climate scenarios 450ppm and 450ppm_DAM, biomass is employed much stronger for the purpose of CO_2 emission reduction. As a result, biomass utilization adds up to almost 13,000 PJ until 2050 in both scenarios. In contrast to the REF scenario, the production of biofuels becomes more and more important in the climate scenarios. Especially the production of Fischer-Tropsch (FT) fuels increases considerably from 2020 onward. Since the overall biomass potential is limited, the growing biofuel production leads to a decreasing biomass utilization of other applications after 2040. This indicates that in the long run, biofuels play an essential role for GHG reduction in the transport sector (especially for road freight transport and aviation) whereas other end use sectors as well as public electricity and heat

production have a higher flexibility in using other alternative options for GHG reduction. Comparing the two climate scenarios 450ppm and 450ppm_DAM it becomes apparent that in the letter one the overall utilization of biomass is always slightly lower between 2020 and 2040. The reason is that the combustion of biomass causes comparably high pollutant emissions which are penalized with external costs in scenario 450ppm_DAM. Nevertheless, until 2050 the tightened limit for GHG emissions provokes that the biomass potentials are completely exhausted in both climate scenarios. The utilization of biomass for the production of biofuels is always higher in scenario 450ppm_DAM because biofuel production causes less additional pollutant emissions than the direct use of biomass for heat production.

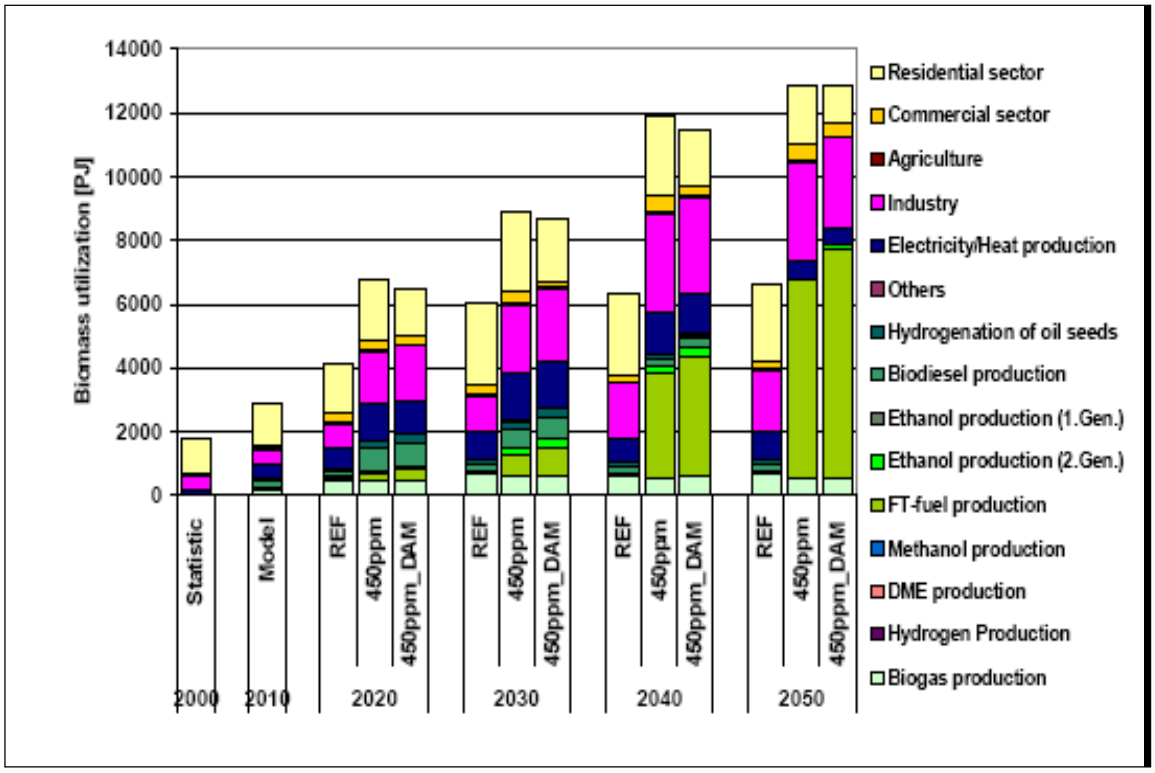

Figure 2-3: Biomass utilisation by application (EU-27)

The development of final energy consumption (Figure 2-4) shows similar effects like the development of primary energy consumption. In the REF scenario, final energy consumption increases from 49,528 PJ in 2010 to 52,816 PJ in 2050 and remains relatively constant afterwards. Fossil fuels and electricity are the dominant energy carriers. From 2030 on, oil based fuels are progressively substituted by CtL (coal to liquid) fuels. District heat plays a minor role in final energy consumption in the REF scenario and the consumption of renewables grows slightly.

The climate scenarios 450ppm and 450ppm_DAM are characterized by a continuously decreasing final energy consumption from 2020 onward, which is based on the already mentioned stronger efficiency improvements and on the implementation of energy savingmeasures. Next to the increasing direct use of renewable energy carriers, which almost quadruples in both climate scenarios between 2010 and 2050, the consumption

of electricityrises also considerably (+26 % (450ppm) and +27% (450ppm_DAM)). As a result of the incessant decarbonisation of electricity production, the use of electric appliances instead of oil or gas based appliances is getting more and more attractive with respect to emission reduction.

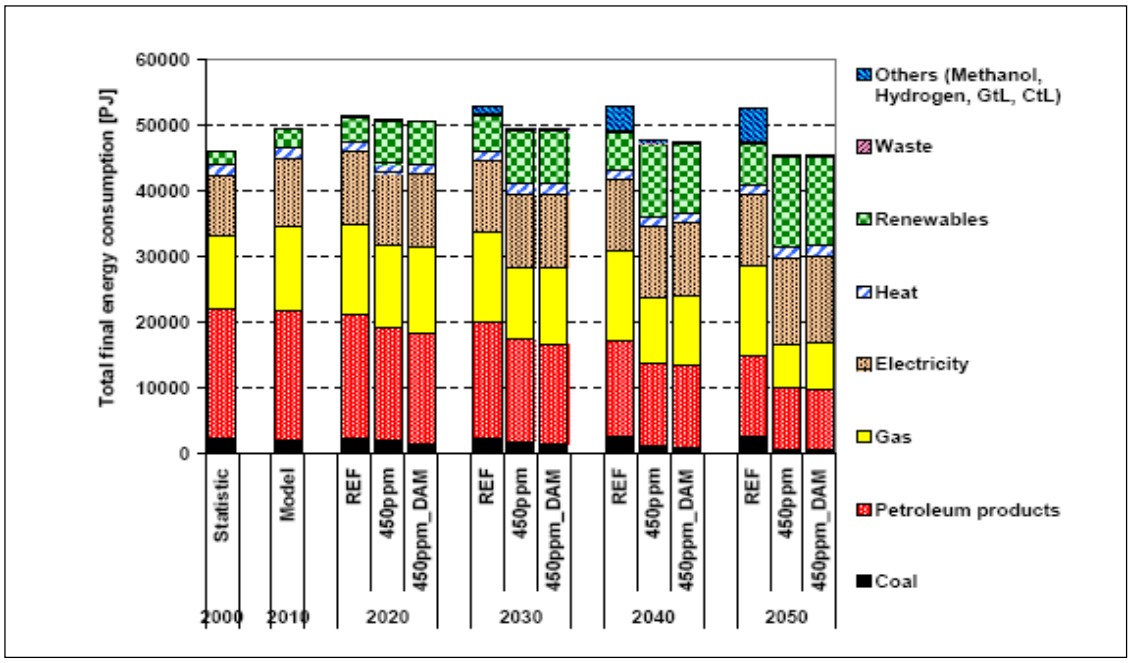

Figure 2-4: Final energy consumption by fuel (EU-27).

The fuel input for electricity and district heat generation from public and industrial power and CHP plants is characterized by a decreasing consumption past 2010, resulting from the increased use of renewable energies (conversion efficiency of hydro, wind, solar and ambient heat technologies 100 %), declining electricity generation from nuclear and efficiency improvements of fossil and nuclear based technologies (Figure 6). Nevertheless coal, lignite and nuclear energy fueled technologies, with their comparably low conversion efficiencies hold the dominant shares of the total fuel input. The total consumption declines from 28 EJ in 2010 to 22 EJ in 2050 in the REF scenario and about 20 EJ in the two 450ppm scenarios. In the reference scenario fossil fuel consumption decreases from 15 EJ in 2010 to 13 EJ in 2050, whereas coal and lignite consumption increases slightly. The average conversion efficiency (electricity and heat) of solid fossil fuels increases from 41 % in 2010 to 55 % in 2050, which means fuel savings of about 4 EJ in 2050. In the 450ppm scenarios two contrary effects determine the fuel consumption for electricity and district heat generation from public and industrial power and CHP plants. The electricity generation in CCS power and CHP plants leads to an increased fuel consumption of natural gas, coal and lignite due to additional energy consumption for the CO2 capture process and the increased share of CHP plants reduces the total fuel consumption due to its higher overall efficiency.

Thus, in 2050 the average conversion efficiency of solid fossil fuels reaches 67 %, mainly determined by the high coal and lignite CHP share of 63 % in 2050.

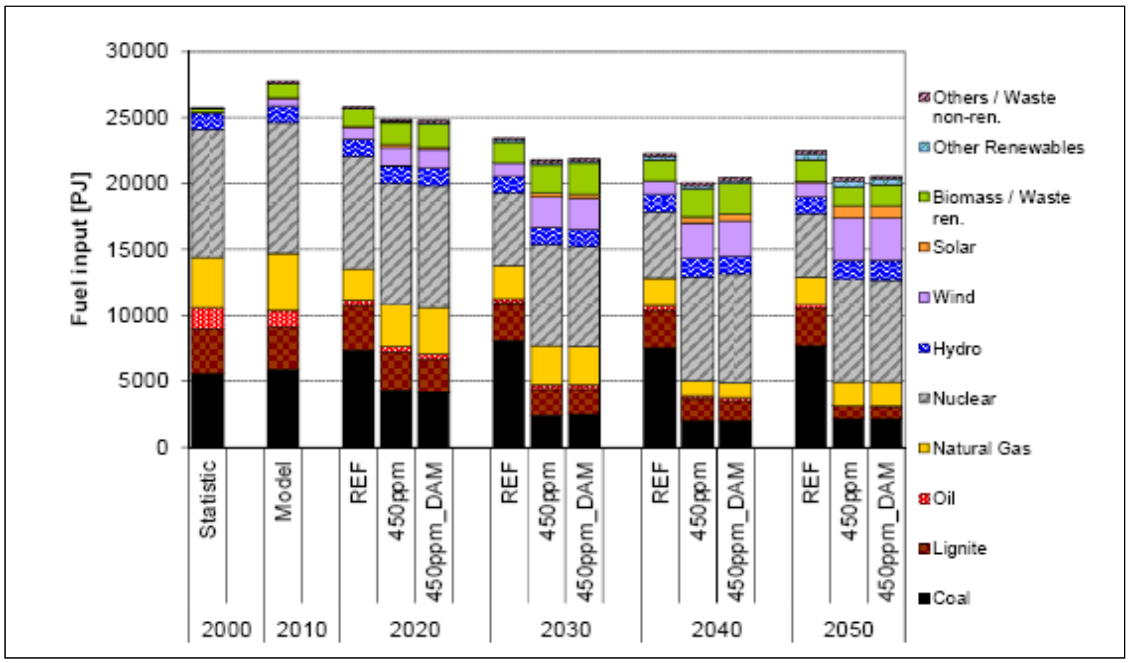

Figure 2-5: Fuel consumption for electricity and district heat generation from public and industrial power and CHP plants by fuel (EU27).

Contrary to the REF scenario, the transport final energy consumption in the scenarios 450ppm and 450ppm_DAM decreases continuously from 2010 onward. This is the result of the stronger efficiency improvements of conventional vehicles and the greater penetration of electric and hybrid electric propulsion technologies. The share of biofuels in transport final energy consumption grows in both climate scenarios. Until 2030 the biofuel consumption is mainly driven by the EU directive on renewable transport fuels that demands a minimum quota of biofuels and renewable electricity in the total consumption of gasoline and diesel fuels, renewable energy carriers and electricity in road and rail transport (minimum 10 % in 2020) (EU 2009). After 2030 biofuels, especially so called secondgeneration biofuels like BtL (biomass-to-liquids) or ethanol from lignocellulosic feedstock are also employed as a consequence of the tightened target for GHG emission reduction. In case of an internalization of the external costs of GHG and pollutant emissions (scenario 450ppm_DAM), the consumption of biofuels is even higher than in the climate scenario without external costs (450ppm). The reason lies in the fact that the conversion of biomass into biofuels and the following substitution of conventional fuels in the transport sector cause less additional pollutant emissions than the direct use of biomass for heat production in households and commercial sector. Due the greater penetration of electric vehicle concepts in both climate scenarios, electricity consumption in the transport sector rises considerably from 72 TWh in 2000 to more than 260 TWh in 2050. Most of this increase occurs at the end of the considered times horizon, when electric vehicles are intensively used as an option for GHG reduction.

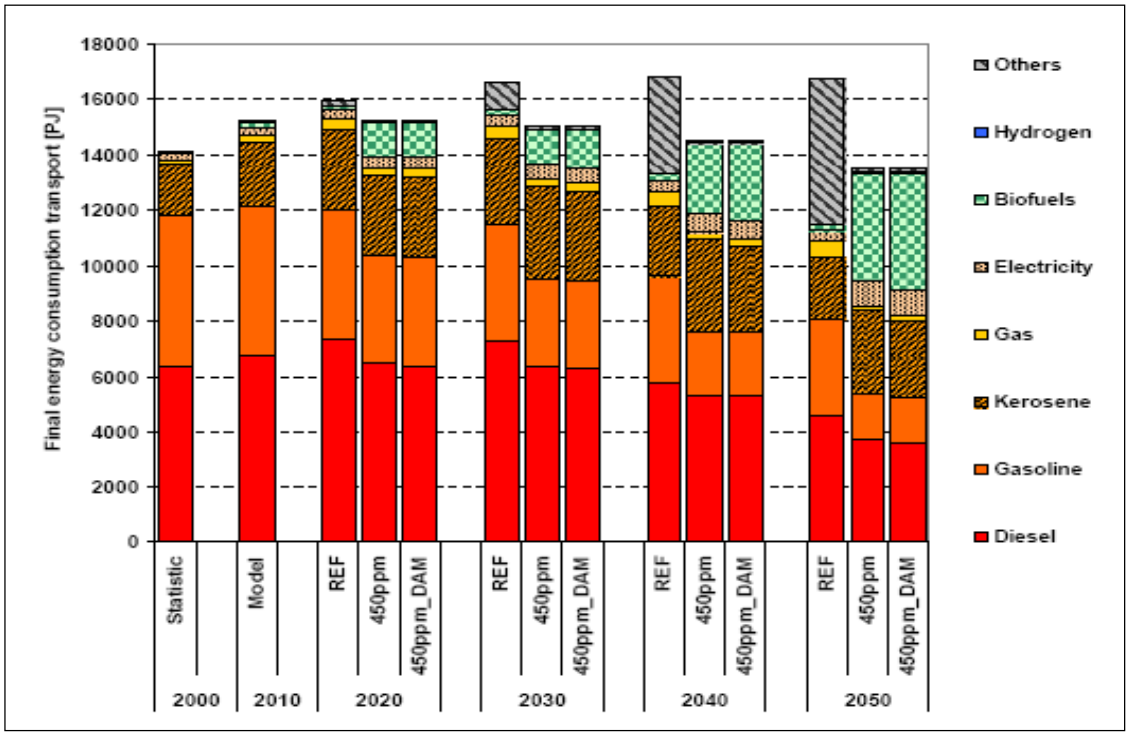

Figure 2-6: Final energy consumption transport by fuel (EU-27).

2.2.4 Activities in agriculture

For the agricultural case study a number of factors are identified, responsible for the influence of the emission estimates, as listed below: a) temperature variation due to climate change, b) changes in the spatial distribution of crops and in yield and c) changes in the AI list. Another issue addressed here is the EU policy on energy crops cultivated in arable land and its effect on human health.

More in detail, the temperature scenarios considered in this study will reflect on changes in agro-climatic zones from 2000 to 2050, as a function of the corresponding air temperature scenario (2 or more degrees C temperature rise). These changes are have been considered as environmental background in the development of the emission scenarios for pesticides from agricultural activities. Overall, they imply lower water availability for agriculture in the European South (in particular Spain) and improved conditions for agricultural development in the European North (UK, northern Germany, Finland, Sweden, the Baltic countries). These developments affect directly and non-homogeneously the spatial extent of the land used for agriculture across Europe and consequently the spatial distribution of crops as well as the agricultural yield. More favorable agro-climatic conditions also imply the faster growth of pests in the European North compared to today and thus the need for more intensive use of pesticides to maintain the current agricultural yield. Two are the main Community

policy areas directly affecting emissions of pesticides and the respective spatial distribution:

a The Plant Protection Products Directive, under the impetus of which a large number of the most toxic active ingredients (AI) in commercial pesticide preparations has been replaced over the last 10 years by more benign ones. This trend, albeit not at the same pace, is assumed to continue in the decades to come due to higher public awareness regarding the dangers to environmental and human health from toxic chemicals entering the environment. Thus, we have simulated the substitution of the most toxic AIs among the ones still allowed to use in the EU with less toxic ones in order to take into account the underlying change in the environmental burden of disease.

b The 20-20-20 policy of the EU, regarding enhanced penetration of renewable energy sources in the internal energy market in combination with the reformed Common Agricultural Policy, which sets aside 15% of agricultural land and allows its use for cultivation of energy crops. Clearly, the proactive introduction of energy crops has to take into account sustainability constraints based on the current and projected state of the European environment. Thus, we have used a relevant study of the European Environment Area, which outlines the level of energy crop production per country in order to respect sustainability criteria, in line with the Sustainable Development Strategy of the EU.

Models Used

Basic data are needed for the agricultural section in the context of the land use, edible and energy crops, animal numbers and general climatic data. Candidate models are selected according to the guidelines based on the Intergovernmental Panel on Climate Change (IPCC). The model identified as matching the IPCC requirements is the Integrated Model to Assess the Global Environment, (IMAGE).

The IMAGE model is developed at PBL[2]; it is an ecological-environmental model that simulates the environmental consequences of human activities worldwide. IMAGE scenarios are commonly presented as representative concentration pathways (RCP) with different radiative forcing (expressed in W/m2) and concentrations of CO2 equivalents. The two scenarios selected as most relevant for the overall climatic scenarios, taken as overarching drivers in the Common Case Study, are the RCP-B2 baseline (equivalent to the A1F scenario) and the RCP-B2.6 (mitigation scenario equivalent to the B1 scenario. IMAGE model maps (50x50 km) include data on, land use (utilized agricultural area, arable and pasture land) and crops (cereal, maize, oilseed, rice etc), but limited information on energy crops (woody energy crops only) and no information on animal numbers. To cope with these limitations, other models are used, provided that the scenarios selected are in accord with the IPCC guidelines.

[2] (http://themasites.pbl.nl/en/themasites/image/index.html)

The models from the PESETA (http://peseta.jrc.ec.europa.eu/)(Projection of Economic impacts of climate challenge in Sectors of the European Union based on bottom-up Analysis) and the ATEAM (Advanced Terrestrial Ecosystem Analysis and Modelling (http://www.pik-potsdam.de/ateam) project and the GAINS (Greenhouse Gas and Air Pollution Interactions and Synergies Model) (IIASA: GAINS model, 2010)) model are integrated into the case study and used to enhance the IMAGE model.

In order to use the IMAGE model maps for the scenarios, the baseline maps (on the land use) are firstly calibrated against the EUROSTAT 2000 data and secondly against the CORINE land cover map in the EU 27. The reason is two-fold, historic trends (25-yr period) on land use and crops are only available at country level and their spatial variation, at the 50x50km^2, is for the year 2000. Information is combined, with objective to update developed spatial allocation models, whose parameters are estimated via optimization (Nelder-Mead simplex method). The models developed are listed below:

- a land use allocation model (incl. arable land and pasture)
- a land allocation model for permanent crops and vineyards
- a crop allocation model for edible crops (cereals, maize and oilseed)
- a crop allocation model for energy crops
- an animal estimation model based on the GAINS model output
- an energy estimation model computed from the energy crops

Some assumptions made for the agricultural sector are:

Crop typology in the BAU and mitigation scenarios

According to the IMAGE model output, changes in the climatic conditions result in spatial variations in crops for the EU-27. Crop typology is kept the same, but depending on the scenario considered there are significant changes between countries.

Increase or reduction of pesticides (use of new substances)

The pesticide list considered takes into account two categories of active substances, i.e., those approved for use and those under evaluation (pending approval), as discussed in Karabelas et al. (2009). It was hence possible to derive a “future list” of pesticides. Nevertheless, it is unclear whether future pesticides usage will increase or decrease.

On biomass for energy crops

In a recent study (EEA, 2006) the European Environment Agency reviewed what is the amount of biomass, potentially available for energy production, without increasing pressures on the environment or counteracting current and possible future EU environmental policies and objectives. This EEA study developed a number of premises for bioenergy production as a basis for modeling the available energy potential, for the sectors of agriculture, forestry and waste. On the production of

biomass for energy, the following policies are considered: (a) EU policy and legislation, (b) land use requirements, (c) water usage, (d) types of plants for biomass-to-energy production, (e) pesticides used on energy crops and (f) the environmental and economic implications.

Please note however, that from 2020 on additional areas are needed for biomass production in the climate protection scenario, which are in principle available, but would lead – according to the EEA study – to increasing pressures on the environment.

Land use requirements for Energy Crops

For the scenarios, arable land was allocated for use by energy crops according to the general requirements of the EEA (2006) study listed below:

i. The only substantial increase of bio-energy production is due to energy crop cultivation.

ii. It is foreseen that forestry can make only a small contribution to energy production in the context of a mitigation scenario; this prediction is in accordance with other stakeholder opinions [e.g. EuropaBio (2007)].

iii. In estimating equivalent energy production, for these scenarios, one has to take into account: a) agricultural residues related to the crops as well as the main product (seeds or grain) and b) appropriate yield for both main crop (grain, seed) and the rest of biomass (from the plant, where applicable), i.e. the total biomass produced per unit area cultivated. A literature review by CERTH estimates yield per crop type and reflects future trends by taking into account the agro-climatic zones in Europe.

iv. Energy crops are assumed to be cultivated on arable and fallow land as well as on ‘excess’ land, considered to be changes in arable land between the baseline year and the scenarios.

Use of agro-climatic zones

According to the PESETA project ((Projection of Economic impacts of climate challenge in Sectors of the European Union based on bottom-up Analysis), the agro-climatic zones are shifted according to climatic conditions based amongst others on temperature and water availability. Those zones are the basis for the selection of the energy crops suitable for the local environmental conditions. Hence, the following energy crops are selected: sunflower, rape, sugar beet, wheat, oilseeds, sorghum, maize, cardoon, willow and poplar. In addition, their spatial variation is taken from the ATEAM project based on the requirements set by an EEA guideline on energy crops (EEA, 2006).

Energy crops needed based on energy model runs

The demand for energy from biomass was determined by application of the Pan-European TIMES energy system model (see Section 2.2.3).

TIMES model results were received in terms of petajoule (PJ) per year for raw products of oil seeds, sugar crops, starch crops, woody biomass and grassy biomass (see Figure 2-7).

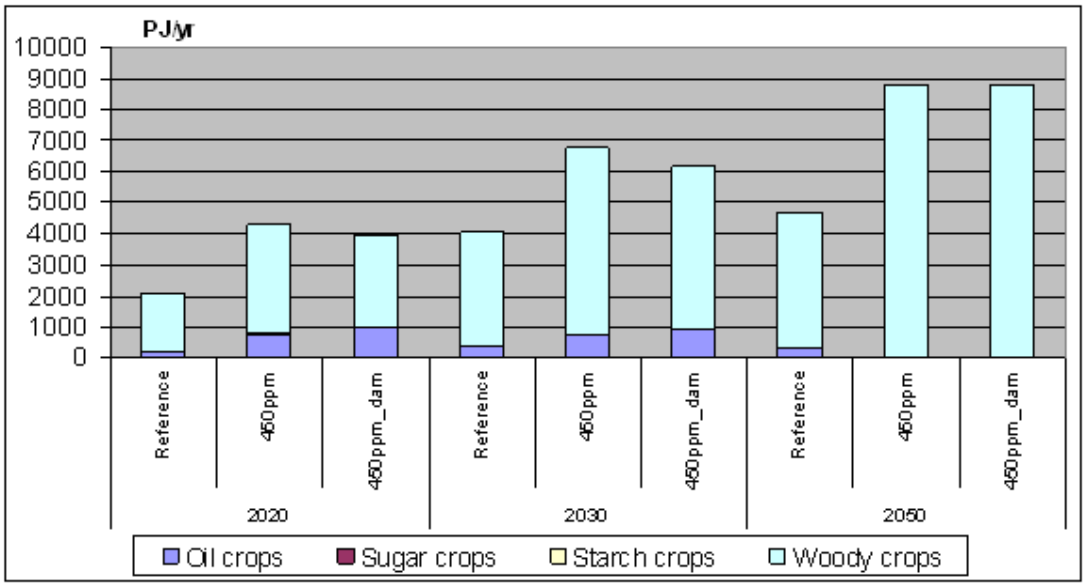

Figure 2-7: Biomass energy demand in EU-27 + CH and NO (TIMES model results, PJ/yr).

Applying energy content conversion factors (in Gigajoule (GJ) per ton of fresh matter (FM) (Table 2-3), the amount of harvested biomass per crop category which is required to meet biomass energy demand was derived. According to TIMES results, no demand for energy from grassy biomass exists.

Table 2-3: Energy content of biomass

TIMES category	Crop category	Energy content (GJ/t FM)
Oil crops	Rape seed	23.8
	Sunflower	26.38
Sugar crops	Sugar beet	18
Starch crops	Wheat	17
Woody biomass	Willow	11.11

Source: Schröder et al (2006)

After the amount of crops needed had been calculated, the respective area had to be estimated. First the average yield per crop for the base year was determined based on Eurostat data (Table “apro_cpp_crop”). The mean of average yield of 2004 to 2006 was calculated in order to smooth the impoacts of climate differences. Starting with the

average yields for the year 2005, future yields were estimated. A distinction was made between Northern European countries and Southern European countries for climatic reasons and future possible climate effects on crop production. For all Northern European countries, an average annual yield increase of 1 % was assumed for all crops. This is based on the assumption that climate effects on Northern Europe are positive for plant growth (EEA 2006). For Southern Europe an average yield increase of 1 % was assumed until the 2020. After 2020 it was assumed that temperature rise will have adverse impacts on plant growth and harvest yields. This is also based on the assumption that a global average temperature increase of 2° C in 2050 leads to a temperature rise of more than 2° C in summer in Mediterranean countries (IPCC 2007). Temperatures in Mediterranean countries can rise between 5 and 8° in summer and precipitation can decrease. This will lead to a decrease in yields.

For the reference scenario, representing an average temperature rise of more than 2°C globally in 2050, it as assumed that from 2021 on yields would decrease by 5% per year. For the Climate scenario the following was assumed: Again in Northern European countries yields will increase by 1 % annually. In Southern European countries, yields will increase by 1 % per year until 2020. After 2020, yields will decrease by 3% annually due to temperature rise. Decrease in yields is not expected to be as high as in the reference scenario because temperature increase is expected to be lower.

Based on the assumed yield developments, the area of biomass crops required to meet biomass energy demand in 2020, 2030 and 2050 was derived (see Figure 2-8). The additional area for energy biomass production is also available per country and even per gridcell of the EMEP 50*50 km² grid.

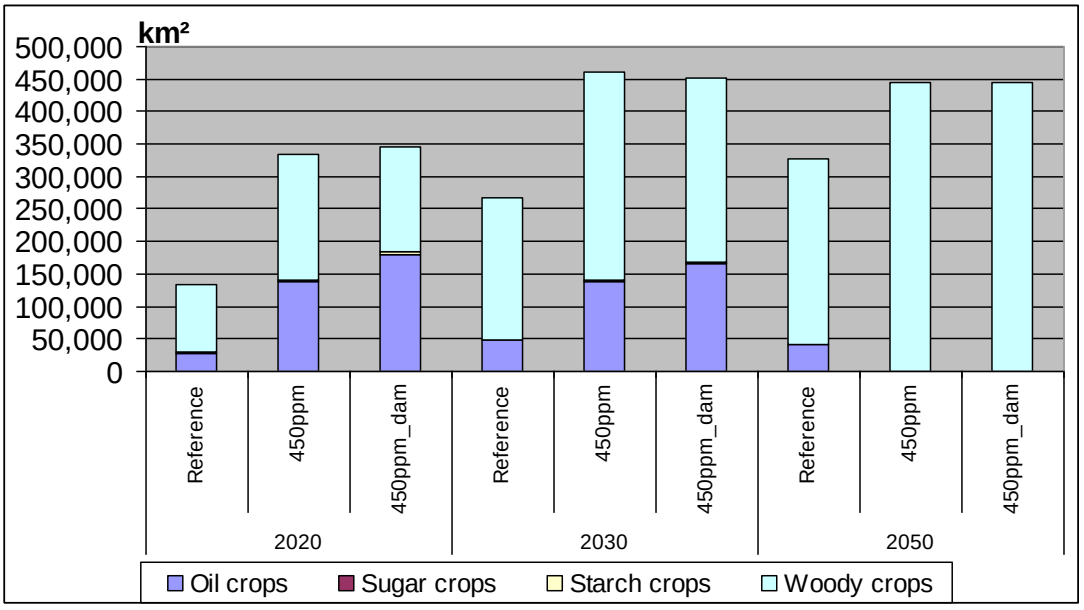

Figure 2-8: Biomass area required to meet TIMES biomass energy demand in EU-27 +CH and NO (km²).

2.2.5 Emissions in the Scenarios for all Sectors

In the following emissions are shown for selected pollutants for all sectors and activities. In agriculture, the emissions from not only the production of energy crops, but also from the production of food are included.

The represented source categories include the following sub-sectors:

- **Agriculture** (livestock management, energy and food crops cultivation)
- **Energy** (Public Electricity and Heat Production, Conversion)
- **Transport** (Civil Aviation, Road Transport, Railways, national Navigation and mobile sources and maschinery)
- **Small and medium plants** (small and medium combustion plants in agriculture, in commercial sector and households)
- **Industry** (energy and non-energy related industrial activities)
- **Waste.**

The following figures show the greenhouse emissions by source categories in EU 27, Switzerland and Norway between 2020 and 2050.

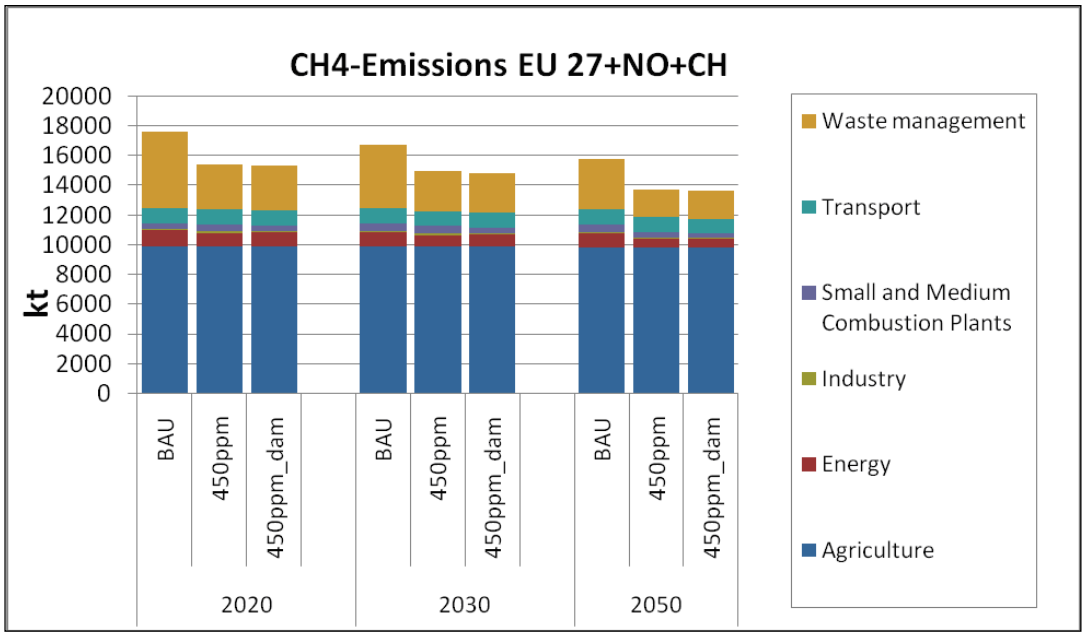

Figure 2-9: Results of Emission Scenarios- CH_4 emissions by source category in EU-27 +CH and NO.

The methane emissions decrease in the 450ppm Scenario compared to the BAU Scenario in 2050 by about 12%. The CH_4-reduction can particularly be attributed to the

sectors waste management (landfills) and energy. The emission reduction on landfills is caused by the installation of landfill gas collection and treatment systems (see DTU 2010).

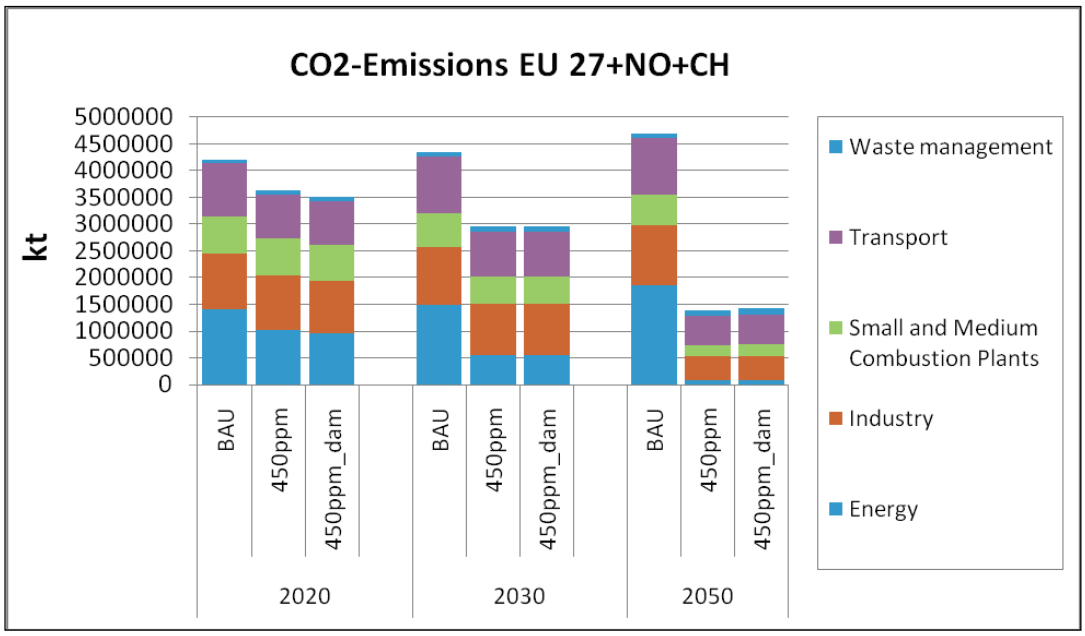

Figure 2-10: Results of emission scenarios- CO_2 emissions by source category in EU-27 +CH and NO.

As Figure 2-10 shows, the sector energy accounts for the largest CO_2 reduction of all sectors (-94 % between 2020 and 2050 in both climate protection scenarios compared to BAU). The main reason for this is the much stronger penetration of renewable energy for electricity production as well as the utilization of CCS (carbon capture and storage) technologies. Nevertheless, the end use sectors also contribute to the reduction of CO_2 emissions. In the transport sector the reduction is caused by the stronger efficiency improvement of conventional vehicles as well as by the penetration of alternative fuels (e. g. biofuels) and power trains (e. g. electric and hybrid electric vehicles). In the sectors households, commercial and agriculture the main instruments for CO_2 reduction are energy saving measures (e. g. improved building insulations), the use of renewables (e. g. solar heating, biomass boilers, heat pumps) as well as a higher use of electric appliances in favour of oil and gas based technologies. The same applies to the industry sector where CO_2 emissions are additionally reduced through the use of CCS. All in all the reduction of CO_2 emissions between 2020 and 2050 in the climate scenarios adds up to 45 % and 54 % in the transport sector, 57 % and 56 % in the industry sector and 73 % and 70 % in the sectors households, commercial and agricultures (see Blesl et al. 2011).

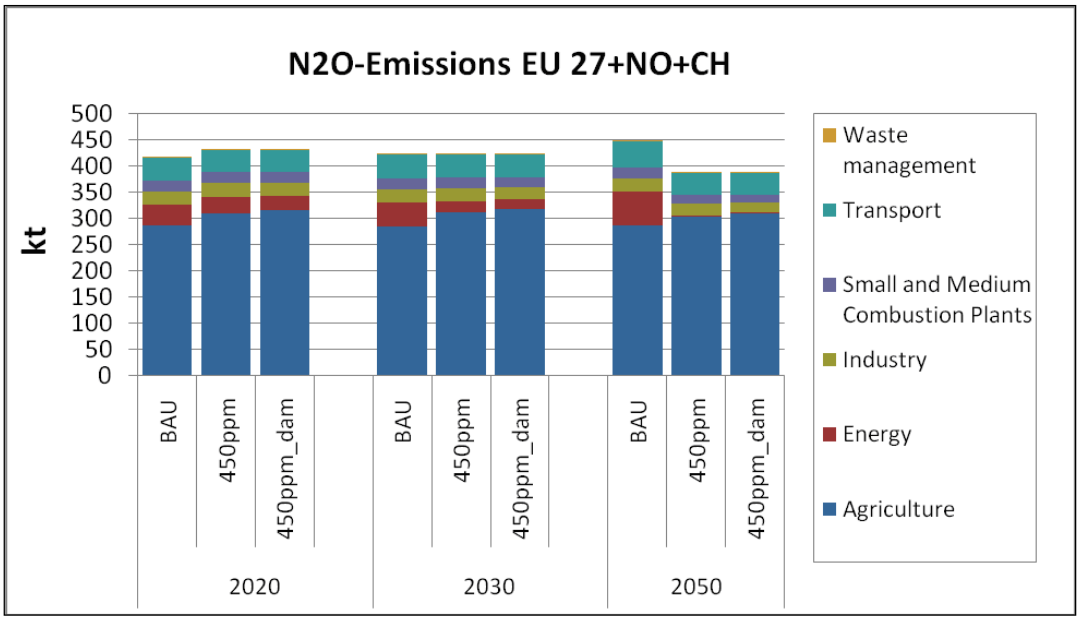

Figure 2-11: Results of Emission Scenarios- N2O emissions by source category in EU-27 +CH and NO.

The N_2O emissions decrease particularly in the energy sector by about 96 % in 2050. In the sector agriculture the emissions increase slightly. This increase can be explained by the intensified cultivation of the energy crops for biofuel production (see Section 3.1.1).

The changes in GHG emissions by source sector and pollutant between 2020 and 2050 are given in Table 2-4. The plus sign indicates an increase of emissions in the climate policy scenario compared to the BAU/REF scenario and the minus sign indicates an emission reduction in the climate policy scenario in comparison to the reference scenario (BAU).

Table 2-4: Changes in Greenhouse Gas Emissions in % for the different scenarios.

	Changes in Emissions in %						
		2020		2030		2050	
Sector	Pollu-tant	450 ppm	450 ppm_dam	450 ppm	450 ppm_dam	450 ppm	450 ppm_dam
Agriculture	CH4	0.0	0.0	0.0	0.0	0.0	0.0
Energy	CH4	-14.5	-13.0	-16.6	-15.0	-40.5	-39.3
Industry	CH4	-1.1	5.9	-4.1	-0.9	-18.1	-18.8
Small and Medium Combustion Plants	CH4	23.4	0.8	-3.7	-23.0	-25.9	-50.2
Transport	CH4	-1.4	-1.4	-1.8	-1.8	-1.8	-1.8
Waste management	CH4	-41.5	-41.5	-37.4	-37.4	-44.1	-44.1
Energy	CO2	-26.6	-32.0	-62.7	-62.5	-95.6	-95.7

		Changes in Emissions in %					
		2020		2030		2050	
Sector	Pollu-tant	450 ppm	450 ppm_dam	450 ppm	450 ppm_dam	450 ppm	450 ppm_dam
Industry	CO2	-2.5	-6.0	-11.3	-12.8	-60.4	-59.4
Small and Medium Combustion Plants	CO2	-1.9	-2.9	-20.8	-19.0	-64.2	-60.6
Transport	CO2	-18.5	-18.5	-21.8	-21.8	-48.5	-48.5
Waste management	CO2	41.7	41.7	27.7	27.7	46.6	46.6
Agriculture	N2O	7.6	9.6	9.4	11.4	6.1	8.1
Energy	N2O	-18.3	-27.2	-55.5	-59.2	-95.7	-96.1
Industry	N2O	6.8	-1.6	4.8	-2.8	-14.4	-30.4
Small and Medium Combustion Plants	N2O	1.0	-3.0	-7.3	-10.8	-23.1	-26.5
Transport	N2O	-4.8	-5.0	-5.9	-6.4	-15.7	-16.8
Waste management	N2O	75.8	75.8	71.1	71.1	121.4	121.4

The next Figures present the development of air pollutants by source categories in EU 27, Switzerland and Norway between 2020 and 2050.

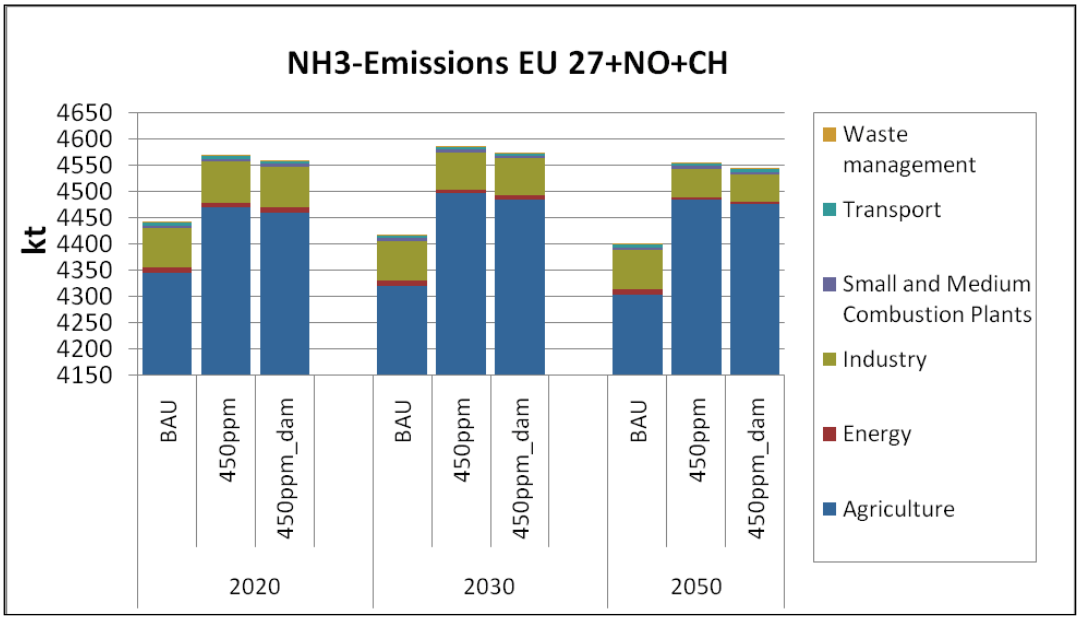

Figure 2-12: Results of Emission Scenarios- NH_3 emissions by source category in EU-27 +CH and NO.

Figure 2-12 shows that the ammonia emissions from agricultural activities increase between 2020 and 2050 in both climate protection scenarios. The higher NH_3

emissions will be caused by increase of cultivation area for energy crops and associated increased fertilization (see Section 3.1.1).

The industrial ammonia emissions remain relatively constant until 2030. From 2030 on an emission reduction by about 30% is expected.

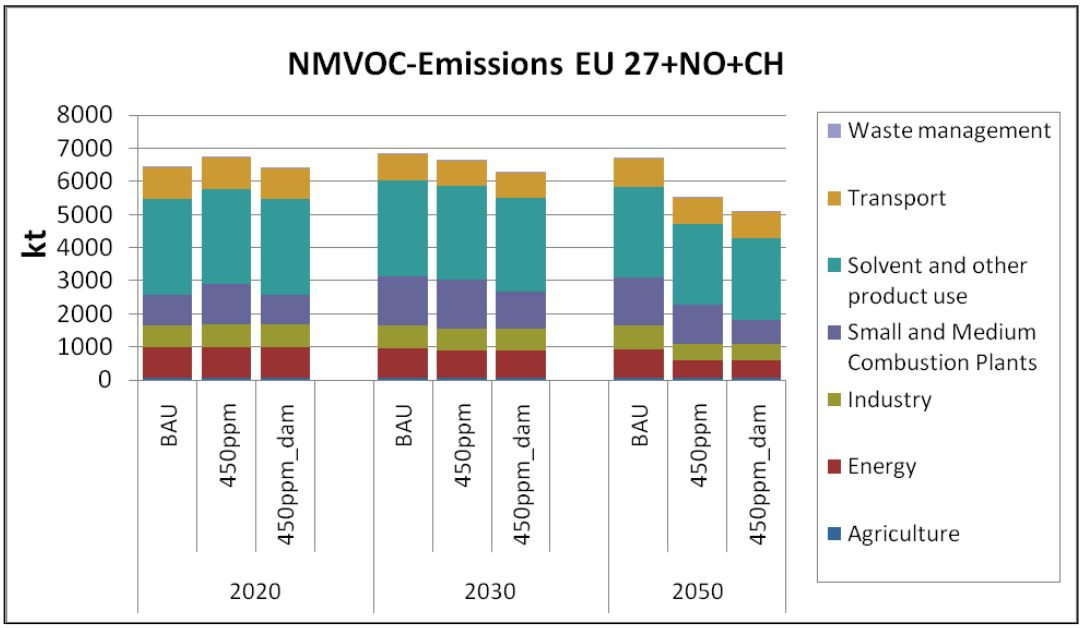

Figure 2-13: Results of Emission Scenarios- NMVOC emissions by source category in EU-27 + CH and NO.

The NMVOC-Emissions in the source category “solvent use” remains constant between 2020 and 2050. In 2020 the sector small combustion plants shows higher emissions in the 450ppm than in BAU scenario. Up to 2050 the NMVOC emissions in this sector are decreasing. This is due to the fact, that in 2020 in the 450ppm scenario a more solid biomass fuel (wood) is burned in small and medium plants than in the BAU Scenario. From 2030 the solid biomass use decreases in the climate scenario (see Section 2.2.3), as the biomass is needed and used more urgently in the transport sector to generate biofuels. The use of solid biofuels like for example split logs, wood chips, pellets in small combustion plants causes significantly higher emissions from incomplete combustion (for example CO, Particulate matter emissions, PAK, NMVOC) than gas or oil systems.

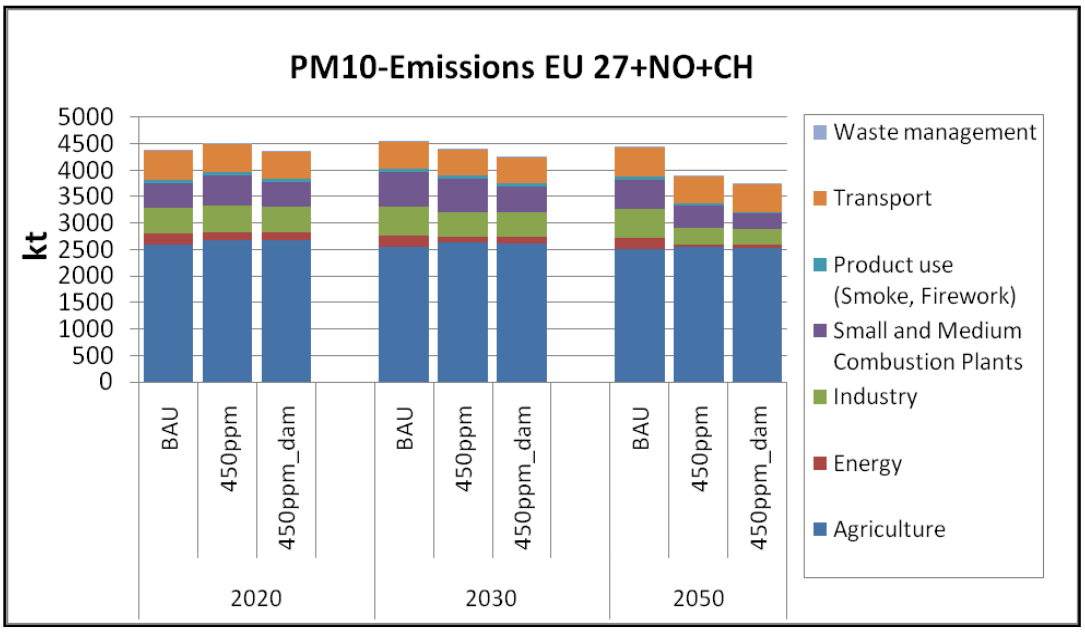

Figure 2-14: Results of Emission Scenarios- PM10 emissions by source category.

Figure 2-14 and Figure 2-15 show a similar emission development as Figure 2-13. Pm emissions form agriculture are courser particles, thus contribute to PM10, but less to PM2.5. The sector small combustion plants is the highest contributor to total PM2.5 emissions. The PM emission from small combustion plants increase in the 450ppm scenario by 2030 by about 27%, as more wood is burnt in small firings. After 2030 the woody biomass produced is more and more used for the generation of biofulels for transport, in addition houses are better insulated, thus the PM2.5 emissions from small combustion decrease again. In the energy sector the PM_{10} emissions decrease up to 2050 by about 70% compared to BAU.

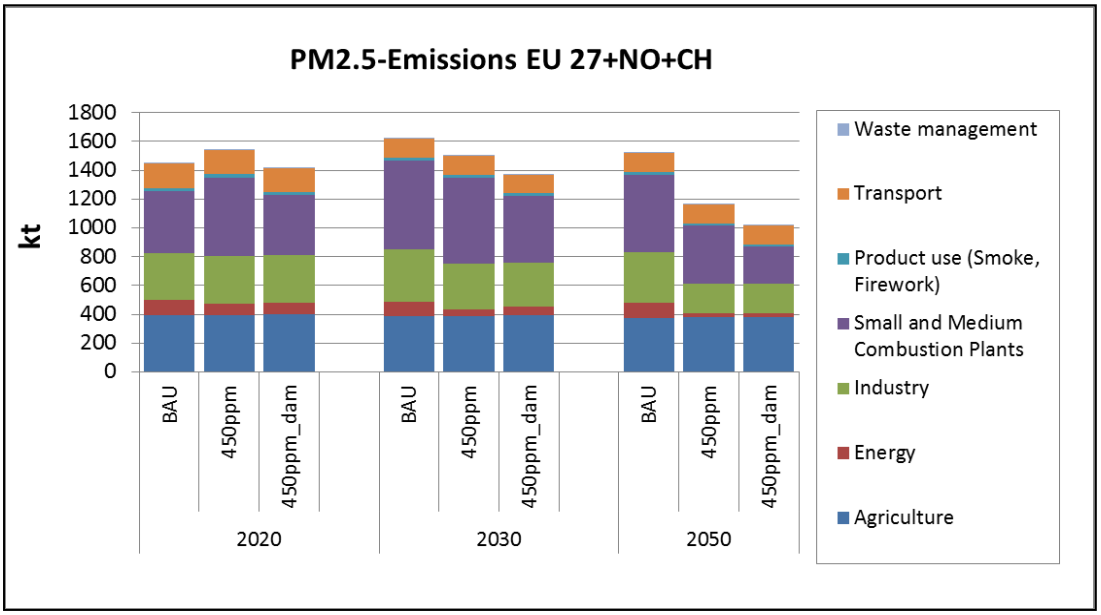

Figure 2-15: Results of Emission Scenarios- PM2.5 emissions by source category.

The SO_2 emissions (see Figure 2-16) decrease in the climate scenario in all sectors except the sector waste management. In transport sector the emission reduction is about 5% up to 2050. The significantly reduction can be archived in 2050 for energy and industry by about 60%. The SO_2 emissions from small combustion plants are in 450ppm scenario in 2050 by about 36% smaller than in BAU Scenario.

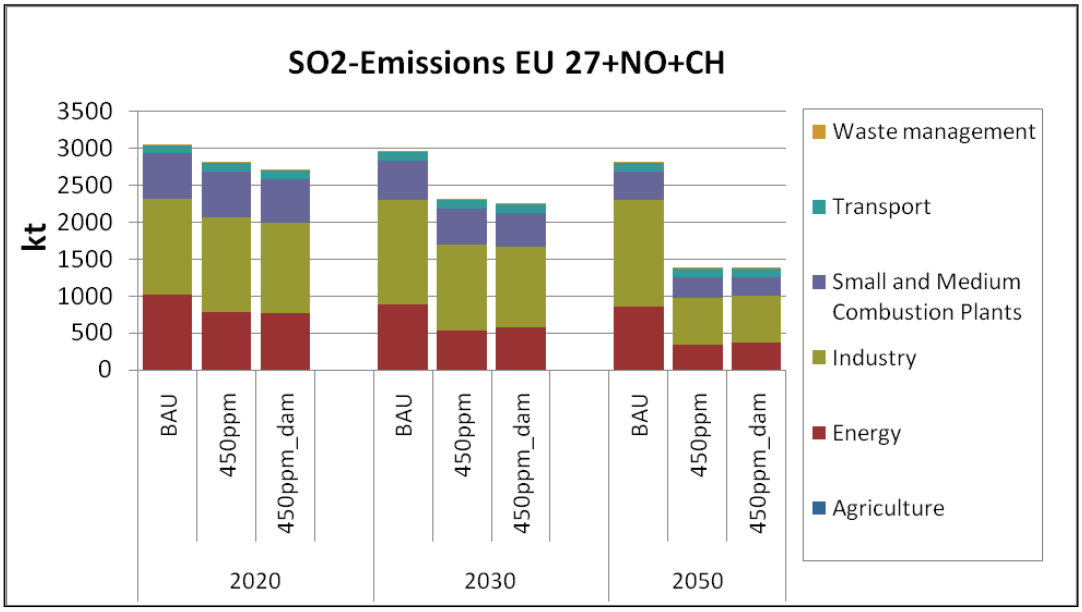

Figure 2-16: Results of Emission Scenarios-SO2 emissions by source category.

The largest NO_x emission reductions in the Climate Policy scenario are expected 2050 from the energy sector (by about 60% in 450ppm) and from small combustion plants (by about 50% in 450ppm Scenario), see Figure 2-17. The NO_x emissions from transport will be reduced 2020 by about 2% and 2050 by about 4%.

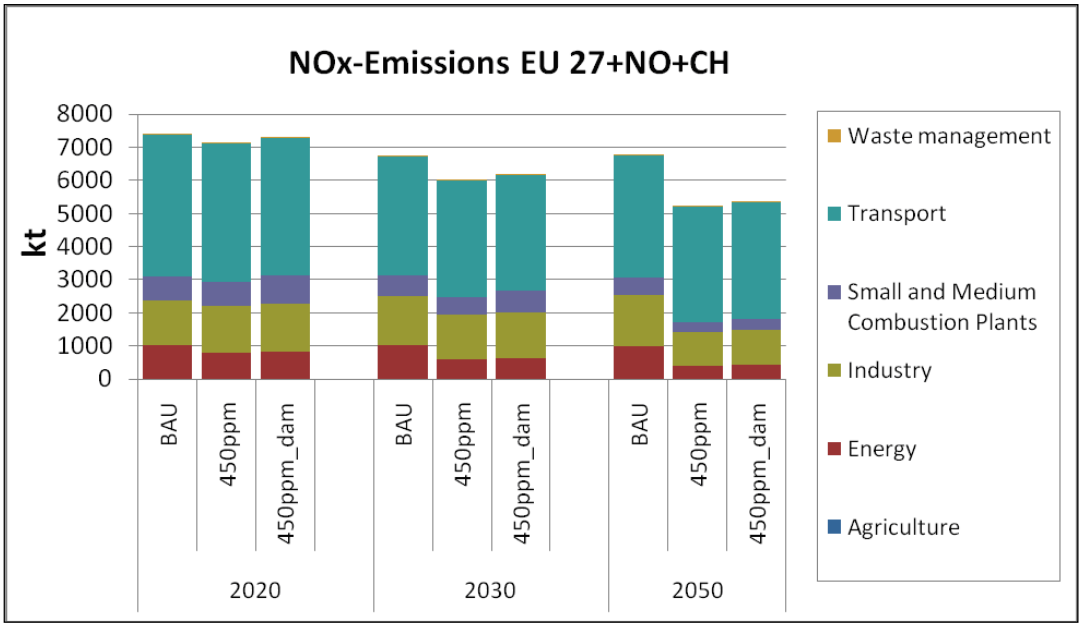

Figure 2-17: Results of Emission Scenarios- NOx emissions by source category.

The changes in emissions by source sector and pollutant between 2020 and 2050 are shown in Table 2-5. The plus sign indicates an increase in emissions in the climate policy scenario compared to BAU and the minus sign indicates an emission reduction in the climate policy scenario in comparison to the reference scenario (BAU).

Table 2-5: Changes in Emissions in % for different scenarios.

	Changes in Emissions in %						
		2020		2030		2050	
Sector	Pollu-tant	450 ppm	450 ppm_dam	450 ppm	450 ppm_dam	450 ppm	450 ppm_dam
Agriculture	NH3	2.9	2.6	4.1	3.8	4.2	4.0
Energy	NH3	-9.8	-4.9	-33.6	-27.7	-56.5	-50.4
Industry	NH3	5.2	5.8	-4.5	-4.3	-30.3	-31.3
Small and Medium Combustion Plants	NH3	9.2	-5.0	15.5	-13.8	79.2	42.7
Transport	NH3	-7.4	-7.4	-10.1	-10.1	-15.1	-15.1
Waste manage-ment	NH3	75.3	75.3	69.9	69.9	121.4	121.4
Agriculture	NMVOC	0.0	0.0	-3.0	-3.0	-3.0	-3.0
Energy	NMVOC	-2.2	-2.2	-9.3	-8.7	-39.9	-39.4
Industry	NMVOC	8.2	8.8	-2.1	-2.5	-26.8	-28.5
Small and Medium Combustion Plants	NMVOC	30.6	-2.5	-0.4	-24.9	-21.5	-51.3
Solvent and other product use	NMVOC	0.0	0.0	-2.4	-2.4	-9.4	-9.4
Transport	NMVOC	-3.2	-3.4	-4.1	-4.4	-5.9	-6.1
Waste management	NMVOC	26.5	26.5	22.2	22.2	39.5	39.5
Agriculture	NOx	0.0	0.0	-1.9	-1.9	-1.9	-1.9
Energy	NOx	-21.9	-18.4	-43.7	-38.6	-62.3	-58.1
Industry	NOx	3.8	7.2	-7.6	-5.8	-31.9	-31.0
Small and Medium Combustion Plants	NOx	0.1	15.8	-13.2	3.1	-49.6	-38.0
Transport	NOx	-2.1	-2.3	-2.5	-2.7	-4.7	-4.8
Waste management	NOx	-68.9	-68.9	-60.2	-60.2	-31.0	-31.0
Agriculture	PM10	2.8	2.8	3.2	3.0	1.1	0.9
Energy	PM10	-24.7	-26.3	-50.3	-42.3	-71.0	-69.2

	Changes in Emissions in %						
		2020		2030		2050	
Sector	Pollu-tant	450 ppm	450 ppm_dam	450 ppm	450 ppm_dam	450 ppm	450 ppm_dam
Industry	PM10	0.6	-0.5	-15.4	-16.6	-44.8	-45.0
Small and Medium Combustion Plants	PM10	26.8	-1.4	-1.8	-24.2	-23.7	-50.4
Product use (Smoke. Firework)	PM10	0.0	0.0	-7.9	-7.9	-38.3	-38.3
Transport	PM10	-3.9	-4.1	-5.0	-5.1	-4.7	-4.7
Waste management	PM10	42.9	42.9	30.6	30.6	46.1	46.1
Industry	PM2.5	0.6	-0.5	-15.4	-16.6	-44.8	-45.0
Small and Medium Combustion Plants	PM2.5	26.8	-1.4	-1.8	-24.2	-23.7	-50.4
Product use (Smoke. Firework)	PM2.5	0.0	0.0	-7.9	-7.9	-38.3	-38.3
Transport	PM2.5	-3.9	-4.1	-5.0	-5.1	-4.7	-4.7
Waste manage-ment	PM2.5	42.9	42.9	30.6	30.6	46.1	46.1
Agriculture	PMTSP	3.0	3.0	3.3	3.1	1.1	0.9
Energy	PMTSP	-26.3	-27.3	-52.6	-43.2	-71.6	-69.8
Industry	PMTSP	0.8	-0.2	-14.0	-15.2	-44.6	-44.6
Small and Medium Combustion Plants	PMTSP	25.8	-1.4	-1.8	-23.8	-23.3	-49.7
Product use (Smoke. Firework)	PMTSP	0.0	0.0	-7.9	-7.9	-38.3	-38.3
Transport	PMTSP	-4.5	-4.6	-5.5	-5.5	-5.0	-5.0
Waste manage-ment	PMTSP	42.9	42.9	30.6	30.6	46.1	46.1
Agriculture	SO2	0.0	0.0	-2.3	-2.3	-2.3	-2.3
Energy	SO2	-22.7	-23.7	-39.8	-34.8	-60.6	-56.5
Industry	SO2	-2.2	-6.9	-18.2	-23.4	-55.9	-55.9
Small and Medium	SO2	1.8	-1.9	-7.3	-12.1	-27.8	-35.9

	Changes in Emissions in %						
		2020		2030		2050	
Sector	Pollu-tant	450 ppm	450 ppm_dam	450 ppm	450 ppm_dam	450 ppm	450 ppm_dam
Combustion Plants							
Transport	SO2	-0.6	-0.6	-0.8	-0.8	-3.9	-3.8
Waste management	SO2	113.1	113.1	133.5	133.5	10.8	10.8
Energy	CO	42.9	42.9	30.6	30.6	46.1	46.1
Industry	CO	0.0	0.0	-2.3	-2.3	-2.3	-2.3
Small and Medium Combustion Plants	CO	-22.7	-23.7	-39.8	-34.8	-60.6	-56.5
Transport	CO	-2.2	-6.9	-18.2	-23.4	-55.9	-55.9
Waste management	CO	1.8	-1.9	-7.3	-12.1	-27.8	-35.9

Some examples of the spatial distribution of emissions for the BAU and climate policy scenarios are shown in Figure 2-18 and Figure 2-19. Note the different scales.

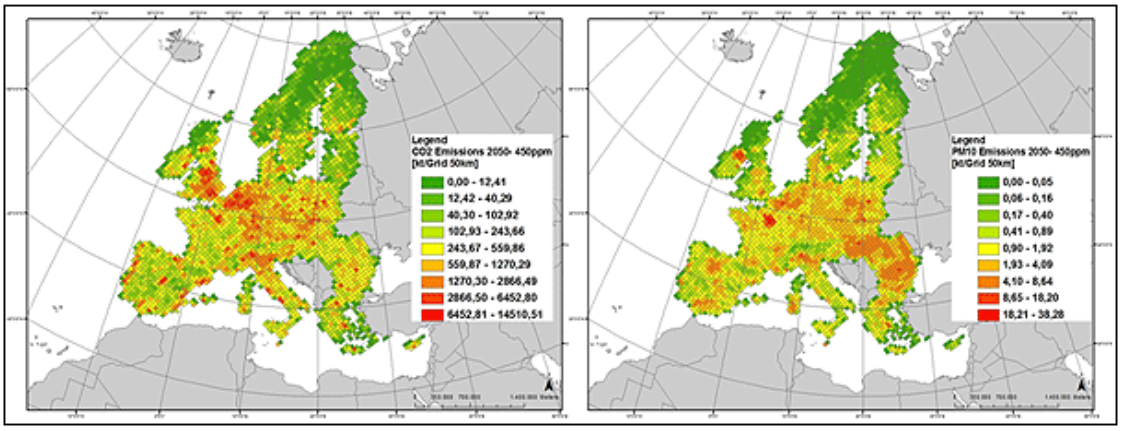

Figure 2-18: Spatial distribution of emissions for CO_2 and PM_{10} in the BAU Scenario 2050.

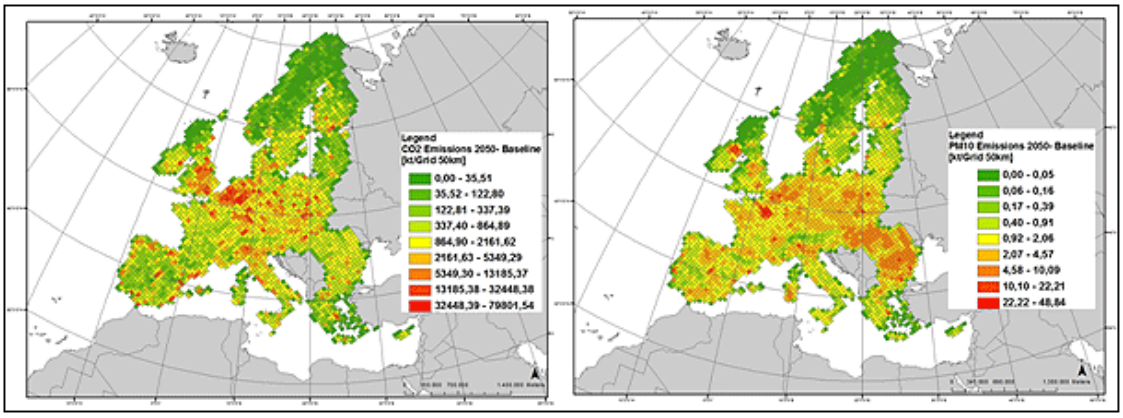

Figure 2-19: Spatial distribution of emissions for CO_2 and PM_{10} in the 450ppm Scenario 2050.

Emissions of POPs to air

The future development of dioxin and PCB emissions from 2010 to 2050 in EU27 as well as Norway and Switzerland is shown in Figure 2-20 and Figure 2-21. The estimation of emissions is based on the results of the FP6 project DROPS (http://drops.nilu.no/). The detailed scenario assumptions are described in the HEIMTSA Deliverables 5.1.1. and 5.1.2. The reduction from 2010 to 2050 is surprisingly high for both scenarios. This is due to the fact that for both scenarios very strict assumptions about the future regulation of POP emissions have been set. This refers especially to industrial processes, especially in the climate policy scenario many industrial processes using coal have been substituted by processes using electricity. For the remaining processes, state of the art abatement technologies have been implemented (for both scenarios). Dioxin emissions from waste incineration are very small compared to emissions from other sources (due to current legislation). PCB emissions from electrical equipment are assumed to be reduced to zero based on current legislation, especially the Aarhus protocol.

The scenarios used here might certainly be seen as underestimating POP emissions, as very far reaching assumptions about the implementation of policies and measures to reduce POP emissions have been made.

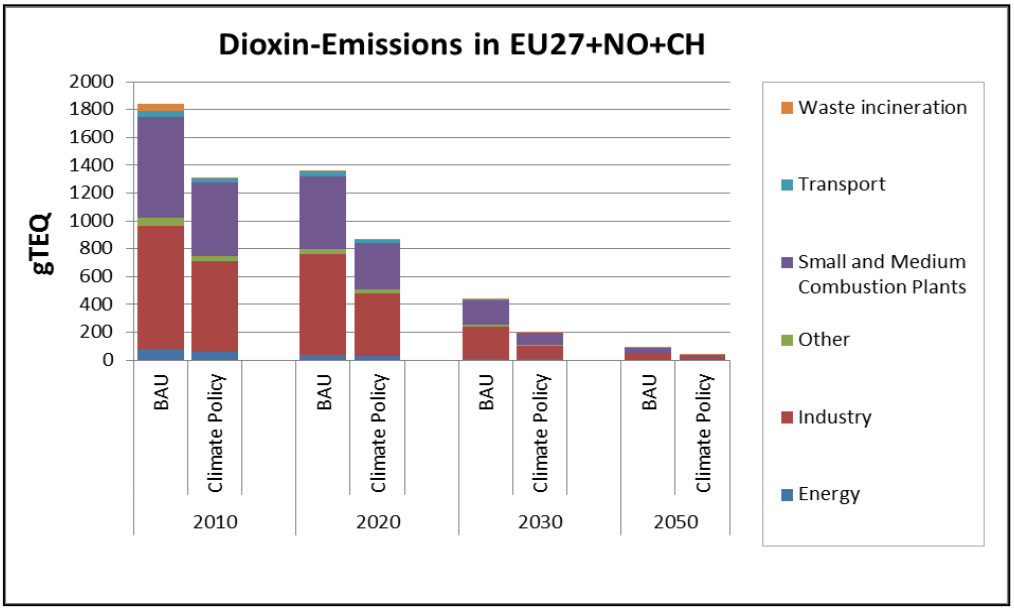

Figure 2-20: Dioxine emissions by source category in EU-27 +CH and NO.

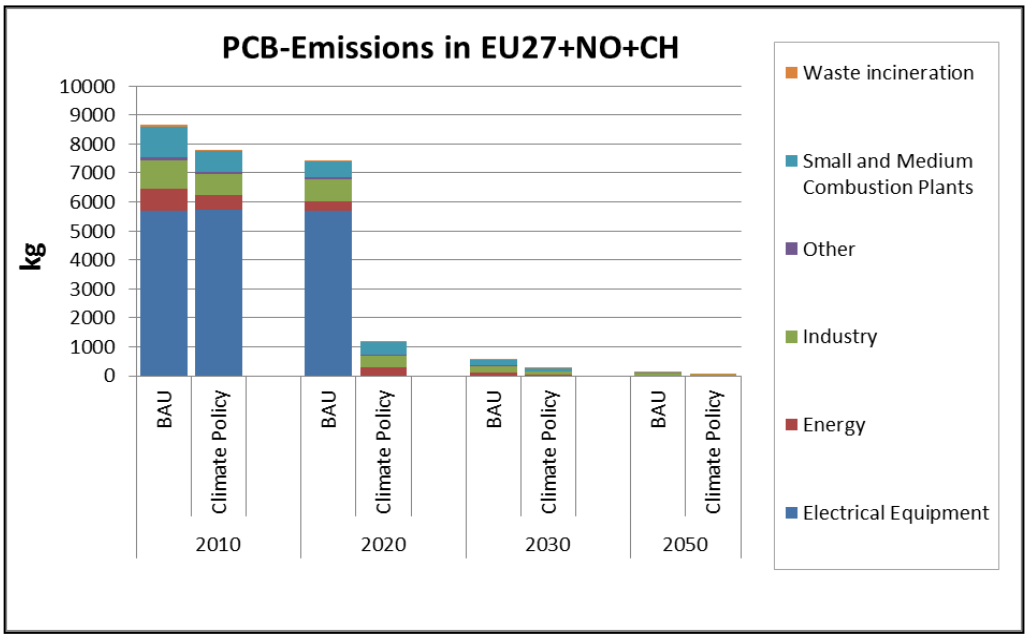

Figure 2-21: PCB emissions by source category in EU-27 +CH and NO.

As well dioxins as PCBs consist of many different species with different features, As the impact assessment described later is made for a specific substances, i.e. congeners 2,3,4,7,8-PeCDF and congener PCB-153, an information about what the share of these congeners on the overall emissions as specified in the Figures above is. These shares are specified in the following table. The shares were taken from Vulykh et al. (2001), Breivik et al. (2002a), Breivik et al. (2002b) and Breivik et al. (2007). They refer to the total dioxin/PCB emissions of the respective sector.

Table 2-6: Share of dioxins/PCB congener on the emissions in the corresponding sector

Sector	Share	Congener	Corresponding Pollutant
Energy Industries	0.48	2,3,4, 7,8 PeCDF	dioxins
Manufacturing Industries and Construction	0.05	2,3,4, 7,8 PeCDF	dioxins
Transport	0.48	2,3,4, 7,8 PeCDF	dioxins
Small Combustion Plants	0.48	2,3,4, 7,8 PeCDF	dioxins
Cement Production	0.05	2,3,4, 7,8 PeCDF	dioxins
Iron and Steel Production	0.64	2,3,4, 7,8 PeCDF	dioxins
Non-Ferrous Industries	0.2	2,3,4, 7,8 PeCDF	dioxins
Waste Incineration	0.08	2,3,4, 7,8 PeCDF	dioxins
Other Sources	0.05	2,3,4, 7,8 PeCDF	dioxins
Energy Industries	0.06	PCB-153	PCB
Manufacturing Industries and Construction	0.06	PCB-153	PCB
Small Combustion Plants	0.06	PCB-153	PCB
Iron and Steel Production	0.06	PCB-153	PCB
Non-Ferrous Industries	0.06	PCB-153	PCB
Electrical Equipment Use	0.06	PCB-153	PCB
Waste Incineration	0.06	PCB-153	PCB
Other Sources	0.06	PCB-153	PCB

Noise emissions

For noise, the emission data were based on activity data (total mileage, see Section 3.3 and Section 2) and emission factors (noise emission per vehiclekilometre), all per vehicle type, road type, country and year.

The total amount of noise emitted by a road segment is determined by two elements (see Figure 2-22):

- the emission levels of single vehicles,
- the number of vehicles that pass per unit time (traffic/vehicle intensity).

Three types of vehicles were distinguished: light vehicles (passenger cars), medium-heavy trucks, and heavy trucks. Noise emission levels of single vehicles were calculated with an engineering traffic noise model. The model is suitable for noise mapping in the framework of the Environmental Noise Directive 2002/49/EC.

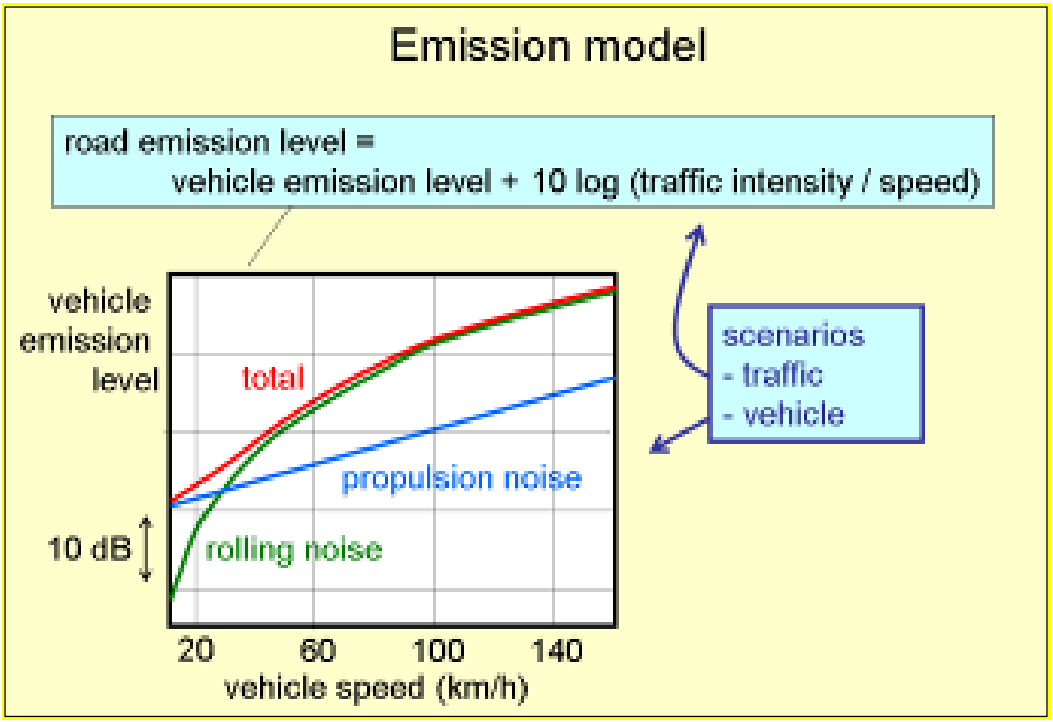

Figure 2-22: Illustration of the noise emission model.

For the BAU scenario, a gradual reduction of the vehicle emission levels was assumed, resulting in a decrease of 2 dB by 2050. For electric vehicles the emission level at 50 km/h was calculated to be 1 dB lower than for conventional vehicles (see Figure 2-23).

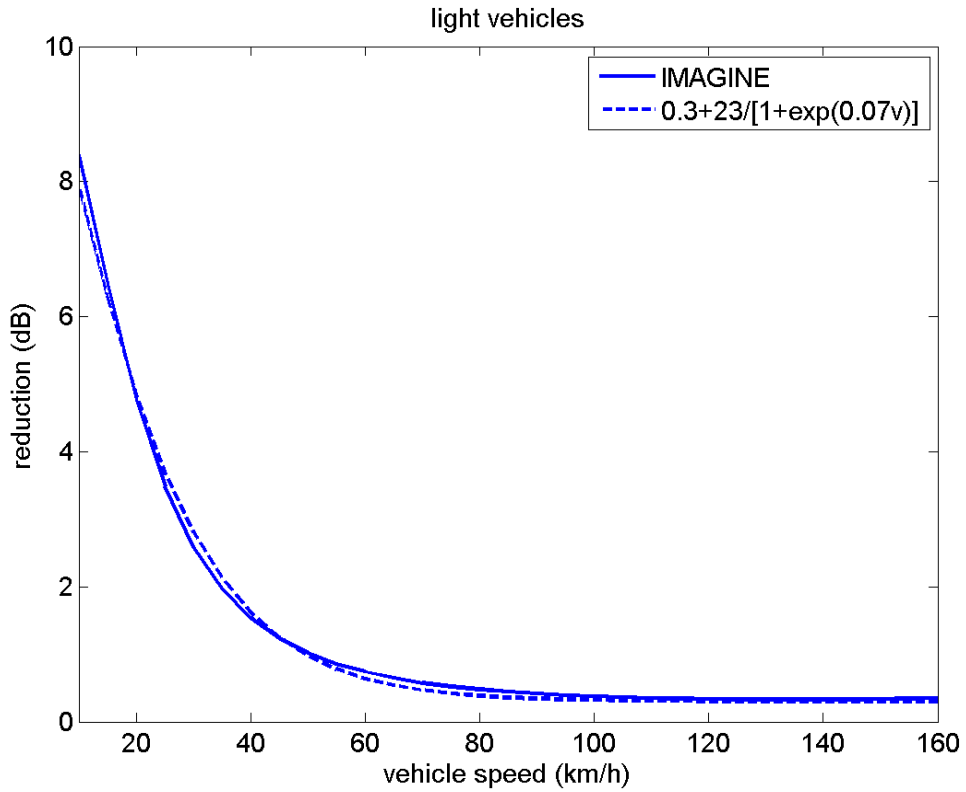

Figure 2-23: Emission reduction for electric vehicles as a function of speed. The solid line is calculated with the Harmonoise/Imagine road vehicle emission model, taking into account separate contributions from tire-road noise and propulsion noise. The dashed line is an exponential fit.

Changes of traffic intensity in the period 2006-2050 were derived from changes in numbers of urban vehicle kilometres in EU countries.

Use of pesticides

Figure 2-24 shows the amount of pesticides that is applied in the REF/BAU scenario per country. The overall amount of pesticides amounts to 59 kt.

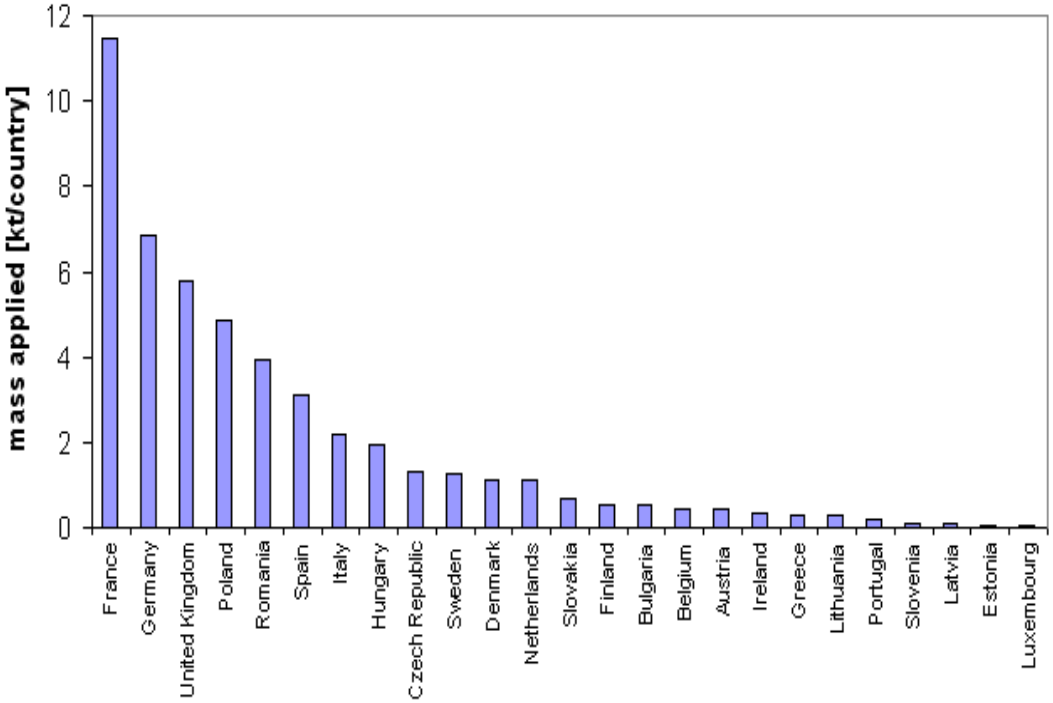

Figure 2-24: amount of pesticides apllied per country in the REF scenario.

Pesticides are composed of many different compounds. As these have different impacts, not only the total sum, but also the composition of the fertilisers has to be known. To estimate this composition for future years is difficult, as due to the Directive 2009/128/EC on establishing a framework for Community action to achieve the sustainable use of pesticides many of the pesticides used in past years are not allowed any more and will thus be replaced by other pesticides. Nevertheless, based on a number of assumptions, a disaggregation per country has been produced stating which pesticides are used in which country.

3 CHANGES OF EMISSIONS DUE TO SINGLE MITIGATION AND ADAPTATION POLICIES

In the results above, the overall changes in emissions due to the combined implementation of many different policies and measures for the mitigation of greenhouse gases have been analysed. This has been done, as the effect of different measures influence each other. For example, the effect of a shift from diesel to electric cars depends on the generation of the electricity. Furthermore it reduces the benefits of shifting from individual to public transport. The results above take all these interdependencies into account.

However, the results above only give insight to the effects of the whole bundle of policies and measures implemented. What can already be seen already is that policies and measures perform quite differently, some lead to large emission reductions, others even increase emissions. Thus it would be beneficial to know how the individual policies and measures perform within the bundle of policies/measures. This would help to change, replace or improve the policies/measures, so that at the end a better bundle of measures/policies canb be identified by the decision maker. Thus we need to assess single policies and measures, however embedded in a strategy where a bundle of measures is implemented. Thus, the influence of single measures on the emissions is assessed in the following sections.

In principal this is done by removing a technology or activity from the climate protection scenario and replacing it with the corresponding technology or activity used in the reference scenario. Then the difference in emissions between the two scenarios is estimated.

The challenge here is obviously to define realistic reference replacements for the technologies and activities used when implementing a climate policy. The assumptions made here are described in the following.

3.1 EFFECT OF AGRICULTURAL MEASURES ON THE EMISSIONS AND OTHER FACTORS RELEVANT TO ENVIRONMENTAL EXPOSURES

3.1.1 Emissions from energy crop production

To estimate NH_3 emissions, the amount of nitrogen (N) fertiliser applied needs to be estimated. The fertiliser application rate was estimated country- and crop specific based on data from FertiStat, FAOSTAT and the World Fertilizer Use Manual (IFA). The N application rate for woody biomass was taken from Schröder et al. (2006). The amount of N applied was split into N from manure and N from mineral fertiliser according to the fractions identified in the GAINS model, developed at the International

Institute for Applied Systems Analysis (IIASA, http://gains.iiasa.ac.at/gains/). Country-specific NH_3 emission factors used were derived from the GAINS model data base considering manure and mineral fertiliser weighted by the expected amount of urea and non-urea fertilisers used.

Concerning emissions of PM_{10} and $PM_{2.5}$, a distinction has been made between the moderate climate in Northern European countries and warmer climates in Southern Europe (Bulgaria, Cyprus, Greece, Hungary, Italy, Malta, Portugal, Romania and Spain). Emission factors for a moderate climate were taken from Hinz & Hoek (2007) and Öttl & Funk (2007). For the warmer climate, emission factors were taken from Cassel et al. (2003) and Yu & Gaffney (2003) (see Table 3-1). For sugar crops, conservation tillage was assumed. For woody crops the emission factors are rather small because conservation tillage was assumed and soil cultivation is carried out only every 3 to 4 years.

Table 3-1: Emission factors for PM_{10} and $PM_{2.5}$ for different crop types and climatic regions

	PM10 emission factors (kg/ha)		**PM2.5 emission factors (kg/ha)**	
Crop category	***Northern Europe***	***Southern Europe***	***Northern Europe***	***Southern Europe***
Oil crops	5.76	10.8	0.71	1.4
Sugar crops	1.86	5.15	0.06	1.14
Starch crops	5.76	10.8	0.71	1.4
Woody crops	0.62	1.72	0.02	0.38

The following figures show the estimated emissions of NH_3, PM_{10}, $PM_{2.5}$ and N_2O resulting from energy crop production based on the energy model runs as described in chapter 2.2.3.

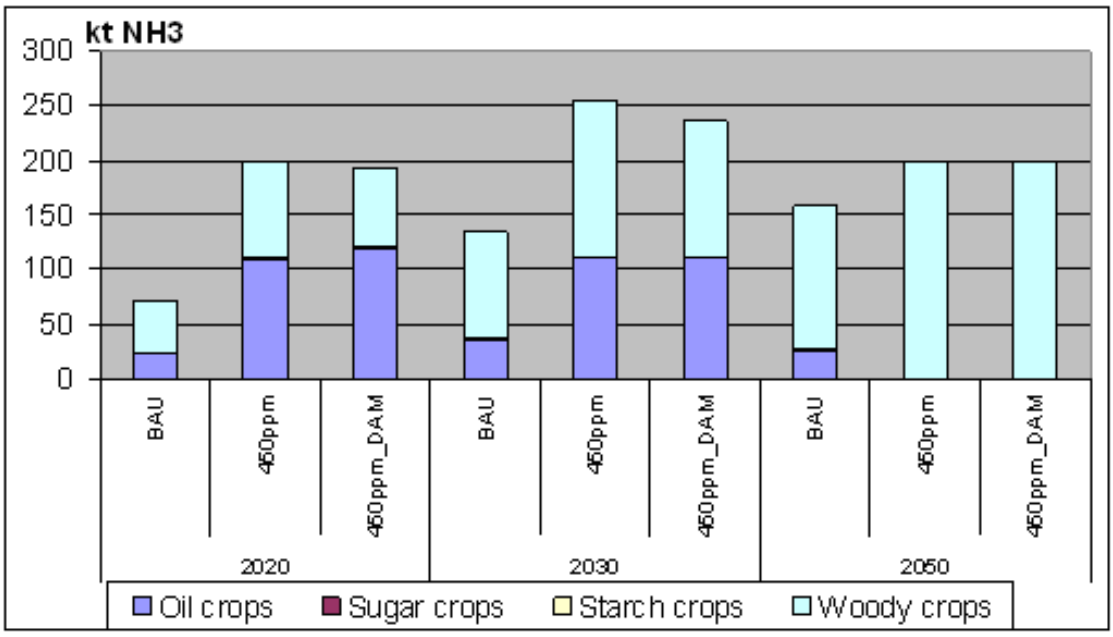

Figure 3-1: NH_3 emissions (kt) from energy crop production in EU-27 +CH and NO

The increase in NH3 emissions (see Figure 3-1) in the climate scenarios (450ppm and 450ppm_DAM) compared to the reference scenario is mainly due to the increase in area. In the year 2050 NH_3 emissions in the climate scenarios are smaller compared to the year 2030 although energy demand and land requirements had increased. This is the case because fertilising intensity is lower for woody biomass than for oil crops.

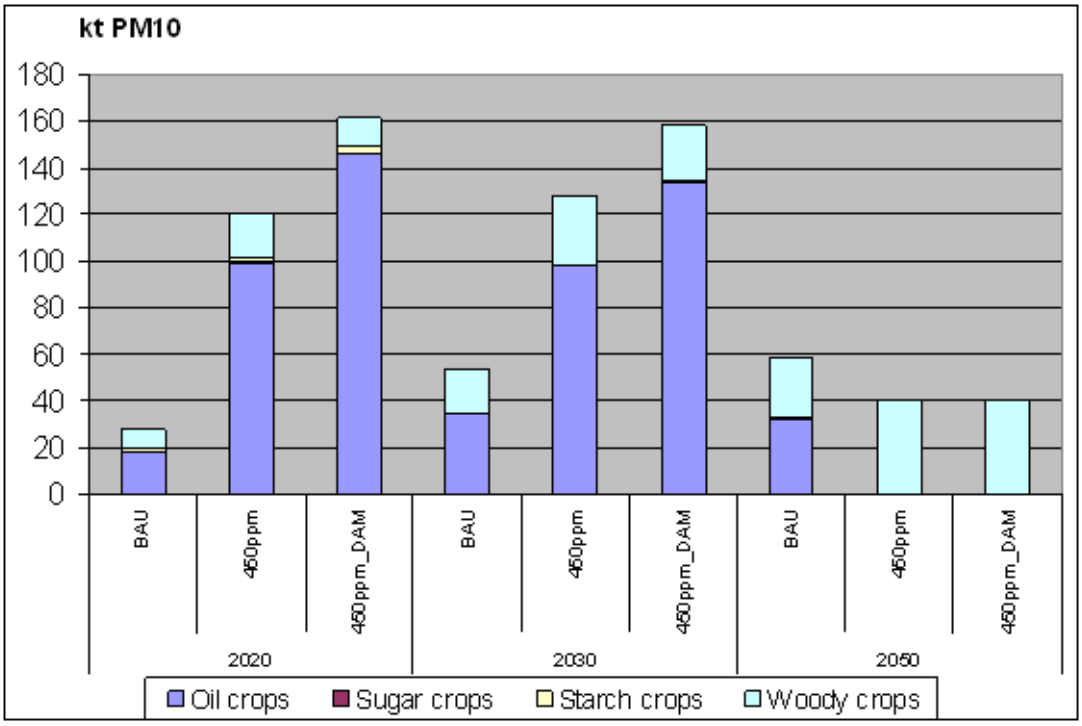

Figure 3-2: PM_{10} emissions (kt) from energy crop production in EU-27 +CH and NO

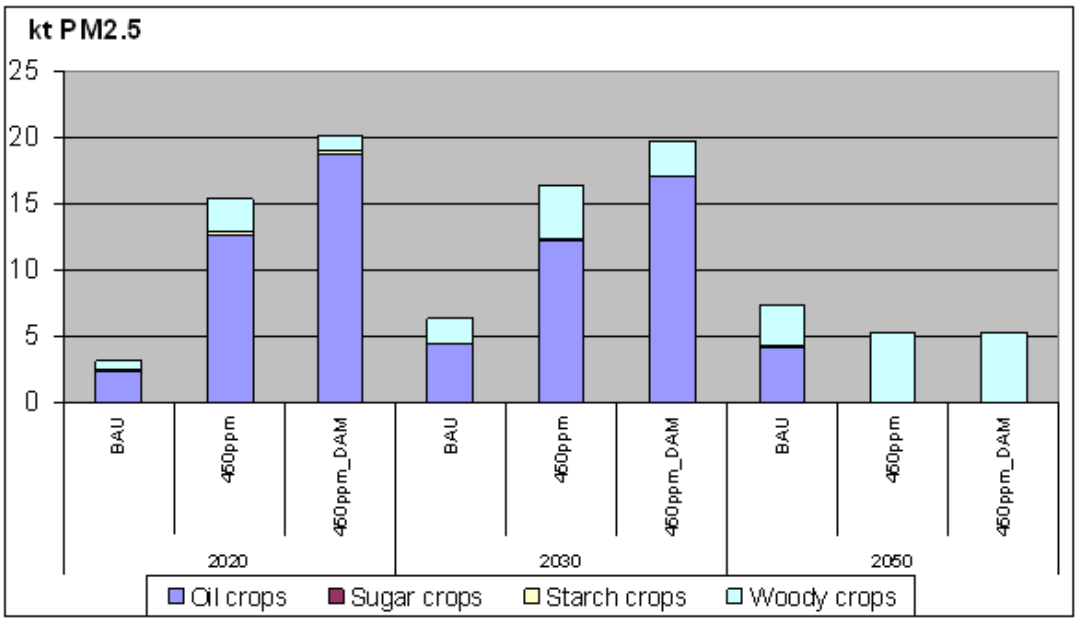

Figure 3-3: $PM_{2.5}$ emissions (kt) from energy crop production in EU-27 +CH and NO

Total PM_{10} and $PM_{2.5}$ (see Figure 3-2 and Figure 3-3) emissions increase in the climate scenarios compared to the reference scenario with emissions from oilseed representing the highest share. This goes back to the general increase in oilseeds area on the one hand; on the other hand oilseeds area considerably increases in Mediterranean countries with dryer climates and higher PM emission rates compared to the moderate climate in Northern Europe. The area for starch crops declines and leads to less PM_{10} emissions. As the area for woody biomass increases significantly, PM10 emissions increase as well. In the year 2050 PM_{10} and $PM_{2.}5$ emissions decrease compared to the years 2020 and 2030 in the climate scenarios. This can be explained by the increase in woody biomass used instead of oil crops and the emission factors for woody biomass are much lower than the emission factors for oil crops.

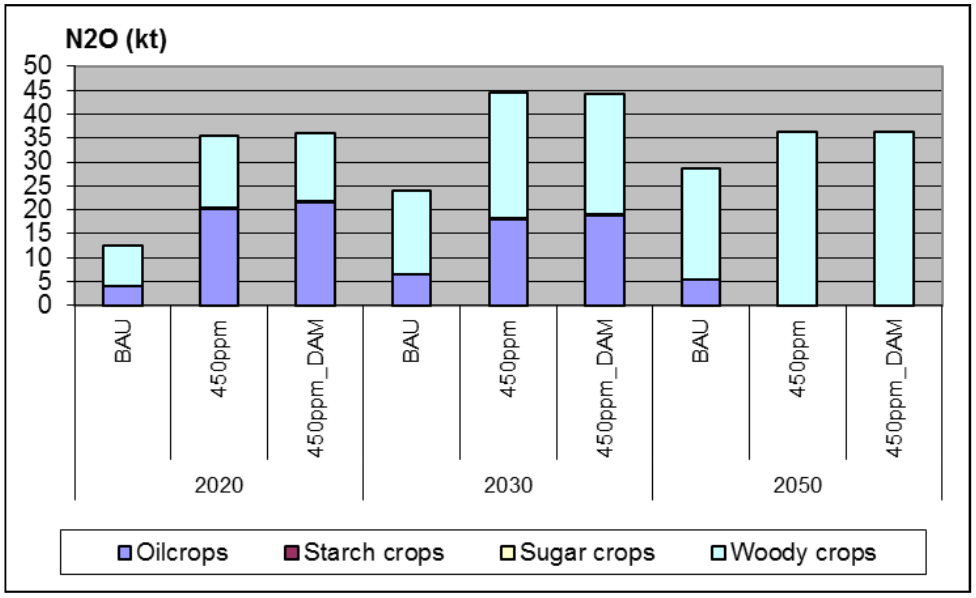

Figure 3-4: N_2O emissions (kt) from energy crop production in EU-27 + CH and NO

3.1.2 Reduced cattle protein consumption in human diets

As an additional measure not included in the climate protection scenario it was investigated, how a change in diet would effect the emissions. The measure is defined as a policy that would bring people to consume 20% less beef and also 20% less dairy products. However it is assumed that instead of meat other animal protein like pork and poultry is consumed.

It was assumed that the number of cattle (i.e. beef and dairy cows and thus the milk yield) would be reduced by 20% in 2020, by 30% in 2030 and by 50% in 2050 compared to the climate protection scenario. The reason for this is that cattle produce large amounts of methane, which can be reduced with this measure. It was also assumed that the amount of protein consumed was kept constant, i.e. the amount of protein reduced via reduced cattle product consumption was to be balanced by an increase in pig and poultry product consumption. The protein content in beef, milk, pork, poultry meat and eggs is shown in Table 3-2. The average protein content of beef and milk served as the base for the protein equivalents of pork, poultry meat and eggs. Starting from protein equivalents, the increased numbers of pigs and poultry were calculated. The historic share of consumption between pork, poultry meat and eggs was kept constant in each country. Animal numbers for “other animals” (sheep, goats, horses and fur animals) were not changed.

Table 3-2: Protein content of animal products.

	Beef	**Milk**	**Pork**	**Poultry**	**Eggs**
kg protein/ kg product	0.22	0.03	0.18	0.20	0.13

Country-specific milk yields per dairy cow were considered based on GAINS data. In the GAINS model database, no information on slaughter weight and number of eggs was given. Therefore for slaughter weights and number of eggs per laying hen and year, average values were assumed. For other poultry including ducks, geese, turkey, the average weight of broilers was assumed. The emission factors for CH_4, NH_3, N_2O, TSP, PM_{10} and $PM_{2.5}$ were also taken from the GAINS model.

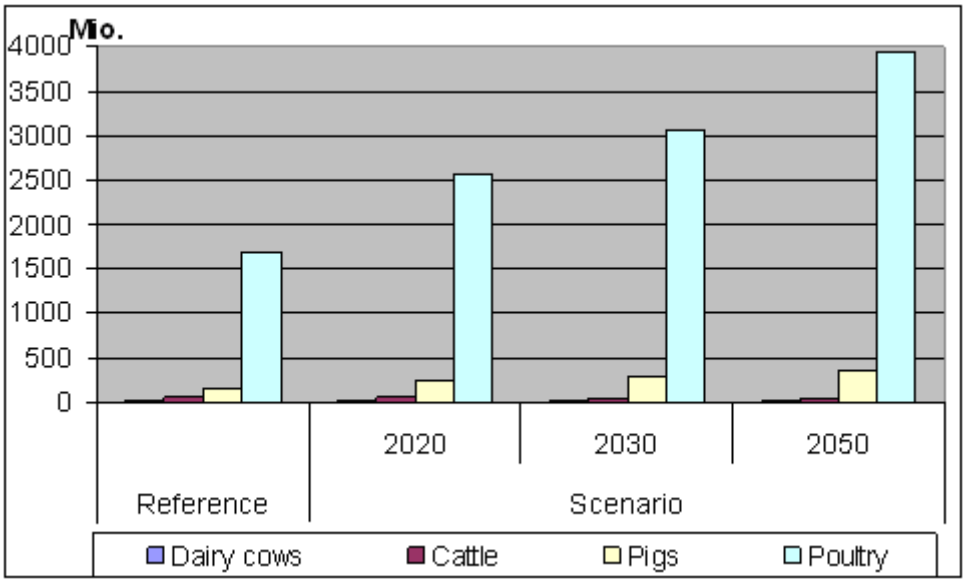

Figure 3-5: Development of animal numbers in the „reduced cattle scenario“ in EU-27+CH,NO.

With this measure, NH3 emissions increase compared to the 450ppm scenario by about 8% in 2020, by about 13% in 2030 and by about 21% in 2050. This is the case as animal numbers for pigs and poultry increase and emission factors are higher for pigs and poultry than for cattle.

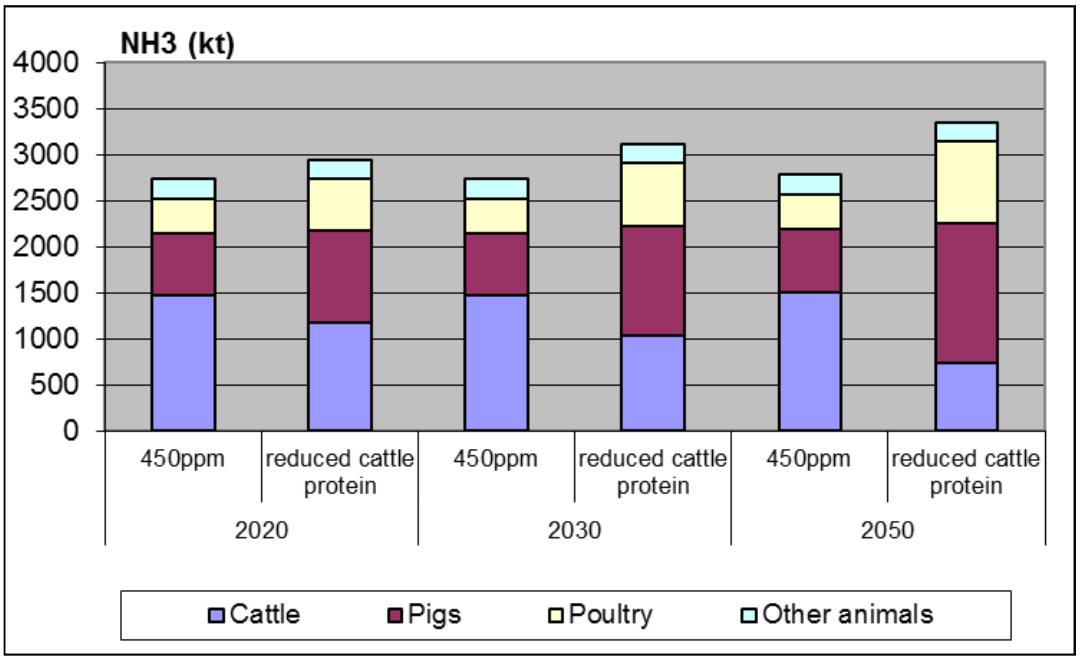

Figure 3-6: NH_3 Emissions from reduced cattle protein consumption in human diets in EU 27+NO+CH

PM_{10} emissions increase by about 39% in 2020, by about 63% in 2030 and by about 104% in 2050. This can be explained on the one hand by the increase in pig and poultry

numbers and by the higher emission factors compared to cattle. The same situation applies to emissions of PM2.5.

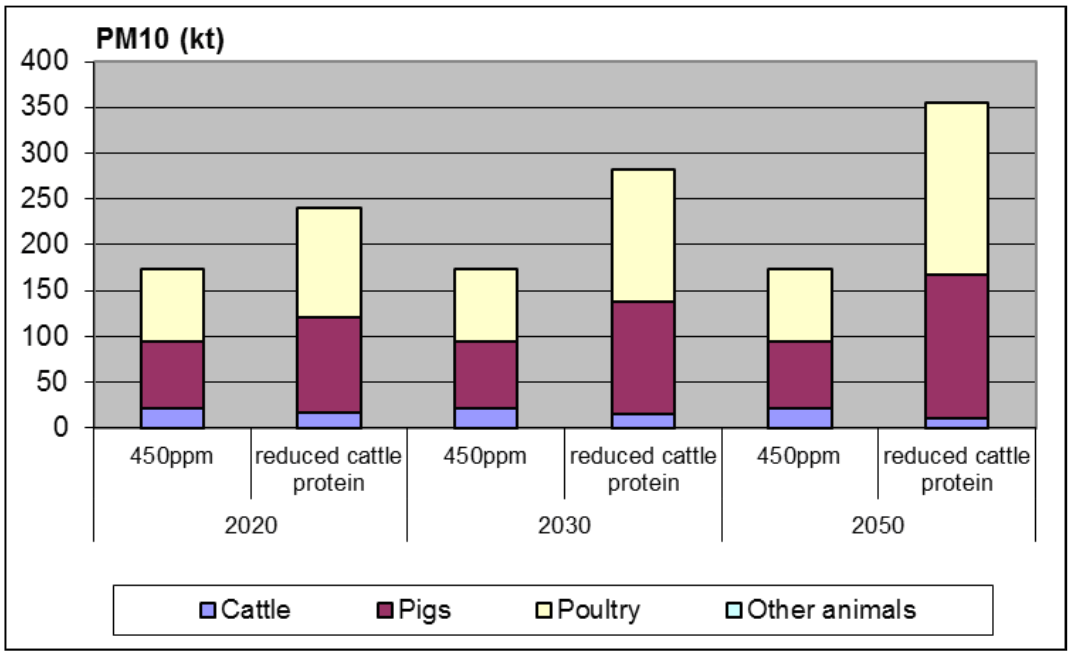

Figure 3-7: PM_{10} Emissions from reduced cattle protein consumption in human diets in EU 27+NO+CH

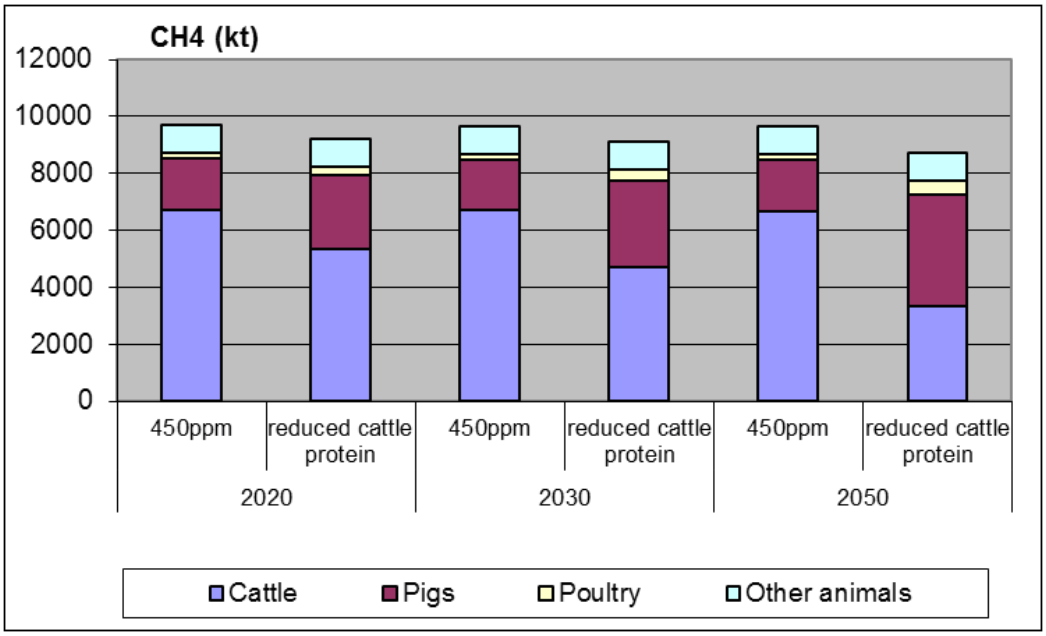

Figure 3-8:CH_4 Emissions from reduced cattle protein consumption in human diets in EU 27+NO+CH

The CH_4 emissions decrease in the 'reduced cattle protein' scenario much less than expected. Of course the emissins from cattle are reduced as assumed, hoever this

reduction is to large part compensated by the increase of methane emissions from pig-keeping.

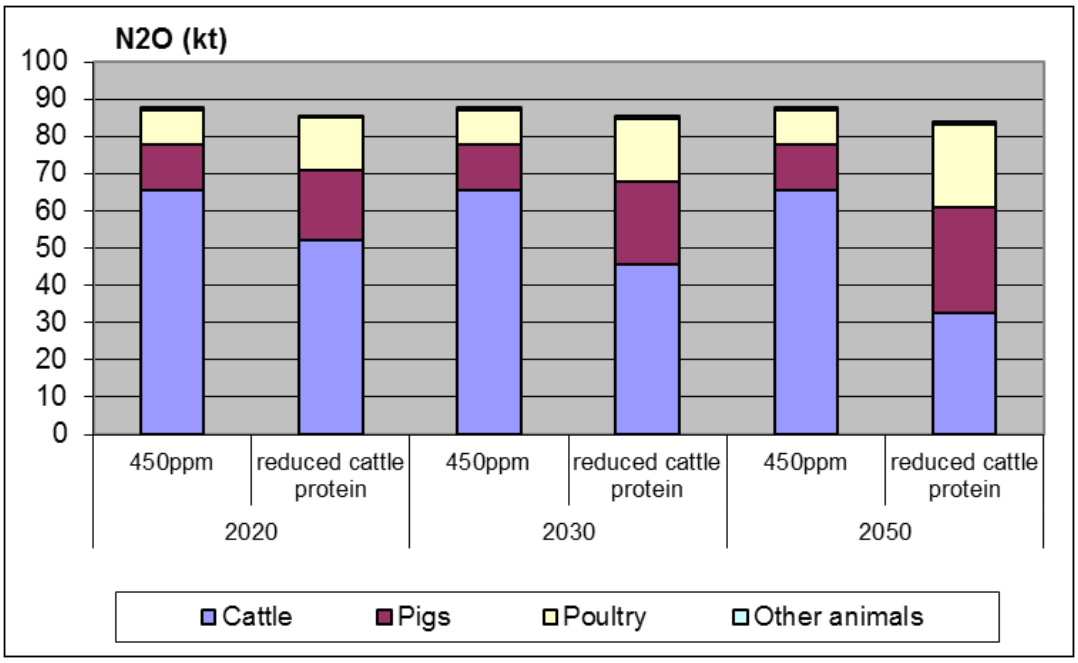

Figure 3-9: N2O Emissions from reduced cattle protein consumption in human diets in EU 27+NO+CH

Overall N_2O emissions from manure show a slight decrease in the 'reduced cattle' scenario compared to the climate (450 ppm) scenario. Figure 3-9 shows that N_2O emissions from cattle and poultry are reduced while N_2O emissions from pigs increase.

3.2 ENERGY POLICIES

3.2.1 Objectives

The main objective of the assessment of scenarios for the energy sector is to quantify the changes of emissions resulting from the additional use of renewable energy sources in electricity and heat production. The analysis divides the assessment of the impacts into the operational phase of electricity and heat production and the other phases of the life cycle, i.e. construction, maintenance, fuel supply, deconstruction and waste disposal.

3.2.1.1 General approach for energy scenarios

This analysis of the impacts on emissions for a single policy was done by assuming that the policy would have have been implemented in the Climate Protection Scenario

scenario. Based on this assumption the amount of electricity and heat would instead have to be produced by other sources as used in the reference scenario.

In principle, a starting point for defining the substitutes is taken from (UBA, 2009), which proposes the following substitution factors:

Table 3-3: Substitution factors for electricity production by renewables.

Renewable electricity	Substitution factors			
	Oil	Gas	Coal	Lignite
Hydro power and geothermal	0%	25%	45%	30%
Wind	2%	24%	63%	11%
Photovoltaic	0%	50%	50%	0%
Thermal	0%	0%	50%	50%
Solid biomass and renewable waste	0%	25%	59%	16%
Liquid biomass and biogas	1%	32%	62%	5%

Source: UBA (2009)

Table 3-4: Substitution factors for heat production by renewables.

Renewable heat	Substitution factors				
	Oil	Gas	Coal	Lignite	Other
Solarthermal	45%	51%	0%	0%	5%
Heat pumps	45%	44%	1%	2%	8%
Solid Biomass (Industry)	17%	55%	10%	12%	7%

Source: UBA (2009)

Electricity

This means, that e.g. electricity produced with wind energy is replaced by electricity from coal (63%), lignite (11%), natural gas (24 %) and oil (2%) fired power plants. However in a next step, these factors, that are representative for Germany, have to be adjusted to other countries. If a country has no domestic lignite reserves, lignite is not used as substitute. Thus depending on the available technologies in the different countries in the reference year, the substitution factors are adjusted.

Secondly, emissions depend not only on the fuel, but also on the technology. E.g. domestic oil heating might mean a low heating boiler or a condensing boiler a.s.o. So for each fuel the technologies used have to be defined And of course the technology are different for the different years, as we assume technological progress. Fortunately the definition and characterisation of future technologies in the energy sector has alredy been made within the EC FP6 projects NEEDS and CASES, whose results are used here.

The result of calculating the changes in emissions for single energy measures is shown in Table 3-5. For each technology analysed, the difference in application between the 450 ppm and the REF/BAU scenario is determined and then the absolute emission

difference resulting from substituting this amount of the technology by alternatives is estimated. Positive figures mean that using the technology reduces emissions, negative figures indicate an increase. What can be seen is that the GHG reduction of wind offshore, PV and solid biomass is high, wind onshore, solar thermal and hydro power have a lower additional potential, as they are already used to a large extent in the reference scenario. The reduction of emissions is often lower in 2050 as in 2020/2030, as the conventional technologies, that replace renewable energies, also are improving their emission factors due to technical progress.

Table 3-5: Resulting total emission changes in EU-27 for electricity generation in 2020 [in kt].

2020	CH_4	N_2O	CO_2	NH_3	NMVOC	NO_X	PM_{10}	$PM_{2.5}$	SO_2
Solid biomass/renewable waste	39.6	-1.8	15,819.0	-1.7	-1.5	-24.8	-0.3	-0.8	4.5
Biogas/biofuels	9.8	0.1	1,697.7	0.0	0.0	-1.3	-1.0	-0.7	-8.3
Hydro power	3.6	0.1	2,179.4	0.0	0.2	1.8	0.0	0.0	1.7
Wind onshore	13.0	0.2	4,533.4	0.1	0.7	4.4	0.3	0.1	3.9
Wind offshore	262.8	4.0	103,809.5	2.3	13.3	98.5	5.5	1.3	87.3
Solar PV	52.8	0.7	20,495.2	0.2	3.4	16.3	0.6	0.2	13.4
Solar Thermal	4.8	0.1	2,398.6	0.0	0.1	1.8	0.1	0.0	1.6

The electricity production using solid biomass and biogas leads to additional emissions, as electricity production in large power plants with effective filters is replaced by electricity generation in smaller stationary plants with less effective air pollution control system or in the case of biogas with combustion engines.

Heat supply

For residential heat supply, the measure ‘more use of wood for residential heating’ has been analysed. Additional wood is burnt especially in new state of the art furnaces, mostly using wood pellets. The following table shows the respective emissions, if wood or alternatively oil or gas would be used to provide the heat.

Wood causes much larger particle and NMVOC emissions.

Table 3-6: Resulting total emissions due to additional wood burning in 2020 in EU-27 [in kt].

kt	CO_2	CH_4	N_2O	CO_{2eq}	NO_x	SO_2	NMVOC	Particles (80%PM2.5)	NH_3
Wood operation	0	21	N/A	525	15	1.6	33	22	N/A

Wood LCA	N/A	N/A	0.469	140	N/A	N/A	N/A	0.091	4,6
If the same amount of heat would be supplied by natural gas firings, the following emissions would occur:									
Gas operation	11,83	0.5	N/A	11843	4.7	0.1	0.14	0.01	N/A
Gas LCA	1,58	33	0.024	2415	4.9	4.8	3.4	0.146	0.005
If the same amount of heat would be supplied by oil firings, the following emissions would occur:									
Oil Operation	15,55	0.01	N/A	15549	8.9	12.5	0.36	0.184	N/A
Oil LCA	2316	9.5	0.04	2565	9.0	21.9	6	0.86	0.04

3.3 TRANSPORT POLICIES

The Mega Case Study uses the following measures for road transportation to achieve the Climate policy scenario.

- Introduction of the threshold levels of EURO 5 and 6 for passenger cars and light duty vehicles
- Speed limit on motorways
- Increased fuel taxes
- Enhanced use of bicycles in cities
- Economic driving
- City toll
- Use of tyre pressure monitoring systems
- Use of gear shift indicators
- Passenger car tolls
- Improved traffic flow (“Green Wave”)
- Increased use of electric cars

3.4 INDOOR AIR POLICIES

For indoor air policies two measures are investigated.

- Insulation of buildings
- Biomass burning for space heating in homes

Insulation of houses leads to two different effects: Less energy demand for heating purposes influences the outdoor air quality; on the other hand the changes in the air exchange rate and penetration factors influences the indoor air quality.

Biomass burning in the residential sector is considered to be a CO_2-neutral process of energy supply (climate mitigation measure). The amount of biomass burned was modelled with the energy model TIMES during the scenario development (see Section 2.2.3).

The scenario definition for the indoor measures can be found in

Table 3-7.

Table 3-7: Scenario definition for the indoor measures.

Description	Name	Definition
Effect of insulation of houses(with paying attention to a minimum hygienic air exchange rate)	„2050 Insulation“	Enhanced insulation with ensuring a minimum hygienic air exchange rate
Effect of insulation of houses without paying attention to a minimum hygienic air exchange rate	„2050 Renovation“	Have of the insulated dwellings, that are insulated as in scenario renovation, are renovated dwellings w/o heat ventilation and air conditioning appliance.
Effect of biomass burning	“2050 Biomass”	Biomass is used Defined as “BAU2050” with biomass like “Policy2050”

The following house types were defined (“old” different air exchange rate and per country; “new” having the same air exchange rate and infiltration factor EU-wide):

- “Old”: penetration and infiltration as status quo (in each country).
- “New or renovated with forced ventilation”: tighter houses; minimum hygienic air exchange rate ensured.
- “Renovated”: tighter houses; very low air exchange rate.

The amount of insulated, renovated and old houses can be found as en EU-average in Table 3-8. The figures are different for each country, however.

Table 3-8: Amount of insulated, renovated and old houses (EU-average).

	New or renovated with forced ventilation	**Renovated without forced ventilation**	**Old**
2050 BAU	58 %		42 %
2050 Policy	81 %		19 %
2050 Insulation	81 %		19 %
2050 Renovation	40.5 %	40.5 %	19 %

The indoor air pollutants covered are $PM_{2.5}$, dampness, radon and ETS originated VOC's (4-(N-nitrosomethylamino)-1-(3-pyridyl)-1-butanone (NNK), benzene and formaldehyde).

3.5 URBAN DEVELOPMENT POLICIES

The objective was to evaluate current and future mortality impacts caused by summertime (April-September) ambient heat exposure in large cities (i.e. densely populated metropolitan areas) in Europe, and to assess the potential for reducing these impacts by implementing different types of policies aimed at mitigating urban heat island effect (UHI). UHI is a phenomenon whereby urban regions experience warmer temperatures than their surrounding rural areas. It is caused by the replacement of open ground and vegetation by buildings and roads, and therefore, permeable and moist surfaces with impermeable and dry ones. UHI can be mitigated by means of, for example, increasing urban vegetation and surface albedo. Trees and vegetation help to cool urban climates by increasing shading and evapotranspiration, whereas increasing urban albedo increases the amount of solar radiation reflected back to the atmosphere and, therefore, decreases the amount of energy absorbed into the city structures. These measures were selected, because they are feasible in most urban settings and likely to be effective in reducing the UHI effect. The specific UHI mitigation policy scenarios evaluated were:

Vegetation: urban vegetation is increased by planting trees on open grassy areas and street curbsides. Open space planting is applied to 10.8 % and curbside planting to 6.7 % of the total surface area of each city. Trees are assumed to be deciduous and mature.

Albedo: albedo of the city is increased by replacing impervious roof and street surfaces (sidewalks and roadways) by light coloured surfaces. From the total surface area of each city, 13.6 % is converted from impervious roof surface to light coloured roof surface and 34.4 % from impervious street surface to light coloured street surface. For

light roof surface, albedo is assumed to increase from 0.15 to 0.5 and for light street level surfaces from 0.15 to 0.2.

Veg+alb: both vegetation and albedo are increased as described above.

In the policy scenarios, characteristics of the urban environment and human behaviour were assumed to be the same as they are currently except for the policy specific measures. All large European cities were considered to undergo similar level of mitigation measures, and the impact of these measures (i.e. the absolute decrease in the city-specific daily temperatures) was assumed to be the same.

The percentages of total city surface area that can be converted from one surface cover type to another in large European cities were based on a modelling study on urban heat island mitigation in New York City (NYSERDA 2006). It is unknown how well these estimates are suited for European urban settings. In reality, European cities probably have quite a wide range in terms of city structure, land use and potential for implementing different mitigation measures. However, in the lack of better knowledge, the average estimates provided for the New York Metropolitan Region are considered to be reasonable for European level assessment.

Impact of policies on heat exposure

The impact of the alternative policies on heat exposure was modelled based on the percentage of a given surface cover type that could be converted to another in a city and the change in near-surface air temperatures caused by these changes per unit area. The city-wide cooling effect then depends on the number of units that is redeveloped and the type of redevelopment. Estimates for both available surface areas that could be converted from one surface cover type to another in large European cities and the unit cooling effects of these changes (Table 3-9) were based on a modelling study on urban heat island mitigation in New York City (NYSERDA 2006). In this study, they used a regional climate model MM5 in combination with observed meteorological, satellite, and GIS data to determine the potential impacts of mitigation strategies on the surface air temperature (2 m height) over space and time in the New York Metropolitan Region.

Table 3-9: Modelled absolute differences in near-surface air temperature (°C, daily average or daily maximum temperature) between different surface cover types in New York City. The difference represents potential for cooling by replacing a unit of one surface cover type with a unit of another.

	Surface cover change		
Temperature	**Grass to trees**	**Impervious surface to trees**	**Impervious surface to light surface**
Average	-0.6	-1.9	-1.1
Maximum	-1.7	-4.8	-2.6

It is unknown how well the NYSERDA estimates for the cooling effect of different measures translate to the widely varying urban settings and climate types in European cities. However, in the lack of better knowledge, the NYSERDA estimates are considered to provide reasonable average estimates for European level assessment in terms of the possible scale of temperature reductions and relative effectiveness of different measures.

Average city-wide reductions in the daily surface air temperature in the evaluated UHI mitigation policy scenarios are presented in Table 3-10. The NYSERDA estimates on the unit cooling effects of different measures indicate that replacing impervious street cover with trees would be the most efficient measure in reducing urban heat island (UHI) effect in terms of the amount of area that would have to be modified to reach a given temperature decrease. However, due to the higher share of area that could be converted to high reflectance surface than vegetation, albedo policy would result in larger absolute reduction in temperature than vegetation policy. Implementation of both policies would, naturally, have the highest impact. The temperature changes were modelled based on the unit decrease in the average daily temperature because it was assumed to better reflect the impact on overall daily heat exposure and mortality effects caused by it.

Table 3-10: The modelled reductions in average city-wide near-surface air temperature in different UHI mitigation policy scenarios.

UHI mitigation policy	**Change in temperature (ºC)**
Vegetation	-0.2
Albedo	-0.5
Veg+alb	-0.7

4 ENVIRONMENTAL FATE MODELLING AND EXPOSURE ASSESSMENT

4.1 INPUT DATA FOR FATE AND EXPOSURE ASSESSMENT

4.1.1 Meteorological Data

Meteorological data is one of the main inputs of any dispersion model as they enable to describe the physical and chemical processes involved in the fate and transport of particles in their journey through the air. As the time frame addressed within the CCS spans over four decades, the inclusion of changes in the future climate due to anthropogenic activities was recognized. For this purpose, meteorological data for the years 2020, 2030 and 2050 provided by the Regional Climate Model (REMO) were implemented in the air dispersion simulations. The REMO (Regional Model) was developed jointly by DKRZ (German High Performance Computing Centre for Climate- and Earth System Research), DWD (German Meteorological Service), and GKSS (Research Centre in Geesthach) at the MPI (Max Planck Institute for Meteorology). REMO is a three dimensional hydrostatic atmospheric circulation model, which solves the discretisation primitive equations of the atmospheric motion (Jacob and Podzun 1997).

IPCC scenarios and their influence on future meteorology

Changes in future meteorological conditions due to anthropogenic activities are taken into account using the scenarios developed by the Intergovernmental Panel on Climate Change (IPCC). The modelling exercises of the IPCC carried out in the year 2000 resulted in four scenarios (A1, B1, A2 and B2) and their scenario family (sub-scenarios). The scenarios consist of different parts: One part is composed by the socio-economic scenarios (e.g. population prospects, economic development); the other part is comprised by the emission scenarios, which consider Greenhouse Gases (e.g. Carbon dioxide emissions, Methane).

Within the framework of the CCS, the scenarios A1B and B1 were chosen to represent the climate expected for the two scenarios REF/BAU and climate protection/450ppm (

Table 4-1).

Table 4-1: Overview over considered SRES scenarios (Nakicenovic et al. 2000).

Scenario	**Main assumptions**
A1B, Used for REF/BAU scenario	Very rapid economic growth Global population peaks in mid-century declines thereafter Rapid introduction of new and more efficient technologies Convergence among regions Capacity building Increased cultural and social interactions Reduction in regional differences in per capita income Balance across all sources of energy
B1, Used for Climate protection/ 450ppm scenario	Population as in A1B (global population peaks in mid-century declines thereafter) Rapid changes in economic structures toward a service and information economy Reductions in material intensity Introduction of clean and resource-efficient technologies Emphasis on global solutions to economic, social and environmental sustainability with improved equity No additional climate initiatives

4.1.2 Population Data

Population density and composition are both highly variable, often over short distances. Substantial changes in population can also occur over periods of a few years not only as a result of natural changes of birth and death but also through migration and urban development.

Obtaining appropriate population data at a suitable spatial and temporal resolution is an important consideration to many risk assessments, and in particular for this case study. Here, where we investigate health impacts under different scenarios at years 2020, 2030 and 2050, estimates of population in future were of upmost importance. As exposures are closely linked to location, spatially resolved data for some components of study (e.g. agriculture) were also needed to reflect local variations in environmental conditions. Additionally, information was needed not only as totals for the whole population, but also for specific population groups defined in terms of age and sex.

To meet the needs of this assessment, spatial and temporal population modelling was required to generate a 50x50km^2 European population data set, to be compatible with the emissions estimates for the EMEP[3] grid, cross-stratified by area, year, and

[3] http://www.eea.europa.eu/data-and-maps/data/emep-grids-reprojected-by-eea

population group. For the agricultural component of the case study, a further stratification was required to distinguish between urban and rural subgroups.

Modelling Approach[4]

This population data set was prepared for the INTARESE and HEIMTSA projects. It includes population data on the EMEP 50 km x 50 km grid for the years 2000, 2010, 2020, 2030 and 2050. The data is stratified by 5 year age bands and by gender.

Data were derived by making use of different data sources: UN data, CIESIN / SEDAC Gridded World Population and national census data.

A) Census data are available on LAU[6] level 2 for the year 2001. They are stratified by gender and age and used as basis data set for 2000/2001. They give spatial information as well as information on age groups and gender. However, they do not give information about the development in the future. Only data for 23 countries are available. BG, CY, LV, RO, CH, NO and IS are missing.

B) UN data[5] are available by country for the years 1950 to 2050 stratified by gender and 5-year age groups. They were used for filling of information gaps on country totals and gender and age stratification for those countries for which no LAU census data was available. Furthermore, they are used for deriving growth rates of population subgroups for future years. If for some reason not gridded data are needed but country totals, UN data can be taken. They give information on a country level. No further spatial information is available.

C) GWP[6] (Gridded World Population) data are available from CIESIN/SEDAC. They provide gridded data on several resolutions for several regions. Interesting for the INTARESE/HEITMSA study were the data for 2000 and 2010 for a resolution of ½°. GWP data are used for filling of spatial information gaps for those countries for which no LAU census data is available. They furthermore give some feeling for spatial shift of population from 2000 to 2010. No information for the years 2020, 2030 and 2050 is available. No stratification regarding gender or age groups is available.

D) EUROSTAT[7] data and projections are available for all required years. EUROSTAT data, including projections to the future, are used as one basic assumption for the energy modelling, which in turn is an important basis for emission scenario modelling. No stratification regarding gender or age groups is available for future years.

---

4 http://www.integrated-assessment.eu/resource_centre/eu_age_and_gender_stratified_population_data_emep_grid_2010_2020_2030_and_2050

5 http://esa.un.org/unpp/index.asp?panel=2%20

6 http://sedac.ciesin.columbia.edu/gpw/global.jsp

7 http://epp.eurostat.ec.europa.eu/tgm/table.do?tab=table&init=1&language=de&pcode=tps00002&plugin=1%20

Comparisons indicate that EUROSTAT data, including projections, does not differ much from UN data, including projections. Thus, consistency is preserved.

Steps to generate the data sets

Step 1a: Processing LAU census data to fit it to the Emep grid cell

- Filling gaps in the available data sets (e.g. for some countries for some LAU regions only the total number of persons was available, not split by age and gender)
- Filling missing age groups (e.g. for some countries no 5-year age bands were given but e.g. 15-year bands: they were further split up using age group fractions derived from the UN data)
- Intersection with Emep 50 km x 50 km grid
- Summing up per grid cell, age and gender

Step 1b: Filling gaps: Filling data for those countries for which no LAU census data was available

- Using UN data for country totals
- Splitting into subgroups on a country level using UN data (subgroup fractions)
- Area-weigh total population using GWP data (using percentages of grid cells compared to the total GWP population)

UN data are used for country totals as country totals for all sources are relatively small, so there is no reason against using them. Furthermore, UN data country totals and growth rates are used for projections to the future (see step 2). Thus, consistency is preserved.

Step 1c: Summing up data from both sources

- Summing up values for each grid cell from both sources

Step 2: Projections to the future

- Growth rates from UN data (for each subgroup separately) are taken to project the basic data set to the future.
- **Result:** Data set including for each grid cell the number of persons of each subgroup in the years 2000, 2010, 2020, 2030 and 2050. For 2020, 2030 and 2050, medium, high and low estimates are available.

Growth rates from UN data are taken because i) UN data are taken whenever possible for consistency reasons, ii) UN data have several growth rates (middle, high, low) which gives some kind of uncertainty bounds, and iii) EUROSTAT growth rates fit quite well with the UN data growth rates so there is no inconsistency here.

4.1.3 Other Input Data

Indoor air related data

The LAMA modelling tool to estimate exposure to air pollutants calculates the exposure by using a microenvironmental approach incorporating an outdoor air model, time activity patterns and an indoor air model (exposure model to $PM_{2.5}$; see Section 4.3.1 and HEIMTSA Deliverable D2.1.5/7 “Exposure methods in the Common Case Study”). The main input data are the parameters for the indoor air model, see Table 4-2. These parameters, mainly derived from measurements performed in the US PTEAM (Özkaynak et al, 1996) and the EXPOLIS (Jantunen et al. 1998) studies, describe the relationship between the indoor concentration of a pollutant in a microenvironment with the outdoor concentration, i.e. building properties, indoor source strengths, additional traffic increment and prevalence of individual habits leading to additional indoor sources.

Table 4-2: Parameters used for the LAMA exposure model.

Parameter	micro-environment	Unit	Distribution	Description
a	home/work	h^{-1}	lognormal	air exchange rate for homes/ workplaces
v	home/work	m^3	lognormal	room volume for homes / workplaces
p	home/work	fraction	lognormal/ uniform	penetration factor for homes / workplaces
k	home/work	h^{-1}	lognormal	decay rate for homes / workplaces
e	travel	ratio	lognormal	urban traffic enrichment factor ($c_{transport}/c_{background}$)
s_cig	home	ug cig^{-1}	lognormal	source strength for ETS
s_bio	home	ug h^{-1}	lognormal	source strength for biomass burning
s_bgr	home	ug h^{-1}	lognormal	source strength for background emissions
n_cig	home	count	lognormal	number of smoked cigarettes per day
f_bio	-	fraction	none	fraction of the population exposed to biomass burning
f_cig	-	fraction	none	fraction of the population exposed to cigarette smoking

To account for uncertainties parameters are represented by distributions taken from the measurements. Parameters from EXPOLIS were estimated for EU-30 by assigning them to 4 geographical regions (Southern - Athens, Central - Prague, Northwestern – Basel, Northern - Helsinki) and extrapolated to the countries within these regions. Parameters from PTEAM (k, p) are constant over Europe.

The parameter values are dependent on the policy scenarios, and each parameter is connected to a certain scenario. Some of the policy scenarios are related to buildings, thus the filtration rate which is dependent on *p*, *a* and *k*, is of importance. Different policy measures call for a categorisation of building types. “Old dwellings” have different values for “a” per country as used in the basic input data set for LAMA (p and k are the same for all countries, again, as used in the basic input data set for LAMA). “New dwellings” and “renovated dwellings w/o HVAC (heat, ventilation and air conditioning appliances)” are assumed to fulfil the same European standards in each country, thus p, a and k are the same for all countries.

The difference between “new” and “renovated” buildings is that “new (and properly renovated dwellings)” include a minimum hygienic air exchange rate versus “renovated dwellings” that are made air tighter but where no attention is paid to ensure a minimum air exchange rate. “p” and “k” were found to be connected to “a” and were, thus, adapted as well.

The total “p”, “a” and “k” for the countries in the scenarios was calculated by Monte Carlo analysis from the “p”, “a” and “k” values of the different dwelling types times the fraction of the different dwelling types. The fraction of insulated dwellings was taken from the energy model assumptions (see Section 2.2.3). It was distinguished between an “insulation” scenario where all insulated dwellings are “new”, and a “renovation” scenario where half of the insulated dwellings are “new” and half are “renovated” (see Section 3.4).

The data used for time use in LAMA is the Multinational Time Use Survey (MTUS) data (see http://www.timeuse.org/mtus/). It includes individual diaries listing the activities of the individuals during a day. A micro-environment was allocated to each activity. Time use data for the EU-30 countries which were not included in MTUS was estimated by creating a new set of diaries for a country by sampling randomly from the diaries of neighbouring countries.

4.2 OUTDOOR AIR

4.2.1 Calculation of concentrations of air pollutants

Three state of the art chemical transport models (CTMs) have been applied: the Unified EMEP model, Polyphemus, and Chimère. These three models were used to estimate concentration fields given the same set of emission data. However, due to the calculation intensity and, thus, long run time of the CTMs only a few scenarios could be calculated, thus the final calculations were made with a parametrised version of the EMEP model. This version uses source receptor matrices (SR-Ms) derived from numerous model runs of the EMEP models, which were obtained during earlier projects. SR-Ms relate a given change in the emissions of a country to changes in concentrations in all grid cells of Europe. The model using the CTMs is included in the integrated assessment model 'ECOSENSE'.

EcoSense[8] is an integrated atmospheric dispersion and exposure assessment system implementing the impact pathway approach. It is designed for the assessment of emissions of air pollutants in Europe. EcoSense was developed to support the assessment of priority impacts resulting from the exposure to airborne pollutants, namely impacts on human health, crops, building materials and ecosystems. The current version of EcoSense covers the emission of 'classical' pollutants SO_2, NO_x, primary particulates, NMVOC, NH_3, as well as some of the most important heavy metals.

In this case study EcoSense was used as an "umbrella" model. Emissions / emission scenarios can be given as input; and calculations are performed through the whole chain to the damage costs. However, as an alternative, concentration fields (modelled with other chemical transport models) can be included and calculations start from there. Monetary values and impact functions have been adapted to the values given in this case study. Health effects and damage costs are given separately per country and in an aggregate form.

The calculations of the three full Eulerian models EMEP, Polyphemus and CHIMERE were used to valdate the ECOSENSE calculations.

Naming of the scenarios in this chapter is as follows: "reduced cattle protein" is a single measure in the agricultural sector and represents a scenario in which less red meat but more white meat is consumed; "dam" means that the energy model has optimised the energy scenario for private and external (= damage) costs (in contrast to the scenario in which it optimised for only private costs); "450ppm" means climate policy (2 °C aim) scenario (the CO_2 concentration is reduced to 450ppm).

[8] http://ecosenseweb.ier.uni-stuttgart.de/

Validation of SR-Ms in EcoSense

In order to test the accuracy of the SR-M implemented within the EcoSense model, a comparison against the unified EMEP model and the Polyphemus model was carried out. For this purpose, the accumulated exposure (i.e., delta concentration in each grid cell multiplied by number of people affected by it) was estimated using the aforementioned models for the scenario 450ppm_reduced cattle protein minus the business as usual for the year 2020. The results for PM_{10} and $PM_{2.5}$ are presented in Figure 4-1, showing a good agreement of the SR-M results with those of the unified EMEP model. In fact, the total difference amount only for 10% in the case of PM_{10} and 5% for $PM_{2.5}$. Furthermore, the differences are larger when compared against Polyphemus where they account for around 50% and 100% for PM_{10} and $PM_{2.5}$, respectively.

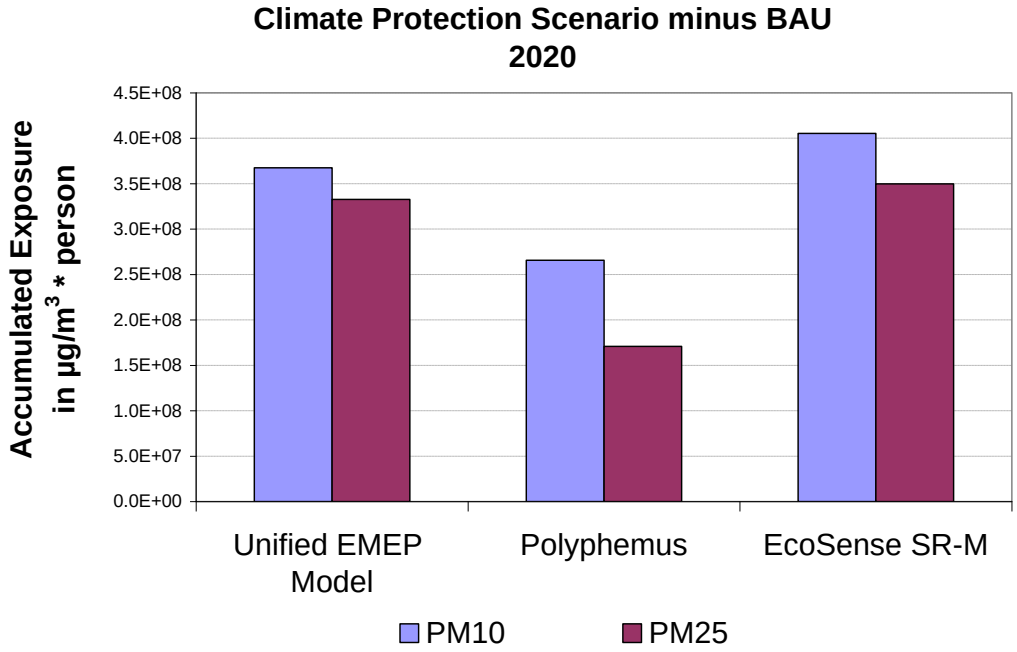

Figure 4-1: Comparison of accumulated exposure to PM_{10} and $PM_{2.5}$ (in $\mu g/m^3$ * person) estimated with the unified EMEP model, Polyphemus and the EcoSense SR-M. The results correspond to the Climate Protection scenario minus Business as Usual for the year 2020.

As for the ozone-indicator SOMO35, Figure 4-2 shows that SR-M overestimates the total accumulated exposure by around 60% in comparison with the EMEP model. On the other hand, the results obtained with Polyphemus differ significantly from the other two models which suggest that Polyphemus may underestimate the SOMO35 indicator. Accumulated exposure estimated for NH_4 were also drawn in this comparison and the results are presented in Figure 4-3. The results provided by the unified EMEP model and the EcoSense SR-M are quite similar and they differ only by around 1% of the total accumulated exposure. Polyphemus on the other hand delivers again lower estimates in comparison with the other two models. Thus, it is considered that the EcoSense SR-M provide estimates similar to those provided by more complex models, such as the unified EMEP model and the Polyphemus model.

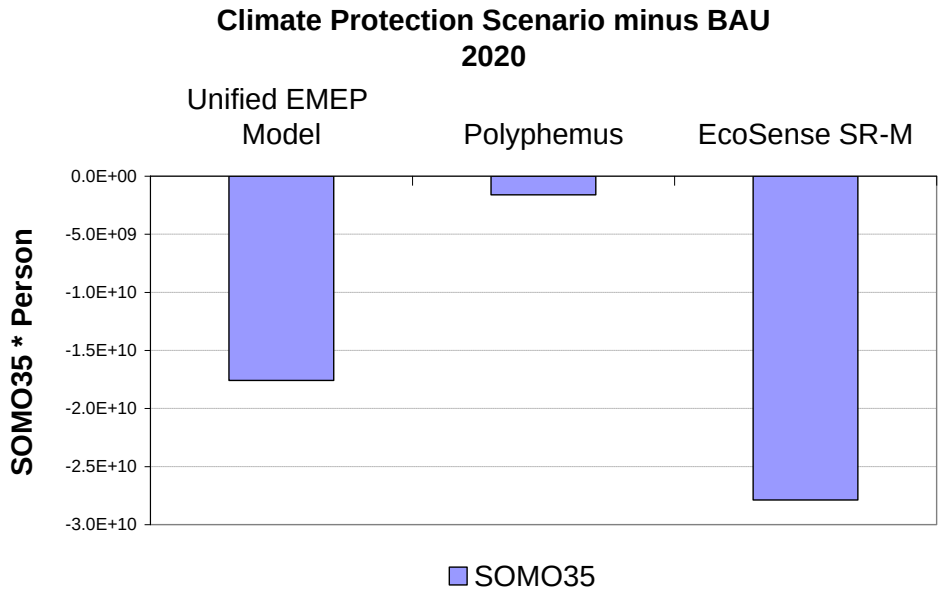

Figure 4-2: Comparison of accumulated exposure [SOMO35 * person] estimated with the unified EMEP model, Polyphemus and the EcoSense SR-M. The results correspond to the Climate Protection scenario minus Business as Usual for the year 2020.

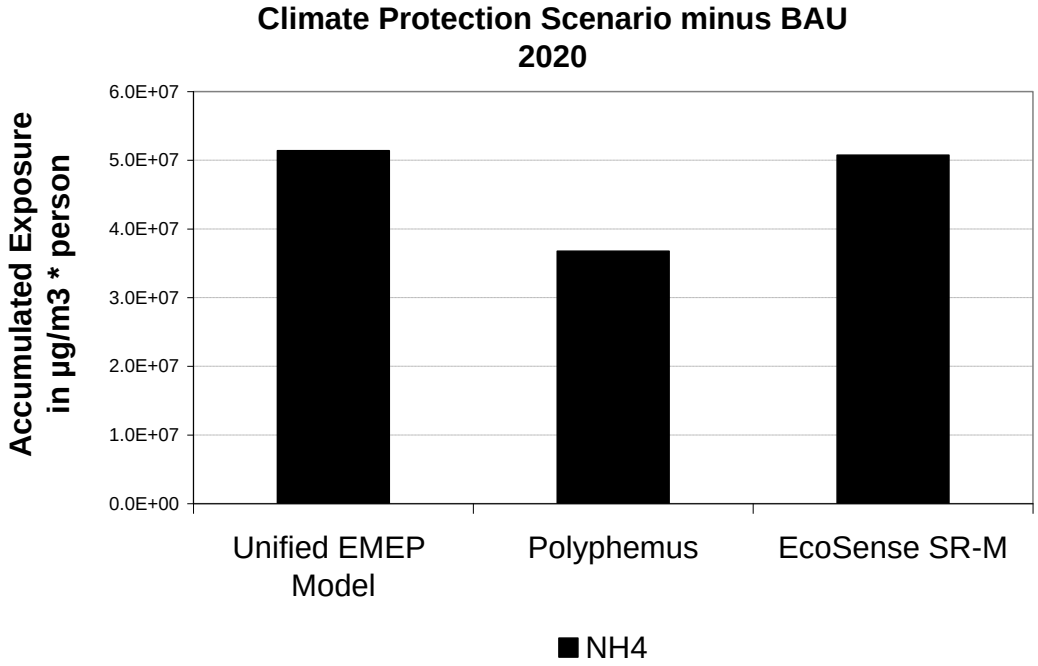

Figure 4-3: Comparison of accumulated exposure to NH_4 (in $\mu g/m^3$ * person) estimated with the unified EMEP model, Polyphemus and the EcoSense SR-M. The results correspond to the scenario Climate Protection scenario minus Business as Usual for the year 2020.

4.2.2 Urban Increment

Over 75% of the European population is living in urban areas; by 2020 it should be 80%, and for some countries will be even 90% (EEA 2006). As a consequence, the number of people affected by elevated pollutant concentrations is notably higher in urban areas than in rural environments. Trying to shed light on the mechanisms accountable for the typical higher pollutant levels in urban areas for most pollutants, the topic has become the subject of a number of studies over the last few decades (De Leeuw et al. 2002; Yin et al. 2005; Charron et al. 2006; Stedman and Derwent 2007). Due to its relevance, the urban increment (i.e., the difference between regional and urban background pollutant concentrations) was included in the analysis carried out within the Common Case Study. A model developed in Torras Ortiz (2010) for German cities was used as the basis for estimating PM10 and $PM_{2.5}$ urban increment for European large cities. In the following sections, the urban increment model for Germany is described along with the approach followed to derive values for European cities.

Urban Increment model for Germany

Torras Ortiz (2010) developed a model to estimate the urban increment for all German cities with over 50 000 inhabitants. The urban background increment for PM10 was estimated using a functional relationship between emissions, city size and average wind speed. Urban areas were defined following Milego (2007) and it was assumed that only primary emissions released from low sources increase concentrations within the cities (Amann et al. 2007). The average wind speed 10-metres-over the surface was estimated using a four-year dataset (1997, 2000, 2001 and 2003). Lastly, the city morphology data (shape and area) were generated using a GIS-Framework.

A pragmatic approach was followed for calculating the observed urban increment: observational data from paired rural and urban background measure stations where used for obtaining the urban increment. For this purpose, observational data for urban and rural background stations for PM_{10} were retrieved from the European Air Quality database. To obtain the relationship between predictor variables and the criterion variable – in this case the measured urban increment – a multiple regression analysis was carried out, using the following formulation:

$$C_{i\ urban} = \varpi_i + \phi_i \frac{E_{iUE}}{A_{UE} \cdot u_{avg}} + \gamma\, C_{i\ rural} \qquad \text{(Eq. 4-1)}$$

where

$C_{i\ urban}$ = Urban increment of pollutant i.

E_{iUE} = Total emission of pollutant i within an urban entity in tons.

A_{UE} = Urban entity area in km^2.

u_{avg} = Urban entity average wind speed in m/s.

$C_{i\ rural}$ = Rural background concentration of pollutant i in µg/m³.

ω_i, φ_i, and γ_i = Multiple-regression parameters for pollutant i.

An urban increment model for $PM_{2.5}$ was not directly estimated due to the limited availability of valid measurements for this pollutant. Instead, the $PM_{2.5/PM10}$ concentration ratio provided by several studies were analyzed (Gehrig and Buchmann 2003; Van Dingenen et al. 2004; Graff 2006) and, as a result, the value of 0.75 for the $PM_{2.5}/PM_{10}$ urban background ratio was considered to be a reasonable assumption.

Model's adaptation for Europe

A straightforward application of the model described in the last section was not feasible for estimating the PM_{10} urban increment of cities outside Germany. The main hurdle was that urban emissions were available only on an EMEP-Grid level (i.e. 50x50 kilometres) and not -for each European city, as it is required in the model presented above. Despite this drawback, an alternative approach was followed to provide a first estimate of the urban increment for European cities: a hierarchical clustering analyse. This type of analysis allows to group a sample of subjects into significantly different groups (called clusters) based upon a number of key variables. Thus, a sample of cases is reduced to a few statistically different groups based upon differences/similarities across a set of multiple variables (Bacher et al. 2010). Once the clusters are identified, the values of the key variables may be transferred to other groups with similar characteristics.

In this study, the values to be clustered were the German cities provided in Torras Ortiz (2010). For this purpose, several variables were chosen as key variables: urban population and urban emissions per EMEP-Grid cell, and the PM_{10} urban increment. Here it is important to note that the PM_{10} urban increment estimated in the original study was linked to individual cities and, therefore, it was necessary to estimate an average PM_{10} urban increment per EMEP-Grid cell. The key variables were z-transformed to enable their comparison. Hereinafter, a WARD-hierarchical clustering using the software Kyplot Version 2.0 was applied to all cities, sorting them into significant different groups where the cities within each group were as homogeneous as possible and the groups were as different from one another as possible. Dissimilarity is defined as the distance between two samples under some criterion or metric. The metric used in this analysis was the standardized Euclidian distance. The analysis identified five clusters with the characteristics showed in Table 4-3.

Table 4-3: Clusters built using data provided in Torras Ortiz (2010).

Cluster	Urban Emissions / Urban population	PM_{10} Urban Increment
1	Low	Moderate - high
2	Moderate – low	Moderate - low
3	Moderate	Moderate
4	Moderate – high	High
5	High	Low

It is noticeable that the emissions, population and urban increment do not follow the same rank order; a low PM_{10} urban increment can be related to high emission density areas. This is because large urban emissions sources have a strong influence on pollutant levels measured at rural stations (i.e., stations located within a distance of 10 to 50 kilometres from built up areas and other major sources) and, thus, the urban background concentration does not stand out as much from the rural background concentration as the urban emission density in the area would suggest. In fact, this is also the reason why the rural background concentration is included in the original regression model.

Once the clusters were identified, the PM_{10} urban increment values were transferred to other cities with similar key variables outside Germany. The European cities were grouped using urban population and emissions per EMEP-Grid cell and, finally, the corresponding urban increment value was assigned to each EMEP-Grid cell.

Concerning $PM_{2.5}$ urban increment, in the original model this value was estimated as a function of the $PM_{2.5}/PM_{10}$ urban background concentration ratio. For this study, PM_{10} and $PM_{2.5}$ concentration values were collected from the European air quality database (Airbase 2010). The concentration values were selected based on several criteria, which are described in the following table:

Table 4-4: Criteria for selection of concentration values.

Name of Field	Criteria
Type of station	Background
Station type of area	Urban
Statistic name	Annual Mean
Statistics average group	Day
Statistic shortname	Mean
Statistics year	2005
Component caption	PM10 / PM2.5
Statistics percentage valid	>80

The limited availability of measurements for the baseline year 2005 hampered developing the estimation of the $PM_{2.5}/PM_{10}$ concentration ratio for all the countries included in the CCS. As a way for dealing with this situation, the analysis scope was

extended to two additional years (2006 and 2007) and the results are presented in Table 4-5.

Table 4-5: $PM_{2.5}/PM_{10}$ concentration ratios for several countries

Country	PM_{25} / PM_{10} ratio	Source
Switzerland	0.75	Gehrig and Buchmann (2003)
Czech Republic	0.67	Average Airbase years 2005, 2006 and 2007
Germany	0.75	Torras Ortiz (2010)
Denmark	0.54	Airbase – Average years 2005, 2006 and 2007
Spain	0.42	Airbase – Average years 2005, 2006 and 2007
Finland	0.58	Airbase – Average years 2005, 2006 and 2007
Norway	0.47	Airbase – Average years 2005, 2006 and 2007
Portugal	0.38	Airbase – Average years 2005, 2006 and 2007
Sweden	0.57	Airbase – Average years 2005, 2006 and 2007
Slovakia	0.73	Airbase – Average years 2005, 2006 and 2007
United Kingdom	0.61	Airbase – Average years 2005, 2006 and 2007

For countries where measurements were lacking, a value of 0.73 for the $PM_{2.5}$/PM10 concentration was assumed based on findings presented in Van Dingenen et al. (2004).

4.3 EXPOSURE TO PM 2.5 AND INDOOR STRESSORS

4.3.1 Exposure to $PM_{2.5}$

Currently, the estimation of health effects from air pollutants is based on concentration response functions (CRFs, e.g. WHO 2004). These CRFs link the ambient concentrations of an air pollutant to health effects that are attributed to this pollutant (e.g. Bickel et al. 2005). The CRFs relate to the ambient concentration of a pollutant but they implicitly include the concept that people do not spend all day outdoors (the CRFs are used as proxies). However, the true exposure of the people depends of the concentration they come into contact with during the time they spend in different microenvironments (e.g. cars, indoors, outdoors). By using the ambient concentration and not the exposure of people as a metric, only those effects of policy measures that influence (decreases) the emissions (and thus the concentration) can be considered. In fact, changes in exposure, and subsequent health effects, can also be influenced by other factors like changes in the infiltration from outdoor into indoor environments, or changes in the time spent in different micro environments.

LAMA is a tool developed for use as a part of the “full-chain” assessment for estimating exposure to air pollutants in a population. It requires air pollution concentration inputs from emissions and atmospheric models and integrates these with time-use data and micro-environmental factors (factors which modify the infiltration of ambient pollutants into microenvironments) to estimate exposures, which constitute LAMA’s output. This

output serves as input to the health effects estimation. This total exposure is spatially distributed due to varying outdoor concentrations, population density and behaviour of humans. The results are in the form of annual averages that can be calculated on a grid or country level (by weighting with the appropriate population). The methodology implemented in LAMA can be used for different air pollutants but has currently only been tested for PM2.5 and so far only input data for PM2.5 is available. For methodological details see HEIMTSA Deliverable D2.1.5/7 “Exposure methods in the Common Case Study” as only a brief overview is presented here.

Methodology

In LAMA the exposure is modelled using a microenvironmental approach by integrating the elements that influence people’s exposure: exposure to outdoor sources and indoor sources, and time spent in different micro-environments. A microenvironment is a term used often in air pollution exposure science and refers to a location or surroundings that a person spends time in where the air concentrations are treated as homogenous (e.g. IPCS 2004).

The time spent by a person is classified into microenvironments (MEs) for which the concentrations are estimated. The microenvironments used in LAMA are:

- work & school
- home
- travel & commute
- outdoor
- other (unspecified location)

The concentration per microenvironment is estimated based on the mass-balance indoor model under steady state, instantaneous and homogenous mixing conditions (Koutrakis et al., 1992):

$$c_{in} = \frac{c_{out}\, pa + \frac{\sum_{i=1}^{n} s_i}{v}}{(a+k)} \qquad (1)$$

Where: c_{in} = indoor concentration [µg m^{-3}]
c_{out} = outdoor concentration [µg m^{-3}]
p = penetration factor
a= air exchange rate [h^{-1}]
k = decay rate [h^{-1}]
s_i = emission rate for source i [µg h^{-1}]
v = room volume [m^3]

LAMA combines the human time activity data with the concentration data and microenvironment-specific parameters to estimate individual exposure. The final

calculation of exposure can be performed either on a diary basis (for each country, eq. 4a), as subgroup average for each grid cell (eq. 4b) or as subgroup average for each country (eq. 4c, derived from 4a or 4b):

$$E_{c,d} = \frac{1}{\sum_{i=1}^{n} pop_i} \sum_{i=1}^{n} \left[pop_i \left(\frac{1}{\sum_{j=1}^{m} t_{d,j}} \sum_{j=1}^{m} \left[t_{d,j} \left(f_j \left(c_{out,i} + c_{urb,i} \right) + c_{in|s,j} \right) \right] \right) \right] \quad (4a)$$

$$E_{i,g} = \frac{1}{q_g} \sum_{d=1}^{q_g} \left[\frac{1}{\sum_{j=1}^{m} t_{d,j}} \sum_{j=1}^{m} \left[t_{d,j} \left(f_j \left(c_{out,i} + c_{urb,i} \right) + c_{in|s,j} \right) \right] \right] \quad (4b)$$

$$E_{c,g} = \frac{1}{q_g} \sum_{d=1}^{q_g} E_{c,d} = \frac{1}{\sum_{i=1}^{n} pop_i} \sum_{i=1}^{n} \left[pop_i E_{i,g} \right] \quad (4c)$$

Where : E = exposure [µg m^{-3}]

c = country

i = grid cell

g = subgroup

d = individual diary of subgroup g

q = number of diaries per subgroup g

f = infiltration or traffic enrichment factor (see eq. 3)

pop = population per subgroup and grid cell

t = time fraction spent in a microenvironment

j = microenvironment

c_{urb} = urban increment for cities in grid cell i [µg m^{-3}], this factor was only added to a number of individuals according to the percentage of people living in an urban area in the grid cell

Uncertainty

In LAMA, there are two main parameter types that have inherent uncertainty and variability – the parameters related to estimating indoor concentrations and the time activity diary data. The greatest uncertainty is likely in the indoor parameters. Therefore uncertainty is explored by simulating a set of realisations for each diary, based on the distributions of the indoor parameters. To account for the uncertainty in the indoor parameter estimations each parameter is represented by a distribution instead of single values (see Section 4.1.3). In LAMA, Monte Carlo sampling is used to draw a large number of realisations from each of the parameter distributions. The variability between the diaries is separated from the uncertainty of the true parameters for each diary within LAMA by keeping both sample dimensions (*r* realisations and *q* diaries) separately. This gives two ways to look at the results: 1) the variability between exposures estimated per diary (averages over the realisations) and 2) the uncertainty

for each diary result between realisations (or the uncertainty of the population average between realisations).

As an example, the results for eq. 4a calculated *r* times for *q* diaries can be visualised as cumulative probability curves for each population realisation (Figure 4-4, black curves). Variability between the diaries of a population is represented by the slope of the curve. Uncertainty between realisations is shown by the difference between the curves. For further calculations (i.e. health effects) we do not distinguish the individuals but make a distribution of the whole sample size (blue curve). This includes the variability of the diaries within the population and the uncertainties of the indoor parameters.

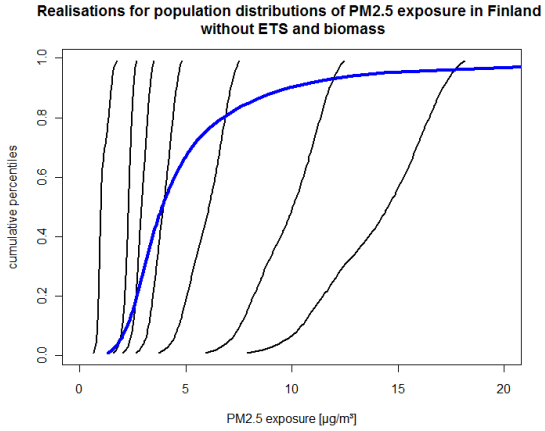

Figure 4-4: Variability within and uncertainty between curves for $PM_{2.5}$ exposure results in Finland.

Results. LAMA was applied for the scenarios developed in Section 2 for grid based and country based subgroup results with 10,000 Monte Carlo realisations. The results on the EMEP grid averaged to the total population for the scenarios in 2020, 2030 and 2050 are shown as maps in Figure 4-5. Generally, the results for the policy scenarios are higher than the results for the respective BAU scenario. There is also a temporal trend visible with increasing exposure results with time. Within the scenario maps there are clearly differences between countries which exceed differences within countries. This is clearly due to the fact that time use data as well as indoor parameters are available on a country level only. Thus, the differences on the grid level within the countries are only caused by differences in population and outdoor concentration of $PM_{2.5}$.

For uncertainty visualisation in Figure 4-6 the average $PM_{2.5}$ exposure map for the 2020BAU scenario is plotted next to the associated standard deviation map. As the uncertainty estimates come from the parameters only, the uncertainty map shows no variation within the grid cells of a country. The maps show that the uncertainty is smaller for Norway, Sweden and Germany compared to the rest of Europe. Maximum

uncertainty can be found in Bulgaria, followed by the rest of Eastern Europe. This result can be explained by the sparse data availability for parameters like room volume for these areas. Thus, the higher uncertainty in the input data is clearly reflected in the exposure results.

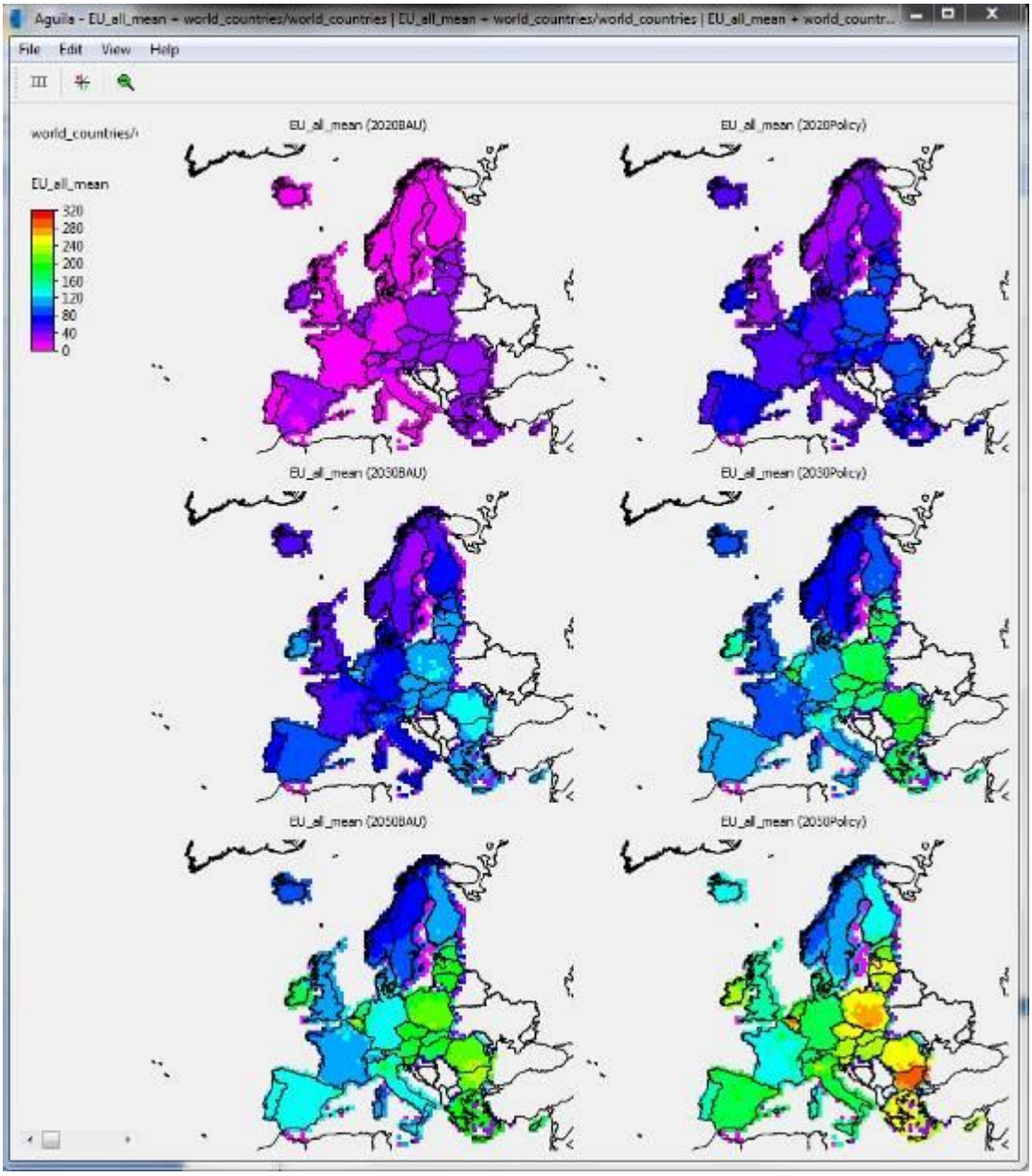

Figure 4-5: Average $PM_{2.5}$ exposure results for the six scenarios on the EMEP grid shown with the visualisation software Aguila (Pebesma et al., 2007).

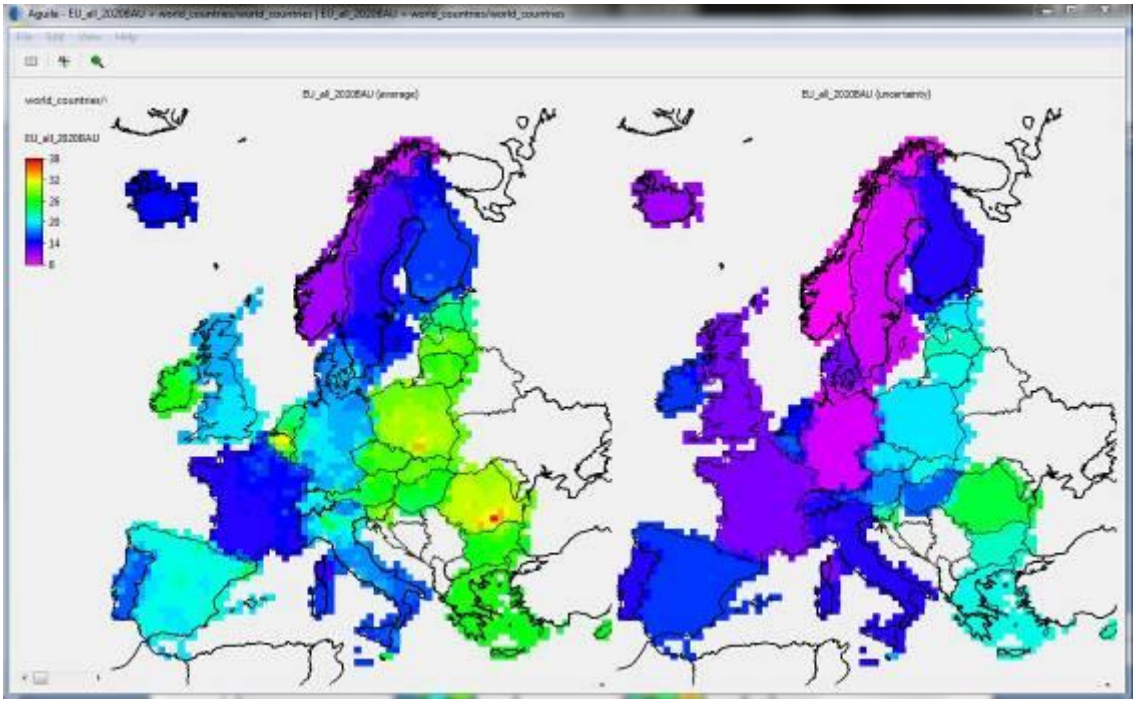

Figure 4-6: Average $PM_{2.5}$ exposure results and uncertainty (standard deviation) for 2020BAU scenario on the EMEP grid shown with the Aguila software.

Subgroup results

The country based results per subgroup as cumulative curves over all realisations are shown exemplarily for Germany and the 2020BAU scenario in Figure 4-7. It is clear from this figure that the uncertainty within the subgroups is relatively large compared to the differences between the subgroups. Furthermore, the average exposure is clearly higher than the average outdoor concentration for $PM_{2.5}$. This is due to the fact that multiple indoor sources occur which elevate the total personal exposure compared to the outdoor concentration.

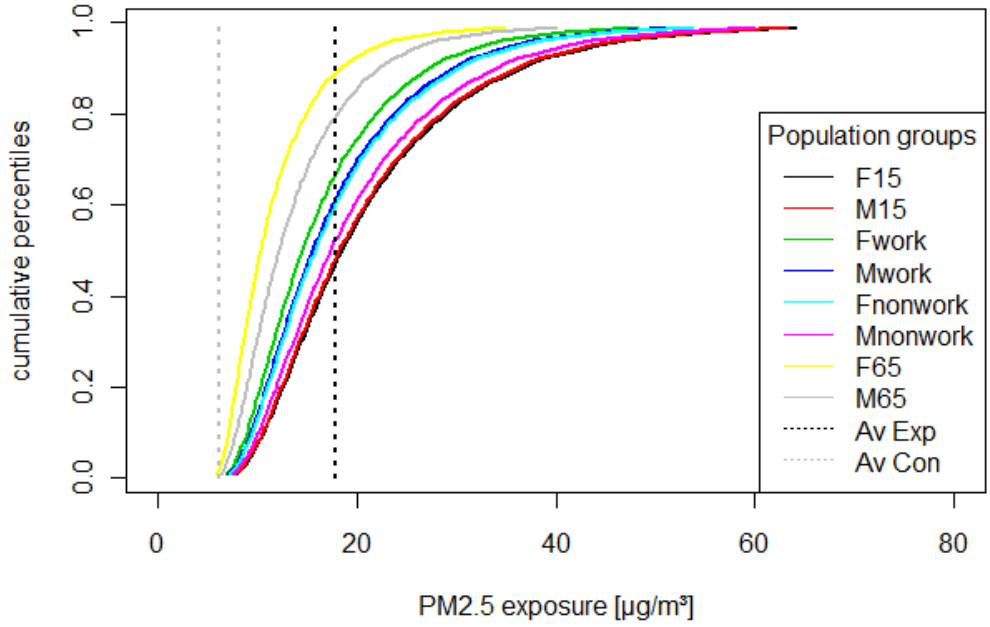

Figure 4-7: Cumulative $PM_{2.5}$ exposure per subgroup for the 2020BAU scenario in Germany.

Scenario comparison

The overall $PM_{2.5}$ exposure results averaged over EU-30 per subgroup and scenario are shown in Figure 4-8. Differences between subgroups are larger than differences between scenarios. However it is visible again that the policy scenario results tend to exceed those for the BAU scenarios. This is due to accumulation of indoor sources (see Figure 4-10 for a comparison to outdoor air sources only).

In general, the older age groups (65 years and older) have the lowest exposure values for all scenarios. Working male and female persons between 15 and 64 years (Fwork/Mwork) also experience a lower exposure than non-working people from the same age class or younger people. This can be explained by the parameters used for the indoor model which assumes no background, ETS or biomass burning sources at working places. Furthermore, infiltration into working environments is assumed to be lower than into residential environments (assuming more heat, ventilation and air conditioning appliances at work than at home and, thus, a better filter mechanism).

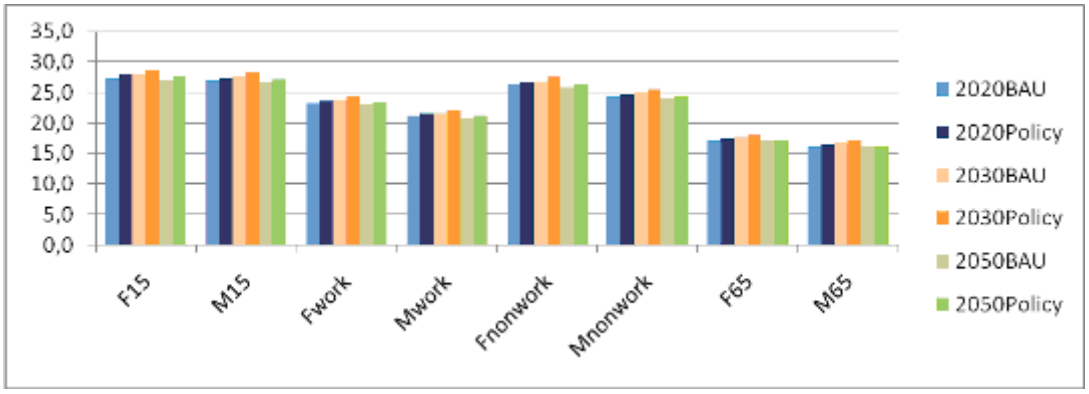

Figure 4-8: Average $PM_{2.5}$ exposure over EU-30 per subgroup for the six scenarios.

The exact differences between BAU and policy for each of the three years are plotted in Figure 4-9. Differences are largest for 2030 and for the youngest age groups younger than 15 years. However, differences are very small and show for the oldest age groups in 2050 even slightly negative results (BAU > Policy).

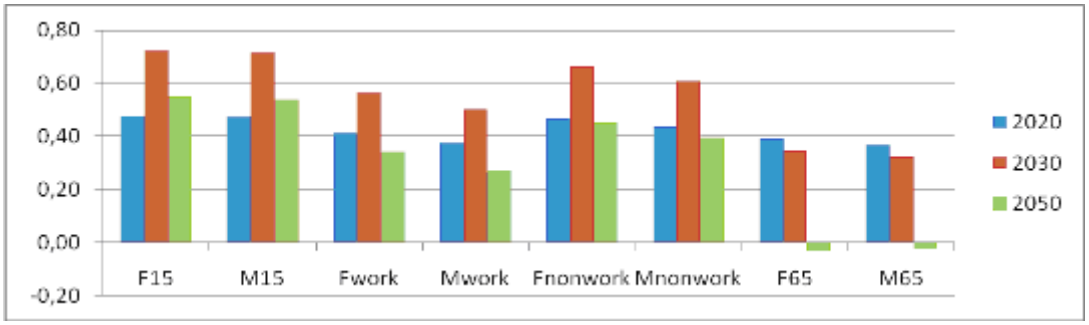

Figure 4-9: Differences for the average $PM_{2.5}$ exposure over EU-30 per subgroup between policy and BAU scenario for each year (Policy – BAU).

If only outdoor air as a source is considered the trends in exposure change (see Figure 4-10). Lower outdoor air concentrations of PM2.5 lead to lower personal exposure in the respective policy scenarios vs. BAU (for 2020 the differences are very small and the concentration in the policy scenario is slightly higher).

Reduced exposure with time and for policy scenarios vs. BAU originates mainly from a reduction in the infiltration (more residential buildings are new or insulated/renovated and the air exchange rate and penetration is assumed to be lower). Based on these findings it can be concluded that the higher exposure with time and for policy vs. BAU scenarios is due to accumulation of the indoor sources in residential micro-environments (home).

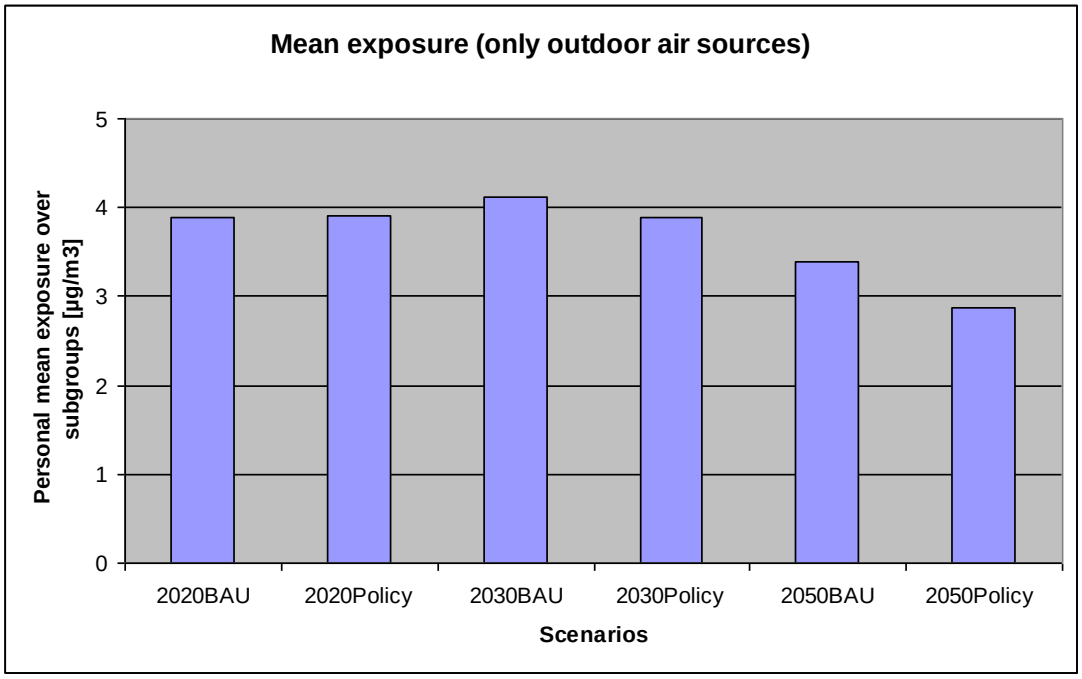

Figure 4-10: Average $PM_{2.5}$ exposure over EU-30 over subgroup for the six scenarios including only outdoor air sources.

4.3.2 Exposure to ETS originated VOCs and formaldehyde

Carcinogenic effects and asthma due to exposure to Environmental Tobacco Smoke (ETS) and formaldehyde (from all sources) were investigated. The carcinogenic health endpoints tackled for ETS are related to three Group I carcinogens (among others) named as NNK (4-(N-nitrosomethylamino)-1-(3-pyridyl)-1-butanone), benzene and formaldehyde, correspondingly related to lung cancer, leukemia and nasopharyngeal cancer. All methodological steps needed for the indoor air case study are integrated in a single advanced simulation software platform using the acslXtreme dynamic simulation environment. The platform (a simplified conceptual visualization presented in the following Figure) is composed by 5 main components, named as:

- Emissions-Concentrations component
- Exposure component
- Internal dose – PBPK/PD (Physiology Based PharmacoKinetic/PharmacoDynamic) model component
- Health outcomes component
- Monetary valuation/DALYs component

All components are directly linked and the output of each previous component is the input of the following one. Most of the blocks correspond to systems of differential

equations that describe a dynamic procedure either related to environmental parameters (e.g. emission and dispersion), either to metabolic ones (kinetic of a stressors in the tissues).

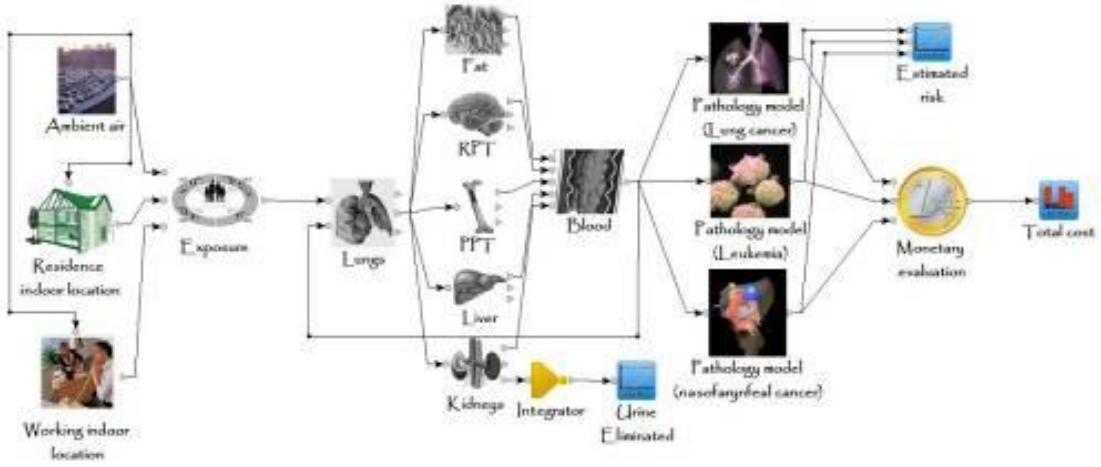

Figure 4-11: Model framework for ETS originated VOCs

Indoor air quality modeling was based on a mass balance model, the concentrations of the contaminants of interested are given by the generic formula:

$$V\frac{dC}{dt} = Q\left(C_0 + C_a - C\right) + E - kC$$

Personal exposure was estimated as a function of the concentrations for a given micro-environment at the given time duration. If over the given period of time, T, the person passes through n locations, spending a fraction fn of the period T in location n where the concentration of the pollutant under consideration is Cn, then the personal exposure for this period T, represented by the concentration CT, is given by:

$$C_T = \sum_n f_n \cdot C_n$$

4.3.3 Exposure to dampness

The assessment is based on a causal model presented in Figure 4-12. Each node in the graph (also called a variable in the model) are described in more detail in the HEITMSA D7.1.15: “Final report on ‘full chain’ analysis of indoor air pollution: Update based on the Common Case study”, and only a summary of the model is presented here.

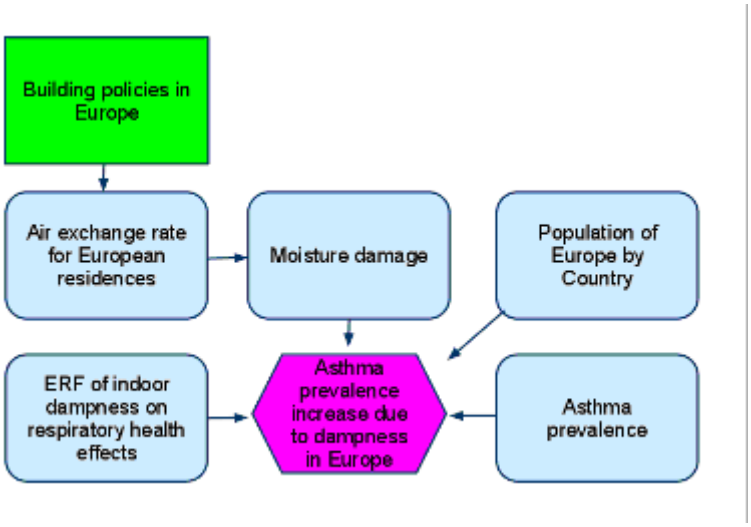

Figure 4-12: A causal diagram of health effects of dampness in Europe.

The logic of the assessment is that the climate change mitigation policies considered affect air exchange rates in buildings. It is expected that moisture problems become more likely if the air exchange decreases. Nation-wide dampness estimates were obtained from several studies reviewed (see Annex B for more information). However, several countries (Luxembourg, Netherlands, Switzerland, Ireland, Norway, United Kingdom, Bulgaria, Hungary, Lithuania, Romania, Slovakia, Slovenia, Malta) were rejected due to lack of data.

4.3.4 Exposure to radon

The assessment is based on a causal model presented in Figure 4-13. Each node in the graph (also called a variable in the model) are described in more detail in the HEITMSA D7.1.15: “Final report on ‘full chain’ analysis of indoor air pollution: Update based on the Common Case study”, and only a summary of the model is presented here.

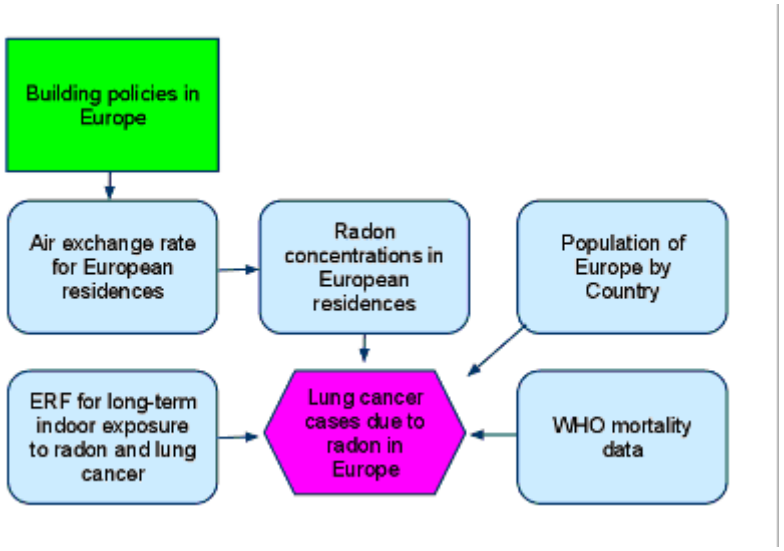

Figure 4-13: A causal diagram of health impacts of radon in Europe

The logic of the assessment is that the climate change mitigation policies considered affect air exchange rates in buildings. There is a simple negative association between air exchange and radon: air exchange removes radon from indoor air. However, there are many complicating factors which are not considered in this assessment. Radon comes to indoor air from soil via gas leakages in the building ground floor structures. The most important omission in the assessment is that there are effective methods to prevent radon leakages into the building in the first place. Although these are typically cheap to implement during construction, they can be very costly if implemented in an existing building. Therefore, this first pass assessment simply assumes that such measures are not taken more in the future than what they have been taken so far, i.e. the radon emissions from soil into indoor air will remain at the current levels. Although this is a somewhat pessimistic assumption, the knowledge about radon and its mitigation have been around for decades, and the current situation is the result of radon policies that societies have been willing to implement in practice. Nation-wide radon estimates were obtained from EnVIE project and UNSCEAR 2000 (UNSCEAR 200) report. However, United Kingdom, Czech Republic, and Slovenia were rejected due to lack of data.

4.4 EXPOSURE TO NOISE

As noise is a very local phenomenon, modelling with very high resolution is needed to obtain meaningful results on exposure. For noise there is not, as for air pollution, a Europe-wide --database on emissions. Therefore Europe-covering modelling as described above for air quality was not feasible. In HEIMTSA two alternative methods for assessing exposure distributions of the EU population to the façade levels, method A and method B (see Figure 4-14) were developed. In the Common Case Study, Method B has been applied.

Method A is based on detailed noise mapping calculations for a few example cities and upscaling the results to the EU urban population in an approximate way.

Method B employs noise maps and exposure distributions previously calculated by many EU cities in the framework of the Environmental Noise Directive (END), for the reference year 2006. Method B is expected to be more reliable for policy changes that can be calculated by scaling the exposure distributions, but it assumes a spatially homogeneous change of noise levels. Future scenarios are often characterized by changes without specific geographical coordinates, for example: numbers of urban vehicle kilometres or percentages of electric vehicles in EU member states. For such scenarios, the future exposure distribution is calculated by *scaling*, i.e. by shifting the 2006 exposure distribution along the horizontal noise level axis (see Figure 4-15)[9]. For more complex scenarios the exposure changes must be derived from detailed noise mapping calculations.

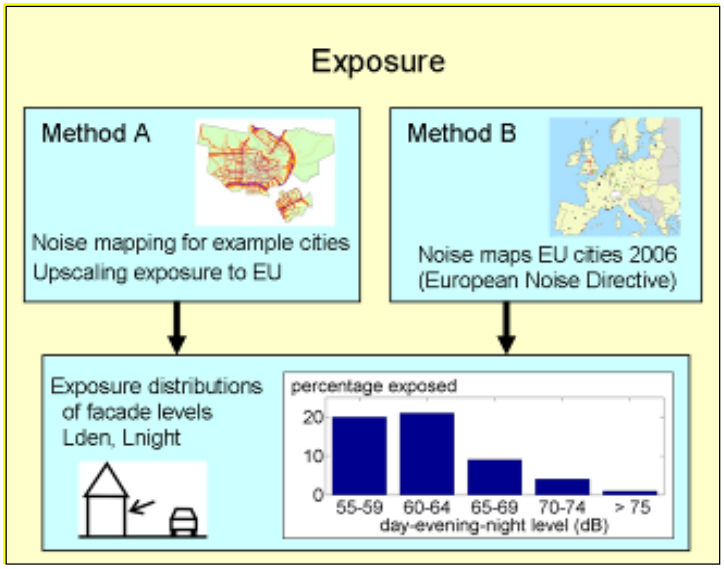

Figure 4-14: Illustration of methods A and B for calculating noise exposure distributions.

[9] This is based on the acoustic relation *immission level = emission level – transmission loss*, where the transmission loss accounts for sound attenuation between source and receiver, which is assumed constant.

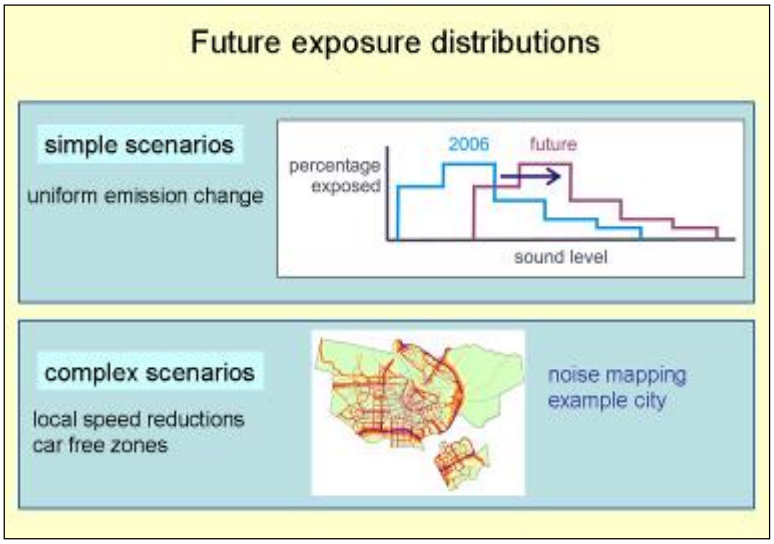

Figure 4-15: Illustration of simple scenarios and complex scenarios for calculating future exposure distributions to noise.

Table 4-6 summarises the results for the number of Europeans exposed in cities above 55 dB (day-evening-night level). Similar results for other noise thresholds were also calculated. The results are also shown in Figure 4-16.

Table 4-6: Number of inhabitants of European cities exposed above 55 dB (day-evening-night level) for the BAU and the climate policy scenario, including the contributions of individual measures within the climate policy scenario.

Scenario/measure	**2005**	**2020**	**2030**	**2050**
BAU (number of Europeans)	156 million	170 million	169 million	157 million
Percentage change in the number of Europeans, compared to the BAU scenario				
450 ppm scenario	0	-5.1	-5.7	-7.2
- Fuel tax	0	-1.0	-1.8	-1.6
- Cycling in cities	0	-1.2	-1.1	-1.0
- City toll	0	-0.2	-0.1	-0.1
- PC toll	0	-2.5	-2.2	-2.0
- Electric vehicles	0	-0.2	-0.6	-2.4

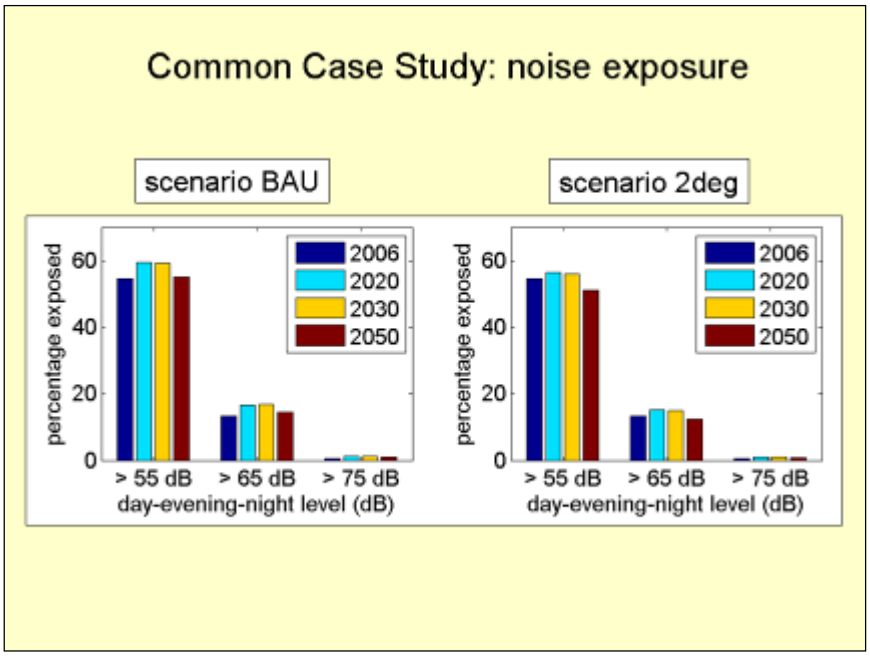

Figure 4-16: Cumulative noise exposure distributions calculated for the BAU scenario and the 450ppm scenario.

4.5 FATE AND EXPOSURE ASSESSMENT OF POPS

4.5.1 Description of models for POPs modelling

MSCE-POP: The multicompartment chemistry transport model MSCE-POP is currently used for operational calculations of transboundary pollution within the European region under the EMEP programme and other activities relating to the LTRAP Convention. The model is a three-dimensional Eulerian type multicompartment chemistry transport model. It can operate with two different grids: hemispheric grid covering the Northern Hemisphere with resolution 2.5º×2.5º and regional grid with resolution 50×50 km. The vertical structure of the model is formulated in the sigma-pressure coordinate system consisting of irregular sigma-layers. The hemispheric grid is formulated on the longitude-latitude basis and covers the entire Northern Hemisphere. The regional one is formulated on the polar stereographic projection covering the European region and surrounding areas. It has a top at 100 hPa (that roughly corresponds to 15 km). A global version of MSCE-POP model covering the entire globe is now under development. The following environmental compartments are considered in the model: the atmosphere, soil, seawater and vegetation. The model considers the following processes governing POP fate in the environment: partitioning and degradation in the considered environmental media, dry and wet deposition processes and gaseous exchange between the atmosphere anr the underlying surface.

Evaluation of contamination by POPs in Europe is performed on a regional scale. However, due to the ability of some POPs to be transported over long distances and to be accumulated for a long time periods in environmental compartments (soil, vegetation) it is reasonable to take into account POP long-range transport (regional and intercontinental) and long-term accumulation. To do that, one-way nesting approach using both model resolutions is used. Under this approach, boundary and initial conditions for regional model runs are prepared with the use of pre-calculations by hemispheric scale simulations for sufficiently long time period (depending on the contaminant under consideration). For example, for such long-living substances as PCDD/Fs and PCBs this period should be several decades whereas for trifluralin and heavy PAHs (B[a]P, B[b]F, B[k]F and IP) pre-calculations are not necessary. Detailed description of the model is available in (Gusev et al., 2005). The model formulation and performance was thoroughly evaluated within the EMEP/TFMM Workshop on the model review (Gusev et al., 2006). The MSCE-POP modelling framework is described in detail in HEIMTSA Deliverable D 2.2.3/4 “Environmental modelling for the HEIMTSA/INTARESE Common Case Study”.

PANGEA: PANGEA, developed conjointly by the School of Public Health (SPH), University of Michigan, United States, and the Institute of Energy Economics and the Rational Use of Energy (IER), University of Stuttgart, Germany, is a multi-scale, multimedia modelling framework that allows to determine and compare local to global impacts of organic pollutants that undergo a multimedia fate and lead to a multi-pathway exposure of the population. The purpose of PANGEA is to analyse all relevant impact pathways of organic contaminants at various spatial scales. The modelling

framework is based on a flexible, multi-scale and multi-compartment system for generating multi-scale grids (covering single or a set of environmental media) according to any user defined criterion with the help of GIS processing. This enables the model to automatically project every available data set onto a flexible grid (i.e. adjacent grid cells may have different extensions) and to solve the underlying numerical equations by means of matrix algebra.

For the Common Case Study, PANGEA was coupled to the atmospheric transport model MSCE-POP, i.e. the atmospheric transport processes in PANGEA are computed by means of the MSCE-POP model as described above and the interfaces between the atmospheric ground layer and the adjacent compartment types, such as ocean water, are calibrated by means of well-defined boundary conditions between the two models. Initial and boundary conditions were defined based on the concentration and deposition fields as calculated by means of MSCE-POP model. However, POPs are considered global pollutants due to their persistence and long-range transport potential (Klecka et al., 2000; Scheringer and Wania, 2003). In addition, the global context is not only limited to the atmospheric compartment, but also involves for instance large ocean currents (Lammel, 2007). Hence, PANGEA runs of the considered POPs focusses on continental Europe, but embedded all scenarios in a global context, i.e. the model domain is not restricted to Europe only.

All environmental compartments, underlying environmental fate processes like degradation, diffusion, deposition, re-emission, sedimentation, re-suspension, sorption, etc. including partitioning between compartments and compartment phases as implemented in the PANGEA model are fully described in the PANGEA development handbook (Wannaz, 2010). The PANGEA modelling framework is described in detail in HEIMTSA Deliverable D 2.2.3/4 “Environmental modelling for the HEIMTSA/INTARESE Common Case Study”.

4.5.2 Results: POPs concentrations including BAU and 2°C aim scenarios and comparison of concentration fields

MSCE-POP: Calculations of projections of POP concentration and deposition fields up to 2050 year were performed for two contaminants: PCDD/Fs (indicator congener 2,3,4,7,8-PeCDF) and PCBs (congener PCB-153). The choice of 2,3,4,7,8-PeCDF for evaluation of PCDD/F levels in the environment is conditioned by the fact that it constitutes bulk of the toxicity of PCDD/F mixture both in emissions and the environment (about 30 – 40%). PCB-153 is chosen as a representative of PCB group since it is present in the atmosphere both in gaseous and particle-bound phases. In addition, the information on physical-chemical properties and environmental levels for this congener is the most detailed among PCB congeners. Initial and boundary conditions for regional calculation runs were prepared by calculations by hemispheric calculations from 1970 to 2050 to take into account long-term accumulation in the environmental media and the transport from non-European sources. Emissions for 2000 (base year), 2010, 2020, 2030 and 2050 for regional calculations were prepared within WP5.1 of the Project. Hemispheric emissions for the period from 1970 to 1999 were adapted from emission inventory (Breivik et al., 2007) (high scenario). For the

period from 2000 to 2050 hemispheric emissions were prepared by converting European emissions following the scenarios into hemispheric grid and complementing them by emission data from [Breivik et al., 2007] for non-European areas. Spatial distributions of 2,3,4,7,8-PeCDF air concentrations and deposition fluxes obtained by model simulations for BAU and 450ppm emission scenarios for 2000 and 2050 are shown in Figure 4-17and Figure 4-18, respectively. Note the different scale for BAU 2050 scenarios.

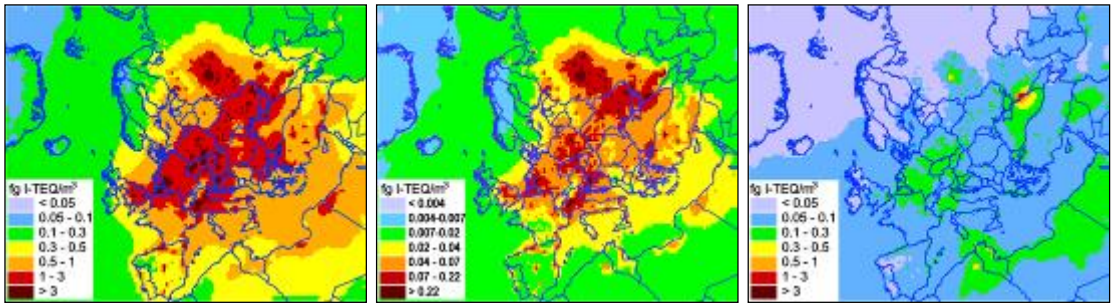

2000 (base) BAU 2050 450ppm 2050

Figure 4-17: Spatial distributions of air concentrations of 2,3,4,7,8-PeCDF for BAU and 450ppm scenarios for 2050 in comparison with those for the base year (2000).

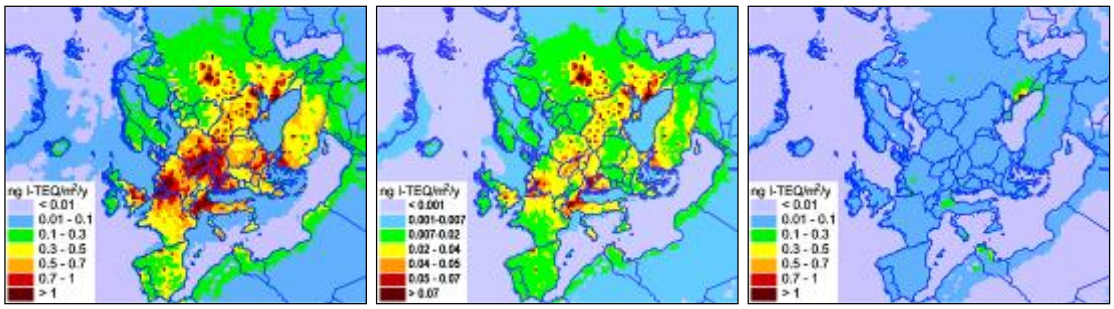

2000 (base) BAU 2050 450ppm 2050

Figure 4-18: Spatial distributions of deposition fluxes of 2,3,4,7,8-PeCDF for BAU and 450ppm scenarios for 2050 in comparison with those for the base year (2000).

Highest reduction of air concentrations and deposition fluxes takes place in western and central parts of Europe. The reduction of 2,3,4,7,8-PeCDF contamination in eastern regions is much weaker. The reduction of pollution levels averaged over the area of all European countries from 2000 to 2050 is shown in Figure 4-19. In general, contamination levels in Europe drops 1.9 times for air concentrations and 2 times for deposition fluxes under BAU scenario and 15 times for air concentrations and 9 times for deposition fluxes under 450ppm scenario.

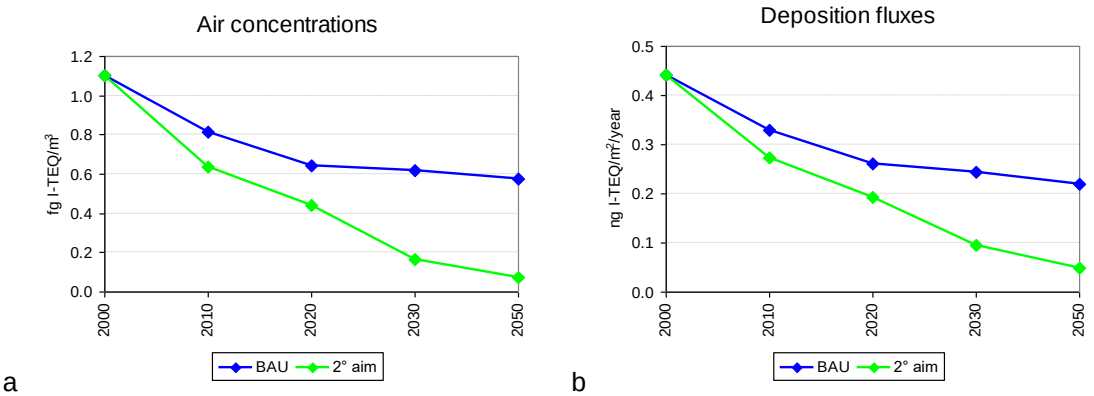

Figure 4-19: Reduction of air concentrations (a) and deposition fluxes (b) of 2,3,4,7,8-PeCDF averaged over the area of European countries for BAU and 450ppm scenarios from 2000 to 2050.

The reduction of air concentrations averaged over the areas of particular countries varies from 1.5 to 2.6 times for the BAU scenario and from 5.1 to 25.9 times for 450ppm scenario. It should be mentioned that the reduction of air concentrations is considerably lower than that of emissions due to the contribution of re-emission process to the formation of air concentrations. The reduction of deposition fluxes of 2,3,4,7,8-PeCDF averaged over particular countries' areas due to BAU scenario vary from 1.5 to 2.5 times. For 450ppm scenario reduction rates are between 4.7 and 13.4. Spatial distributions of PCB-153 contamination (air concentrations and deposition fluxes) obtained by model simulations for BAU and 450ppm emission scenarios are shown in Figure 4-20 and Figure 4-21. Note the different scale for BAU 2050 scenarios.

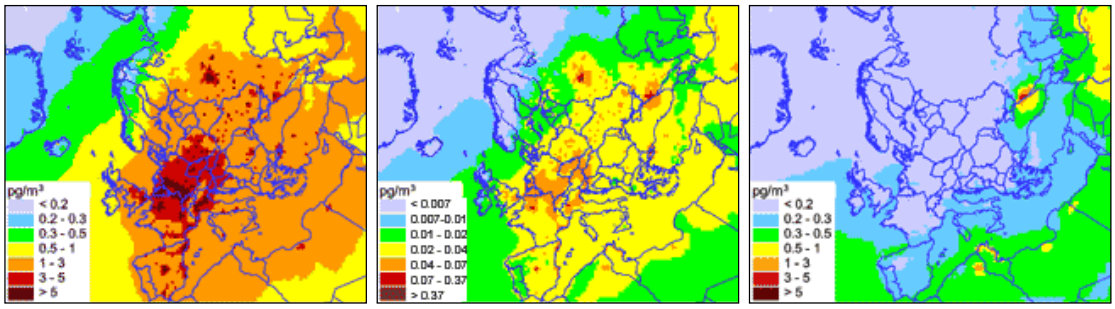

2000 (base) BAU 2050 2ºaim 2050

Figure 4-20: Spatial distributions of air concentrations of PCB-153 for BAU and 450ppm scenarios for 2050 in comparison with those for the base year (2000).

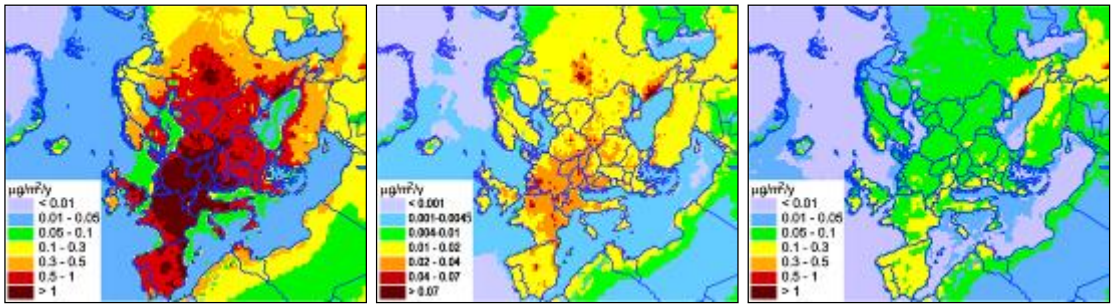

2000 (base) BAU 2050 2ºaim 2050

Figure 4-21: Spatial distributions of deposition fluxes of PCB-153 for BAU and 450ppm scenarios for 2050 in comparison with those for the base year (2000).

The reduction of air concentration levels under 450ppm scenario is much higher than under BAU one. Similar to the case of PCB-153, geographical location can play essential role in the reduction of pollution levels. General trend of the reduction of PCB-153 contamination averaged over the total territory of all European countries is shown in Figure 4-22. Total reduction of air concentrations and deposition fluxes under BAU scenario from 2000 to 2050 is about 4 times. With the 450ppm aim scenario, the reduction of air concentrations and deposition fluxes is 12 and 10 times, respectively.

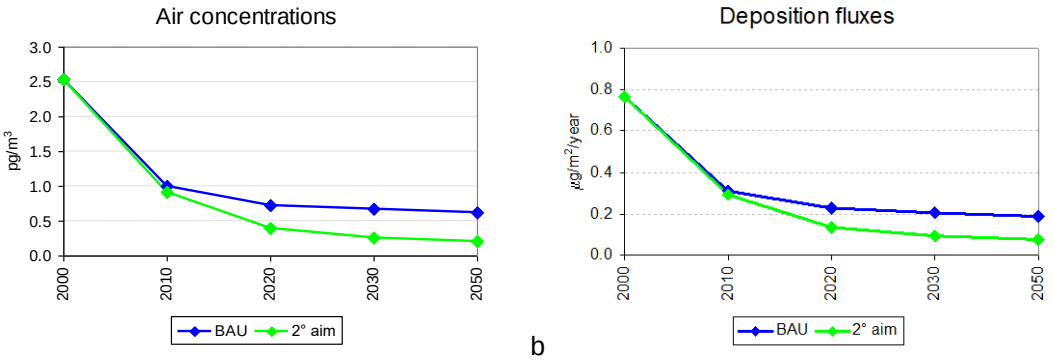

a b

Figure 4-22: Reduction of air concentrations (a) and deposition fluxes (b) of PCB-153 averaged over the area of European countries for BAU and 450ppm scenarios from 2000 to 2050.

For different countries these reductions vary from 2.3 to 4.9 times under BAU scenario and from 3.5 to 22 times under 450ppm scenario. Again it can be noted that the reduction of air concentrations is much slower than that of emissions. In fact, for 450ppm scenario air concentrations are mostly supported by re-emission flux. For example, the projection of emission reduction in the Germany from 2000 to 2050 is accounted to 3.5 and 270 times under BAU and 450ppm scenarios, respectively. However, the reduction of air concentrations differs from emission reduction. Namely, air concentrations under BAU scenario dropped 4.9 times, and under the 450ppm scenario – 20.6 times only. The reduction of deposition fluxes of PCB-153 following the BAU scenario varies between particular countries from 2.1 to 5.1 times. For 450ppm scenario reduction rates are between 4.5 and 18. Thus, for both above considered substances it can be concluded that under strong emission reduction re-emission process can support contamination for long time periods (tens of years).

PANGEA: Initial and boundary conditions were defined based on the concentration and deposition fields as calculated by means of MSCE-POP model and based on harmonization of environmental compartments across the two models MSCE-POP and PANGEA. For the two selected POPs, i.e. PCB-153 and 2,3,4,7,8-PeCDF, not only air (and therewith the concentration in air as calculated by means of the MSCE-POP model), but also other environmental compartments including freshwater, i.e. the continental water network mainly consisting of rivers and lakes, the freshwater body underlying sediment as well as natural and agricultural land. This is due to the fact that assessing human health impacts caused by environmental releases of POPs requires to consider multiple media, whenever organic substances show low degradability, persistence and/or long-range transport potential, as emphasized by e.g. Lammel et al. (2007) and Scheringer et al. (2009). Hence, concentrations in media other than air are shown and discussed in the following as calculated by using the multimedia modelling framework PANGEA.

Concentration of POPs in freshwater is mainly driven by the dry and wet deposition from air, by re-volatilisation to air, by surface water runoff from natural and agricultural land as well as by transport and degradation within the frewhwater compartment itself. Concentrations in freshwater are shown in Figure 4-23 for PCB-153 and in Figure 4-24 for 2,3,4,7,8-PeCDF, respectively.

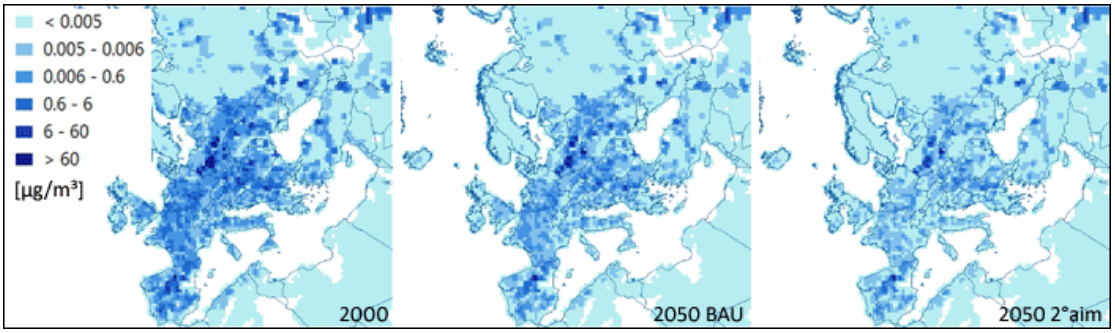

Figure 4-23: Reduction of PCB-153 concentrations in freshwater averaged over the area of European countries for BAU and 450ppm scenarios from 2000 to 2050.

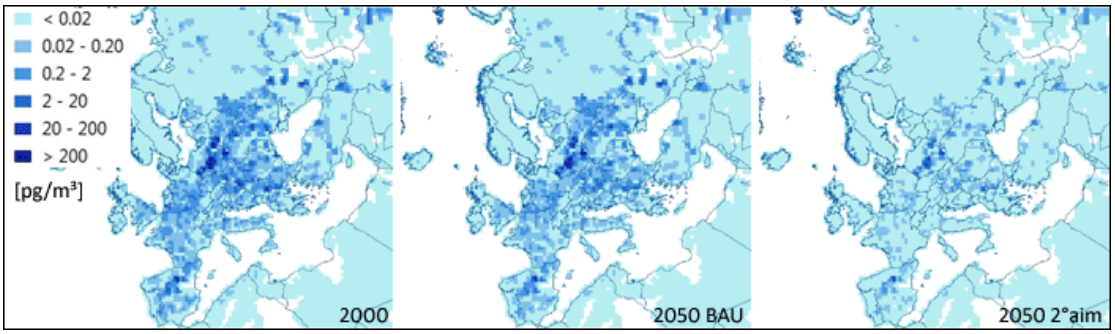

Figure 4-24: Reduction of 2,3,4,7,8-PeCDF concentrations in freshwater averaged over the area of European countries for BAU and 450ppm scenarios from 2000 to 2050.

The highest reduction potential for both POPs in freshwater is found in western Europe. Compared to the PCB-153 concentration, the concentration of 2,3,4,7,8-PeCDF in freshwater is significantly lower. However, the spatial pattern does not change a lot between the scenarios. The concentration reduction of the two POPs in freshwater varies from country to country with Ireland at the lower end with a reduction between 2000 and 2050 of only a factor of 3.36 PCB-153 reduction and a factor of 3.93 of 2,3,4,7,8-PeCDF reduction, and with Belgium at the upper end with a reduction of a factor of around 30 reduction of both POPs.

Concentration of POPs in freshwater sediment is mainly influenced by the transfer processes between freshwater and the underlying sediment including sedimentation, diffusion, adsorption and re-suspension as well as by the degradation in freshwater sediment itself. Concentrations in freshwater sediment are shown in Figure 4-25 for PCB-153 and in Figure 4-26 for 2,3,4,7,8-PeCDF, respectively.

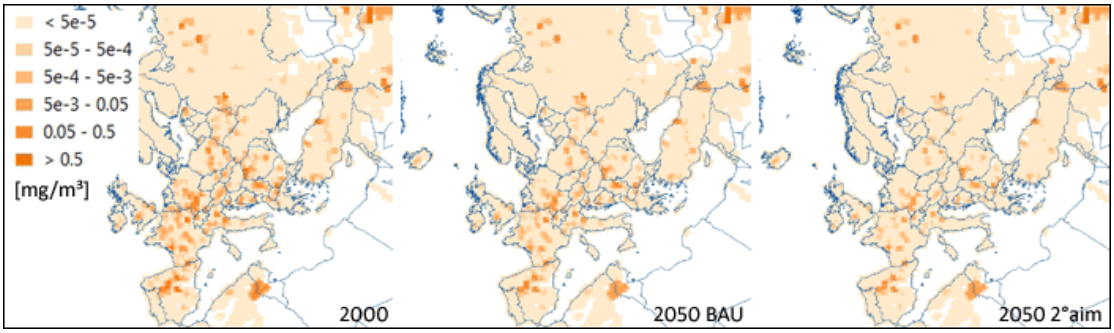

Figure 4-25: Reduction of PCB-153 concentrations in freshwater sediment averaged over the area of European countries for BAU and 450ppm scenarios from 2000 to 2050.

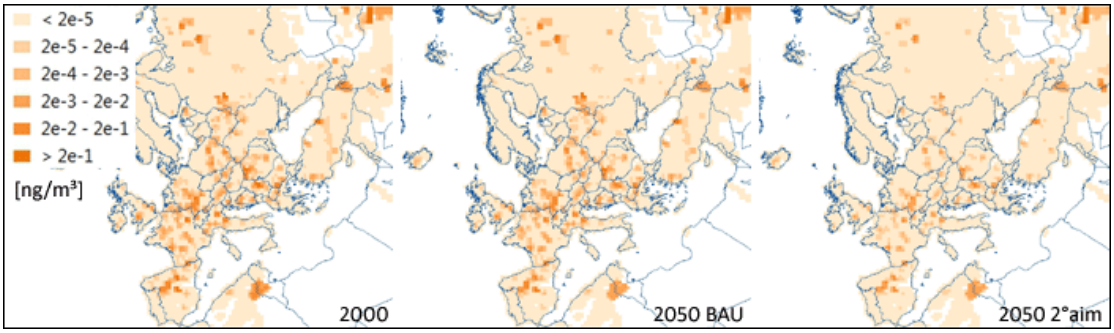

Figure 4-26: Reduction of 2,3,4,7,8-PeCDF concentrations in freshwater sediment averaged over the area of European countries for BAU and 450ppm scenarios from 2000 to 2050.

Similar to freshwater, compared to the PCB-153 concentration, the concentration of 2,3,4,7,8-PeCDF in freshwater sediment is significantly lower. The concentration reduction of the two POPs in freshwater sediment varies from country to country, thereby following the same pattern as for concentration reduction in freshwater, with Ireland at the lower end with a reduction between 2000 and 2050 of only a factor of 3 to 3.5 reduction of PCB-153 and 2,3,4,7,8-PeCDF, and with The Netherlands at the upper end with a reduction of a factor 25 to 28 reduction of both POPs.

Concentration in natural and agricultural land is mainly driven by the dry and wet deposition from air, by re-volatilisation to air, by loss processes from the bulk soil towards freshwater and the saturated sub-surface soil lacer (groundwater table) including most importantly surface water runoff and leaching as well as by the degradation and soil intrinsic inter-phase partitioning in soil itself. In addition, however, the active uptake into vegetation is considered as further loss from bulk agricultural land required for the subsequent human exposure assessment, to which vegetation grown on agricultural land serves as source for human food ingestion as well as for animal feed ingestion. Concentrations in agricultural land are shown in Figure 4-27 for PCB-153 and in Figure 4-28 for 2,3,4,7,8-PeCDF, respectively.

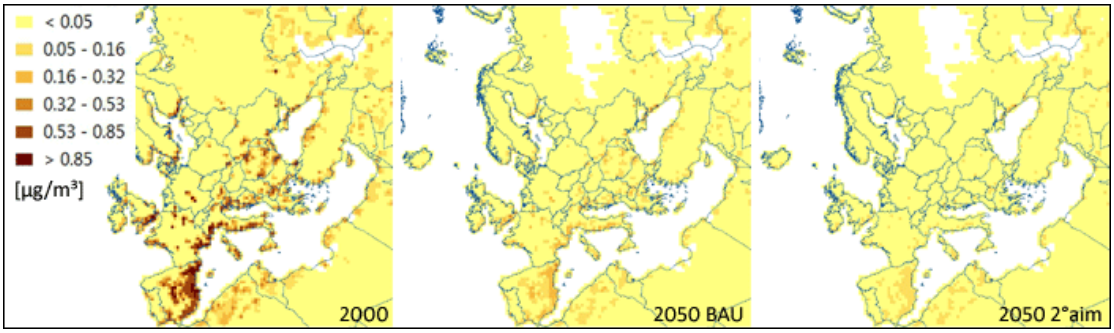

Figure 4-27: Reduction of PCB-153 concentrations in agricultural land averaged over the area of European countries for BAU and 450ppm scenarios from 2000 to 2050.

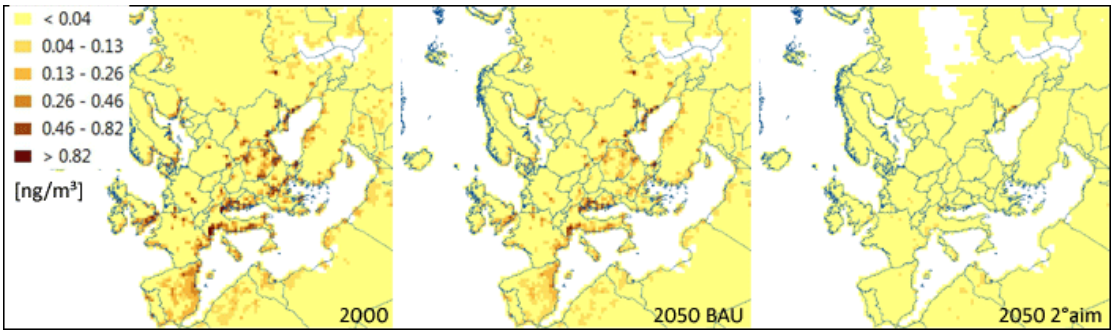

Figure 4-28: Reduction of 2,3,4,7,8-PeCDF concentrations in agricultural land averaged over the area of European countries for BAU and 450ppm scenarios from 2000 to 2050.

Also in agricultural land, the concentration of 2,3,4,7,8-PeCDF is significantly lower compared to the PCB-153 concentration. However, the same as for all other terrestrial compartments, the spatial pattern does not change a lot between the scenarios. The concentration reduction of the two POPs in agricultural land varies from country to country, thereby showing almost the same distribution pattern as reduction in natural land, with Ireland at the lower end with a reduction between 2000 and 2050 of only a factor of less than 3.5 reduction of PCB-153 and 2,3,4,7,8-PeCDF, and with Belgium, Czech Republic, Luxembourg and Switzerland at the upper end with a reduction of a factor between 20 and 22.5 reduction of both POPs.

4.5.3 Uncertainties

MSCE-POP: The overall uncertainty of the model simulating POP fate and transport in the environment can be split into the following groups: (a) Intrinsic model uncertainties. This includes simplifying assumptions in the description of environmental processes included to the model as well as uncertainties if calculation schemes applied. Uncertainties of this group depend just on the model design but do not depend on particular pollutant being considered. (b) Parameterization uncertainties. These are uncertainties in the definition of physical-chemical parameters used in the model for the description of the environmental fate of each particular contaminant. (c) Uncertainties of environmental parameters. This includes

uncertainties in meteorological data, land cover, soil properties, etc. (d) Emission uncertainties. This includes uncertainties in determination both emission totals of particular countries and uncertainties in the determination of emission spatial distribution. Additional emission uncertainties can be related to the determination of emission height, temporal variations, etc.

Evaluation of uncertainties from the first three groups for pollutants included into the scope of EMEP activities (in particular, PAHs, PCBs and PCDD/Fs) was performed in the course of the EMEP model review in 2005 (see Gusev et al., 2005). The uncertainties in air concentrations and deposition are evaluated as 30% and 40%, respectively if only parameterization uncertainties are taken into account. For combined influence of first three uncertainty groups uncertainty in calculations of air concentrations is evaluated as 50% and in calculations of deposition flux - as 70%.

One more direction of the model review was the comparison of modelling results with available measurement data. In particular, for 2,3,4,7,8-PeCDF it was concluded that about 50% of calculated values of concentrations agree with measurements within a factor of 2 and about 60% - within a factor of 3. This is exemplified by comparison with measurements at Bayreuth (Germany) and Hazelrigg (the UK) in Figure 4-29.

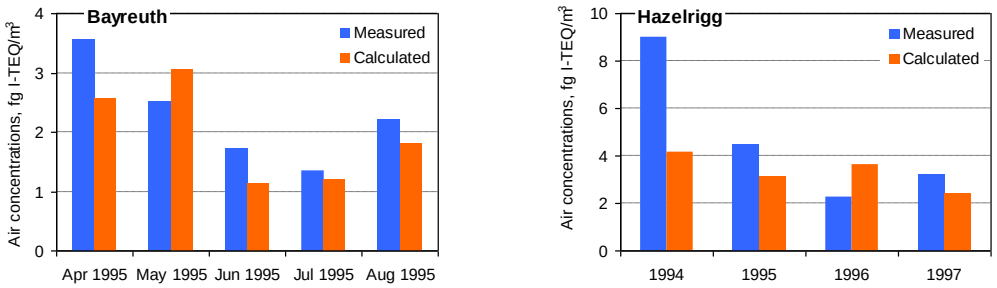

Figure 4-29: The comparison of 2,3,4,7,8-PeCDF air concentrations calculated by MSCE-POP model with measurements at Bayreuth and Hazelrigg.

Unfortunately, the lack of measurement data on PCDD/Fs at European background sites hampers carrying out reliable comparison of calculated results with measurements. The comparison of calculated PCB-153 air concentrations with available measurement data for a number of EMEP monitoring sites is shown in Figure 4-30.

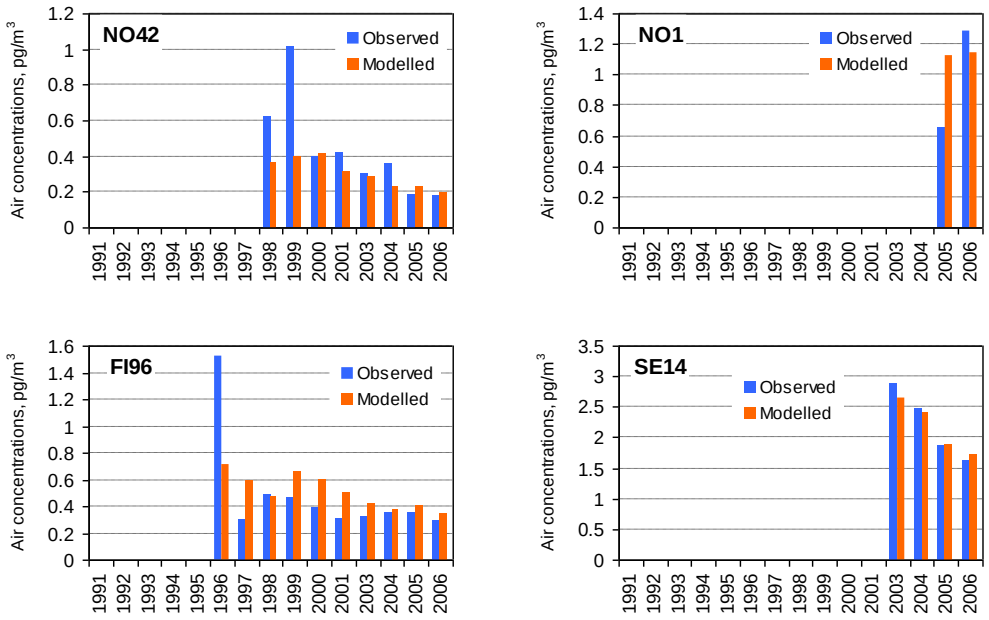

Figure 4-30: The comparison of PCB-153 air concentrations calculated by MSCE-POP model with measurements at a number of EMEP sites.

In general, it can be concluded that most of calculation values of PCB-153 agree with available measurements within a factor of three.

PANGEA: The overall uncertainty of the PANGEA model simulating environmental fate of organic substances, more specifically POPs, can be split into the following groups: (a) Intrinsic model uncertainties. This includes simplifying assumptions in the description of environmental processes. These uncertainties only depend on the model design, but not on substance properties or scenario characteristics. (b) Parameter uncertainties of substances. These uncertainties are related to the definition of physical-chemical substance parameters for describing the environmental fate processes. (c) Parameter uncertainties of boundary conditions and environmental compartments. These uncertainties refer to assumptions for environmental data, such as rain rate, soil properties, etc., most importantly their spatial distribution at the European scale. (d) Input data uncertainties. These uncertainties are related to the input provided by e.g. other models, such as MSCE-POP for air concentrations and deposition fields, as well as related to emission conditions.

Evaluation of uncertainties included the comparison of modeling results against independent data from experimental studies. All model results are within the range of a factor between 2 to 10 compared with measured concentrations for all considered compartments, more specifically with respect to concentrations in freshwater, freshwater sediment, natural land and agricultural land. Measurement data for evaluation of model results, i.e. concentrations of PCB-153 and 2,3,4,7,8-PeCDF in different environmental media are available e.g. in BLMP (2005), Iljina (2007), Meijer et al. (2003), Motelay-Massei et al. (2004), Seike et al. (2007), Schuhmacher et al. (2006) and Sharma et al. (2007).

4.6 FATE AND EXPOSURE ASSESSMENT OF PESTICIDES

4.6.1 Atmospheric fate modelling of indirect pesticide emissions

Methodology: Calculations of projections of trifluralin air concentrations for 2020 were performed using MSCE-POP model on regional scale as described in Section 4.5.1.

Results: Due to relatively short residence time of the contaminant in the environment (for example, half-life in soil is estimated as about 60 days) and moderate ability to long-range transport, no preliminary runs by hemispheric model version are used. Since the levels of atmospheric concentrations for trifluralin strongly depend on emission seasonal variations, additional calculations with conventional seasonal variations of emissions were performed. These calculations showed that air concentrations of trifluralin calculated taking into account conventional seasonal variations of its emissions are essentially lower than those calculated under assumption of uniform temporal distribution of emissions. This is conditioned by strong temperature dependence of trifluralin degradation rates. As a result, if essential mass of the pollutant is emitted in summer months, total trifluralin degradation is higher due to higher temperature. However, since no data of trifluralin emission seasonal variations are available, below the results obtained under the assumption of uniform temporal distribution of emissions over the year are presented.

Spatial distributions of air concentrations calculated under BAU and 450ppm scenarios are presented in in Figure 4-31. These results were obtained under the assumption of uniform distribution of emissions throughout the year.

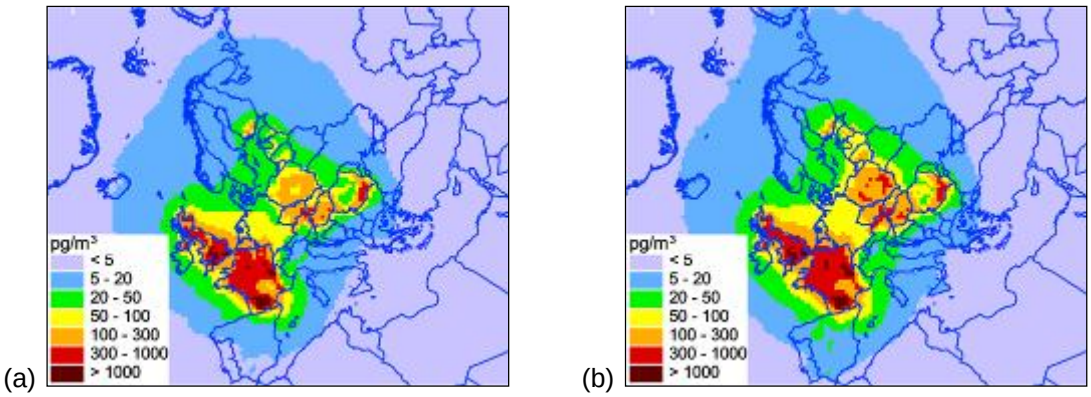

Figure 4-31: Spatial distributions of air concentrations of trifluralin for BAU (a) and 450ppm (b) scenarios for 2020 calculated by MSCE-POP model.

It is seen that spatial distributions of air concentrations are rather similar for BAU and 450ppm scenarios though in general concentrations under 450ppm scenario are somewhat higher. The comparison of air concentrations averaged over European countries calculated under BAU and 450ppm scenarios is given in Figure 4-32.

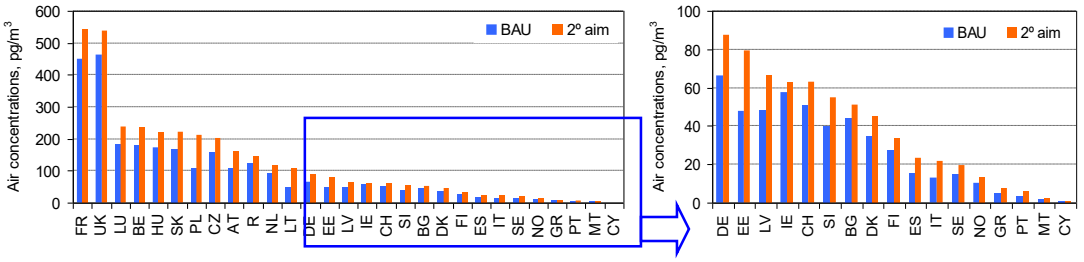

Figure 4-32: Air concentrations of trifluralin for BAU and 450ppm scenarios for 2020 averaged over European countries (MSCE-POP model calculations).

It can be seen that maximum concentration levels are reached in the countries with high emissions (France and the UK). However, air concentrations comparable with those in countries with moderate emissions are calculated for Luxembourg, Belgium and the Netherlands where emissions are essentially lower. This manifests the importance of transboundary transport in formation of contamination levels in Europe.

Uncertainties: Uncertainties related to the assessment of trifluralin air concentrations for 2020 were assessed using MSCE-POP model on regional scale as described in Section 4.5.3. It should be noted that calculated air concentrations agree in order of magnitude with available measurements (see Vulyh et al., 2009).

4.6.2 Environmental fate and ingestion exposure modelling after direct application

Methodology: To assess environmental fate and ingestion exposure of pesticides after direct application, the dynamiCROP model was used, i.e. a dynamic framework for the quantification and valuation of human health impacts caused by the direct application of plant protection products onto agricultural field crops, such as wheat, and subsequent intake by humans via ingestion. The modelling framework is based on a crop-specific multi-compartment system and analyses the mass evolution in the different compartments of the system over time. The underlying analytical first order differential equations are solved by means of matrix algebra. Despite the fact that the dynamiCROP model domain is aspatial, the assessment of human health impacts can be performed in a spatial differentiated way according to the underlying input parameters, such as application pattern, crop production area, population etc.

The physical multimedia plant-environment system consists of environmental compartments (i.e. atmospheric ground layer, paddy water layer, wich is only relevant for paddy rice, and root-zone soil layer) and vegetation compartments (i.e. leaf and fruit surface deposit, leaf and fruit interior, stem and root including thick root and fine root system). In contrast to many existing plant uptake models (e.g. Charles, 2004, Contreras et al., 2008), the protected grains of cereals are explicitly taken into account as separate compartment for substance accumulation. Hence, the model output can directly be compared with measured residues in the edible parts of these agricultural crops and contrasted to MRLs as stated according to current legislation. The

dynamiCROP modelling framework is described in detail in HEIMTSA Deliverable D 2.2.3/4 “Environmental modelling for the HEIMTSA/INTARESE Common Case Study”.

Results: Some of the pesticides foreseen to be considered in the Common Case Study have already been excluded from the Annex I of 91/414/EC as of 2010 (EC, 1991; EC, 2009) and, thus, are not allowed for further usage on field crops including cereals, maize and oilseeds in the EU. Hence, all substances already banned were reallocated to the considered substances which remained avialable for future usage, i.e. which are included in Annex I of 91/414/EC, under the assumption that they will be included also in future years due to lack of further knowledge of which pesticides will be available and authorised for use in future years. The final set of selected substances accounts for approximately 90% of total application amount of pesticides in Europe.

The evolution of pesticide masses in harvested crops under realistic assumptions (i.e. multiple applications, varying growth stages of the considered crops, etc.) serve as input into the subsequent human exposure assessment. A typical mass evolution in edible components of harvested maize for a cascade of four applications of the fungicide cymoxanil (in line with current agricultural practice, see e.g. BVL, 2010) is shown in Figure 4-33 as an example of a realistic application scenario of pesticides according to the standards of good agricultural practice in Europe.

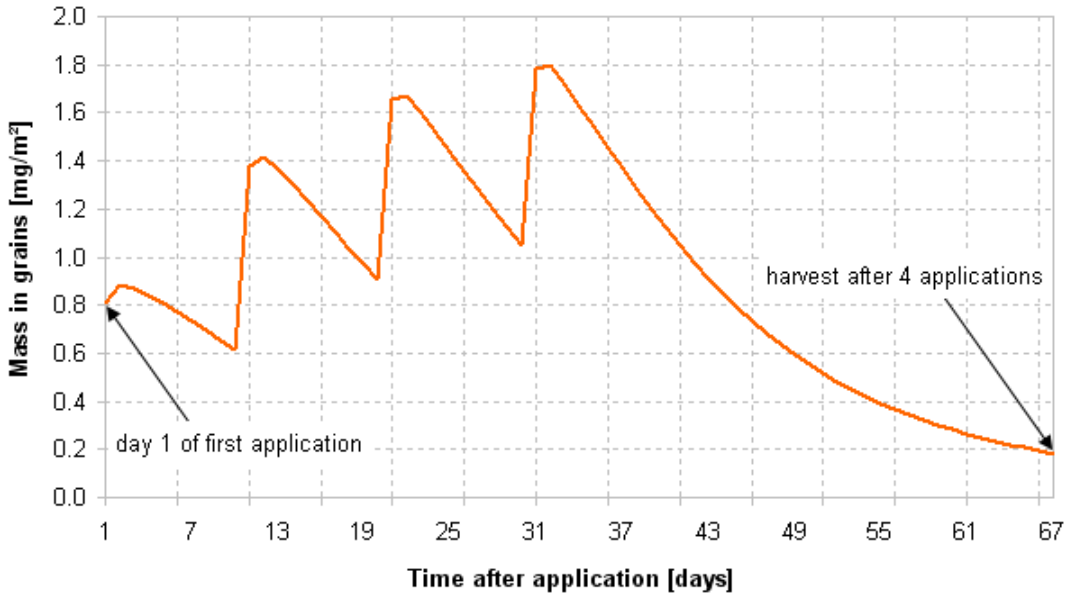

Figure 4-33. Mass evolution of cymoxynil [kg substance/m² treated area] in maize over a time period of 67 days for a cascade of 4 consecutive applications.

As can be seen in Figure 4-33, the driver of the substance mass at harvest time is the last pesticide application before harvest only. All other applications that are prior to the last application before harvest do only negligibly contribute to the overall substance mass at harvest time. Based on these findings, onyl the latest application of the considered pesticides is accounted for for calculating the masses at harvest time in the respective crop components and the subsequent human ingestion intake fractions per country. The distribution pattern of the intake fraction via ingestion of pesticides containing crops are very heterogeneous, i.e. the ingestion intake fraction varies from

5E-03 kg intake per kg applied substance in Italy to 9E-06 kg intake per kg applied substance in Luxembourg. In addition, it can be seen from that same figure that in most countries that largest share of intake is caused by the residue of herbicides and in some countries by the residue of fungicides in crops, while insecticides and plant growth regulators usually only contribute with a smaller fraction to the overall residue due to the relatively small application amount compared with e.g. herbicides. Note that the residues are not necessarily stemming from the same country, since import and export was considered before intake of the respective food crops in a particular country.

The reduction between the climate and the BAU scenarios in each year is mainly caused by the assumptions behind the selection of the areas reserved for food crop production. In the BAU scenarios, on the one hand, the main factor reducing the food crop production area is the increase in area used for energy crop production, which is in line with the larger contribution of renewable energies on the energy mix in future years (see Chapter 3). In line with this development, the lack in food production must be compensated by the import of food crops with higher loadings of pesticides according to less restrictive good agricultural practice outside Europe compared to EU regulations – an information that can be e.g. derived from different MRLs in the EU and other countries (Drogue and DeMaria, 2010). On the other hand, in the climate scenarios, in some countries the overall area available for food crop production is still less than in the baseline scenario, but compared to BAU scenarios in the same years as the climate scenarios the area available for food crops is slightly larger, which is due to the effect of less energy consumption compared to BAU scenarios, thereby also reducing the area used for energy crop production. In other countries, however, there is an increase of intake even higher than in the corresponding BAU scenarios, which is mainly due to the different assumptions behind the crop yield in the different scenarios.

Uncertainties: The overall uncertainty of the dynamiCROP model simulating environmental fate and ingesion exposure of pesticides after direct application onto field crops can be split into the following groups: (a) Intrinsic model uncertainties. This includes simplifying assumptions in the description of environmental processes. These uncertainties only depend on the model design, but not on substance properties, crop properties or scenario characteristics. (b) Parameter uncertainties of substances. These uncertainties are related to the definition of physical-chemical substance parameters for describing the environmental fate processes. (c) Parameter uncertainties of crops. These uncertainties are related to the simplifications of crop components and life cycle stages. (d) Parameter uncertainties of boundary conditions and environmental compartments. These uncertainties refer to assumptions for environmental data, such as rain rate, soil properties, etc. (d) Initial conditions uncertainties. These uncertainties are related to the application techniques and country-specific pesticide application rates.

Evaluation of uncertainties included (a) parameter uncertainties with main focus on the aggregated environmental fate processes expressed as transfer rate coefficients, each coefficient representing an aggregated set of underlying phyisical processes including

degradation, diffusive and advective transfers, (b) scenario uncertainty with respect to the different substance-crop combinations as well as (c) the comparison of modeling results against independent data from experimental studies.

For assessing the sensitivity of the model output an analytical Taylor series expansion algorithm was implemented based on concepts described in Hong et al. (2010) and Imbeault-Tétreault et al. (2010). In Figure 4-34, the contribution of all considered rate coefficients to the sensitivity of the model output is presented.

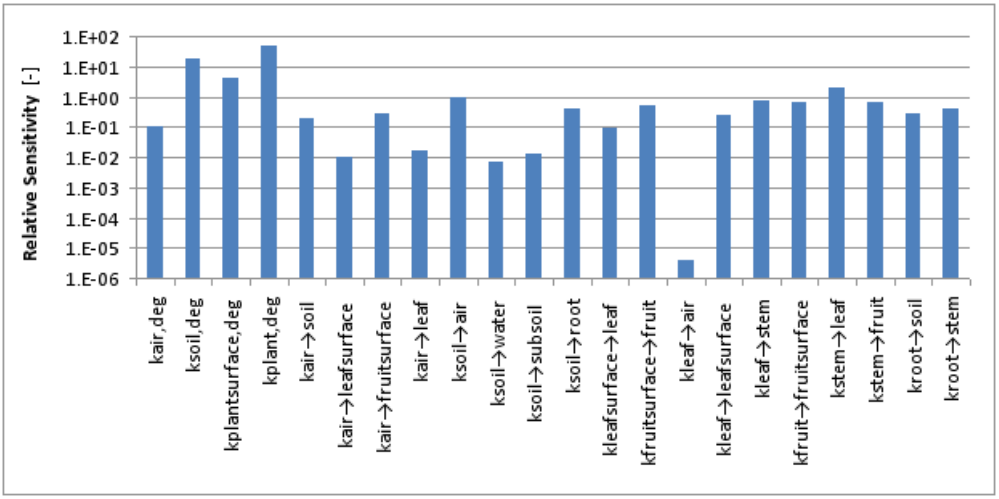

Figure 4-34: Relative sensitivity of dynamiCROP model (example: azoxystrobin residues in harvested cereals) to variation in aggregated input parameters, i.e. contributing rate coefficients *k* either referring to degradation rate (*deg*) or intermedia transfer rate from source medium to target medium (indicated by direction of *arrows*).

It can be seen that the degradation rate in plant interior as well as in soil is predominating the sensitivity of the system, which is due to the facts that (a) soil can be identified for most pesticides as dominating the long-term behaviour of the whole compartmental system with the smallest half-life of the pesticides in contrast to the half-lives in the other compartments and (b) plant-internal translocation and degradation processes finally are responsible for the behaviour of the system during plant growth as well as during intial conditions, i.e. where leafe area and plant transpiration rate play a significant role.

Uncertainties related to different substance-crop combinations vary up to 2 orders of magnitude, mainly influenced by the substance-specific physicochemical properties and the crop-specific properties, which vary up to 14 orders of magnitude for example in Kow values of substances and up to a factor of 5 in substance capture values of crops.

In addition to a parameter sensitivity analysis and uncertainties between different substance-crop combinations, all results have been compared with (a) independent data that were experimentally derived and (b) against current legal European Maximum Residue Levels (MRLs) as stated by the European Commission (EC, 2005). All results are well in line with measured data, i.e. modeled and measured concentrations fitted very well at harvest and deviated over time from less than a factor of two for glyphosate on cereals to more than two orders of magnitude for prosulfocarb

on oilseeds, when accounting for lower detection limits in the latter. In addition, model results are all below existing MRLs according to good agricultural practice.

4.6.3 Inhalation exposure modelling after direct application

Methodology: The Intake fraction (iF) relates population exposure directly to the source that emits the pollutants. It is defined as the integrated incremental intake of a pollutant released from a source, summed over all exposed individuals during a given exposure time, per unit of emitted pollutant (Bennett et al., 2002):

$$iF = \frac{\sum_{people,time} \text{mass intake of pollutant by an idividual}}{\text{mass release into the environment}} \qquad \text{(Eq. 4-2)}$$

on the assumption that iF refers to Intake fraction of an average person. An Intake fraction of 10^{-6} means that for every million grams emitted, one gram is inhaled an exposed person. In Figure 4-35 local emissions to air and intake rate for carcinogenic pesticides in EU27 for the baseline year 2000 are depicted, respectively.

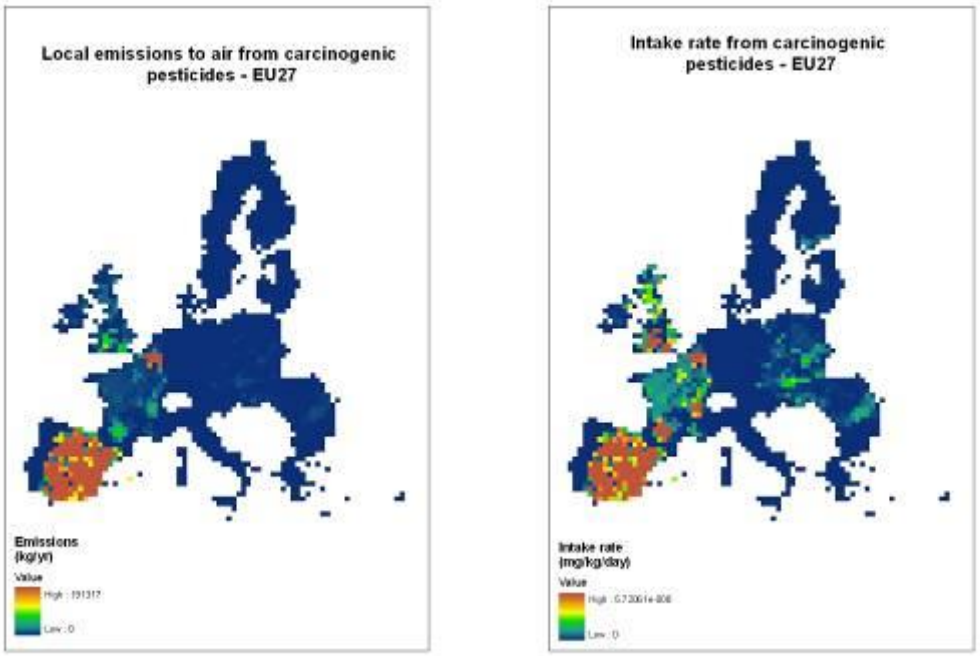

Figure 4-35: Local emissions to air and intake rates from carcinogenic pesticides for EU 27 (year 2000).

4.6.4 Conclusions

Out of the set of selected pesticides, trifluralin was chosen as representative substance to compare ingestion intake with inhalation intake at the European level, where the former is based on dynamically assessing ingestion exposure with the dynamiCROP model and the latter is based on environmental fate modeling including long-range transport by means of MSCE-POP model, both as described above. The purpose was to directly compare the relative importances of the different exposure pathways. The results of this section demonstrate that intake of pesticides from air after atmospheric dispersion modelling as well as intake of pesticides from the different food crops after multimedia plant uptake modelling are highly heterogeneous. Average annual individual intake of trifluralin via inhalation exposure varies from some mg to less than a µg. In contrast, average annual individual intake of trifluralin via ingestion exposure varies from some grams to some ten mg. These results underline the fact that ingestion exposure is by far the predominant exposure route for directly applied pesticides, which is in line with state-of-the-art knowledge on pesticide exposure according to e.g. Margni et al. (2002), Charles (2004), Humbert et al. (2007) and Juraske et al. (2009a,b).

4.7 EXPOSURE TO HEAT

4.7.1 Methodology

Evaluation of the European wide health impacts of heat exposure in large cities requires determination of the weather conditions and the number and characteristics of population living within the cities. This depends on how a large city is defined. In the context of this assessment, the number and geographical location of large cities was based on EMEP grid level data on total population. If the population density within a grid cell surpassed 200 per square kilometre (i.e. 500,000 within a 50 km x 50 km grid cell), the grid cell was considered to represent a large city. The number of people living in the cities was then defined based on EMEP grid level data on the fraction of the total population living in an urban as opposed to rural environment in each grid cell (see Section 4.1.2 for more information on the population data). The mortality impacts of heat exposure were evaluated based on meta-analytical exposure-response functions for two sub-regions of Europe, North-continental and Mediterranean. Because of this, the cities (i.e. grid cells considered to represent a large city) were classified into one of the sub-regions based on the country in which they reside:

- North-continental: Austria, Belgium, Czech Republic, Denmark, Estonia, Finland, France, Germany, Hungary, Ireland, Lithuania, Luxemburg, Netherlands, Poland, Slovakia, Sweden, United Kingdom
- Mediterranean: Greece, Italy, Malta, Portugal, Slovenia, Spain

The impact assessment of heat exposure includes fewer countries than the sub-assessments within the Common Case Study on other environmental exposures. This is because of a lack of data on the fraction of urban population on EMEP grid level in Bulgaria, Cyprus, Iceland, Latvia, Norway, Romania and Switzerland. Heat exposure high enough to lead to increased mortality in reference and policy scenarios was evaluated by determining the number of days between April and September when the sub-region-specific apparent temperature (AT) threshold (North-continental 23.3°C (95% CI 22.5-24), Mediterranean 29.4°C (25.7-32.4)) is exceeded. These days were then classified into different exposure classes based on the level of threshold exceedance on 1°C accuracy. Apparent temperature (AT) is a measure of relative discomfort of heat and is derived from air temperature (Temp) and dew point (Dew) as follows: $AT = -2.653 + 0.994\ Temp + 0.0153\ (Dew)^2$

In the reference scenarios, city-specific daily maximum apparent temperatures were calculated based on EMEP grid level data on hourly air temperatures and dew points modelled for IPCC climate scenarios A1B (corresponds with reference scenario 1) and B1 (corresponds with reference scenario 2) using the Max Planck Institute for Meteorology Regional Model (REMO). Reductions in the city-specific temperatures due to the different UHI mitigation policies were estimated by first subtracting the policy-specific city-wide average decrease in the near-surface air temperature (see Section 3.5) from the daily maximum air temperature in each city. The daily maximum apparent temperature (AT) was then calculated based on this and the original dew point data. The methodology for heat exposure assessment and uncertainties related to it are described in more detail in Annex A.2.

4.7.2 Results

Table 4-7 provides indicators on how the heat exposure in large European cities will change in the future in the reference scenarios and in case different urban heat island mitigation policies are implemented. Heat sum is an indicator derived by adding up the temperature threshold exceedance from all days between April and September. The range in the estimates is based on the 95% confidence limits for the sub-region specific temperature thresholds. In the reference scenario 1, heat exposure increases in both sub-regions over the years. By 2050, the average exposure in the North-continental cities is estimated to be 200% and in Mediterranean cities 68% higher than in the current climate conditions. In the reference scenario 2, the exposure in the North-continental cities first increases, but then begins to decrease by 2050. In the Mediterranean region, the exposure levels in reference scenarios are more similar but somewhat lower in the later years in the scenario 2. Increasing both trees and surface albedo would result in approximately 14% reduction in the exposure averaged over all large cities, while increasing albedo alone would decrease exposure by 11% and increasing trees by 4%. The effects of UHI mitigation policies are similar across both IPCC climate scenarios and sub-regions. Of the total population, approximately 46% in the North-continental countries and 40% in the Mediterranean countries were estimated to live in large cities, but there were substantial differences between

countries. The main uncertainties in the assessment relate to the reliability of the temperature data, the methodology for estimation of the exposed population and the impact of the mitigation measures on city-wide air temperatures and heat exposure. The results of the assessment and uncertainties are discussed in more detail in Annex E (Annexes

Heat and Urban Heat Island (UHI) Mitigation).

Table 4-7: Average daily maximum apparent temperature, no. of days when temperature threshold is exceeded, the average exceedance on these days, and heat sum (95% confidence limits) in April-September averaged over all large cities. The temperature thresholds: North-continental region 23.3°C (22.5-24.0), Mediterranean region 29.4°C (95% CI 25.7-32.4).

		North-continental cities				Mediterranean cities			
Climate scenario & year	Reference / UHI mitigation scenario	Averge daily max AT (°C)	No. days above threshold	Average threshold exceedance (°C)	Heat sum (°C)	Averge daily max AT (°C)	No. days above threshold	Average threshold exceedance (°C)	Heat sum (°C)
2010	Current	16.9	27 (23-32)	4.0 (4.0-4.2)	107 (90-130)	24.2	51 (29-79)	4.5 (3.5-5.8)	222 (103-458)
A1B									
2020	Reference 1	17.7	31 (27-34)	4.8 (4.7-5.1)	147 (127-172)	24.4	50 (31-80)	4.6 (3.6-5.8)	227 (109-465)
	Vegetation	17.5	30 (27-33)	4.8 (4.6-5.0)	141 (121-166)	24.2	49 (30-78)	4.6 (3.5-5.7)	218 (104-449)
	Albedo	17.1	28 (25-32)	4.7 (4.5-4.9)	131 (113-155)	23.9	46 (28-76)	4.5 (3.4-5.6)	202 (94-424)
	Veg+alb	16.9	27 (24-31)	4.6 (4.4-4.9)	126 (108-149)	23.7	45 (27-74)	4.4 (3.3-5.6)	194 (89-409)
2030	Reference 1	19.2	43 (38-49)	4.6 (4.4-4.7)	194 (166-230)	25.7	72 (43-101)	4.5 (3.4-6.3)	312 (145-631)
	Vegetation	19.0	42 (36-48)	4.5 (4.4-4.7)	186 (159-221)	25.5	70 (41-99)	4.4 (3.3-6.2)	299 (136-612)
	Albedo	18.7	39 (34-45)	4.5 (4.4-4.6)	173 (147-206)	25.1	66 (38-97)	4.3 (3.2-6.0)	277 (123-579)
	Veg+alb	18.5	38 (33-44)	4.4 (4.3-4.6)	165 (141-197)	25.0	64 (37-96)	4.2 (3.1-5.9)	264 (116-560)
2050	Reference 1	20.5	63 (57-70)	5.2 (5.0-5.4)	323 (281-375)	26.5	75 (48-103)	5.1 (3.9-6.8)	373 (191-702)
	Vegetation	20.3	61 (55-68)	5.1 (4.9-5.4)	311 (270-362)	26.3	74 (47-101)	5.0 (3.9-6.8)	359 (181-682)
	Albedo	19.9	59 (52-65)	5.0 (4.9-5.3)	291 (252-340)	26.0	71 (44-99)	4.8 (3.8-6.6)	336 (166-648)
	Veg+alb	19.8	57 (51-63)	5.0 (4.8-5.2)	280 (242-327)	25.8	69 (42-98)	4.8 (3.7-6.5)	322 (158-629)
B1									
2020	Reference 2	17.9	32 (28-37)	4.6 (4.5-4.7)	146 (126-174)	25.1	58 (33-88)	4.2 (3.2-5.7)	238 (106-505)
	Vegetation	17.7	31 (27-35)	4.6 (4.5-4.7)	140 (121-167)	24.9	56 (31-86)	4.2 (3.1-5.7)	228 (100-488)
	Albedo	17.3	29 (25-33)	4.6 (4.4-4.7)	131 (112-155)	24.5	53 (29-83)	4.1 (3.1-5.5)	210 (89-459)
	Veg+alb	17.1	28 (25-32)	4.5 (4.3-4.6)	125 (107-149)	24.3	51 (27-81)	4.0 (3.0-5.5)	200 (84-443)
2030	Reference 2	17.5	35 (32-40)	5.2 (5.1-5.4)	182 (159-212)	25.3	65 (39-94)	4.6 (3.5-6.2)	288 (136-580)
	Vegetation	17.3	34 (30-38)	5.2 (5.0-5.3)	175 (153-204)	25.1	63 (38-92)	4.5 (3.4-6.1)	276 (129-562)
	Albedo	17.0	33 (29-37)	5.1 (5.0-5.3)	164 (143-192)	24.8	60 (36-90)	4.4 (3.3-5.9)	256 (117-531)
	Veg+alb	16.8	32 (28-36)	5.1 (4.9-5.2)	158 (137-185)	24.6	58 (34-88)	4.3 (3.2-5.8)	245 (110-514)
2050	Reference 2	18.1	27 (23-32)	4.5 (4.5-4.5)	120 (102-143)	25.8	66 (44-92)	5.2 (4.1-6.8)	340 (177-630)
	Vegetation	17.9	26 (22-31)	4.5 (4.4-4.5)	115 (98-137)	25.6	65 (42-91)	5.2 (4.0-6.7)	327 (169-612)
	Albedo	17.5	24 (21-29)	4.5 (4.4-4.5)	106 (91-127)	25.3	62 (40-88)	5.0 (3.8-6.6)	306 (155-582)
	Veg+alb	17.3	23 (20-27)	4.4 (4.4-4.5)	102 (87-122)	25.1	60 (39-87)	5.0 (3.8-6.5)	295 (147-565)

5 HEALTH EFFECTS CAUSED BY AIR POLLUTANTS

5.1 EXPOSURE RESPONSE FUNCTIONS

5.1.1 Generic methodology

The health effects of simple pathway pollutants were calculated using impact functions. Each impact function is comprised of three basic components: the concentration-response function (CRF), the background rate of disease within the population and the proportion of the population exposed. Details of each of these components are summarised below. The exception to this basic methodology is the relationship between exposure to air pollution and mortality which is described separately in Section 5.1.3.

Impact functions

Identification of concentration-response functions

In the early years of HEIMTSA, a scoping study was carried out which identified the health effects associated with a wide range of pollutants. Health effects related to with both long and short term exposures were described and those health effects for which quantified CRFs are available were identified. In addition, more detailed work on selected pollutants was carried out for the HEIMTSA and INTARESE case studies. For the common case study, the scoping reports and case study reports for the selected pollutants were reviewed, and updated where newer, relevant information was available.

The CAFE report (Hurley et al, 2005) was used as a starting point for identifying CRFs for outdoor air pollution. Quantification in CAFE had been based on relationships of health with particulate matter (PM, expressed variously as PM_{10} or $PM_{2.5}$) and ozone. The Common Case Study, like CAFE, focuses on EU-wide health impacts of EU-wide policies and measures; and for the CCS we decided, once again, to base quantification on CRFs in PM and in O_3.

Within the framework of quantifying the health effects of air pollution via CRFs in PM and ozone, an update of the CRFs reported in the CAFE report was considered for health endpoints which were known to strongly influence the overall outcome of the health impact assessment (Watkiss et al, 2005). These were:

- Effects on mortality in adults of long-term exposure to $PM_{2.5}$
- Development (new cases) of chronic bronchitis and long-term exposure to PM; and
- PM, ozone and Restricted Activity Days.

We have done substantial additional work on mortality in adults and long-term exposure to $PM_{2.5}$ which, in many applications, is the dominant health effect of air

pollution (Watkiss et al, 2005). This work is described briefly in Section 5.1.3 below and in more detail in the Outdoor Air Pollution Case Study Final Report (D3.1.2/3/4). CRFs for the relationships between PM_{10} and chronic bronchitis and respiratory hospital admissions were the only morbidity CRFs updated from the CAFE report – chronic bronchitis because it is influential; respiratory hospital admissions because they are a very widely studied health outcome, and INTARESE colleagues at IRAS had carried out a new meta-analysis. Other health endpoints for air pollution either contributed only a small amount to the overall health impacts of air pollution, or had no new information available.

Identification of background rates

Availability of background rates was reviewed for each of the identified health endpoints. The most recent rates for the EU as a whole were sought from sources including national statistics, WHO databases and multi-centre studies. In sourcing the background rates, a general hierarchy was used to determine the most appropriate rate to be included. Firstly, data from national statistics and WHO databases were used. If no information was available then information from multi-centre studies from multiple countries was used. Finally, single country studies were used, as was the case for respiratory symptoms, with an assessment of the transferability of the background rate from the study population to the entire EU. Where feasible, rates from European studies were used but in a few instances (e.g. Restricted Activity Days) only data from the US were available.

For some health endpoints, rates for the EU as a whole were not available in the required format and in these cases, relevant rates were extracted for individual countries and an EU rate derived by combining these with adjustment for differing population sizes. For health endpoints associated with air pollutants, most of the background rates used were those from CAFE (Hurley et al, 2005) as these were the most up-to-date available, or were for health endpoints which contributed very little to overall health impact from air pollutants.

Calculation of impact functions

The simplest case for calculating an impact function occurs when the total population is exposed; the CRF is a relative risk and the background rate of disease refers to annual incidence or prevalence. In this calculation the CRF is multiplied by the background rate of disease within the population to obtain an impact function expressed as the number of additional cases of disease per 10 $\mu g/m^3$ of pollutant per 100,000 population per year.

In many instances the information available is not in the required form and it is necessary to adapt what is available into the form required for the calculation described above. This includes addressing issues such as:

- CRFs expressed as Odds Ratios rather than relative risks
- Diseases where background rates need to be adjusted for disease remission
- Background rates which apply to different time periods (e.g. per day rather than annual)
- Pollutants for which not all of the population are exposed, so that background rates need to be adjusted to apply to the unexposed population only
- Converting CRFs from one exposure metric to another (e.g. from PM_{10} to $PM_{2.5}$)

Details of how the CRFs were converted from one exposure metric to another are shown in Section 5.1.2 below. Details of how the other issues have been addressed in the common case study are described in the Impact Functions deliverable (D3.1.2/3/4).

Table 5-1 summarises the outdoor air pollution and personal exposure impact functions calculated for the common case study. The table includes details of the CRFs used, the background rates and the calculated impact functions. Full details of the calculation of the impact functions in this table are given in the Impact Function deliverable (D3.1.2/3/4). Information on the impact functions used for the other pollutants in the Common Case Study, i.e. heat, noise, homes with mould and/or dampness, radon and ETS originated VOCs and formaldehyde, are described below in Sections 5.1.6 to 5.1.10.

5.1.2 Conversion of CRFs to ERFs for use with personal exposure to $PM_{2.5}$

The outdoor air pollution risk functions included in the Common Case Study are concentration-response functions (CRFs), i.e. the health effects relate to background concentrations of outdoor air pollutants. Within the CCS, the CRFs for $PM_{2,5}$ and PM_{10} were adapted to exposure-response functions (ERFs) in order to estimate the health effects of personal exposure to $PM_{2.5}$ from indoor and outdoor sources. This adaption requires two steps:

1. As the modelling of personal exposure was in the metric of $PM_{2.5}$, the PM_{10} CRFs were converted to $PM_{2.5}$ CRFs; and
2. The $PM_{2.5}$ CRFs were then scaled to $PM_{2.5}$ ERFs.

Both of these steps are described below.

Converting PM_{10} CRFs to $PM_{2.5}$ CRFs

The PM_{10} CRFs were converted to $PM_{2.5}$ CRFs by multiplying the PM_{10} CRFs by a conversion factor obtained from the con-current measurements of PM_{10} and $PM_{2.5}$ in the Apheis-3 study (APHEIS, 2004). Apheis-3 measured PM10 and $PM_{2.5}$ in 26 cities – 11 of the cities had PM10 and PM2.5 measurements. The ratio of measured $PM_{2.5}$ to PM_{10} ranged from 0.5 in Gothenburg, Sweden to 0.71 in Rouen, France. The overall ratio was used as the conversion factor between $PM_{2.5}$ and PM_{10}. On average, the levels of PM2.5 were about 0.65 times the corresponding levels of PM10.

As the relationship between PM measurements and health effects is log-linear, the conversion from PM_{10} CRFs to $PM_{2.5}$ CRFs was done on the log (base e) scale. The log of the PM_{10} CRF was divided by 0.65 to obtain the log of the $PM_{2.5}$ CRF which was then exponentiated. The end result was a CRF in the exposure metric of $PM_{2.5}$. The $PM_{2.5}$ CRF can then be combined with the original background rate to obtain an impact function in the exposure metric of $PM_{2.5}$.

The following equation was therefore used to convert PM_{10} CRFs to $PM_{2.5}$ CRFs using a conversion factor of 0.65.

$$PM_{2.5}CRF = \exp(\ln(PM_{2.5}CRF) = \exp(\frac{\ln(PM_{10}CRF)}{0.65})$$

Scaling factor from CRFs to ERFs in $PM_{2.5}$

Concentration response functions (CRFs) for $PM_{2.5}$ are based on outdoor air background concentration and do not capture the health effects from indoor sources. Thus, an approach was developed to scale the existing CRFs for use with personal exposure. CRFs were scaled to exposure response functions (ERFs) based on the relationship between background concentrations and personal exposure to $PM_{2.5}$ experienced indoors from outdoor sources. This resulted in dividing the CRFs by 0.7 to obtain the ERFs. In a next step it is assumed that these ERFs can be applied to estimate the health effects of $PM_{2.5}$ from indoor and outdoor sources (although it is acknowledged that probably indoor sources from combustions have other toxicity levels than secondary particles from outdoor air). For a detailed explanation see Annex A.2.

5.1.3 Mortality and long-term exposure to outdoor air pollution

Pollutant principally responsible

The Transport Case Study of INTARESE WP3.1 uses quantification in terms of $PM_{2.5}$, ultrafine PM, and NO_2. However, the HEIMTSA and INTARESE teams agreed that while quantification in NO_2 and ultrafine were relevant for local (within-city) effects of traffic air pollution, as used in the INTARESE Transport case study, $PM_{2.5}$ was the best indicator for the Common Case Study, with its many sectors and EU-wide population.

Concentration-response function

HEIMTSA, working with and within the UK Committee on the Medical Effects of Air Pollutants (COMEAP), considered in detail the evidence and uncertainties regarding the concentration-response function (CRF). COMEAP (2009) recommended a CRF of 6% change in mortality hazards per 10 μg/m^3 annual average $PM_{2.5}$, from Pope et al's (2002) analysis of the American Cancer Society (ACS) cohort. This is the same function as was used by CAFE (Hurley et al., 2005), and in the INTARESE case studies (Ref).

In early 2010 INTARESE carried out a formal meta-analysis of 5 cohort mortality studies principally from North America and Europe (Transport Case Study of INTARESE WP3.1) which supported the CRF of 6% change in mortality hazards per 10 μg/m^3 annual average $PM_{2.5}$.

This CRF was reviewed again within HEIMTSA in early 2010, taking account of updates during 2009 of the ACS cohort and of the Dutch NLCS-AIR cohort, and of new assessments by the US EPA, the WHO Global Burden of disease project (ongoing), and the INTARESE meta-analysis. That review (Chapter 5 of the HEIMTSA Outdoor Air Case Study Final Report (D7.1.7)) recommended the same CRF, an approach later endorsed by the WHO Task Force on Health of the Convention on Long-Range Transboundary Air Pollution in its meeting of April 2010 (WHO, 2010); and so this value was used in the Common Case Study.

From CRF to mortality impacts

Changes in mortality risks lead, over time, to changes in the size and age structure of the population at risk, and this affects both the numbers of deaths, and the distribution of age at death, in future years, compared to a baseline scenario. These complications can be addressed using life table methods (Miller and Hurley, 2003). However there is still widespread confusion on how best to express mortality impacts, and in particular on the relationships between life expectancy, total population survival time expressed as life years, and annual numbers of deaths.

Further methodological work on survival concepts and life table methods within HEIMTSA, in collaboration with COMEAP in the UK, has greatly clarified the relationships between these indicators. Results are reported most fully in COMEAP (2010), which concluded that the mortality impacts of a change in annual average $PM_{2.5}$ were best analysed using total population survival (life years), not deaths or life expectancy. The main points are summarised in Chapter 6 of the HEIMTSA Outdoor Air Pollution Case Study (D7.1.7), which describes further methodological work on the mortality impacts of a one-year change in annual average $PM_{2.5}$. This is necessary for the Common Case Study, which looks at changes in emissions in specific years (e.g. 2020, 2030).

We estimated the impact in life-years of a 1-year reduction in 2010 of 1μg/m^3 annual average PM_2, with consequent reductions in all-cause hazards for those aged 30+,

scaling from a hazard ratio impact coefficient of 1.06 per 10µg/m^3. Analyses in England and Wales, Italy and Sweden gave consistent results over countries and sexes, and we took a weighted average unit impact to apply to areas in Western European countries, with or without discounting at 3%. Impacts for Poland were somewhat higher, and we recommended applying the average there for areas in Eastern European countries. Results for Western and Eastern European countries (without discounting) are given in Table 5-2.

Assessment of uncertainty

Qualitative uncertainty methods were used to make an assessment of the possible effects of uncertainty on the calculation of the impact functions. The methodology used for this qualitative uncertainty assessment was developed in WP1.2 of HEIMTSA as described in D1.2.4/5.2.3.

For estimation of uncertainty in the calculation of impact functions, we used the methodology described in D1.2.4/5.2.3 and adapted it to encompass the specific issues in the impact function calculation. We identified broad sources of uncertainty as follows:

- Conceptual model – causality, health outcome
- Mathematical model – model, coherence, regionalisation, target population
- Parameters – baseline rates, future rates, change co-efficient

For some specific pollutant-health endpoints additional sources of uncertainty were also assessed. Information on the uncertainty analysis of impact functions included in the Common Case Study can be found in the Impact Functions deliverable (D3.1.2/3/4).

5.1.4 Impact functions for air and other pollutants

Table 1-1, below, shows the outdoor air pollution and personal exposure impact functions included in the Common Case Study. Information on the impact functions used for the other pollutants included in the CCS can be found in the following sections:

- Risk functions for heat extremes: Section 5.1.6;
- Risk functions for noise: Section 5.1.7;
- Risk functions for homes with mould and/or dampness: Section 5.1.8;
- Risk functions for radon: Section 5.1.9; and
- Risk functions for ETS originated VOCs and formaldehyde: Section 5.1.10.

Table 5-1: Table of outdoor air pollution impact functions.

Pollutant	Health effect	Relative Risk	Total Population Background Rate of Disease (per year)	Age Group	Population	Impact Function
PM2.5						
	Mortality (all cause)	6% (95% CI: 2%, 11%) change per 10 µg/m^3 $PM_{2.5}$	Not applicable	Adults 30 years and older	General Population	Impact Function : see separate table 5.2.
	Work loss days (WLDs)	4.6% (95% CI: 3.9%, 5.3%) increase per 10 µg/m^3 $PM_{2.5}$	450,000 WLDs per 100,000 people aged 15-64 per year	15-64 Years	General Population	20,700 (95% CI: 17,600, 23,800) additional work lost days per 10 µg/m^3 increase in $PM_{2.5}$ per 100,000 people aged 15-64 in the general population per year
	Minor Restricted Activity Days (MRADs)	7.4% (95% CI: 6.0%, 8.8%) change per 10 µg/m^3 $PM_{2.5}$	780,000 MRADs per 100,000 people in employment aged 18-64 per year	18-64 Years	General Population	57,700 (95% CI: 46,800, 68,600) additional MRADs per 10 µg/m^3 increase in $PM_{2.5}$ per 100,000 adults aged 18-64 (general population) per year
	Restricted activity days (RADs)	4.75% (95% CI: 4.17%, 5.33%) change per 10 µg/m^3 $PM_{2.5}$	1,900,000 RADs per 100,000 people aged 18-64 per year	18-64 Years	General Population	90,200 (95% CI: 79,200, 101,300) additional RADs per 10 µg/m^3 increase in $PM_{2.5}$ per 100,000 adults aged 18-64 (general population) per year
PM10						
	Infant Mortality	4% (95% CI: 2%, 7%) change per 10 µg/m^3 PM_{10}	145 postneonatal deaths per 100,000 live births	1 month to 1 year	General Population	5.8 (95% CI: 2.9, 10.2) additional infant deaths per 10 µg/m^3 increase in PM_{10} per 100,000 live births, per year
	Chronic bronchitis	22% (95% CI: 2%, 38%) change per 10 µg/m^3 PM_{10}	390 new cases annually per 100,000 adults at risk (adjusted for remission - remission rate of 56.2%)	Adults aged 18 years and older	General Population without symptoms (90% of population)	86 (95% CI 7.8, 150) new cases of chronic bronchitis per 10 µg/m^3 increase in PM_{10} per 100,000 at-risk adults aged 18 and older, per year
	Cardiovascular hospital admissions	0.6% (95% CI: 0.3%, 0.9%) change per 10 µg/m^3 PM_{10}	723 emergency cardiac admissions per 100,000 population, all ages, per year	All Ages	General Population	4.3 (95% CI: 2.2, 6.5) additional emergency cardiac hospital admissions per 10 µg/m^3 increase in PM_{10} per 100,000 people (all ages) per year
	Respiratory hospital admissions	0.9% (95% CI: 0.7%, 1.0%) change per 10 µg/m^3 PM_{10}	617 emergency respiratory hospital admissions per 100,000 population, all ages, per year	All Ages	General Population	5.6 (95% CI: 4.3, 6.2) additional emergency respiratory hospital admissions per 10 µg/m^3 increase in PM_{10} per 100,000 people (all ages) per year

Pollutant	Health effect	Relative Risk	Total Population Background Rate of Disease (per year)	Age Group	Population	Impact Function
	Asthma medication use among asthmatic children	0.4% (95% CI: -1.7%, 2.6%) change per 10 µg/m^3 PM_{10}	10% mean daily prevalence of bronchodilaotor usage among children meeting the PEACE criteria	5-14 Years	Children with Asthma (14.4% of children aged 5-14 in EU27)	14,600 (95% CI: -62,050, 94,900) additional days of bronchodilator usage per 10 ug/m^3 increase in PM_{10} per 100,000 children aged 5-14 years meeting the PEACE study criteria, per year
	Bronchodilator usage among asthmatic adults	0.5% (95% CI: -0.5%, 1.5%) change per 10 µg/m^3 PM_{10}	Background probability of bronchodilator use of 0.5 of daily usage among adults 20+	Adults aged 20 years and older	Adults with asthma (10.2% of adults aged 20 and older in EU27)	91,300 (95% CI: -91,300, 274,000) additional days of bronchodilator usage per 10 µg/m^3 increase in PM_{10} per 100,000 adults aged 20 and older with well-established asthma, per year
	Lower respiratory symptoms including cough among children	3.4% (95% CI: 1.7%, 5.1%) change per 10 µg/m^3 PM_{10}	15% mean daily prevalence rate for LRS including cough (all-year rate) among children	5-14 Years	General Population	186,000 (95% CI: 93,100, 279,000) additional lower respiratory symptom days per 10 µg/m^3 increase in PM_{10} per 100,000 children aged 5-14, per year
	Lower respiratory symptoms (including cough) in symptomatic adults	1.2% (95% CI: 0.1%, 2.2%) change per 10 µg/m^3 PM_{10}	30% mean daily prevalence for LRS including cough in symptomatic adults	Adults	Adults with chronic respiratory symptoms (30% of adults)	131,000 (95% CI: 11,000, 241,000) additional lower respiratory symptom days per 10 µg/m^3 increase in PM_{10}, per 100,000 adults with chronic respiratory symptoms, per year
Ozone						
	Mortality (all cause)	0.3% (95% CI: 0.1%, 0.4%) change per 10 µg/m^3 O_3	920 deaths per 100,000 population	All Ages	General Population	2.8 (95% CI: 0.92, 3.7) additional deaths (or life years lost) per 10 µg/m^3 increase in O_3 per 100,000 population (all ages), per year
	Respiratory hospital admissions	0.5% (95% CI: -0.2%, 1.2%) change per 10 µg/m^3 O_3	2496 hospitalisations per 100,000 adults aged 65+	Adults aged 65 years and older	General Population	12.5 (95% CI: -5.0, 30.0) additional emergency respiratory hospital admissions per 10 µg/m^3 increase in O_3 per year per 100,000 people aged 65+, per year
	Bronchodilator usage in children	21% (95% CI: 2.9%, 39%) change per 10 µg/m^3 O_3	40% mean daily prevalence of bronchodilator useage among asthmatic children. 292,000 (0.8%) days at risk per 100,000 children in the general population	5-14 Years	General Population	24,500 (95% CI: 3,400, 45,600) additional days of bronchodilator usage per 10 µg/m^3 increase in O_3 per 100,000 children aged 5-14 (general population), per year

Pollutant	Health effect	Relative Risk	Total Population Background Rate of Disease (per year)	Age Group	Population	Impact Function
	Bronchodilator use among asthmatic adults	0.6% (95% CI: -0.2%, 1.4%) change per 10 µg/m^3 O_3	Mean daily prevalence of 32% for bronchodilator usage during the summer months	Adults aged 20 years and older	Adults with asthma (10.2% of adults in EU27)	70,100 (95% CI: -23,400, 164,000) additional days of bronchodilator usage per 10 ug/m^3 increase in O_3 per 100,000 adults aged 20 and older with persistent asthma, per year
	Lower respiratory symptoms (excluding cough) among children	3.0% (95% CI: -7.9%, 15%) change per 10 µg/m^3 O_3	1.5% mean daily prevalence of LRS excluding cough in general population of children (summer-time rate)	5-14 Years	General Population	16,000 (95% CI: -43,000, 82,000) additional days of LRS (excluding cough) per 10 µg/m^3 increase in O_3 per 100,000 children aged 5-14 years, per year
	Cough (days) among children	4.7% (95% CI: -0.9%, 11%) change per 10 µg/m^3 O_3	5.4% mean daily prevalence of cough in general population of children (summer-time rate)	5-14 Years	General Population	93,000 (95% CI: -17,700, 217,000) additional cough days per 10 µg/m^3 increase in O_3 per 100,000 children aged 5-14 years per year
	Minor Restricted Activity Days (MRADs)	1.48% (95% CI: 0.57%, 2.38%) change per 10 µg/m^3 O_3	780,000 MRADs per 100,000 people in employment aged 18-64 per year	18-64 Years	General Population	11,500 (95% CI: 4,400, 18,600) additional MRADs per 10 µg/m^3 increase in O_3 per 100,000 adults aged 18-64 (general population) per year
PM2.5 including PM10 CRFs converted to PM2.5 CRFs						
	Mortality (all cause)	6% (95% CI: 2%, 11%) change per 10 µg/m^3 $PM_{2.5}$	Not applicable	Adults aged 30 years and older	General Population	Impact Function : see table 5.2.
	Work loss days (WLDs)	4.6% (95% CI: 3.9%, 5.3%) increase per 10 µg/m^3 $PM_{2.5}$	450,000 WLDs per 100,000 people aged 15-64 per year	15-64 Years	General Population	20,700 (95% CI: 17,600, 23,800) additional work lost days per 10 µg/m^3 increase in $PM_{2.5}$ per 100,000 people aged 15-64 in the general population per year
	Minor Restricted Activity Days (MRADs)	7.4% (95% CI: 6.0%, 8.8%) change per 10 µg/m^3 $PM_{2.5}$	780,000 MRADs per 100,000 people in employment aged 18-64 per year	18-64 Years	General Population	57,700 (95% CI: 46,800, 68,600) additional MRADs per 10 µg/m^3 increase in $PM_{2.5}$ per 100,000 adults aged 18-64 (general population) per year
	Restricted activity days (RADs)	4.75% (95% CI: 4.17%, 5.33%) change per 10 µg/m^3 $PM_{2.5}$	1,900,000 RADs per 100,000 people aged 18-64 per year	18-64 Years	General Population	90,200 (95% CI: 79,200, 101,300) additional RADs per 10 µg/m^3 increase in $PM_{2.5}$ per 100,000 adults aged 18-64 (general population) per year
	Infant Mortality	6% (95% CI: 3%, 11%) change per 10 µg/m^3 $PM_{2.5}$	145 postneonatal deaths per 100,000 live births	1 month to 1 year	General Population	8.7 (95% CI: 4.4, 16) additional infant deaths per 10 µg/m^3 increase in $PM_{2.5}$ per 100,000 live births, per year
	Chronic bronchitis	36% (95% CI: 3%, 64%) change per 10 µg/m^3 $PM_{2.5}$	390 new cases annually per 100,000 adults at risk (adjusted for remission - remission rate of 56.2%)	Adults aged 18 years and older	General Population without symptoms (90% of population)	140 (95% CI 12, 250) new cases of chronic bronchitis per 10 µg/m^3 increase in $PM_{2.5}$ per 100,000 at-risk adults aged 18 and older, per year

Pollutant	Health effect	Relative Risk	Total Population Background Rate of Disease (per year)	Age Group	Population	Impact Function
	Cardiovascular hospital admissions	0.9% (95% CI: 0.5%, 1.4%) change per 10 µg/m^3 $PM_{2.5}$	723 emergency cardiac admissions per 100,000 population, all ages, per year	All Ages	General Population	6.5 (95% CI:3.6, 10) additional emergency cardiac hospital admissions per 10 µg/m^3 increase in $PM_{2.5}$ per 100,000 people (all ages) per year
	Respiratory hospital admissions	1.4% (95% CI: 1.1%, 1.5%) change per 10 µg/m^3 $PM_{2.5}$	617 emergency respiratory hospital admissions per 100,000 population, all ages, per year	All Ages	General Population	8.6 (95% CI: 6.8, 9.3) additional emergency respiratory hospital admissions per 10 µg/m^3 increase in $PM_{2.5}$ per 100,000 people (all ages) per year
	Asthma medication use among asthmatic children	0.6% (95% CI: -2.6%, 4.0%) change per 10 µg/m^3 $PM_{2.5}$	10% mean daily prevalence of bronchodilaotor usage among children meeting the PEACE criteria	5-14 Years	Children with Asthma (14.4% of children aged 5-14 in EU27)	22,000 (95% CI: -95,000, 146,000) additional days of bronchodilator usage per 10 ug/m^3 increase in $PM_{2.5}$ per 100,000 children aged 5-14 years meeting the PEACE study criteria, per year
	Bronchodilator usage among asthmatic adults	0.8% (95% CI: -0.8%, 2.3%) change per 10 µg/m^3 $PM_{2.5}$	Background probability of bronchodilator use of 0.5 of daily usage among adults 20+	Adults aged 20 years and older	Adults with asthma (10.2% of adults in EU27)	146,000 (95% CI: -146,000, 420,000) additional days of bronchodilator usage per 10 µg/m^3 increase in $PM_{2.5}$ per 100,000 adults aged 20 and older with well-established asthma, per year
	Lower respiratory symptoms including cough among children	5.3% (95% CI: 2.6%, 8.0%) change per 10 µg/m^3 $PM_{2.5}$	15% mean daily prevalence rate for LRS including cough (all-year rate) among children	5-14 Years	General Population	290,000 (95% CI: 142,000, 438,000) additional lower respiratory symptom days per 10 µg/m^3 increase in $PM_{2.5}$ per 100,000 children aged 5-14, per year
	Lower respiratory symptoms (including cough) in symptomatic adults	1.9% (95% CI: 0.2%, 3.4%) change per 10 µg/m^3 $PM_{2.5}$	30% mean daily prevalence for LRS including cough in symptomatic adults	Adults	Adults with chronic respiratory symptoms (30% of adults)	208,000 (95% CI: 22,000, 372,000) additional lower respiratory symptom days per 10 µg/m^3 increase in $PM_{2.5}$, per 100,000 adults with chronic respiratory symptoms, per year

Table 5-2: Results for impact assessment of mortality in relation to air pollution

Western Countries -			
Weighted average of England & Wales, Italy and Sweden			
	Female	**Male**	**Total**
Population 30+	42,415,896	38,784,956	81,200,852
Life years gained per µg/m3	37,656	39,757	77.412
Life years gained per 100k popn 30+ per µg/m3	**88.8**	**102.5**	**95.3**

Eastern Countries -			

based on Poland			
Population 30+	12,307,810	10,714,244	23,022,054
Life years gained per µg/m3	12,545	16,358	28,903
Life years gained per 100k popn 30+ per µg/m3	**101.9**	**152.7**	**125.5**

5.1.5 Exposure response functions for $PM_{2.5}$

We present in this report a description of the impact functions for the two most important health effects of $PM_{2.5}$ - mortality and restricted activity days (RADs) – more detailed descriptions of these impact functions and of impact functions for other health endpoints are reported in D3.1.2/3/4. The impact function for $PM_{2.5}$ in relation to mortality is described in section 5.1.3 above.

Restricted activity days (RADs) include both work loss days (WLDs) and minor restricted activity days (MRADs), defined as follows (i) days when a person needs to stay bed; (ii) days when a person stays off work or school (or whatever may be their usual place to go, if they have a usual place to go) but doesn't need to stay in bed (includes WLDs); and (iii) other, less serious, restrictions on normal activity (MRADs).

Concentration-Response Function

The concentration response function was derived from Ostro (1987), based on the HIS study on RADs and $PM_{2.5}$ for 12,000 adults aged 18-64 from the US general population. The study was conducted over the course of six years from 1976 to 1981 and the overall CRF was calculated as a weighted mean of the six individual coefficients with weights that were inversely proportional to the variances of the coefficients. The overall CRF (relative risk) was:

4.75% (95% CI: 4.17%, 5.33%) change per 10 µg/m^3 $PM_{2.5}$

Stieb et al (2002) studied the relationship between 'disability days' (which were defined in a similar way to RADs) and $PM_{2.5}$ levels and estimated a 33% (95% CI: 6%, 58%) increase in disability days per 10 µg/m^3 $PM_{2.5}$ which is much higher than the Ostro (1987) estimate; however they state that the higher result may be due to the use of a two-week average $PM_{2.5}$ concentration instead of daily concentrations of $PM_{2.5}$. As the Stieb et al (2002) study does show that there is an effect between RADs and $PM_{2.5}$ and that the effect estimated in the Ostro (1987) paper is not necessarily high, we followed CAFE and used the Ostro (1987) estimate.

Background rate of disease

The US Coal Fuel Cycle Report (ORNL/RFF, 1994) reported on the background rate of RADs, with an estimate of 19 RADs per person per year, and this was supported by results from the study by Stieb et al (2002) and the results of the UK General

Household Survey. Therefore, in HEIMTSA we will use a background rate of 19 Restricted Activity Days per person per year, which is equivalent to 1,900,000 RADs per 100,000 population per year.

Impact Function

As the CRF is a relative risk, the background rate is an annual rate and the entire population is exposed to $PM_{2.5}$, the impact function was calculated by multiplying the CRF by the background rate for RADs which then produces an impact function of:

90,200 (95% CI: 79,200, 101,300) additional RADs per 10 μg/m^3 increase in $PM_{2.5}$ per 100,000 adults aged 18-64 (general population) per year.

5.1.6 Exposure response functions for PM_{10}

We present here a description of the impact functions for the two most important health effects of PM_{10} – respiratory hospital admissions and chronic bronchitis – more detailed descriptions of these impact functions and of impact functions for other health endpoints are reported in D3.1.2/3/4.

Respiratory hospital admissions

There are numerous studies linking daily variations in air pollution with the numbers of people admitted to hospital on the same day, or on days immediately following. Many studies of hospital admissions and air pollution are based on general hospital admissions, i.e. both planned admissions and emergency admissions. It is to be expected, however, that daily variations in air pollution will impact on emergency admissions rather than on planned admissions. We have, therefore, used background rates for emergency admissions only.

It is unclear to what extent these 'extra' hospital admissions in the days immediately following higher air pollution are genuinely extra new and additional admissions, or to what extent they reflect a 'bringing forward' (by days or weeks or months) of events that would have occurred anyway (COMEAP, 1998). This is, in effect, the counterpart for hospital admissions of the 'harvesting' issue often discussed with regard to daily variations in pollution and mortality. It is conventional to treat the attributable admissions as if they were genuinely new, and we have followed that convention.

Concentration-Response Functions

The WHO meta-analysis of hospital admissions and PM_{10}, provides European risk estimates at different age groups (WHO, 2004). For adults aged 65 and older, studies in eight cities, were included in the meta-analysis producing a CRF of 0.7% (95% CI: 0.2%, 1.3%) per 10 μg/m^3 PM_{10} in adults aged 65 and older; while for people aged 0-64, information on daily variations in PM_{10} and respiratory hospital admissions in three European cities (WHO, 2004) produced a CRF of 1% (95% CI: 0%, 2%) per 10 μg/m^3 PM_{10}. In the Apheis-3 report, Atkinson et al (2005) developed a new CRF for PM_{10} and respiratory hospital admissions at all ages, where possible using data on emergency

admissions with an overall CRF for emergency respiratory hospital admissions, all ages, of 1.14% (95% CI: 0.62, 1.67%) per 10 μg/m^3 PM_{10}.

The meta-analysis conducted by the INTARESE WP3.1 Transport Case Study team included the Apheis-3 study results and more recent studies on the relationship between PM_{10} and respiratory hospital admissions. Previously published systematic reviews and meta-analyses from Europe as well as North America were incorporated into the meta-analysis ensuring that the most up-to-date estimates were included in the overall risk estimate. Eleven risk estimates were included producing a CRF (relative risk) for respiratory hospital admissions of:

0.9% (95% CI: 0.7, 1%) change in respiratory hospital admissions per 10 μg/m^3 PM_{10}

The risk estimate obtained in the INTARESE Transport Case Study was lower than that reported in the Apheis-3 study. However, as the Transport Case Study estimate includes more updated information than the Apheis-3 study; we have used the more recent meta-analysis result.

Background rate of disease

The incidence rate of emergency respiratory admissions was obtained from the Apheis-3 city-specific appendices (APHEIS, 2004). Information on emergency respiratory admissions was available for eight cities. The rates ranged from 511 (Gothenburg) to 708 (London), with an average rate (unweighted arithmetic mean of the eight values) of 617 emergency respiratory hospital admissions per 100,000 population, all ages.

Impact Function

As the CRF is a relative risk, the background rate is an annual rate and the entire population is exposed to PM_{10}, the impact function was calculated by multiplying the CRF by the background rate for emergency respiratory hospital admissions which produces an impact function of:

5.6 (95% CI: 4.3, 6.2) additional emergency respiratory hospital admissions per 10 μg/m^3 increase in PM_{10} per 100,000 population (all ages) per year

Chronic bronchitis

The CRF for chronic bronchitis was based on the SAPALDIA study, conducted in 1991 and 2002 in Switzerland (SAPALDIA, 2008). The Schindler et al (2009) paper reported on the relationship between chronic bronchitis in the SAPALDIA cohort and modelled PM_{10} measurements from outside the participants' homes for the 12 months preceding both questionnaires. Chronic bronchitis was defined as chronic cough and/or chronic phlegm. i.e. cough and/or phlegm, which persisted for at least 3 months per year for the last 2 years.

Concentration-Response Function

Schindler et al (2009) examined the relationship between PM_{10}, defined as the difference in PM_{10} levels between 1991 and 2002 as experienced by individuals, and

two aspects of chronic bronchitis experienced between the two surveys. One set of analyses examined new occurrences reported in 2002, i.e. how PM_{10} between surveys influenced the chances of reporting a new occurrence of chronic bronchitis in 2002 among those without chronic cough and/or phlegm in 1991. The other examined how PM_{10} between surveys affected the chances of people with chronic cough and/or phlegm in 1991 again reporting those symptoms in 2002. As in CAFE, we want to calculate an impact function for new cases of chronic bronchitis. For this, we have used the former relative risk producing a CRF of:

22% (95% CI: 2%, 38%) increase per 10 µg/m^3 PM_{10}

It is worth noting that this estimate is substantially larger than the CRF reported by Abbey et al (1995) (22% vs. 7% per 10 µg/m^3 PM_{10}, respectively).

Background rate of disease

The Schindler et al (2009) paper provides details on the percentage of new cases of chronic bronchitis and the percentage of persistent chronic bronchitis, i.e. reported symptoms in 1991 and 2002. Based on these data, there are two background rates that we could use for chronic bronchitis – one being a more transient outcome of new cases of chronic bronchitis with no account taken for remission and one being for persistent new cases of chronic bronchitis which has been adjusted for remission. As the remission rate in the study was greater than 50%, we calculated background rates of chronic bronchitis adjusting for remission which resulted in an annual net incidence rate of 0.39% or 3.9 new cases annually per 1,000 adults at-risk.

It is worth noting that the estimated net incidence rate from the SAPALDIA study (3.9 new cases per 1,000) is very similar to that calculated in the CAFE report based on data from the Abbey et al (1995) study (3.78 new cases per 1,000).

Impact Function

As the CRF is a relative risk, the background rate is an annual rate and the entire population is exposed to PM_{10}, the impact function was calculated by multiplying the CRF by the incidence rate of persistent chronic bronchitis which then produces an impact function of:

86 (95% CI: 7.8, 150) new persistent cases of chronic bronchitis per 10 µg/m^3 PM_{10} per 100,000 adults aged 18 and older at-risk, per year

The at-risk population is defined as the proportion of adults in the population without symptoms of chronic bronchitis. In the Schindler et al (2009) study, approximately 90% of adults did not have persistent chronic bronchitis; therefore, the impact function should be applied to only 90% of the total EU adult population.

The corresponding impact function for the total population would be:

77 (95%: 7.0, 140) new persistent cases of chronic bronchitis per 10 µg/m^3 PM_{10} per 100,000 adults aged 18 and older, per year.

5.1.7 Exposure response functions for ozone

Mortality

The information below on the CRFs for ozone and their applicable background rates of disease has largely been drawn from the CAFE study (Hurley et al, 2005). Refer to Hurley et al, 2005 for full details of the impact functions used in the CAFE study.

Concentration-Response Function

As there have been few studies of long-term exposure to ozone and mortality, we have quantified the effects of short-term exposure to ozone on mortality, in terms of deaths postponed/attributable cases avoided. The CAFE report provides details of the guidance from WHO to RAINS on calculating the effects of ozone on mortality. After the WHO recommendations to RAINS were published, Gryparis et al (2004) conducted a study of mortality and ozone based on the results of the APHEA-2 study in which the relationship between daily mortality and ozone in 23 cities/areas was studied. The CRF reported by Gryparis et al (2004) was very similar to that recommended by the WHO, with a CRF of 0.33% (95% CI: 0.17%, 0.52%) increase in daily mortality per 10 μg/m^3 O_3 during the warm season.

The results of the Gryparis et al (2004) study lend further support to the use of the WHO meta-analysis results. Therefore we have used a CRF (relative risk) of:

0.3% (95% CI: 0.1-0.4%) increase in daily mortality per 10 μg/m^3 O_3

Background rate of disease

Information on the number of all-cause mortality deaths (non-violent) was obtained by country from the WHO European detailed mortality database (European DMDB, 2010). Numbers of deaths were available for all EU 27 countries for the years ranging from 2003 (Portugal) to 2008. Population figures for the appropriate year (all ages) were obtained from the Eurostat database (EC, 2010). The population-weighted background rate of mortality (all-cause, non-violent) in the EU 27 was found to be:

920 deaths per 100,000 population, all ages

Impact function

As the CRF is a relative risk, the background rate is an annual rate and the entire population is exposed to ozone, the impact function was calculated by multiplying the CRF by the background rate for all-cause, non-violent deaths which then produces an impact function of:

2.8 (95% CI: 0.92, 3.7) additional deaths per 10 μg/m^3 increase in O_3 per 100,000 population (all ages) per year.

5.1.8 Exposure response functions for heat

Assessment concentrated on mortality effects of short-term heat exposure. Impacts were evaluated based on the results of the PHEWE-project (Baccini et al. 2008, Michelozzi et al. 2007), which investigated acute health effects of weather in European cities. In PHEWE, epidemiological time-series studies on the association between daily heat exposure and mortality were conducted in 15 cities. The city-specific estimates were then pooled into two groups based of meteorological and geographical criteria, Mediterranean (7 cities) and North-continental (8 cities), to produce meta-analytical ERFs for these sub-regions.

ERFs for heat exposure and natural mortality (all non-accidental causes of death) were available for three age categories (15-64, 65-74, 75+, Table 5-3). The ERFs are based on a linear threshold model and describe the percent change in daily mortality associated with a 1°C increase in daily maximum apparent temperature above a sub-region specific temperature threshold in the warm season (April-September).

Table 5-3: Percent change in daily natural mortality associated with a 1°C increase in maximum apparent temperature above the region specific threshold (95% confidence intervals, Baccini et al 2008).

	Region	
	North-continental	**Mediterranean**
AT threshold	23.3 (22.5-24.0)	29.4 (25.7-32.4)
Age		
15-64	1.31 (-0.94, 3.72)	0.92 (-1.29, 3.13)
65-74	1.65 (-0.51, 3.87)	2.13 (-0.42, 4.74)
75+	2.07 (0.24, 3.89)	4.22 (1.33, 7.20)
All	1.84 (0.06, 3.64)	3.12 (0.60, 5.73)

In PHEWE, heat exposure in cities was evaluated based on weather data from the nearest airport. Thus, the ERFs describe the association between background ambient temperature level and mortality risk in a city. Because of the urban heat island effect, heat exposure in a city is in reality likely to be higher than the background temperature indicates. Therefore, the impact of the urban heat island effect is embedded in and inseparable from these ERF estimates, and the health effects of heat exposure and the changes in these effects due to different UHI mitigation policies have to be evaluated against ambient background temperature data.

Specifics of the methodology applied in the modelling of mortality impacts of heat exposure are presented in Annex E (Annexes

Heat and Urban Heat Island (UHI) Mitigation).

5.1.9 Exposure response functions for noise

Three health endpoints were taken into account for noise:

- annoyance, expressed as number of *annoyed* people and number of *highly annoyed* people,[10]
- sleep disturbance, expressed as number of *sleep-disturbed* people and number of *highly sleep-disturbed* people,
- myocardial infarction, expressed as number of *fatal* infarctions and number of *non-fatal* infarctions.

The prevalence of these effects was calculated from existing statistical exposure-response relations relating to exposure expressed as the noise level at dwelling façade. This is illustrated in figure X5. The graph in the figure shows an example: about 25% of people exposed to a level of 70 dB are highly annoyed by the noise.

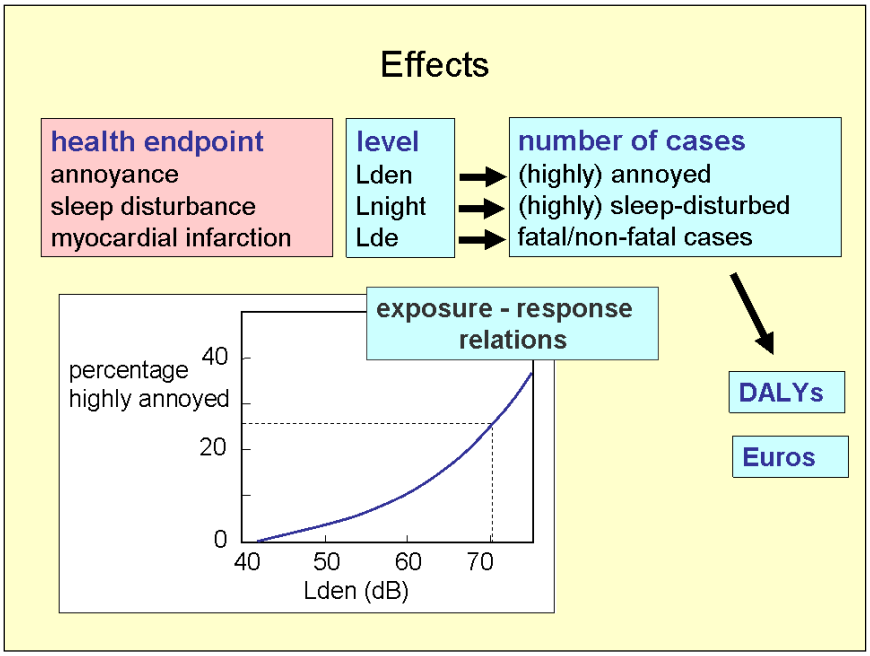

Figure 5-1: Illustration of the calculation of health impact parameters (noise).[11]

For annoyance, sleep disturbance and myocardial infarction the exposure response functions, known from literature, were applied in the Common Case Study (the various L parameters refer to segments of daytime):

- The percentages annoyed (%A) and highly annoyed (%HA):
  $\%A_{road} = 1.795 * 10^{-4} (L_{den} - 37)^3 + 2.110 * 10^{-2} (L_{den} - 37)^2 + 0.5353 (L_{den} - 37)$,
  $\%HA_{road} = 9.868 * 10^{-4} (L_{den} - 42)^3 - 1.436 * 10^{-2} (L_{den} - 42)^2 + 0.5118 (L_{den} - 42)$.

[10] The category 'highly annoyed' represents all people with annoyance ratings higher than 72% on a rating scale from 0% (not annoyed at all) to 100% (extremely annoyed). The category 'annoyed' represents people with annoyance ratings higher than 50%. The categories 'highly sleep-disturbed' and 'sleep-disturbed' are defined analogously.
[11] The façade level L_{de}, or day-evening level, is derived from the day-evening-night level Lden.

- The percentage highly sleep disturbed (%HSD):
  $\%HSD_{road} = 20.8 - 1.05*L_{night} + 0.01486\ (L_{night})^2$.
- Myocardial infarction:
  Odds Ratio = $1.629657 – 0.000613(L_{day,16h})^2 + 0.000007357(L_{day,16h})^3$
  (valid for $55 \leq L_{day,16h} \leq 80$ dB).

5.1.10 Exposure response functions for dampness

Asthma prevalence (number of asthma cases) attributable to indoor problems due to residential mould or dampness was chosen as the outcome of interest for two reasons. First, there are plausible information about the causal association between dampness and asthma; second, asthma is a fairly common and severe disease, and therefore it is likely that focusing on this single endpoint can produce a reasonable estimate about the total magnitude of the problem.

The current scientific epidemiological literature contains plausible exposure-response functions for the association of moisture problems and asthma. In this assessment, number of current asthma cases (i.e., prevalence) is used as the outcome indicator. The current exposure-response estimate is 1.56 (odds ratio OR) for current asthma risk (prevalence) due to existing dampness problem (Fisk et al., 2007). Linear no-threshold exposure-response function was assumed for the whole population in each country.

The prevalence of dampness-induced asthma depends also on the background prevalence of asthma and the population size. Asthma and population size differ by country and the population also changes in time. However, the determinants of asthma are not known well enough to predict time trends into the future and so the asthma background is assumed constant in time in this assessment.

5.1.11 Exposure response functions for radon

Lung cancer mortality (number of deaths due to lung cancer) attributable to indoor radon concentrations was chosen as the outcome of interest for two reasons. First, there is clear evidence about the causal association between indoor radon and lung cancer; second, lung cancer is the only known endpoint of radon exposure, and as a deathly disease, focusing on mortality can produce a reasonable estimate about the total magnitude of the problem.

The current epidemiological literature contains plausible exposure-response functions for the association of indoor radon and lung cancer. The current exposure-response estimate is 1.16 (risk ratio RR) for lung cancer mortality per 100 Bq/m3 radon concentration increase (Darby 2004 and 2005). Linear no-threshold exposure-response function was assumed for the whole population in each country.

Lung cancer mortality due to radon depends also on the background mortality of lung cancer and the population size. Population size differs by country and also in time; data from the Common Case Study was used also in this sub-assessment. The same lung cancer background mortality is assumed for the whole Europe: 58.2 cases/100000 person-years (Globocan 2008). The main exposures causing lung cancer are known fairly well: smoking, asbestos, radon, and smoke from any source. Many of these exposures are decreasing at some rate in Europe. However, for simplicity we assume no change in the background risk of lung cancer, and this somewhat overestimates the impacts of radon and also the impacts of policies on lung cancer in the future.

5.1.12 Exposure response functions for ETS originated VOCs and formaldehyde

Internal dose modeling was conducted by physiologically based pharmacokinetic models (PBPK), which are modeling tools describing the mechanisms of absorption, distribution, metabolism and elimination (ADME) of chemicals in the body resulting from acute and/or chronic exposure regimes. They are independent structural models, comprising the tissues and organs of the body with each perfused by, and connected via, the blood circulatory system. In PBPK models the organism is frequently represented as a network of tissue compartments (e.g., liver, fat, slowly perfused tissues, and richly perfused tissues) interconnected by systemic circulation. The general formula describing these procedures in a tissue is the following one:

$$V_i \frac{dC_{ij}}{dt} = Q_i(CA_j - CV_{ij}) - Metab_{ij} - E\lim_{ij} + Absorp_{ij} - \Pr Binding_{ij}$$

For assessing risks for long term effects, a mechanistic approach was followed, allowing us the development of a BBDR (Biology Based Dose Response) model, linking exposure, to internal dose and following the modeling of a biological process leading to adverse health effects. Instead of trying to quantify the relation between dose and response probability directly, it is useful to decompose the causal relation between exposure history and health risk probability into biologically meaningful causal links called "micro-relations" to quantify these links, and then to estimate the full dose-response relation by composing its constituent micro-relations. As an example, the dose-response relation for benzene can be described as the composition of two micro-relations, one linking administered dose (or the external exposure) to internal dose of benzene metabolites, the other linking internal dose to cancer probability by the formula:

$$P(y) = 1 - e^{\left(-0.04296940\,y + 0.0263373\,y^2 - 0.00764081\,y^3\right)}$$

Similarly, the corresponding formulas linking DPX (formaldehyde-DNA adducts) formation and the risk for nasopharyngeal cancer is given by the formula:

$$P(y) = 1 - e^{\left(-0.04296940\,y + 0.0263373\,y^2 - 0.00764081\,y^3\right)}$$

While the respective formula for NNK and risk of lung cancer is given by the formula:

$$P(y) = 1 - e^{\left(-0.0239 \cdot y \cdot N^{1.3}\right)}$$

Asthma was estimated by an epidemiologically derived exposure-response function (17% new cases change per 10 µg/m^3).

5.2 RESULTS (HEALTH EFFECTS)

5.2.1 Health effects due to outdoor air pollutants

Health effects caused by air pollutants in EU 29 for the different scenarios are listed in Table 5-4 and Table 5-5. It needs to be noted that e.g. if someone is in hospital this is counted as Cardiac/Respiratory Hospital Admission but also as a certain number of Restricted Activity Days (same for Work Loss Day and Minor Restricted Activity Day). Thus, for aggregation and valuation (see Sections 7.1.6 and 7.2.5) netRADs (net Restricted Activity DAYs) have to be calculated as otherwise double counting occurs. See also Section 5.1.

netRADs = RAD – WLD – MRAD – (RHA and CHA) x 10 days

Table 5-4: Health effects due to air pollutants, per endpoint, pollutant and year for the BAU Scenario EU29.

				Health effects		
Endpoint	**Unit**	**Pollutant**	**Population subgroup**	**2020**	**2030**	**2050**
YOLL chronic	Add. life years lost	PM25	30+	1,954,000	2,044,000	1,870,000
Mortality	Add. life years lost	SOMO35	all	11,500	10,500	10,200
Infant Mortality	Add. infant deaths	PM10	1 month - 1 year	266	265	244
Chronic bronchitis	New cases	PM10	18+	308,000	313,000	288,000
Respiratory Hospital Admissions	Add. emergency RHA	PM10, SOMO35	all	40,000	41,000	41,000
Cardiac Hospital Admissions	Add. emergency CHA	PM10	all	17,900	18,000	16,600

Bronchodilator Usage Adults	Add. days of usage	PM10, SOMO35	20+, asthmatics	126,716,000	122,006,000	113,314,000
Bronchodilator Usage Children	Add. days of usage	PM10, SOMO35	5-14 (asthmatics for PM)	10,489,000	9,339,000	9,203,000
Cough Days	Add. cough days	SOMO35	5-14	36,842,000	32,139,000	31,590,000
Lower respiratory symptoms Adults	Add. symptom days	PM10	adults with chronic resp. symptoms	156,580,000	158,689,000	146,385,000
Lower respiratory symptoms Children	Add. symptom days	PM10	5-14	85,133,000	82,559,000	76,691,000
Lower respiratory symptoms Children Excl Cough	Add. symptom days	SOMO35	5-14	6,339,000	5,529,000	5,435.000
Minor Restricted Activity Days	Add. MRADs	PM25, SOMO35	18-64	126,616,000	121,414,000	102,129,000
Restricted Activity Days	Add. RADs	PM25	18-64	152,248,000	149,736,000	124,733,000
Work Loss Days	Add. WLDs	PM25	15-64	409,000	403,000	336,000
Net Restricted Activity Days	Add. netRADs	Mix	Mix	10,300,000	13,202,000	10,060,000

Table 5-5: Health effects due to air pollutants, per endpoint, pollutant and year for the Policy Scenario EU29.

				Health effects		
Endpoint	**Unit**	**Pollutant**	**Population subgroup**	**2020**	**2030**	**2050**
YOLL chronic	Add. life years lost	PM25	30+	1,965,000	1,894,000	1,520,000
Mortality	Add. life years lost	SOMO35	all	11,200	9,700	8,200
Infant Mortality	Add. infant deaths	PM10	1 month - 1 year	265	248	206
Chronic bronchitis	New cases	PM10	18+	307,000	292,000	243,000
Respiratory Hospital Admissions	Add. emergency RHA	PM10, SOMO35	all	40,000	38,000	34,000

Cardiac Hospital Admissions	Add. emergency CHA	PM10	all	17,900	16,900	14,000
Bronchodilator Usage Adults	Add. days of usage	PM10, SOMO35	20+, asthmatics	125,617,000	113,924,000	94,959,000
Bronchodilator Usage Children	Add. days of usage	PM10, SOMO35	5-14 (asthmatics for PM)	10,288,000	8,545,000	7,406,000
Cough Days	Add. cough days	SOMO35	5-14	36,120,000	29,436,000	25,443,000
Lower respiratory symptoms Adults	Add. symptom days	PM10	adults with chronic resp. symptoms	155,988,000	148,383,000	123,232,000
Lower respiratory symptoms Children	Add. symptom days	PM10	5-14	85,041,000	77,286,000	64,450,000
Lower respiratory symptoms Children Excl Cough	Add. symptom days	SOMO35	5-14	6,214,000	5,064,000	4,377,000
Minor Restricted Activity Days	Add. MRADs	PM25, SOMO35	18-64	126,681,000	112,182,000	82,620,000
Restricted Activity Days	Add. RADs	PM25	18-64	153,283,000	138,689,000	101,051,000
Work Loss Days	Add. WLDs	PM25	15-64	411,000	373,000	272,000
Net Restricted Activity Days	Add. netRADs	Mix	Mix	11,807,000	12,254,000	7,146,000

Table 5-6: Difference in health effects due to air pollutants for Policy – BAU scenario, per endpoint, pollutant and year, EU29.

				Health effects		
Endpoint	**Unit**	**Pollutant**	**Population subgroup**	**2020**	**2030**	**2050**
YOLL chronic	Add. life years lost	PM2.5	30+	11,000	-150,000	-350,000
Mortality	Add. life years lost	SOMO35	all	-300	-800	-2,000
Infant Mortality	Add. infant deaths	PM10	1 month - 1 year	-1	-17	-38
Chronic bronchitis	New cases	PM10	18+	-1,000	-21,000	-45,000

Respiratory Hospital Admissions	Add. emergency RHA	PM10, SOMO35	all	0	-3,000	-7,000
Cardiac Hospital Admissions	Add. emergency CHA	PM10	all	0	-1,100	-2,600
Bronchodilator Usage Adults	Add. days of usage	PM10, SOMO35	20+, asthmatics	-1,099,000	-8,082,000	-18,355,000
Bronchodilator Usage Children	Add. days of usage	PM10, SOMO35	5-14 (asthmatics for PM)	-201,000	-794,000	-1,797,000
Cough Days	Add. cough days	SOMO35	5-14	-722,000	-2,703,000	-6,147,000
Lower respiratory symptoms Adults	Add. symptom days	PM10	adults with chronic resp. symptoms	-592,000	-10,306,000	-23,153,000
Lower respiratory symptoms Children	Add. symptom days	PM10	5-14	-92,000	-5,273,000	-12,241,000
Lower respiratory symptoms Children Excl Cough	Add. symptom days	SOMO35	5-14	-125,000	-465,000	-1,058,000
Minor Restricted Activity Days	Add. MRADs	PM2.5, SOMO35	18-64	65,000	-9,232,000	-19,509,000
Restricted Activity Days	Add. RADs	PM2.5	18-64	1,035,000	-11,047,000	-23,682,000
Work Loss Days	Add. WLDs	PM2.5	15-64	2,000	-30,000	-64,000
Net Restricted Activity Days	Add. netRADs	Mix	Mix	1,507,000	-948,000	-2,914,000

The increase of PM2.5 related health effects 2020 in the climate protection scenario is due to the increase in PM2.5 emissions, which especially results from burning of solid biomass in small stoves.

Health effects can be aggregated to make scenarios comparable. DALYs and damage costs can be found in Sections 7.1.6 and 7.2.5.

5.2.2 Health effects due to exposure to PM2.5

The health effects presented above are estimated based on concentration-response functions. However as mentioned earlier, exposure modelling has also been made. As the exposure-response functions are derived from the concentration-response function, the overall number of health damage is very similar when using the exposure approach. However the method allows distinguishing between population groups with different behaviours. Furthermore it allows for the first time to add indoor sources into the assessment.

As an example, health effects for Germany for 2020BAU are given in Figure 5-2. For the exposure response functions applied see Section 5.1. It was decided that health effects would not only be estimated due to $PM_{2.5}$ but also to PM_{10}, based on the personal exposure to $PM_{2.5}$. PM_{10} impact functions were scaled accordingly (see Section 5.1.2).

F15

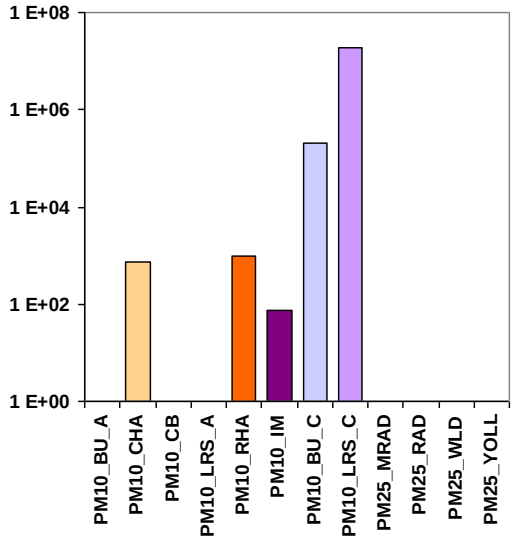

M15

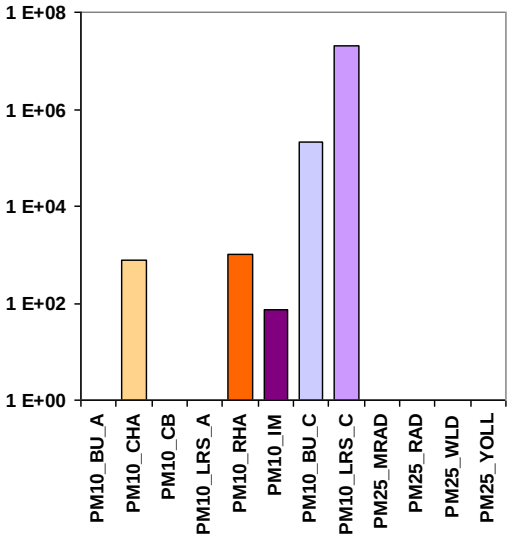

Fwork

Mwork

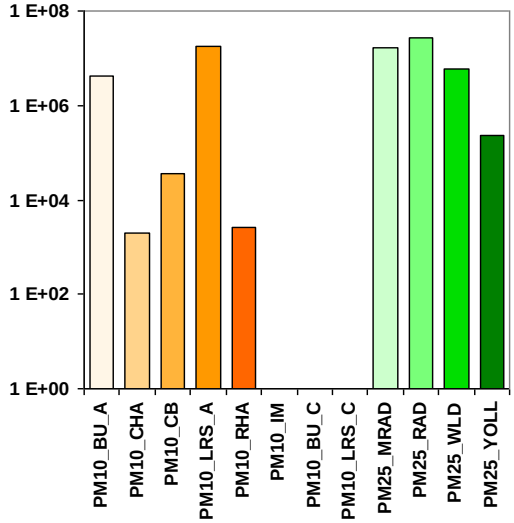

Fnonwork

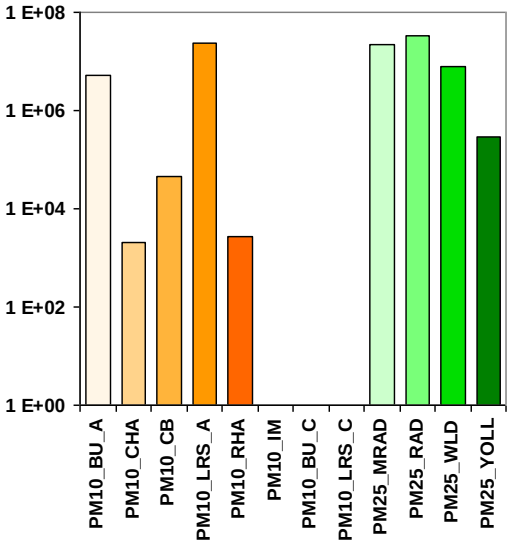

Mnonwork

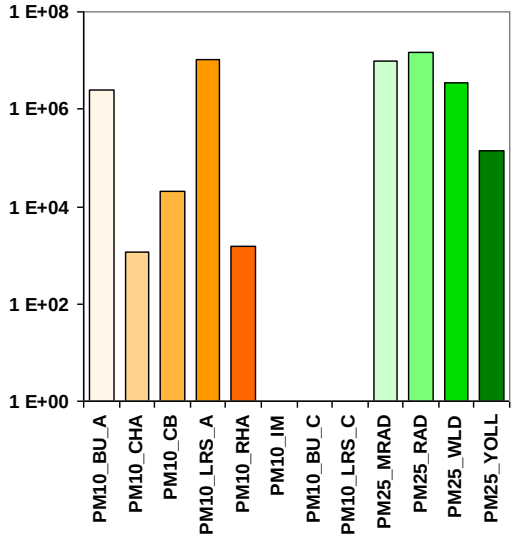

F65

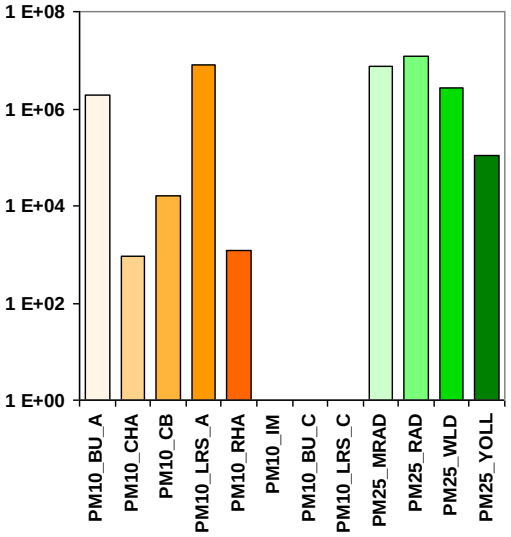

M65

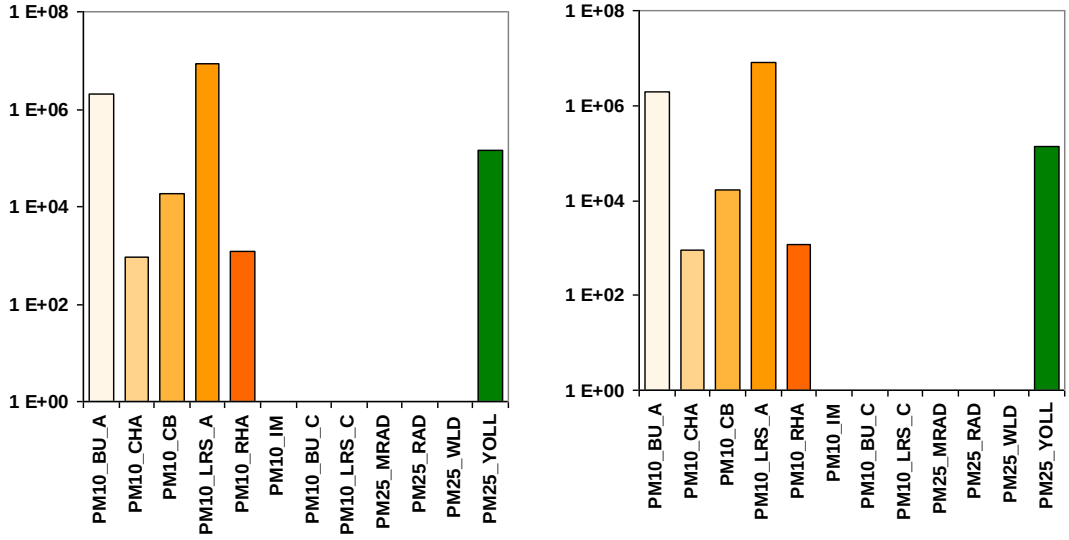

Figure 5-2: Health effects due to personal exposure to $PM_{2.5}$ (including additionally effects allocated to PM10 but scaled to PM2.5 exposure) in Germany for the 2020BAU scenario for the different subgroups

BU_A	Bronchodilator usage adults	BU_C	Brochodilator usage children
CB	New cases of chronic bronchitis	LRS_A	Lower resp. symptoms adults
IM	Infant mortality	LRS_C	Lower resp. symptoms children
RAD	Restricted activity days	MRAD	Minor restricted activity days
WLD	Work loss days	YOLL	Years of life lost
RHA	Respiratory Hospital Admissions	CHA	Cardiac Hospital Admissions

Table 5-7 shows the health effects due to personal exposure to PM (indoor and outdoor sources).

Table 5-7: Health effects due to personal exposure to PM, number of cases per endpoint and year for EU30.

	PM10_BU_A	PM10_BU_C	PM10_CHA	PM10_CB	PM10_IM	PM10_LRS_A	PM10_LRS_C	PM10_RHA
2020 BAU	125.9 mio	3.57 mio	66.6 thd	1 mio	909	542 mio	327 mio	88.1 thd
2020 ppm450	123.9 mio	3.53 mio	65.6 thd	1 mio	897	534 mio	323 mio	86.8 thd
2030 BAU	127.4 mio	3.39 mio	66.7 thd	1.1 mio	901	549 mio	310 mio	88.2 thd
2030 ppm450	131.4 mio	3.51 mio	68.8 thd	1.1 mio	934	566 mio	322 mio	91 thd
2050 BAU	118.6 mio	3.22 mio	62.3 thd	1 mio	857	510 mio	295 mio	82.4 thd
2050 ppm450	121.9 mio	3.35 mio	64.1 thd	1.1 mio	892	524 mio	306 mio	84.8 thd

	PM25_MRAD	PM25_RAD	PM25_WLD	PM25_YOLL
2020 BAU	404 mio	632 mio	145 mio	7.29 mio
2020 ppm450	398 mio	322 mio	143 mio	7.17 mio
2030 BAU	390 mio	309 mio	140 mio	7.42 mio
2030 ppm450	403 mio	630 mio	145 mio	7.65 mio
2050 BAU	338 mio	529 mio	121 mio	6.93 mio
2050 ppm450	348 mio	544 mio	125 mio	7.12 mio

Table 5-8 shows the health effects due to ETS from PM in EU30. Although the source strength and the fraction of people exposed are the same in all scenarios and only the total population changes between the years, the (average) exposure is not the same as insulation of residential buildings leads to accumulation of PM indoors. Thus, from BAU to policy scenarios the exposure to ETS and the health effects increase (except for 2020 where in the BAU the PM emissions are higher than in the Policy scenario so that also the exposure in the BAU is higher). From 2030 to 2050 the exposure decreases – which is probably due to higher average indoor volume of residential buildings.

Table 5-8: Health effects due to ETS (PM based), per endpoint and year for EU30.

	PM10_BU_A	PM10_BU_C	PM10_CHA	PM10_CB	PM10_IM	PM10_LRS_A	PM10_LRS_C	PM10_RHA
2020BAU	70 mio	2.3 mio	38 thd	611 thd	590	303 mio	214 mio	51 thd
2020Policy	67 mio	2.3 mio	37 thd	586 thd	570	290 mio	209 mio	49 thd
2030BAU	68 mio	2.2 mio	37 thd	590 thd	580	292 mio	201 mio	49 thd
2030Policy	71 mio	2.3 mio	38 thd	617 thd	610	306 mio	211 mio	51 thd
2050BAU	65 mio	2.2 mio	35 thd	566 thd	570	280 mio	198 mio	47 thd
2050Policy	69 mio	2.3 mio	38 thd	600 thd	610	297 mio	211 mio	50 thd

	PM25_MRAD	PM25_RAD	PM25_WLD	PM25_YOLL
2020BAU	242 mio	378 mio	87 mio	4 mio
2020Policy	232 mio	363 mio	83 mio	3.8 mio

2030BAU	226 mio	354 mio	81 mio	3.9 mio
2030Policy	237 mio	371 mio	85 mio	4.1 mio
2050BAU	205 mio	321 mio	74 mio	3.7 mio
2050Policy	217 mio	340 mio	78 mio	4 mio

Table 5-9: Health effects due to ETS (PM based), per endpoint and year for EU30, Difference between Policy and BAU scenario.

	PM10_BU_A	PM10_BU_C	PM10_CHA	PM10_CB	PM10_IM	PM10_LRS_A	PM10_LRS_C	PM10_RHA
2030	3 mio	108 thd	1 thd	27 thd	30	14 mio	10 mio	2 thd
2050	4 mio	136 thd	3 thd	34 thd	40	17 mio	12 mio	3 thd

	PM25_MRAD	PM25_RAD	PM25_WLD	PM25_YOLL
2030	11 mio	17 mio	4 mio	200 thd
2050	12 mio	19 mio	4 mio	300 thd

As can be seen in Table 5-9 in 2030 and 2050 in the Policy scenario there are more health effects than in the BAU. This is due to an accumulation of PM in residential buildings due to better insulation and a smaller air exchange rate.

Exposure to ETS is very high. Only to about 20 µg/m^3 background concentration (corresponding to about 30 µg/m^3 personal exposure) is the exposure response function believed to be linear. With higher doses the effect per unit exposure decreases. Thus, we might overestimate the health effects due to ETS.

5.2.3 Health effects due to heat exposure

Currently, almost 15,000 deaths are attributable to summertime heat exposure annually in the densely populated European metropolitan areas within the countries included in the assessment (

Table 5-10). Over 70% of these deaths occur in those aged 75 or older.

Table 5-10: Deaths (all natural causes, average and 95% confidence limits) attributable to heat exposure in large European cities in different reference and UHI mitigation scenarios.

Climate scenario & year	Reference / UHI mitigation scenario	Region		Total
		North-continental	Mediterranean	
2010	Current	7104 (3252-11186)	7516 (2893-15323)	14 639 (8142-22847)
A1B				
2020	Reference 1	13760 (5544-22968)	11412 (4192-23547)	25172 (13682-40539)
	Vegetation	13220 (5326-22101)	10904 (3988-22600)	24123 (13112-38929)
	Albedo	12301 (4957-20607)	10075 (3653-21034)	22376 (12156-36211)
	Veg+alb	11813 (4763-19808)	9589 (3456-20176)	21402 (11627-34718)
2030	Reference 1	21701 (8722-36913)	19552 (7142-40453)	41253 (22284-66631)
	Vegetation	20774 (8347-35396)	18685 (6781-38819)	39459 (21266-63937)
	Albedo	19307 (7758-32865)	17267 (6144-36286)	36574 (19543-59504)
	Veg+alb	18403 (7395-31303)	16329 (5722-34685)	34732 (18391-56714)
2050	BAU	44867 (17406-77214)	33489 (12507-66637)	78357 (42046-123275)
	Vegetation	43110 (16720-74134)	23138 (11980-64412)	75248 (40184-118849)
	Albedo	40520 (15712-69611)	29943 (11081-60713)	70462 (37534-111824)
	Veg+alb	39119 (15161-67230)	28763 (10536-58739)	67882 (36154-108226)
B1				
2020	Reference 2	13066 (5331-21844)	12695 (4571-26552)	25761 (13721-41806)
	Vegetation	12489 (5098-20867)	12078 (4322-25392)	24568 (13063-39917)
	Albedo	11553 (4718-19330)	11112 (3931-23679)	22665 (11905-37098)
	Veg+alb	11066 (4520-18544)	10539 (3673-22668)	21605 (11345-35529)
2030	Reference 2	20325 (8137-34303)	18121 (6640-37088)	38446 (20884-61501)
	Vegetation	19521 (7812-32932)	17287 (6313-35682)	36808 (19969-58953)
	Albedo	18318 (7332-30917)	15984 (5808-33241)	34303 (18569-55122)
	Veg+alb	17629 (7057-29776)	15250 (5520-31990)	32878 (17759-52977)
2050	Reference 2	16059 (6242-27807)	30282 (11515-59608)	46341 (24366-77494)
	Vegetation	15417 (5995-26692)	29019 (11016-57430)	44436 (23406-74422)
	Albedo	14323 (5573-24797)	27103 (10129-54246)	41426 (21876-69871)
	Veg+alb	13681 (5326-23689)	26011 (9670-52433)	39692 (20897-67081)

The number of heat related deaths is likely to increase drastically during the following 40 years as the climate becomes warmer and the population ages. In the reference scenario 1 the attributable deaths increase over 400% by 2050. In the reference scenario 2 the increase in deaths by 2050 is lower, approximately 200%, which is mainly due to the declining trend in heat exposure in the North-continental region cities towards the later years of the assessment time frame. The mortality impacts of heat exposure were not quantified in years of life lost, because it is currently unclear what role mortality displacement, i.e. the so-called harvesting effect, has in heat exposure induced mortality (Basu 2008).

Thousands of heat exposure related deaths could be averted annually by implementing the evaluated urban heat island mitigation policies (Figure 5-3 and Figure 5-4). The benefits from the policies increase substantially in the future and are higher in the IPCC climate scenario A1B, which represents stronger climate change and warming and seems, at the moment, to be the more probable of the two evaluated climate scenarios.

In attributable death estimation, the quantitative uncertainty assessment took into consideration only the uncertainty in the exposure-response functions and exposure thresholds related to them. These two factors alone cause a high range of uncertainty in the results. However, there are also several other sources of uncertainty, the impact of which could not be quantified. These relate to the reliability of the temperature data,

the basic assumptions in the UHI mitigation policies and the effect of the policies on temperatures and heat exposure within cities, the methodology used in defining the large cities and population living within them, assumptions on the background mortality risk in different countries in the future, as well as the suitability of the exposure-response functions to reflect mortality impacts in the future.

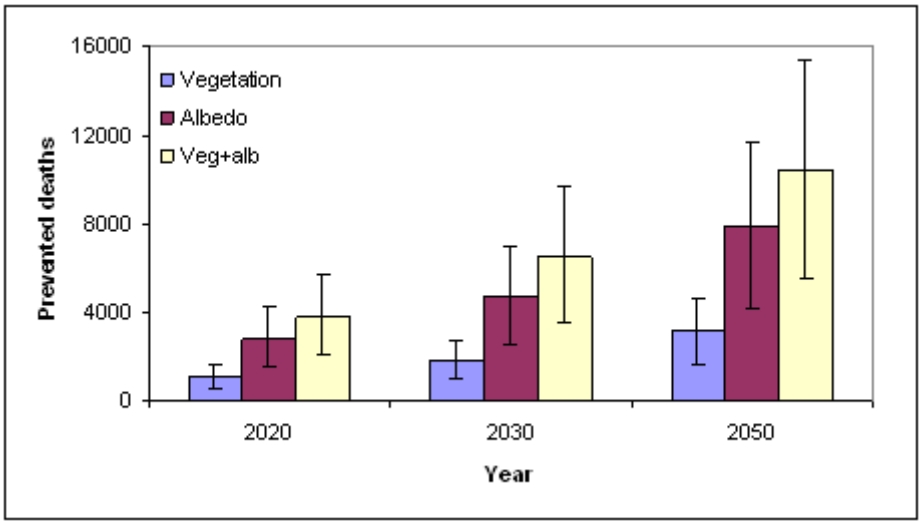

Figure 5-3: Heat exposure related deaths prevented annually in IPCC climate scenario A1B if different UHI mitigation policies are implemented.

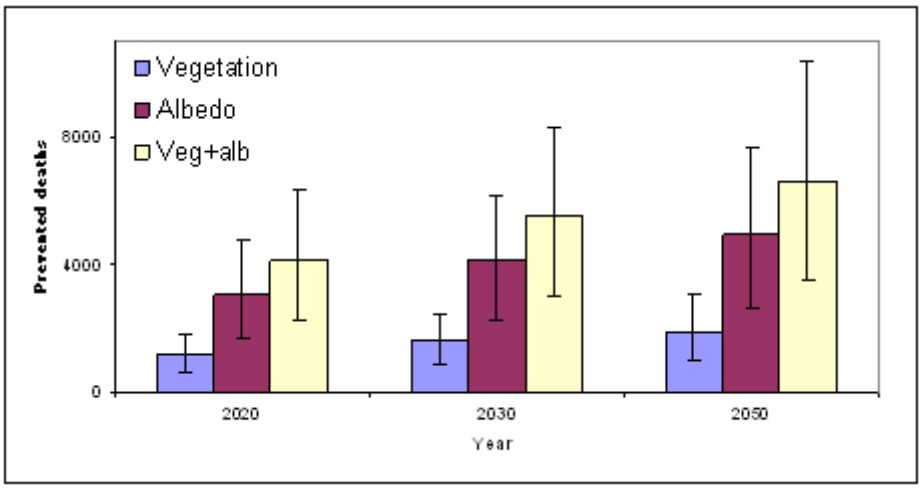

Figure 5-4: Heat exposure related deaths prevented annually in IPCC climate scenario B1 if different UHI mitigation policies are implemented.

It is currently unclear what role mortality displacement, i.e. the so-called harvesting effect, has in heat exposure induced mortality (Basu 2009). Mortality displacement refers to a phenomenon where the environmental exposure advances the deaths of ill people by only a few days. Nevertheless, an attempt was made to quantify the health impacts also in DALYs and monetary costs (see Sections 7.1.9 and 7.2.9). Life years lost due to a heat attributable death was defined as a uniform probability distribution

with a lower boundary of three months and upper boundary of ten years. Because of this, and the uncertainty in the number of the attributable deaths, the uncertainty range in the DALY and monetary cost estimates is very wide. However, if mortality displacement is considered as an important factor in heat related mortality, then the lower boundary estimates should be considered as more representative. Monetary costs were calculated by assuming a uniform distribution for the value of a life year with a lower boundary of 60 000 and upper boundary of 89 715 euros.

The results of the assessment and the uncertainties related to it a discussed in more detail in Appendix E (Annexes

Heat and Urban Heat Island (UHI) Mitigation).

5.2.4 Health effects due to noise

Table 5-11, Table 5-12, Table 5-13 and Table 5-14 present the results for annoyance, high annoyance, high sleep disturbance and myocardial infarction for the BAU and 2degree scenario.

Table 5-11: Prevalence of high annoyance due to road traffic noise in the urban population of Europe for the BAU and the 2degree scenario, including the contributions of individual measures within the 2degree policy

Scenario/measure	**2005**	**2020**	**2030**	**2050**
BAU (number of Europeans)	25.7 million	28.1 million	28.2 million	26.3 million
Percentage change in the number of Europeans affected, compared to the BAU scenario				
Climate policy scenario	0	-4.2	-5.1	-6.5
- Fuel tax	0	-0.8	-1.5	-1.5
- Cycling in cities	0	-1.0	-1.0	-0.9
- City toll	0	-0.2	-0.2	-0.2
- PC toll	0	-2.0	-1.9	-1.8
- Electric vehicles	0	-0.2	-0.6	-2.1

Table 5-12: Prevalence of annoyance due to road traffic noise in the urban population of Europe for the BAU and the 2degree scenario, including the contributions of individual measures within the 2degree policy

Scenario/measure	**2005**	**2020**	**2030**	**2050**
BAU (number of Europeans)	61.3 million	65.2 million	65.4 million	62.1 million
Percentage change in the number of Europeans affected, compared to the BAU scenario				
Climate policy scenario	0	-3.1	-4	-5
- Fuel tax	0	-0.6	-1.1	-1.2
- Cycling in cities	0	-0.7	-0.7	-0.7
- City toll	0	-0.1	-0.1	-0.2
- PC toll	0	-1.4	-1.4	-1.4
- Electric vehicles	0	-0.1	-0.4	-1.6

Table 5-13: Prevalence of high sleep disturbance due to road traffic noise in the urban population in Europe for the BAU and the 2degree scenario, including the contributions of individual measures within the 2degree policy

Scenario/measure	**2005**	**2020**	**2030**	**2050**
BAU (number of Europeans)	15.6 million	16.6 million	16.7 million	15.9 million
Percentage change in the number of Europeans affected, compared to the BAU scenario				
Climate policy scenario	0	-3.1	-3.7	-4.3
- Fuel tax	0	-0.6	-1.1	-1.0
- Cycling in cities	0	-0.8	-0.7	-0.6
- City toll	0	-0.1	-0.1	-0.1
- PC toll	0	-1.5	-1.4	-1.2
- Electric vehicles	0	-0.1	-0.4	-1.4

Table 5-14: Prevalence of myocardial infarction due to road traffic noise in the urban population in Europe for the BAU and the 2degree scenario, including the contributions of individual measures within the 2degree policy

Scenario/measure	**2005**	**2020**	**2030**	**2050**
BAU (number of Europeans)	7.1 thousand	9.4 thousand	9.6 thousand	8.1 thousand
Percentage change in the number of affected Europeans, compared to the BAU scenario				
Climate policy scenario	0	-9.8	-11.8	-15.8
- Fuel tax	0	-1.9	-3.5	-3.6
- Cycling in cities	0	-2.5	-2.2	-2.4
- City toll	0	-0.4	-0.4	-0.5
- PC toll	0	-4.6	-4.3	-4.5
- Electric vehicles	0	-0.4	-1.4	-4.9

The dependence of the above results on the assumptions for the BAU scenario was investigated by comparing results for two different baseline scenarios: one with and one without the emission reduction up to 2 dB in 2050. The effects of the measures were similar for the two baseline scenarios, indicating that the effects are not very sensitive to the actual baseline scenario assumed.

5.2.5 Health effects due to dampness

Table 5-15: Asthma cases (prevalence) in Europe due to residential building dampness (mean and 95% confidence interval) (Luxembourg, Netherlands, Switzerland, Ireland, Norway, United Kingdom, Bulgaria, Hungary, Lithuania, Romania, Slovakia, Slovenia, Malta)

	Year			
Policy	**2010**	**2020**	**2030**	**2050**
BAU	1715846 (794208-2918407)	2069089 (929518-3645690)	2300513 (1007103-4193891)	2417413 (1016202-4559645)
All	NA	2071501 (940391-3650210)	2634778 (1139578-4745158)	3009693 (1251020-5519308)
Insulation	NA	NA	NA	3002498 (1239186-5524389)
Renovation	NA	NA	NA	3416010 (1443227-6233562)

5.2.6 Health effects due to radon

Table 5-16: Lung cancer cases in Europe due to indoor radon in residences (mean and 95% confidence interval) (without UK, Czech Republic and Slovenia).

	Year			
Policy	**2010**	**2020**	**2030**	**2050**
BAU	43074 (7186-104660)	51801 (8934-129303)	58716 (9427-155621)	63718 (10407-178566)
All	NA	52660 (8892-130780)	68086 (10544-180827)	81022 (11983-235695)
Insulation	NA	NA	NA	80149 (11898-228747)
Renovation	NA	NA	NA	92783 (13365-275851)

5.2.7 Health effects due to ETS originated VOCs and formaldehyde

The cases for each country where estimated by multiplying the individual risk by the exposed population.

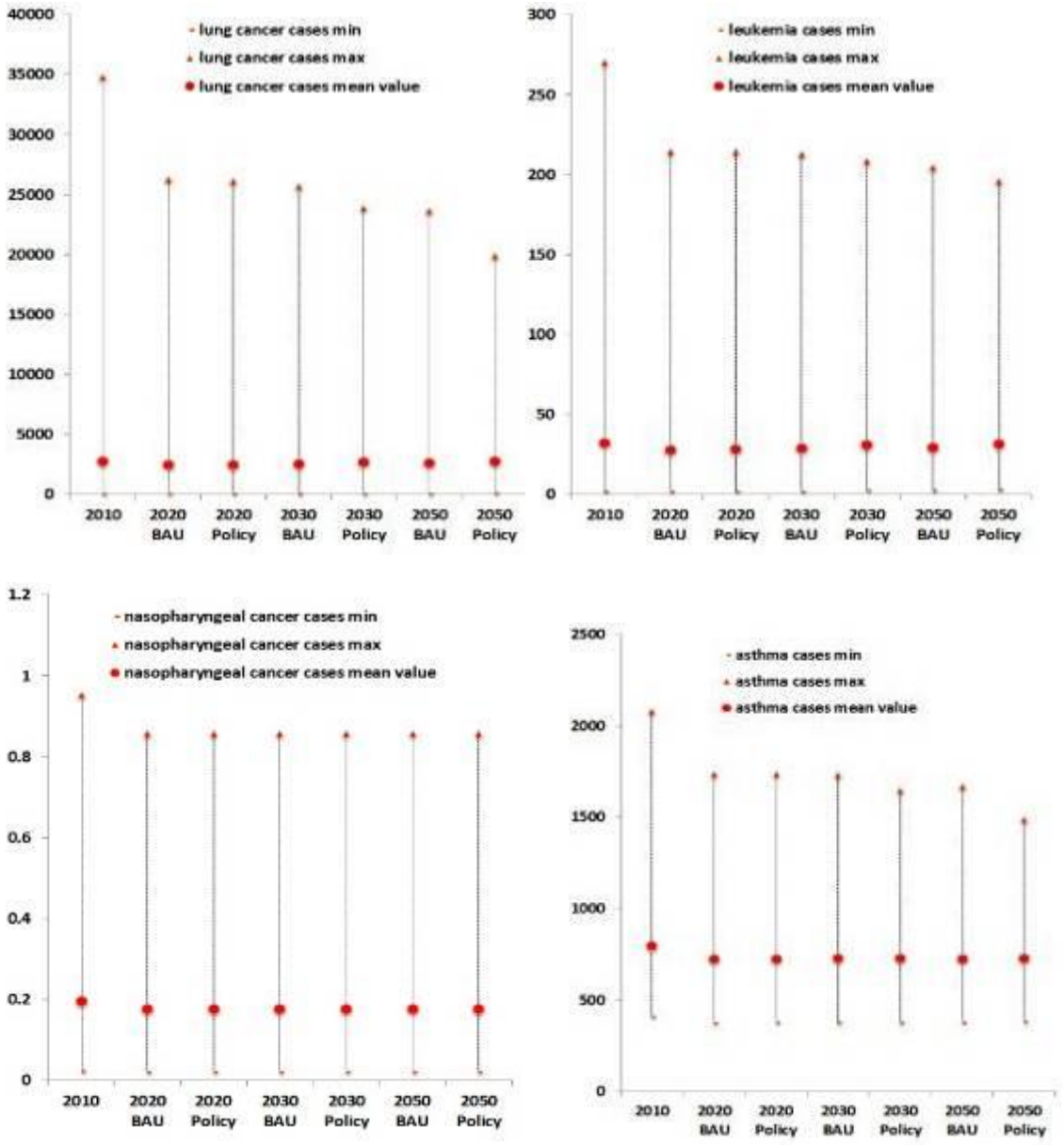

Figure 5-5: Health effects due to ETS originated VOCs (cancer and asthma) for EU27

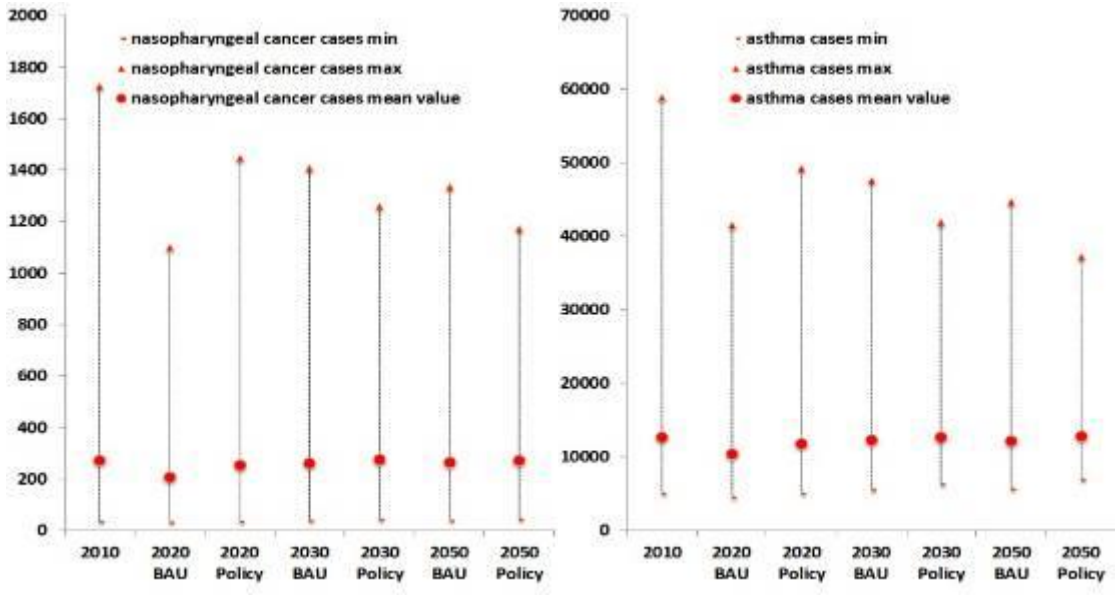

Figure 5-6: Health effects due to formaldehyde (cancer) for EU 27Health Effects caused by Complex Pathway Pollutants

6 HEALTH EFFECTS CAUSED BY MULTIMEDIA PATHWAY POLLUTANTS

6.1 HEALTH EFFECTS CAUSED BY EMISSIONS OF POPS

6.1.1 Followed Approach

The health effects caused by emissions of POPs, in particular caused by emissions of PCB-153 and 2,3,4,7,8-PeDCDF as reference congeners are calculated based on the concentrations in the environmental media, which are discussed in Section 4.5. Intake via inhalation thereby follows the simple approach of relating the air concentration of a chemical to the concentration in humans via the respective inhalation rate, which is assumed to be constant for all persons. The same procedure was followed for the estimation of concentration in humans via drinking water ingestion by applying the respective water ingestion rate, which is also assumed to be constant for all persons. In contrast to these two approaches, health effects via ingestion of food items are calculated based on bioaccumulation factors (BAF) and biotransfer factors (BTF) for relating a concentration in a food product (such as fish) to the environmental concentration of its surrournding medium (in case of fish this would be water) and the concentration in a food product to a particular feed item (e.g. concetration in cows related to the concentration in the produce that is consumed by the cow), respectively. Subsequent human intake of food products is then based on the consumption pattern of the respective food products, which differ significantly between European countries, e.g. in countries like Denmark the per capita intake per year of fish is much higher than in Austria.

The overall health effects caused by emissions of POPs via all considered exposure pathways, i.e. inhalation, ingestion of drinking water and ingestion of food, are finally aggregated.

6.1.2 Results: Health effects due to exposure to POPs including BAU and 2°C aim scenarios

Calculations of health impacts caused by emissions of POPs, in particular emissions of PCB-153 and 2,3,4,7,8-PeCDF, via inhalation and ingestion intake of drinking water and food have been performed by using the PANGEA model as described in Section 4.5.1. Exposure results, i.e. human ingestion intake per country, have been combined with the dose-response information (DRFs) available for the different exposure pathways as described above. Number of cases of cancer for all countries are listed in for PCB-153 and in for 2,3,4,6,7-PeCDF, respectively.

Table 6-1: Number of cancer incidences due to intake of PCB-153 in Europe for all considered scenarios.

Country	Number of cases for cancer, PCB-153 [cases]						
	2000	2020	2030	2050	2020	2030	2050
Austria	1.4E-13	4.8E-14	3.4E-14	2.1E-14	2.9E-14	1.7E-14	1.1E-14
Belgium	6.8E-13	1.5E-13	4.1E-14	2.7E-14	5.6E-14	3.3E-14	2.5E-14
Bulgaria	4.1E-13	7.2E-14	4.9E-14	2.6E-14	4.5E-14	2.8E-14	1.8E-14
Cyprus	1.5E-13	1.2E-14	2.4E-15	1.9E-15	7.9E-15	7.4E-15	7.8E-15
Czech Republic	4.2E-13	2.6E-14	1.4E-14	8.5E-15	1.4E-14	7.7E-15	4.7E-15
Denmark	3.8E-12	9.7E-14	6.1E-14	3.9E-14	5.4E-14	4.1E-14	3.6E-14
Estonia	5.7E-13	1.8E-13	8.8E-14	5.2E-14	1.1E-13	7.3E-14	5.2E-14
Finland	3.3E-13	1.9E-14	2.6E-15	1.6E-15	1.2E-14	8.9E-15	7.3E-15
France	8.2E-12	4.1E-12	2.9E-12	1.8E-12	2.0E-12	1.4E-12	1.2E-12
Germany	6.8E-12	2.5E-12	3.3E-13	1.8E-13	1.3E-12	7.0E-13	4.1E-13
Greece	8.0E-13	1.3E-13	5.4E-14	3.4E-14	8.2E-14	5.8E-14	4.6E-14
Hungary	5.5E-12	3.7E-14	4.5E-15	2.8E-15	2.1E-14	1.2E-14	8.1E-15
Ireland	1.8E-13	1.5E-13	3.3E-14	2.5E-14	1.1E-13	1.1E-13	1.2E-13
Italy	4.1E-12	1.5E-12	4.8E-13	3.0E-13	7.9E-13	5.2E-13	3.9E-13
Latvia	8.9E-13	6.9E-15	3.3E-16	1.8E-16	4.2E-15	2.6E-15	1.8E-15
Lithuania	1.3E-12	1.4E-14	3.8E-15	2.1E-15	7.9E-15	4.8E-15	3.1E-15
Luxembourg	8.8E-15	3.1E-15	1.8E-15	1.4E-15	1.4E-15	8.9E-16	7.5E-16
Malta	n/a	n/a	n/a	n/a	n/a	n/a	n/a
Netherlands	3.4E-12	1.9E-14	7.0E-15	4.5E-15	8.6E-15	4.3E-15	2.9E-15
Norway	2.0E-12	2.8E-14	9.4E-15	6.4E-15	2.2E-14	2.0E-14	1.9E-14
Poland	2.5E-10	9.1E-13	4.3E-13	2.3E-13	4.8E-13	2.6E-13	1.5E-13
Portugal	8.8E-12	6.2E-14	1.2E-14	7.4E-15	3.9E-14	3.3E-14	2.9E-14
Romania	3.9E-12	2.1E-13	1.1E-13	6.0E-14	1.2E-13	7.5E-14	4.7E-14
Slovakia	3.5E-13	1.0E-14	2.1E-15	1.2E-15	5.9E-15	3.2E-15	1.9E-15
Slovenia	6.9E-14	2.2E-14	5.8E-15	3.5E-15	1.2E-14	7.1E-15	4.9E-15
Spain	4.3E-11	1.5E-11	3.7E-12	2.5E-12	8.2E-12	6.5E-12	5.9E-12
Sweden	4.5E-13	1.2E-14	1.9E-15	1.2E-15	6.6E-15	5.0E-15	4.4E-15
Switzerland	7.6E-15	7.6E-15	6.9E-15	4.6E-15	2.9E-15	1.9E-15	1.4E-15
United Kingdom	3.5E-12	1.4E-12	6.0E-13	5.0E-13	6.8E-13	5.2E-13	4.8E-13
SUM	5.9E-10	4.2E-11	1.3E-11	8.4E-12	2.2E-11	1.7E-11	1.5E-11

Table 6-2: Number of cancer incidences due to intake of 2,3,4,7,8-PeCDF in Europe for all considered scenarios.

Country	Number of cases for cancer, 2,3,4,7,8-PeCDF [cases]						
	2000	2020	2030	2050	2020	2030	2050
Austria	0.877	0.584	0.367	0.093	0.410	0.165	0.070
Belgium	2.617	1.597	0.999	0.256	1.137	0.431	0.179
Bulgaria	0.562	0.216	0.120	0.026	0.160	0.055	0.020
Cyprus	0.190	0.161	0.111	0.033	0.118	0.078	0.062
Czech Republic	0.110	0.053	0.036	0.009	0.039	0.013	0.004
Denmark	2.176	1.139	0.708	0.179	0.856	0.365	0.181
Estonia	0.120	0.081	0.050	0.012	0.055	0.023	0.010
Finland	0.168	0.128	0.080	0.020	0.086	0.034	0.016
France	5.607	4.011	2.660	0.671	2.760	1.258	0.633
Germany	3.316	1.908	1.128	0.257	1.469	0.547	0.208

Country	Number of cases for cancer, 2,3,4,7,8-PeCDF [cases]						
	2000	2020	2030	2050	2020	2030	2050
Greece	0.954	0.535	0.326	0.082	0.369	0.170	0.085
Hungary	0.258	0.092	0.056	0.014	0.061	0.019	0.007
Ireland	0.312	0.419	0.282	0.084	0.294	0.162	0.126
Italy	11.761	8.217	5.194	1.297	4.950	1.919	0.847
Latvia	0.004	0.003	0.001	0.000	0.002	0.001	0.000
Lithuania	0.009	0.006	0.003	0.001	0.004	0.001	0.000
Luxembourg	0.004	0.003	0.002	0.001	0.002	0.001	0.000
Malta	n/a	n/a	n/a	n/a	n/a	n/a	n/a
Netherlands	0.016	0.010	0.004	0.001	0.007	0.002	0.001
Norway	0.105	0.076	0.066	0.018	0.052	0.027	0.019
Poland	1.803	0.965	0.611	0.141	0.669	0.217	0.070
Portugal	0.549	0.361	0.226	0.056	0.225	0.094	0.049
Romania	2.724	1.291	0.812	0.187	0.901	0.323	0.122
Slovakia	0.202	0.098	0.057	0.014	0.071	0.026	0.010
Slovenia	0.591	0.469	0.256	0.064	0.265	0.102	0.039
Spain	10.116	8.770	5.695	1.521	6.051	2.890	1.656
Sweden	0.227	0.133	0.081	0.022	0.096	0.043	0.022
Switzerland	0.009	0.006	0.004	0.001	0.004	0.002	0.001
United Kingdom	6.155	4.238	2.774	0.766	2.807	1.124	0.580
SUM	62.43	43.76	28.04	7.25	29.56	12.82	6.61

6.1.3 Uncertainties

Uncertainties related to the assessment of POPs environmental fate for all scenarios were assessed using the MSCE-POP and PANGEA model as described in Section 4.5.3. However, additional uncertainty aspects are introduced by following the chain from exposure to health effects. This uncertainty is mainly related to the distribution of differently exposed population, i.e. consumption pattern and the actural residual concentrations in ingested drinking water and food commodities due to e.g. further processing of cow meat or milk. In addition, uncertainty is introduced by the fact that dose-response information is available only for a specific health endpoint, i.e. carcinogenicity.

6.2 HEALTH EFFECTS CAUSED BY APPLICATIONS AND EMISSIONS OF PESTICIDES

6.2.1 Health Effects via Ingestion Exposure after Direct Application

Results: Calculations of health impacts due to ingestion of pesticides with food crops after direct application have been performed by using the dynamiCROP model as described in Section 4.6.2 for the environmental fate and ingestion exposure part of the full chain. Exposure results, i.e. human ingestion intake per country, have been combined with the dose-response information (DRFs) available for the ingestion pathway as described above. Since DRFs have been available only for few substances

out of the list of considered pesticides for this study, effects caused by all other pesticides had to be estimated based on extrapolation from the existing DRFs.

Based on the effect assessment applied for selected pesticides with available DRF information for carcinogenic potential, the number of human cancer incidences per country are derived as shown in Table 6-3.

Table 6-3: Number of cancer incidences due to ingestion exposure of pesticides after direct application in European countries between 2000 and 2050 for pesticides with available effect information.

Country	Number of cancer cases [cases]						
	2000base	2020BAU	2020climate	2030BAU	2030climate	2050BAU	2050climate
Austria	1.016	1.080	1.080	1.092	1.092	1.077	1.077
Bulgaria	1.7E-12	1.5E-12	1.5E-12	1.4E-12	1.4E-12	1.1E-12	1.1E-12
Cyprus	n/a	n/a	n/a	n/a	n/a	n/a	n/a
Greece	2.5E-12	2.5E-12	2.5E-12	2.5E-12	2.5E-12	2.5E-12	2.5E-12
Hungary	0.129	0.124	0.124	0.120	0.120	0.113	0.113
Italy	n/a	n/a	n/a	n/a	n/a	n/a	n/a
Malta	n/a	n/a	n/a	n/a	n/a	n/a	n/a
Portugal	0.224	0.212	0.212	0.158	0.191	0.104	0.148
Romania	0.358	0.330	0.330	0.315	0.315	0.279	0.279
Slovenia	0.008	0.009	0.009	0.003	0.008	0.005	0.008
Spain	n/a	n/a	n/a	n/a	n/a	n/a	n/a
Switzerland	n/a	n/a	n/a	n/a	n/a	n/a	n/a
Belgium	0.066	0.077	0.077	0.083	0.066	0.095	0.096
Czech Republic	0.228	0.236	0.236	0.235	0.235	0.230	0.230
Denmark	0.011	0.011	0.011	0.011	0.011	0.011	0.011
Estonia	0.018	0.018	0.018	0.017	0.017	0.017	0.017
Finland	0.414	0.437	0.437	0.441	0.441	0.433	0.433
France	5.883	6.528	6.528	6.683	6.683	6.803	6.803
Germany	n/a	n/a	n/a	n/a	n/a	n/a	n/a
Ireland	0.009	0.018	0.018	0.019	0.019	0.021	0.021
Latvia	0.234	0.212	0.212	0.202	0.202	0.183	0.183
Lithuania	0.044	0.038	0.038	0.037	0.037	0.032	0.032
Luxembourg	0.011	0.014	0.014	0.014	0.014	0.018	0.018
Netherlands	0.005	0.006	0.006	0.006	0.006	0.008	0.008
Norway	n/a	n/a	n/a	n/a	n/a	n/a	n/a
Poland	1.453	1.425	1.425	1.375	1.375	1.216	1.216
Slovakia	1.200	1.215	1.215	1.194	1.194	1.097	1.097
Sweden	0.004	0.004	0.004	0.004	0.004	0.004	0.004
United Kingdom	45.473	51.830	51.830	54.112	54.112	57.623	57.623
SUM	**56.79**	**63.82**	**63.82**	**66.12**	**66.14**	**69.37**	**69.42**

Uncertainties: Uncertainties related to the assessment of pesticide environmental fate and ingestion exposure for all scenarios were assessed using the dynamiCROP model as described in Section 4.6.2. However, additional uncertainty aspects are introduced by following the chain from ingestion exposure to health effects. This uncertainty is mainly related to the distribution of differently exposed population, i.e. consumption pattern and the actural residual concentrations in the ingested food commodities due to e.g. further processing of harvested crops. In addition, uncertainty is introduced by

the fact that only for a fraction of considered substances dose-response information is available and this only for a specific health endpoint, i.e. carcinogenicity.

Since no information is available on the uncertainty of the applicability of the applied dose-response information that was available for only few substances and that has been extrapolated to also cover the considered substance for which no specific dose-response functions were available. However, the uncertainty introduced by extrapolating effect information is assumed to be relatively high compared to the uncertainty discussed for the environmental fate and exposure of pesticides as discussed in Section 4.6.2.

6.2.2 Health Effects via Inhalation Exposure after Direct Application

A PBPK model for atrazine as model compound has been developed and implemented to estimate internal dose. Coupling this model with toxicogenomics, and other toxicological evidence we have also developed an internal dose-response function for this compound as methodological proof-of-concept. On the basis of the results and on the fact that we could readily estimate the intake fraction (by inhalation and ingestion) for a relatively significant number of active ingredients in pesticides we have developed a concept based on a intake fraction and intake dose estimation to use as the appropriate exposure metric. Thus, total intake dose was estimated and coupled to the dose-response functions given in the table below to derive estimates of carcinogenicity risk.

The toxicologically-derived dose-response functions for carcinogenic active ingredients in commercial pesticide preparations used in Europe are summarised in the following table. This is only a fraction of the overall number of pesticides currently in the EU internal market. However, these are the ones with a carcinogenicity characterisation by either European or American regulatory authorities. Given the lack of robust quantitative evidence for health endpoints relating exposure metrics (dose/concentration) and physiological response other than in the case of carcinogenicity we have not addressed any other health effect of pesticides.

Table 6-4: Dose response functions for carcinogenic pesticides (Rowland, 2006; Public Notice, 2001).

Name	Action[1]	Chemical class	Carcinogenicity (U.S. EPA)	Slope factors $(mg/kg/day)^{-1}$
1,3-Dichloropropene	ZR	Halogenated organic	Probable (B2)	9.10E-02
Amitrol	H	Triazole	Likely (high doses), Not likely (low doses)	1.13 E+0
Boscalid	F	Carboxamide	Possible (C)	2.59E-02
Bromoxynil	H	Hydroxybenzonitrile	Possible (C)	1.03E-01

Name	Action[1]	Chemical class	Carcinogenicity (U.S. EPA)	Slope factors (mg/kg/day)$^{-1}$
Captan	F	Thiophthalimide	Likely (high doses), Not likely (low doses)	2.30E-03
Carbendazim	F	Benzimidazole	Possible (C)	2.39E-03
Chlorothalonil	F	Chloronitrile	Probable (B2)	7.66E-03
Difenoconazole	F	Azole	Possible (C)	1.13 E+0
Dimethoate	I	Organophosphorus	Possible (C)	5.30E-01
Dithianon	F	Quinone	Suggestive	4.39E-02
Folpet	F	Thiophthalimide	Probable (B2)	1.86 E-3
Iprodione	F	Dicarboximide	Probable (B2)	4.39E-02
Isoxaflutole	H	Isoxazole	Probable (B2)	1.02E-02
Kresoxim Methyl	F	Strobin	Likely	4.39E-02
Linuron	H	Urea	Possible (C)	1.10E-01
Mancozeb	F	Dithiocarbamate, Inorganic-Zinc	Probable (B2)	6.01 E-2
Mecoprop-P	H	Aryloxyalkanoic acid	Possible (C)	1.10E-01
Methidathion	I	Organophosphorus	Possible (C)	5.30E-01
Metiram	F	Dithiocarbamate, Inorganic-Zinc	Probable (B2)	6.01 E-2
Molinate	H	Thiocarbamate	Possible (C)	1.10E-01
Pendimethalin	H	2,6-Dinitroaniline	Possible (C)	2.93E-03
Propiconazole	F	Triazole	Possible (C)	1.13 E+0
Propyzamide	H	Benzamide	Probable (B2)	2.59E-02
Pyrimethanil	F	Pyrimidine	Possible (C)	4.39E-02
S-Metolachlor	H	Chloroacetamide	Possible (C)	2.59E-02
Tebuconazole	F	Triazole	Possible (C)	1.13 E+0
Tebufenpyrad	I	Pyrazole	Suggestive	1.13 E+0
Tolylfluanid	F	Sulphamide	Likely	1.59 E-3
Tralkoxydim	H	Cyclohexadione derivative	Probable (B2)	1.68E-02
Trifluralin	H	2,6-Dinitroaniline	Possible (C)	2.93E-03
Ziram	F	Dithiocarbamate, Inorganic-Zinc	Suggestive	6.01 E-2

DRFs are only available for few carcinogenic pesticides. For the purposes of this study DRFs for the rest of carcinogenic pesticides had to be estimated by extrapolation from the existing DRFs based on the same chemical class.

The incidence rate for carcinogenic pesticides is given by the following formula: I = R x P, where I is the Incidence rate, R is the risk for carcinogenic pesticides and P is the exposed population. Incidence rates for 45 carcinogenic pesticides in arable and permanent crops are presented in the following table (baseline 2000).

Table 6-5: Incidence rates (in cases/yr) for 45 carcinogenic pesticides in arable and permanent crops for the baseline year 2000.

	Incidence rates (in cases/yr)	
Country	**In Permenent Crops**	**In Arable land**
Austria	1.34E-05	6.89E-05
Belgium	1.98E-03	1.69E-04
Bulgaria	1.04E-06	1.26E-05
Cyprus	3.27E-07	0.00E+00
Czech Republic	4.10E-06	2.43E-05
Germany	5.13E-04	8.74E-03
Denmark	5.50E-07	3.88E-06
Spain	1.02E-02	1.87E-03
Estonia	1.82E-10	3.46E-06
Finland	0.00E+00	6.59E-06
France	1.39E-03	2.87E-04
UK	4.11E-07	2.20E-04
Greece	1.55E-05	1.00E-05
Hungary	5.51E-04	2.65E-03
Ireland	2.45E-09	2.06E-03
Italy	2.04E-03	3.83E-04
Lithuania	4.92E-07	1.01E-04
Luxembourg	1.96E-05	6.03E-06
Latvia	5.55E-08	4.97E-06
Malta	0.00E+00	0.00E+00
Netherlands	1.52E-04	3.29E-03
Poland	5.44E-05	2.09E-04
Portugal	1.01E-04	3.64E-02
Romania	1.09E-05	6.03E-05
Slovakia	1.90E-05	2.35E-04
Slovenia	1.86E-05	5.50E-05
Sweden	1.28E-06	4.90E-04

Incidence rates (in cases/year/ha) for 45 carcinogenic pesticides for year 2000 and 59 carcinogenic pesticides for scenario BAU 2030 are presented in Figure 6-1 and Figure 6-2.

The health impact of pesticide inhalation due to direct application by farmers, workers, applicators and their families and bystanders is a local phenomenon; thus, the right spatial scale of health impact estimation is the highest possible spatial resolution - in our case a grid of 100x100 m across Europe. Nevertheless, in order to provide the possibility to intercompare risks in the frame of the CCS at the spatial scale as well,

the health impact results have been resampled to a 50x50km^2 grid that is coherent with the spatial grid of the EMEP model in Europe. These results are given below in map form:

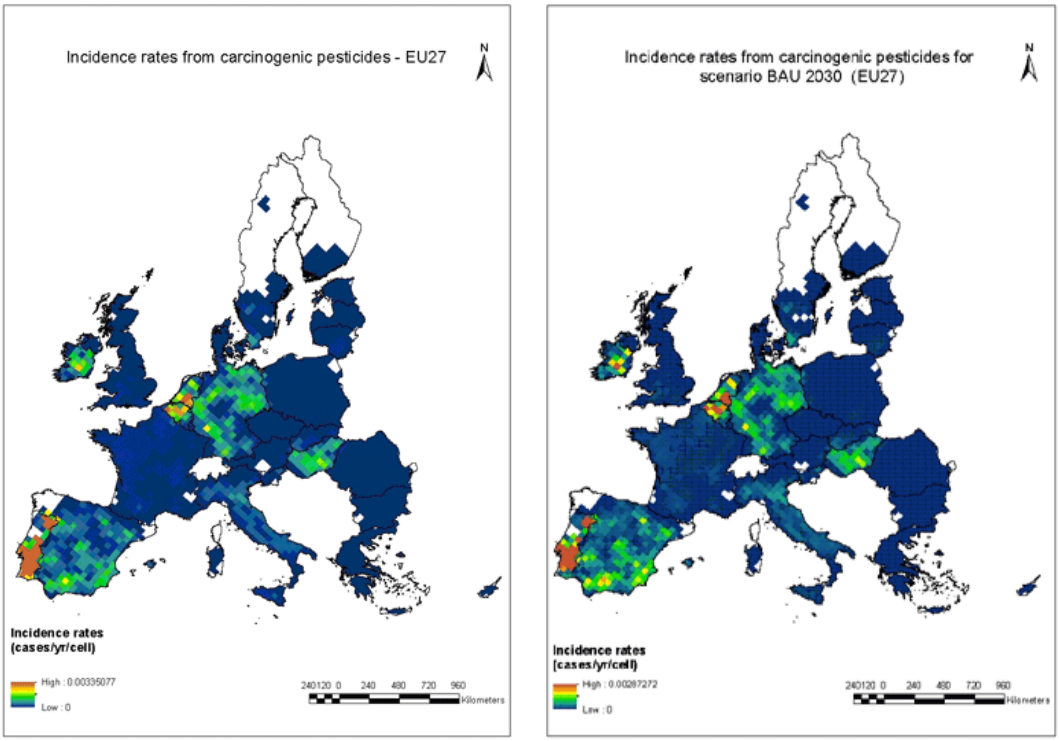

(a) (b)

Figure 6-1: Incidence rates (in cases/year/cell) for a) 45 carcinogenic pesticides (year 2000) and b) 59 carcinogenic pesticides for scenario BAU 2030 – EU27.

Incidence rates from carcinogenic pesticides at 100x100 resolution are shown in Figure 6-2.

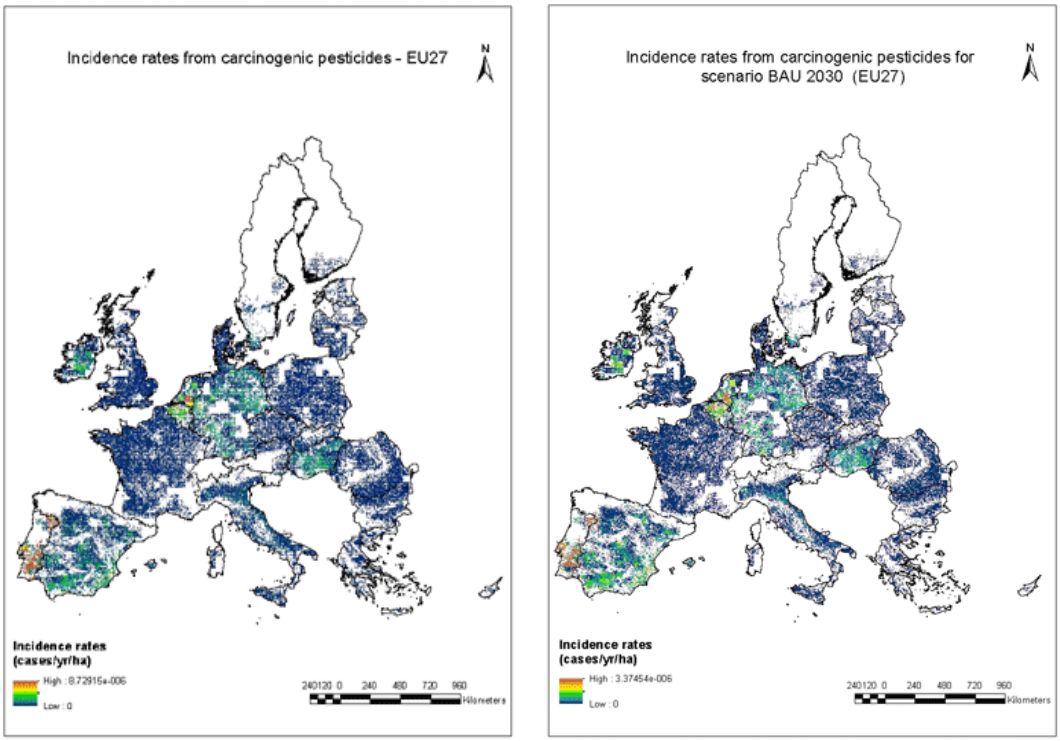

(a) (b)

Figure 6-2: Incidence rates (in cases/year/ha) for a) 45 carcinogenic pesticides (year 2000) and b) 59 carcinogenic pesticides for scenario BAU 2030 – EU27.

7 AGGREGATION AND VALUATION OF HEALTH EFFECTS

Health effects from environmental pressures can vary considerably with regard to their severity, duration, the number of people affected or the impact on society at large. This can make it difficult to compare different (environmental) health effects or evaluate the effects of policy measures that impact on a variety of health outcomes. An integrated measure for health, using the same denominator for all health effects, can help with interpretation and comparison of health problems and policies (scenarios or single measures).

Such measures can quantify and summarise (environment-related) health effects and can be used for e.g.:

- Comparative evaluation of environmental health impacts (“How bad is it?”)
- Evaluation of the effectiveness of (environmental) policies
- Communication of health risks

Two integrated health measures that can be used for this purpose include 1) the calculation of the burden of disease in DALYs (disability adjusted life years) or similar metrics, and 2) monetary valuation, which generally expresses the willingness to pay to avoid certain health effects. Both these options include a weighing scheme in order to compare health effects with a different severity and duration.

Basically, monetary valuation and DALYs are two quite different approaches to weigh and aggregate health outcomes. Monetary valuation is usually based on general population surveys of ‘ordinary’ people’s willingness to pay to avoid various kinds of health risks, augmented by some other measures of costs to society (e.g. health service, time off work etc.). The burden of disease method is based on the assessments of experts about the severity and implications for quality of life of various health outcomes, which is translated into a weighing factor.

While aggregation of health outcomes can be very convenient, any scheme for ‘translating’ complex health outcomes into a single metric necessarily has limitations, so that the two different ways of doing it – both of which are widely used – sometimes give different answers.

7.1 AGGREGATION OF HEALTH EFFECTS – THE BURDEN OF DISEASE APPROACH

DALYs combine information on both the quality and the quantity of life. They give an indication of the (potential) number of healthy life years lost due to premature mortality or morbidity. In these calculations, morbidity is weighted for the severity of the disorder. Thus, the total DALYs include both effects on morbidity and mortality (DALY = Years of Life Lost + Years Lived with Disability).

Calculating DALYs

Simplified, the formula for calculating DALYs is as follows:

Number of people with environment-related morbidity or mortality x

Severity factor (ranging from 0 to 1, with 0 = full health and 1 = death) x

Duration (the duration of disease for morbidity and YLL for mortality)

Uncertainty

DALYs capture the number of people affected and the duration and severity of health conditions in one number, thereby greatly simplifying reality. This simplification can be very useful to make different health states or environmental disease burdens comparable, but it may also lead to significant uncertainty in the output.

Such uncertainty can relate for example to (Knol, 2010):

- Definitions (what is ‘health’? what is ‘environment’?)
- Assumptions (for example about causality, stable situations, etc)
- Environment and health data (e.g. concentrations / emissions, exposed population, dose effect relationships, baseline disease data)
- DALY specific data (estimates of duration and severity of the effect)

Some of these uncertainties can be quantitatively assessed, others can be qualitatively described, and yet others are difficult to assess at all. Therefore, DALYs should always be interpreted taking their context and input data into account. They can only be used to give an indication of the potential order of magnitude of different (environmental) health problems, and cannot be presented as absolute or completely representative numbers.

A thorough assessment of uncertainty has not been carried out in this assessment. We do not have full (quantitative) estimates of the related uncertainty ranges.

Table 7-1: DALY weights and duration for health effects due to air pollutants.

Health endpoint	Weight	Duration	Pollutant
Bronchodilator Usage Adults	0.22	0.00274	PM10
Bronchodilator Usage Children	0.22	0.00274	PM10
Cardiac Hospital Admissions	0.71	0.038	PM10
Chronic Bronchitis	0.099	10	PM10
Infant Mortality	1	80	PM10
Lower Respiratory Symptoms Adults	0.099	0.00274	PM10
Lower Respiratory Symptoms Children	0.099	0.00274	PM10
Respiratory Hospital Admissions	0.64	0.038	PM10
Minor Restricted Activity Days	0.07	0.00274	PM2.5
Restricted Activity Days	0.099	0.00274	PM2.5
Work Loss Days	0.099	0.00274	PM2.5
Years of Life Lost chronic	1	1	PM2.5
Bronchodilator Usage Adults	0.22	0.00274	SOMO35
Bronchodilator Usage Children	0.22	0.00274	SOMO35
Cough Days	0.07	0.00274	SOMO35
LRS Children Excl Cough	0.099	0.00274	SOMO35
Mortality	1	1	SOMO35
Minor Restricted Activity Days	0.07	0.00274	SOMO35
Resp. Hospital Admissions	0.64	0.038	SOMO35

7.1.1 DALYs due to noise

The health effects of noise were also expressed in Disability Adjusted Life Years (DALYs), with a DALY weight factor of 0.02 for high annoyance and 0.07 for high sleep disturbance. For myocardial infarction the WHO definition DALY = Years of Life Lost + Years Lived with Disability was used. It was assumed that 25% of myocardial infarctions fatal with a life loss of 8 years. For the other 75% a DALY weight of 0.405 was used for the duration of one year. Highly annoyance was only considered at daytime (16 hours out of 24), while high sleep disturbance was only considered at nighttime (8 hours out of 24), thus, avoiding double counting. For further calculations see the noise report.

Total DALYs for noise were calculated by summing the values for the three endpoints, neglecting the fact that some overlap of annoyance, sleep disturbance, and myocardial infarction may be expected. For the BAU scenario and the 2degree scenario the results in Table 7-2 were obtained. The results for BAU and 2degree are also shown in Figure 7-1.

Table 7-2: Number of DALYs due to road traffic noise in the urban population in Europe for the BAU and the 450ppm scenario.

Scenario/measure	**2005**	**2020**	**2030**	**2050**
BAU (DALYs per year)	717,000	777,000	781,000	734,000
Climate policy scenario	717,000	747,000	745,000	693,000
Difference: BAU - Policy	-	30,000	36,000	41,000

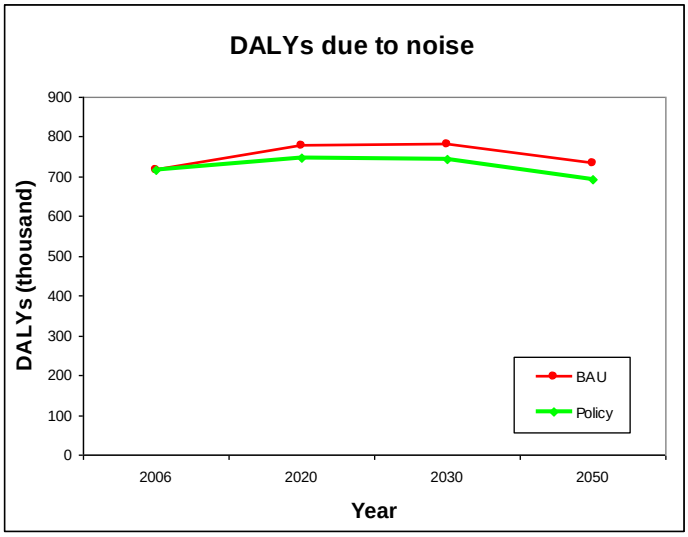

Figure 7-1: DALYs for noise in the BAU and Climate policy scenarios.

7.1.2 DALYs due to dampness

Table 7-3 shows the DALYs due to asthma in parts of Europe due to residential building dampness. For the scenario definition see Section 3.4. For a description of how the exposure to dampness was derived see Section 4.3.3.

Table 7-3: Asthma DALYs in Europe due to residential building dampness (mean and 95% confidence interval) (Luxembourg, Netherlands, Switzerland, Ireland, Norway, United Kingdom, Bulgaria, Hungary, Lithuania, Romania, Slovakia, Slovenia, Malta)

	Year			
Policy	**2010**	**2020**	**2030**	**2050**
BAU	101 000 (46,858-172,186)	122 000 (54,842-215,096)	136 000 (59,419-247,440)	143 000 (59,956-269,019)
All	NA	122 000 (55,483-215,362)	155,000 (67,235-279,964)	178 000 (73,810-325,639)
Insulation	NA	NA	NA	177 000 (73,112-325,939)
Renovation	NA	NA	NA	202 000 (85,150-367,780)

7.1.3 DALYs due to radon

DALYs were estimated for lung cancer due to radon (see Section 4.3.4). The disability weight (estimated by WHO) used in the burden of disease calculation for lung cancer is 0.146. We assume that each case of lung cancer causes a period of 2 to 36 months under disease, and a life expectancy loss of 1 to 15 years. Lung cancer is a rather deadly disease and few patienta that get a lung cancer diagnosis will actually be cured. Therefore, lung cancer mortality covers most DALYs involved, especially when the years with disease before death are included. However, there is also a fraction of patients that eventually die from something else, and their DALYs are not included in an assessment about mortality cases only. Therefore, we used slightly higher estimates for life expectancy loss to compensate for the non-mortality cases. We thought this was more reliable than trying to count lung cancer morbidity separately and then end up with double counting problems.

Table 7-4: Lung cancer DALYs in Europe due to indoor radon in residences (mean and 95% confidence interval). (without UK, Czech Republic and Slovenia)

	Year			
Policy	**2010**	**2020**	**2030**	**2050**
BAU	358 000 (54,193-940,205)	428 000 (65,203-1,156,026)	483 000 (70,921-1,335,438)	524 000 80,215-1,545,369)
All	NA	433 000 (65,625-1,140,190)	563 000 (78,874-1,614,252)	663 000 (89,720-2,045,648)
Insulation	NA	NA	NA	664 000 (88,638-2,108,941)
Renovation	NA	NA	NA	773 000 (107,764-2,392,599)

7.1.4 DALYs due to ETS originated VOCs and formaldehyde

Figure 7-2 and Figure 7-17 show the DALYs due to exposure to ETS originated VOCs and to formaldehyde. For a description of how the exposure was derived see Section 4.3.2.

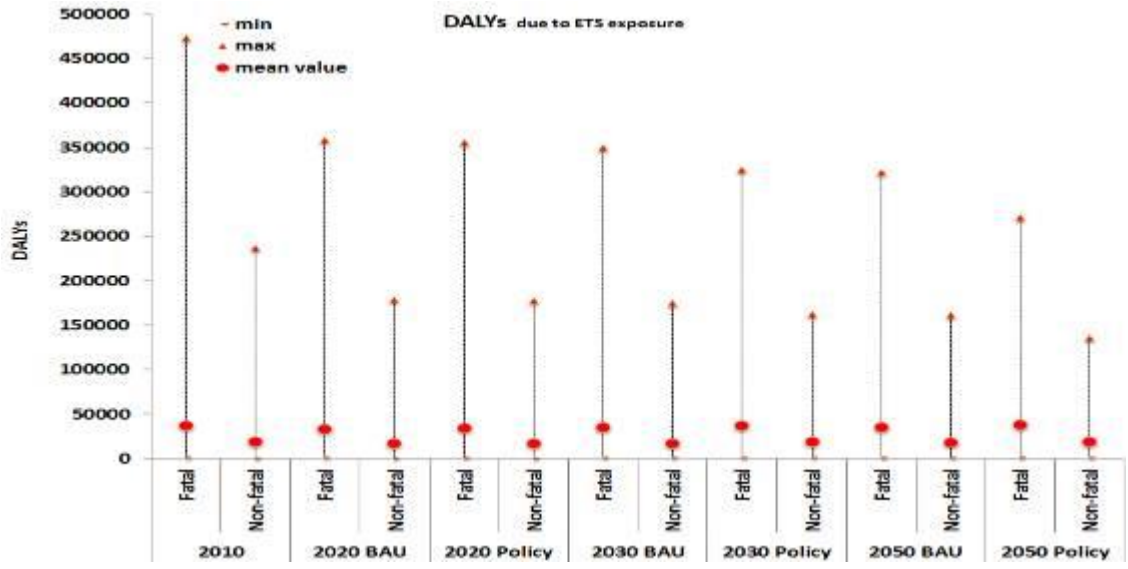

Figure 7-2: DALYs due to exposure to ETS originated VOCs in the EU 27.

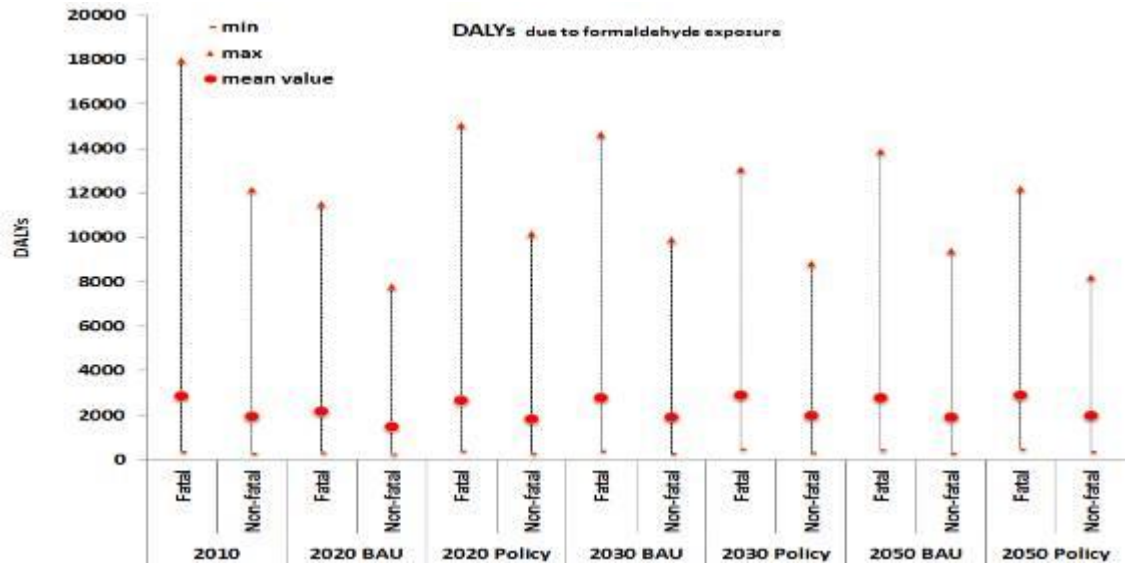

Figure 7-3: DALYs due to exposure to formaldehyde in the EU 27.

7.1.5 DALYs due to personal exposure to $PM_{2.5}$

DALYs for all scenarios are shown in Figure 7-4. For the DALY weights and duration applied see Section 7.1. DALYs were estimated excluding exposure to indoor background sources as it was assumed that e.g. skin particles or home dust does not lead to adverse effects on human health.

DALYs follow the same trends as the exposure. See Section 4.3.1 for a description and explanation of the trends.

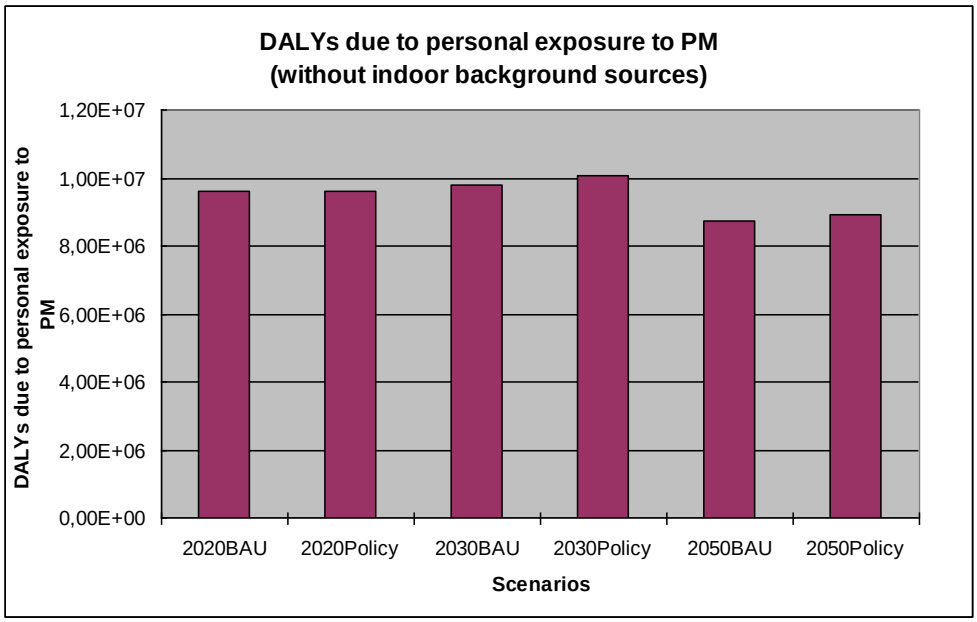

a)

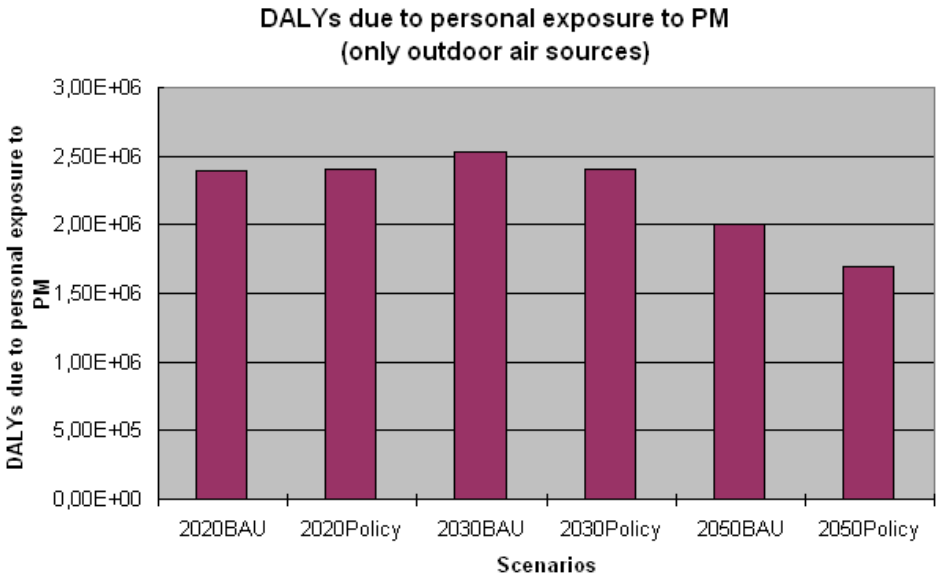

b)

Figure 7-4: DALYs due to personal exposure to $PM_{2.5}$ in EU30 (including additionally effects allocated to PM_{10} but scaled to $PM_{2.5}$ exposure), a) without indoor background sources, b) only with outdoor air sources.

DALYs due to personal exposure to PM from ETS are estimated as 7 mill / 6.7 mill in 2020 (BAU, Policy), 6.7 mill / 7 mill. in 2030 (BAU, Policy) and 6.5 mill / 6.7 mill in 2050 (BAU, Policy). However, theses values are based on mean exposure and do not include uncertainty or variability in the population.

As nearly half of all health effects of personal exposure to PM is originating from ETS, and as the exposure thus is very high, we might be overestimating the DALYs (see Section 5.2.2).

7.1.6 DALYs due to air pollutants

For aggregation of health effects the measure of DALYs is used in this Section. DALYs are given for the BAU (Figure 7-6 to Figure 7-10) and the Policy scenario (Figure 7-11 to Figure 7-15) for the different health endpoints separately and as aggregate values for mortality and morbidity.

Three different weighing schemes are applied as sensitivity analysis (Table 7-5). The idea is to weigh nitrates, sulphates and primary particles differently due to different toxicity, i.e. to investigate the impact of giving more importance to primary particles. A discussion about the differences in toxicity can be found in Bickel et al. 2005.

Table 7-5: Weighing scheme for different fractions of particulate matter.

	Variant 1	Variant 2	Variant 3
PPM2.5	1	* 1.5	* 1.75
nitrates	1	* 0.5	* 0.25
sulphates	1	* 0.6	* 0.25
PPMcoarse	1	* 1	* 1
nitratescoarse	1	* 0.5	* 0.25

Table 7-6: DALYs due to air pollutants, per year for BAU and Policy Scenario EU29 (all variants).

Variant 1			Variant 2			Variant 3		
	BAU	Policy		BAU	Policy		BAU	Policy
2020	2.5 mill	2.5 mill	2020	2 mill	2.1 mill	2020	1.7 mill	1.8 mill
2030	2.6 mill	2.4 mill	2030	2.2 mill	2 mill	2030	1.9 mill	1.8 mill
2050	2.4 mill	1.9 mill	2050	2 mill	1.6 mill	2050	1.7 mill	1.4 mill

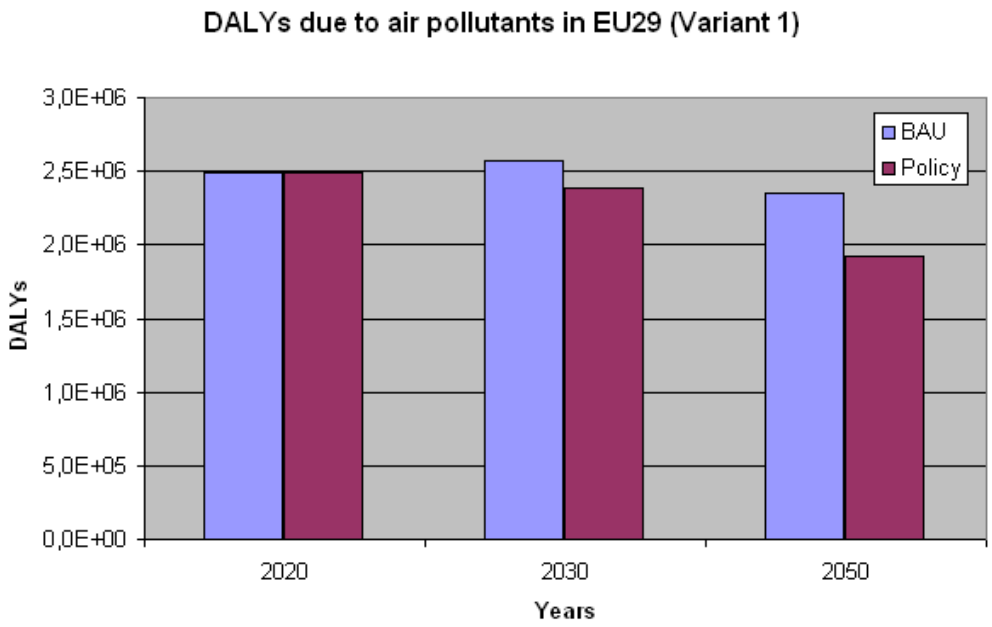

Figure 7-5: DALYs due to air pollutants, per year for BAU + Policy Scenario EU29 (variant 1).

Figure 7-5 shows that 2030 and 2050 the policy scenarios yield less DALYs than the BAU scenarios, with a bigger difference in 2050.

In the BAU scenario the DALYs increase in 2030 but decrease in 2050 (yielding less DALYs than 2020). DALYs for the policy scenario decrease from 2020 to 2050. For a comparison to damage costs see Section 7.2.5.

Different valuation schemes for particle toxicity lead to different number of DALYs for most health endpoints (Figure 7-6 to Figure 7-8 and Figure 7-11 to Figure 7-13). Only cough days are staying the same as they are caused only by SOMO35 and not by particles. The more weight is allocated to primary particles and the less to secondary particles, the less DALYs result. This might mean that more health effects are caused by secondary particles than by primary particles. Only for netRADs the DALYs increase – which might be an artificial effect considering the formula in Section 5.2.1.

BAU

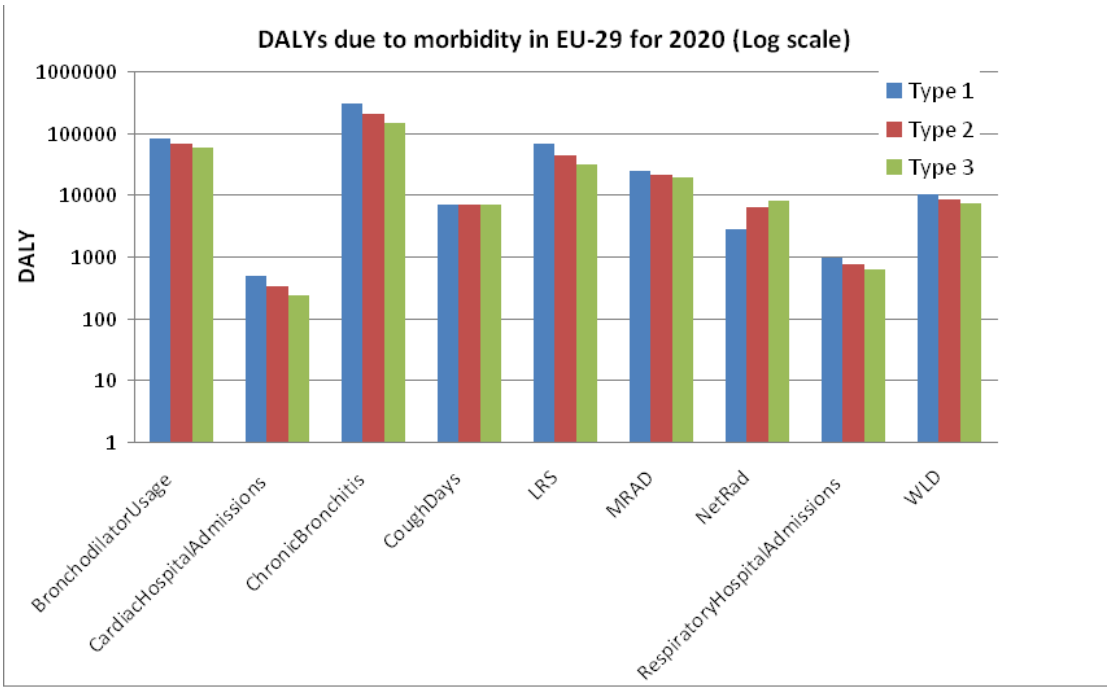

Figure 7-6: DALYs due to air pollutants for 2020 EU29, BAU, all three weighing variants.

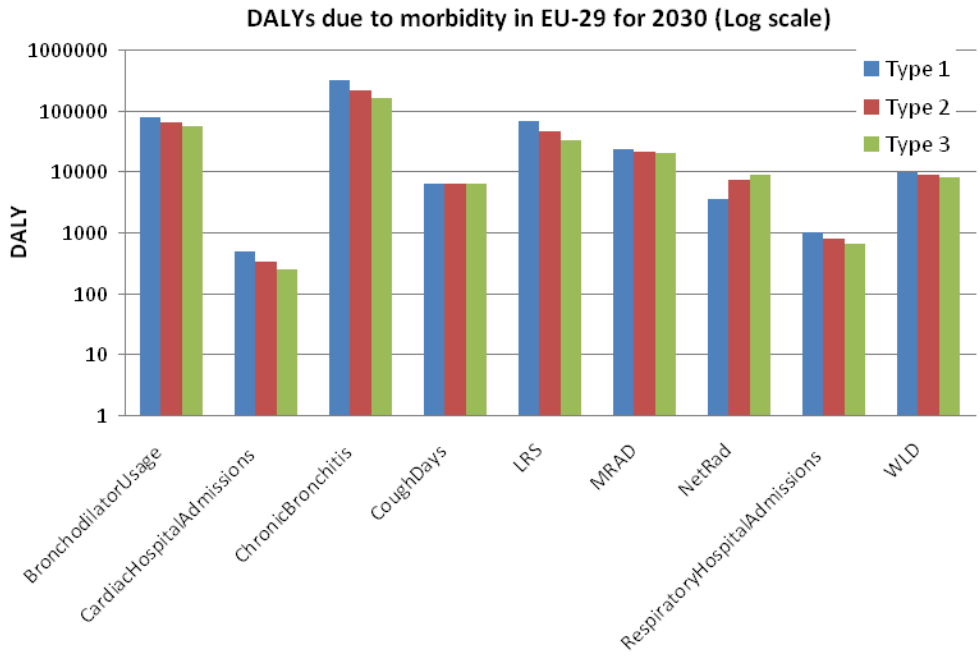

Figure 7-7: DALYs due to air pollutants for 2030 EU29, BAU, all three weighing variants.

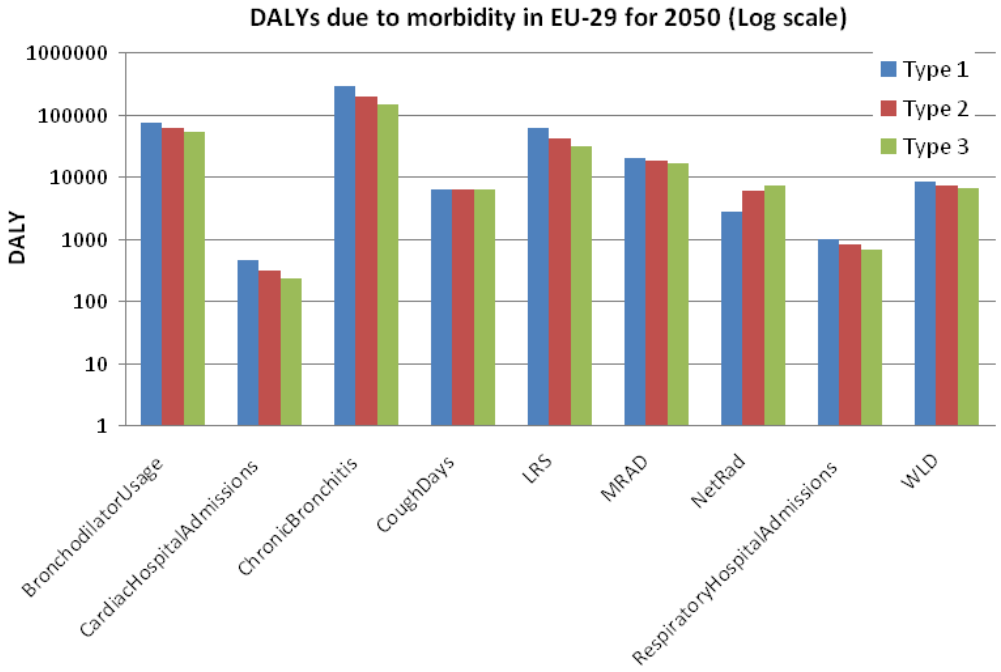

Figure 7-8: DALYs due to air pollutants for 2020 EU29, BAU, all three weighing variants.

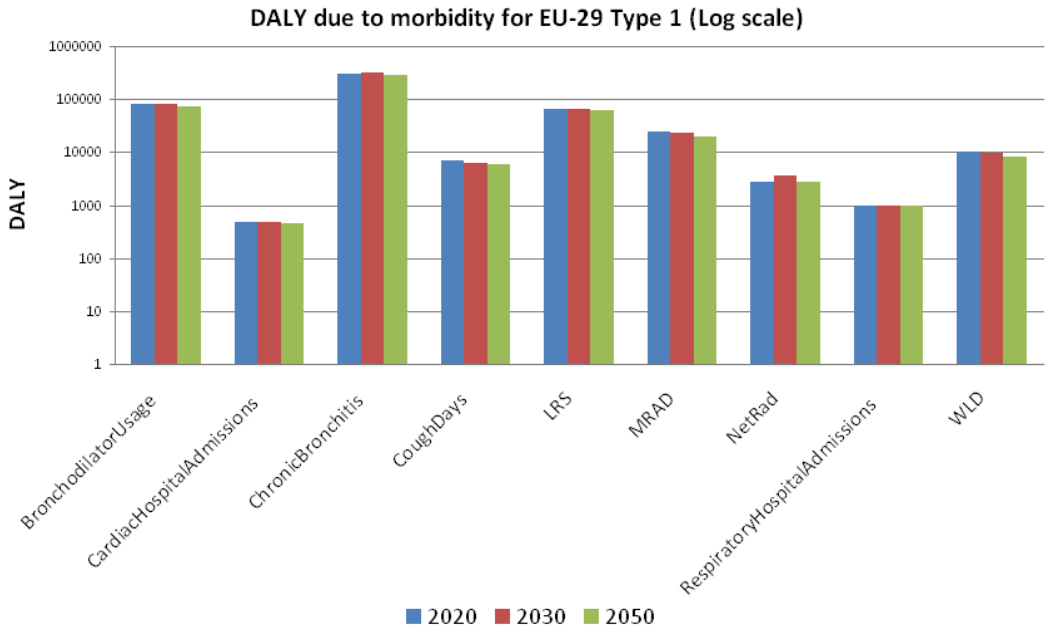

Figure 7-9: DALYs due to air pollutants for all years EU29, BAU, weighing variant 1.

In Figure 7-9 and Figure 7-10 it can be seen that DALYs increase in 2030 for most health endpoints and decrease in general in 2050 (at least compared to 2030). This shows that different pollutants (causing different health effects) do not increase/decrease from 2020 to 2050 in the same way/tendency (see also Section 2).

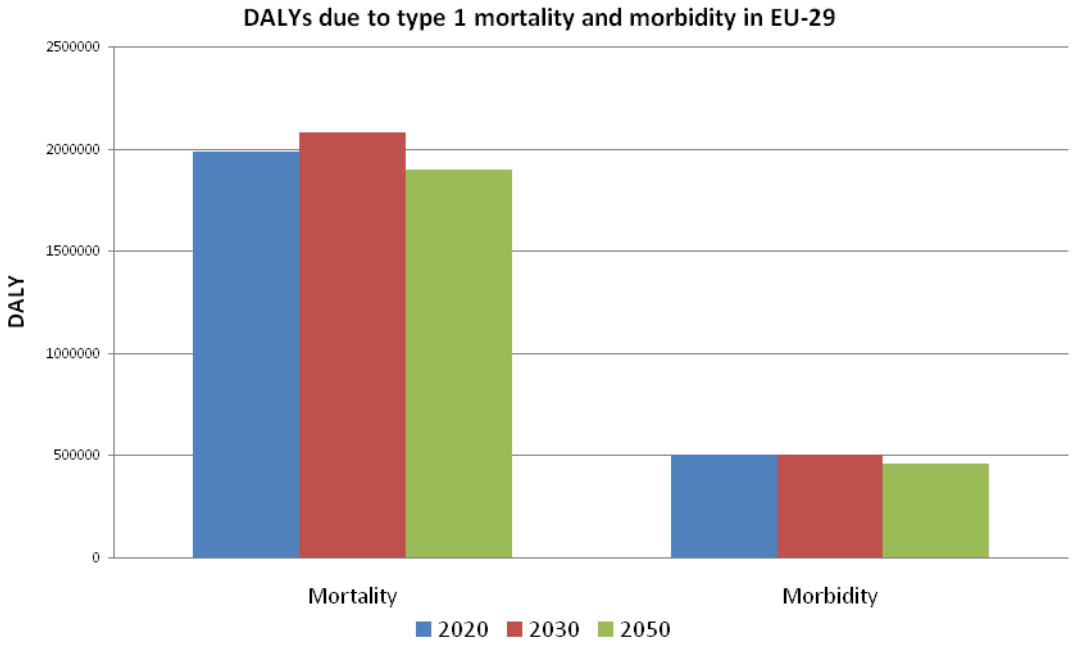

Figure 7-10: DALYs due to air pollutants for all years EU29, BAU, weighing variant 1, mortality and morbidity.

DALYs due to mortality exceed around four times DALYs due to morbidity (Figure 7-10).

Policy

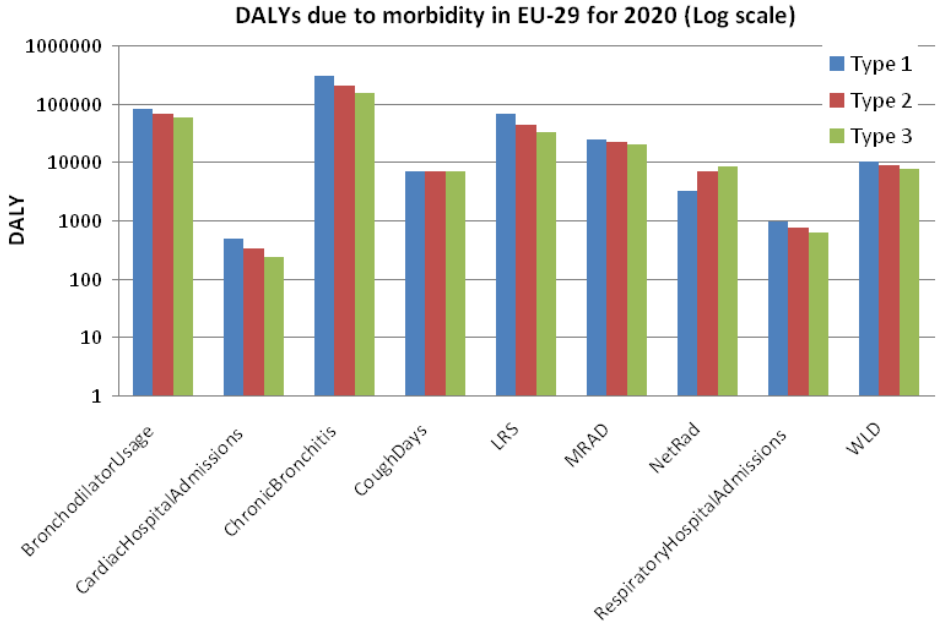

Figure 7-11: DALYs due to air pollutants for 2020 EU29, Policy, all three weighing variants.

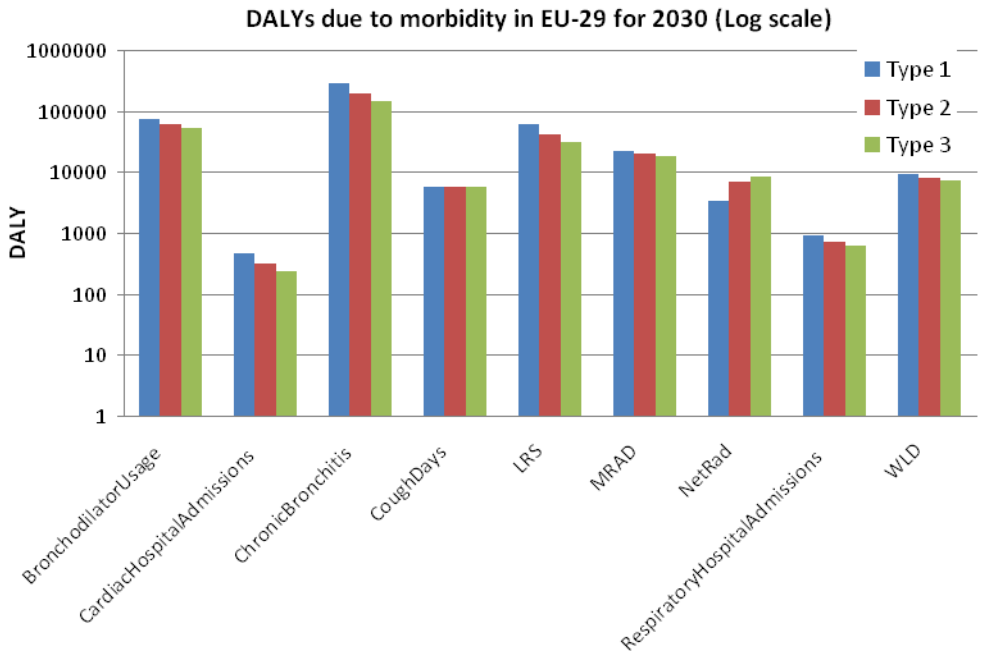

Figure 7-12: DALYs due to air pollutants for 2030 EU29, Policy, all three weighing variants.

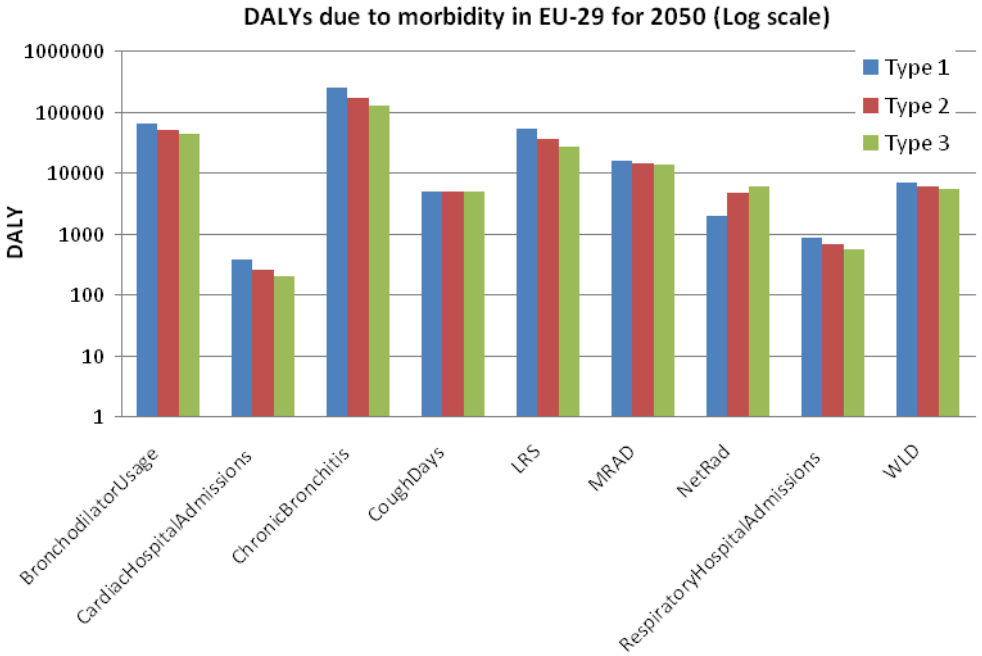

Figure 7-13: DALYs due to air pollutants for 2050 EU29, Policy, all three weighing variants.

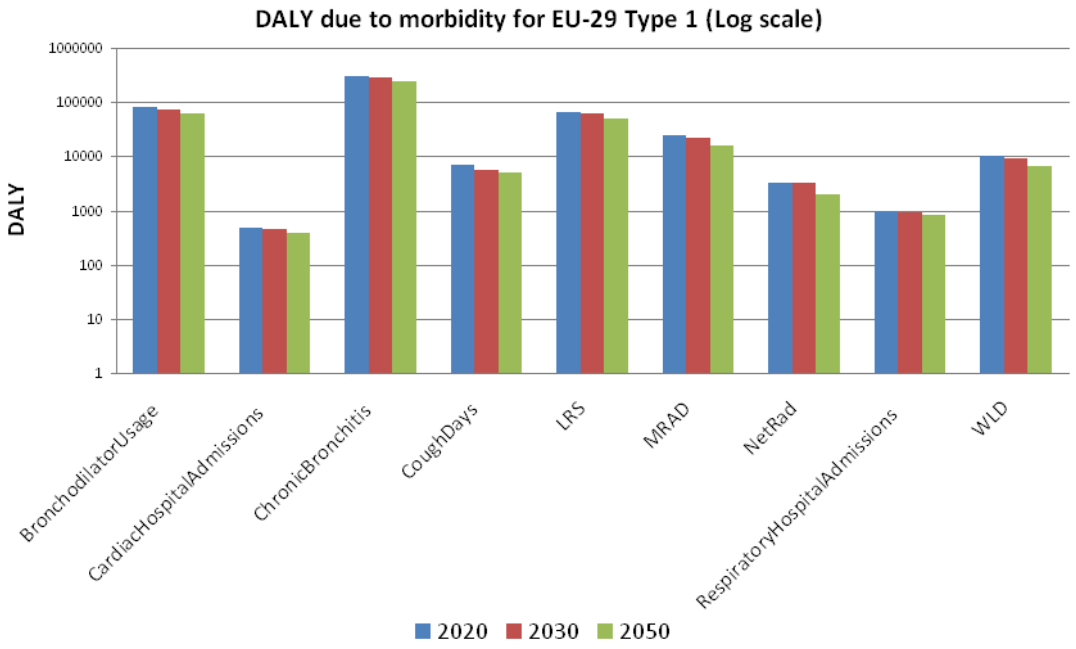

Figure 7-14: DALYs due to air pollutants for all years EU29, Policy, weighing variant 1.

In the policy scenario DALYs in general decrease from 2020 to 2050. This is true for all health endpoints considered (Figure 7-14 and Figure 7-15).

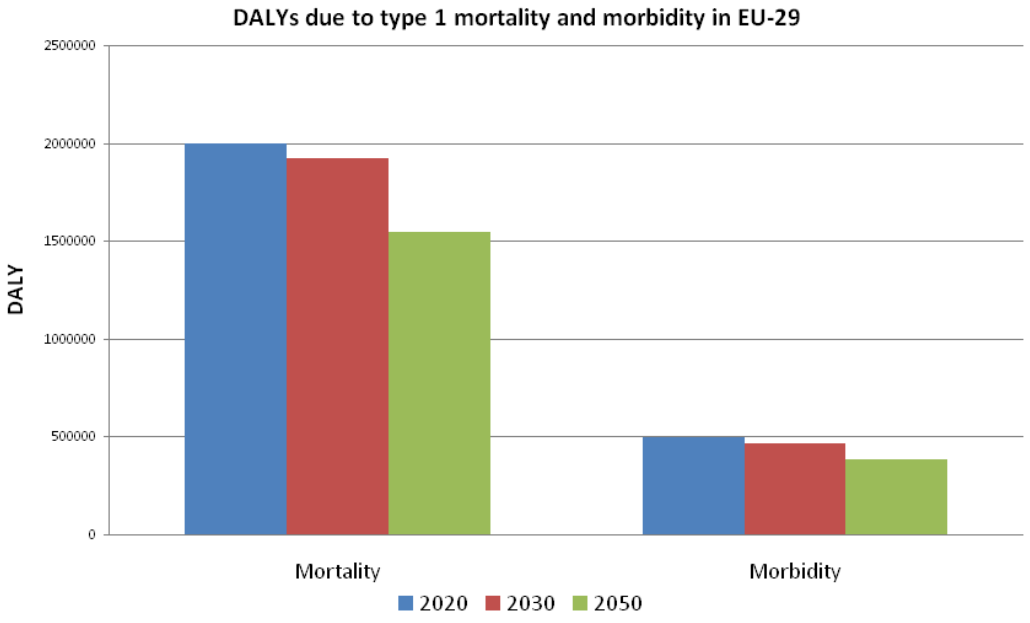

Figure 7-15: DALYs due to air pollutants for all years EU29, Policy, weighing variant 1, mortality and morbidity.

7.1.7 DALYs due to POPs

Based on the available slope factors, the total number of DALYs related to POP exposure are derived as shown in Figure 7-16 for PCB-153 and in Figure 7-17 for 2,3,4,7,8-PeCDF, respectively.

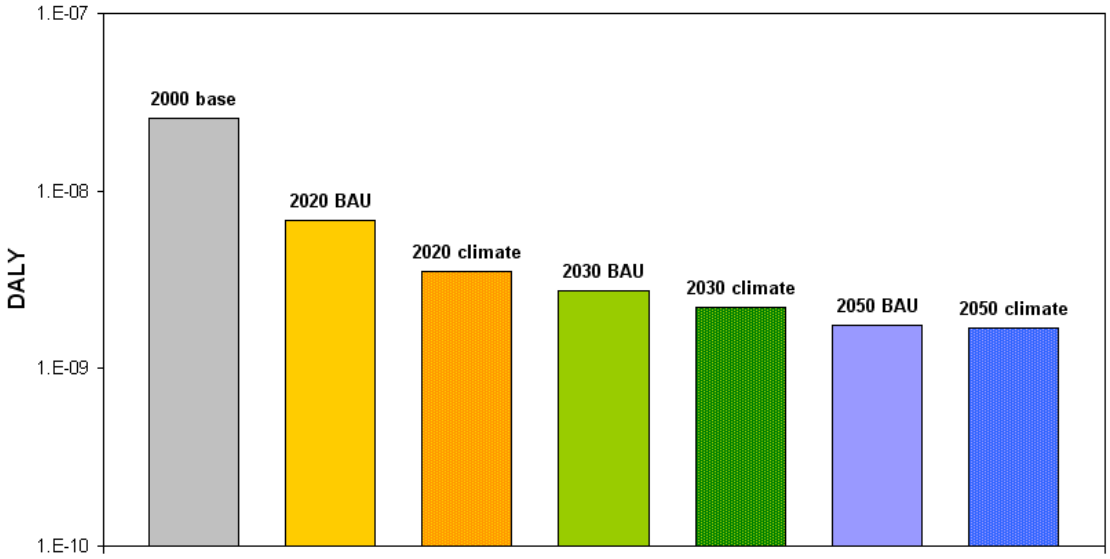

Figure 7-16: Number of DALYs due to cancer caused by intake of PCB-153 via inhalation, ingestion of drinking water and ingestion of food crops for all scenarios from years 2000 to 2050.

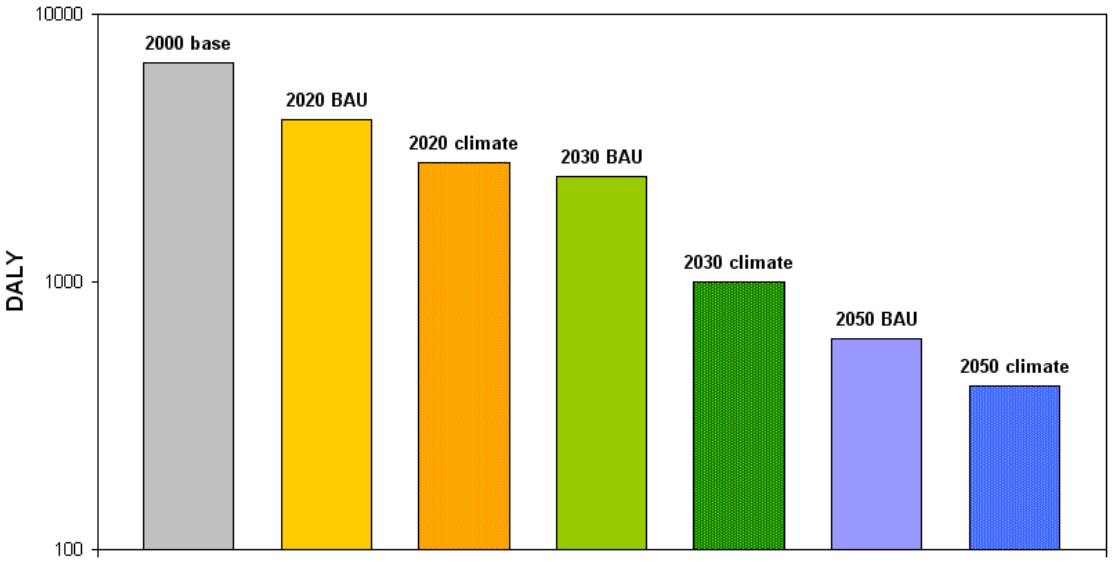

Figure 7-17: Number of DALYs due to cancer caused by intake of 2,3,4,7,8-PeCDF via inhalation, ingestion of drinking water and ingestion of food crops for all scenarios from years 2000 to 2050.

As can be seen from the DALY figures, the effects caused by PCB-153 are rather negligible, whereas the effects caused by 2,3,4,7,8-PeCDF are rather high. This is despite the fact that emissions of PCB-152 are about a factor 10 higher than emissions of 2,3,4,7,8-PeCDF (see Section). However, the driver of the huge difference between

the two DALY figures are the differences in the slope factors, which are several orders of magnitude higher for 2,3,4,7,8-PeCDF than for PCB-153, thereby stressing the high hazard potential of the former.

7.1.8 DALYs due to pesticides

Based on the available ERFs for selected pesticides, the number of DALYs related to ingestion exposure of pesticides is shown in Figure 7-18. Note that the sum of DALYs related to inhalation exposure is too small to show up in a figure with DALYs that are aggregated over the ingestion and inhalation expsoure pathways.

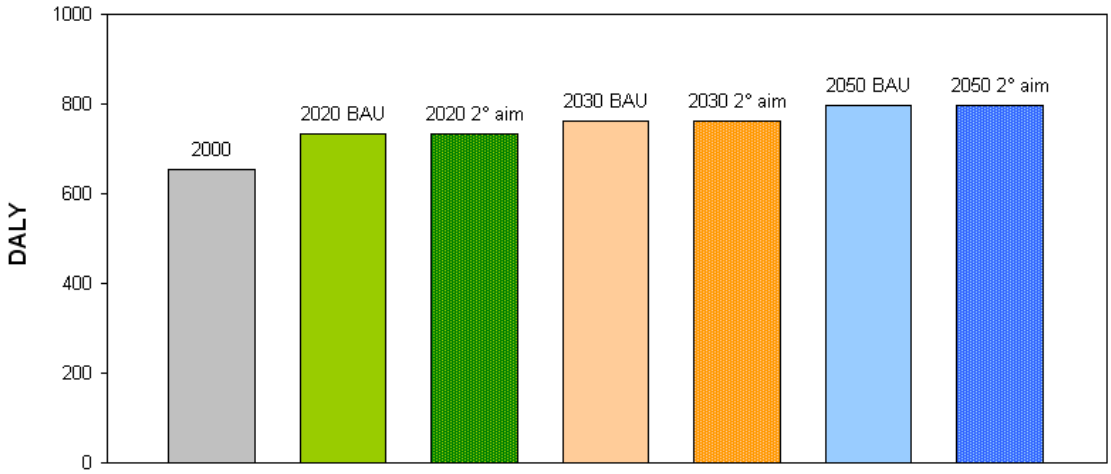

Figure 7-18: Number of DALYs due to cancer caused by intake of pesticides via ingestion of food crops after direct application for all scenarios from years 2000 to 2050.

Since effect information was only available for a certain number of the assessed pesticides, it is not possible to estimate to total health impacts, i.e. for all investigated substances, without extrapolation. A possibility ot estimate – not without introducing further uncertainties, of course – health impacts for the total set of selected pesticides is based on the effect information available for substances of a certain chemical class. This effect information is assumed to be similar also for other substances belonging to the same chemical class as the chemical with existing effect information. The list of chemicals that has been chosen to extrapolate available effect information based on the same chemical classification is shown in Table 7-7.

Table 7-7: Substances for which the slope factor of a pesticides with available effect information has been extrapolated to based on assumed similarities in mode of action for substances belonging to the same chemical class.

Target Class	Chemical Class	Slope Factor	Substance
Fungicides	Carbamate	0.00239	CARBENDAZIM
			METHIOCARB
	Nitrile (Fungicides)	0.00766	CHLOROTHALONIL
	Dicarboximide	0.0439	IPRODIONE
Herbicides	Nitrile (Herbicides)	0.103	BROMOXYNIL
	Oxazole	0.0102	ISOXAFLUTOLE
			VINCLOZOLIN
	Thiocarbamate	0.11	MOLINATE
			THIRAM
			EPTC
			PROSULFOCARB
	Amide	0.0259	PROPYZAMIDE
			NAPROPAMIDE
			BEFLUBUTAMID
			DIFLUFENICAN
			BOSCALID
			ACETOCHLOR
			ALACHLOR
			DIMETHACHLOR
			DIMETHENAMID
			DIMETHENAMID-P
			METOLACHLOR
			S-METOLACHLOR
	Oxime	0.0168	TRALKOXYDIM
			CYMOXANIL
			TEPRALOXYDIM
	Dinitroaniline	0.00293	TRIFLURALIN
			PENDIMETHALIN

Based on the extrapolation as explained above, the total number of DALYs in Europe for all given scenarios is given in Figure 7-19.

Table 7-8 and Table 7-9 present Number of DALYs for morbidity and mortality due to lung cancer caused by 45 carcinogenic pesticides via inhalation for the baseline year 2000.

Table 7-8: Number of DALYs for morbidity due to lung cancer for 45 carcinogenic pesticides used in arable and permanent crops for the baseline year 2000.

	DALYs - morbidity	
Country	**Permanent crops**	**Arable crops**
Austria	1.98E-05	1.02E-04
Belgium	2.93E-03	2.50E-04
Bulgaria	1.53E-06	1.87E-05
Cyprus	4.84E-07	0.00E+00
Czech Republic	6.07E-06	3.61E-05
Germany	7.59E-04	1.30E-02
Denmark	8.15E-07	5.75E-06
Spain	1.51E-02	2.77E-03
Estonia	2.70E-10	5.13E-06
Finland	0.00E+00	9.77E-06
France	2.06E-03	4.25E-04
UK	6.09E-07	3.25E-04
Greece	2.29E-05	1.49E-05
Hungary	8.16E-04	3.92E-03
Ireland	3.64E-09	3.05E-03
Italy	3.02E-03	5.67E-04
Lithuania	7.28E-07	1.50E-04
Luxembourg	2.90E-05	8.94E-06
Latvia	8.22E-08	7.36E-06
Malta	0.00E+00	0.00E+00
Netherlands	2.24E-04	4.87E-03
Poland	8.05E-05	3.09E-04
Portugal	1.49E-04	5.39E-02
Romania	1.61E-05	8.93E-05
Slovakia	2.82E-05	3.48E-04
Slovenia	2.75E-05	8.14E-05
Sweden	1.89E-06	7.25E-04

Table 7-9: Number of DALYs for mortality due to lung cancer for 45 carcinogenic pesticides used in arable and permanent crops for the baseline year 2000.

	DALYs - mortality	
Country	**Permanent crops**	**Arable crops**
Austria	1.81E-04	9.30E-04
Belgium	2.67E-02	2.28E-03
Bulgaria	1.40E-05	1.71E-04
Cyprus	4.41E-06	0.00E+00
Czech Republic	5.54E-05	3.29E-04
Germany	6.92E-03	1.18E-01
Denmark	7.43E-06	5.24E-05
Spain	1.38E-01	2.52E-02
Estonia	2.46E-09	4.67E-05
Finland	0.00E+00	8.90E-05
France	1.87E-02	3.87E-03
UK	5.55E-06	2.96E-03
Greece	2.09E-04	1.35E-04
Hungary	7.44E-03	3.58E-02
Ireland	3.31E-08	2.78E-02
Italy	2.75E-02	5.17E-03
Lithuania	6.64E-06	1.37E-03
Luxembourg	2.65E-04	8.14E-05
Latvia	7.49E-07	6.71E-05
Malta	0.00E+00	0.00E+00
Netherlands	2.05E-03	4.44E-02
Poland	7.34E-04	2.82E-03
Portugal	1.36E-03	4.91E-01
Romania	1.47E-04	8.13E-04
Slovakia	2.57E-04	3.17E-03
Slovenia	2.51E-04	7.42E-04
Sweden	1.72E-05	6.61E-03

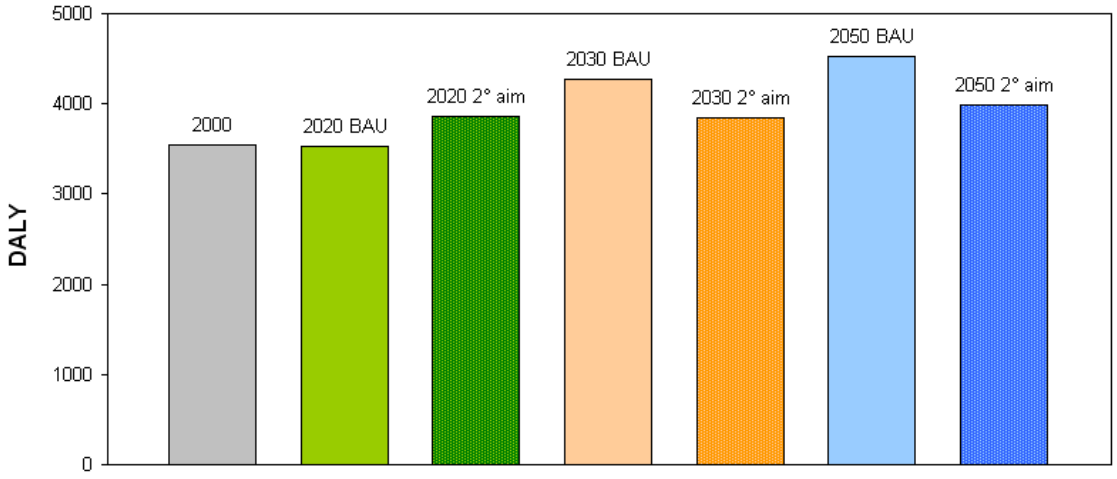

Figure 7-19: Number of DALYs due to cancer caused by intake of pesticides via ingestion of food crops after direct application for all scenarios from years 2000 to 2050.

Number of DALYs for morbidity and mortality due to lung cancer caused by 45 carcinogenic pesticides via inhalation for EU27 (year 2000) are presented in Figure 7-20 and Figure 7-21.

The health impact of pesticide inhalation due to direct application by farmers, workers, applicators and their families and bystanders is a local phenomenon; thus, the right spatial scale of health impact estimation is the highest possible spatial resolution - in our case a grid of 100x100 m across Europe. Nevertheless, in order to provide the possibility to intercompare risks in the frame of the CCS at the spatial scale as well, the health impact results have been resampled to a 50x50km grid that is coherent with the spatial grid of the EMEP model in Europe. These results are given below in map form:

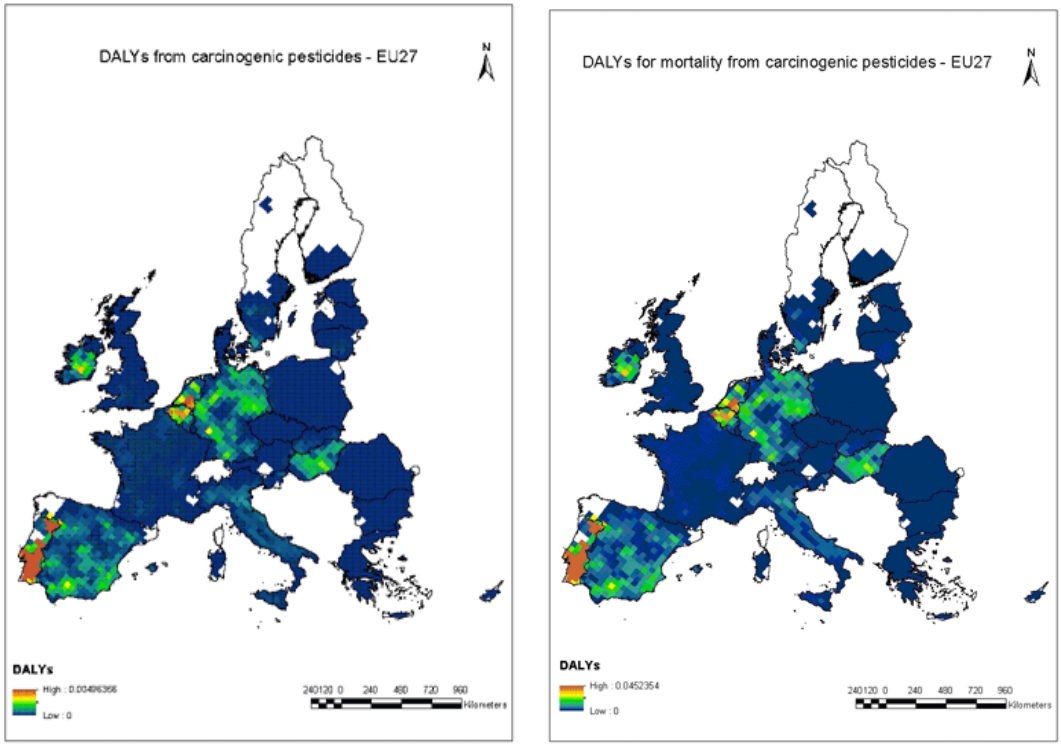

(a) (b)

Figure 7-20: Number of DALYs for a) morbidity and b) mortality due to lung cancer for 45 carcinogenic pesticides at EMEP grid (year 2000) – EU27.

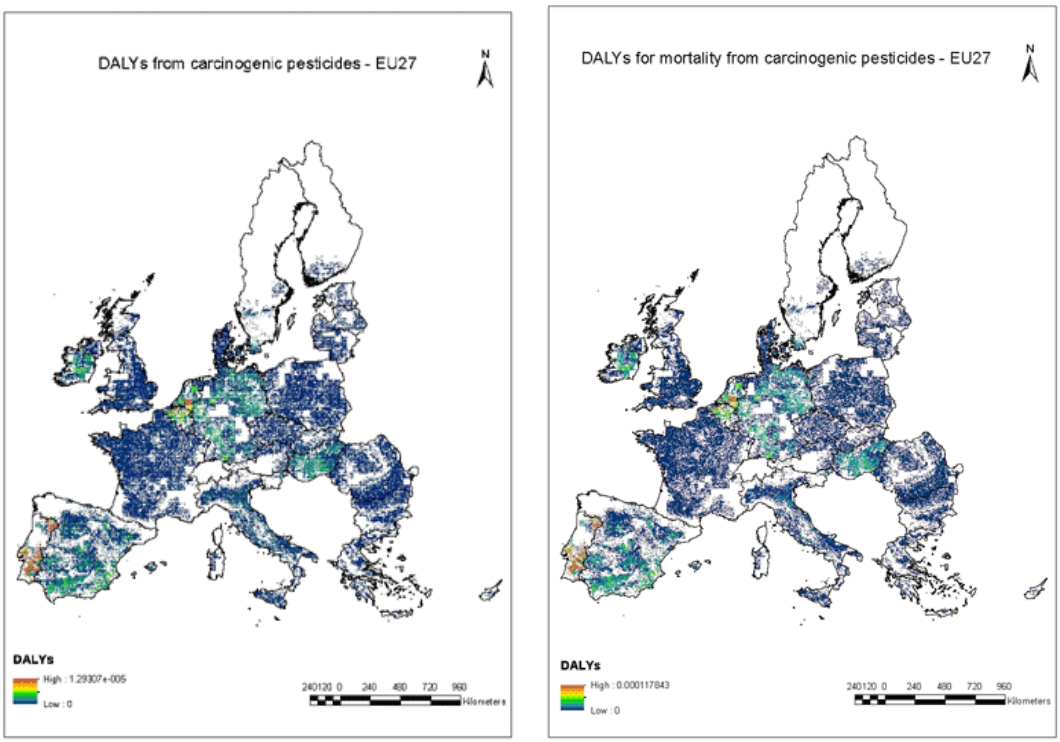

(a) (b)

Figure 7-21: Number of DALYs for a) morbidity and b) mortality due to lung cancer for 45 carcinogenic pesticides at 100x100 spatial resolution (year 2000) – EU27.

Number of DALYs for morbidity and mortality from carcinogenic pesticides at 100x100 spatial resolution are presented in Figure 7-21.

In addition, DALYs median estimate, together with its corresponsing uncertainty is presented in Figure 7-22.

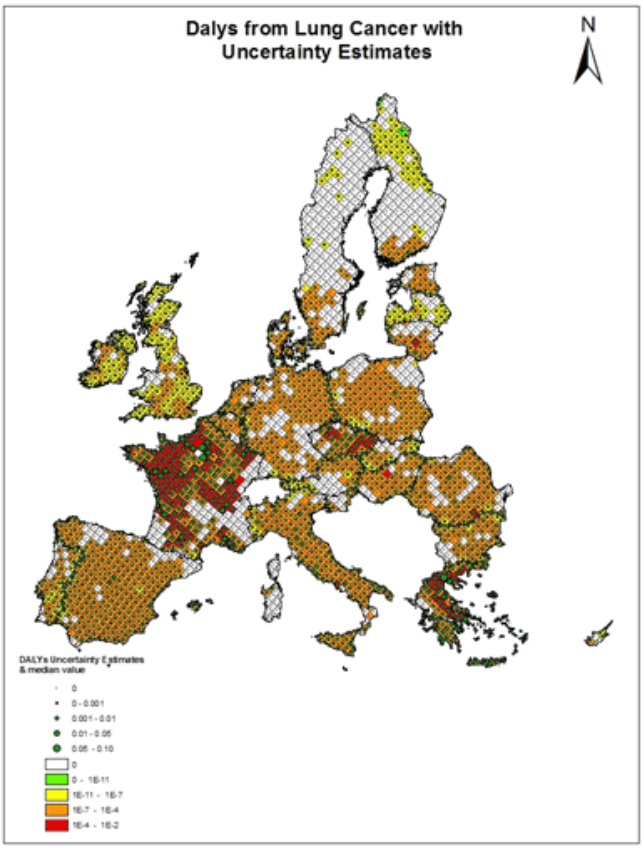

Figure 7-22: Estimates of DALYs in the EU27 together with the uncertainty estimates – spread between the 5 to the 95 percentile (year 2000).

Number of DALYs for morbidity and mortality due to lung cancer caused by 59 carcinogenic pesticides via inhalation for EU27 at EMEP grid for scenario BAU 2030 are presented in Figure 7-23, respectively.

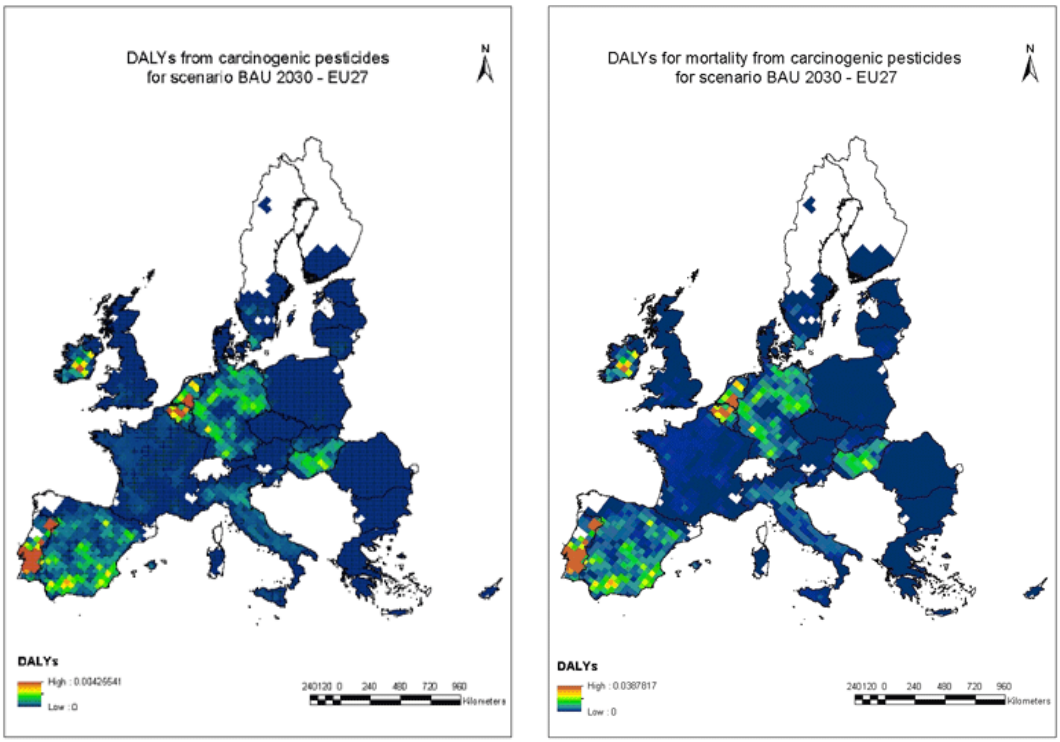

(a) (b)

Figure 7-23: Number of DALYs for a) morbidity and b) mortality due to lung cancer for 59 carcinogenic pesticides for scenario BAU 2030 (EMEP grid) – EU27.

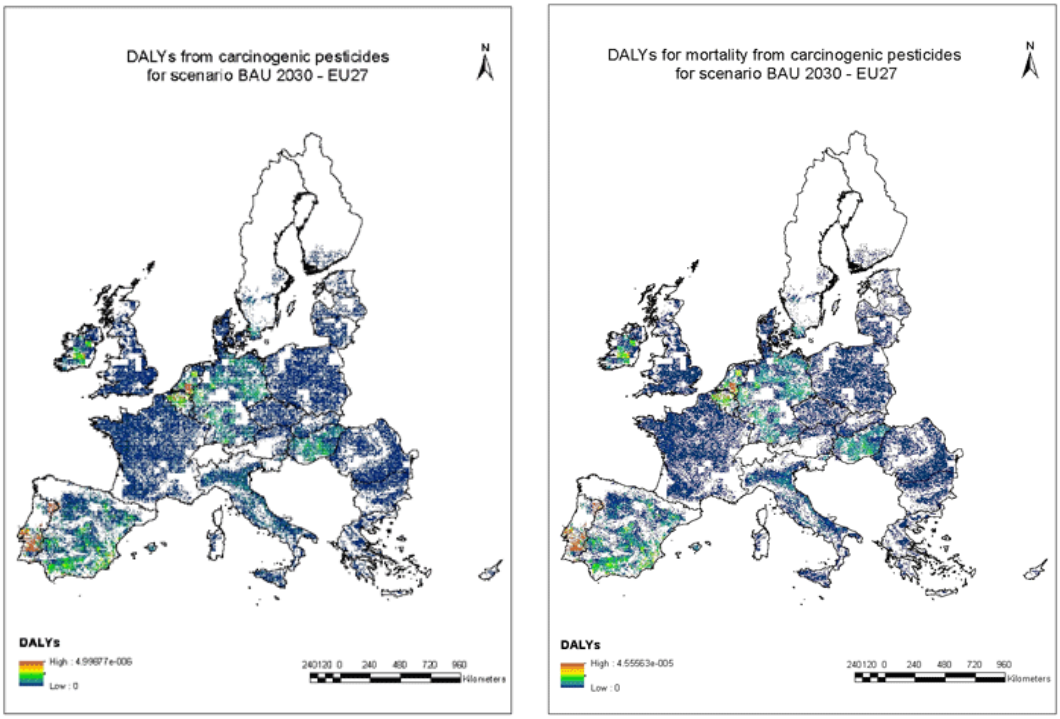

(a) (b)

Figure 7-24: Number of DALYs for a) morbidity and b) mortality due to lung cancer for 59 carcinogenic pesticides for scenario BAU 2030 – EU27.

Number of DALYs for morbidity and mortality from carcinogenic pesticides at 100x100 spatial resolution (BAU 2030) are presented in Figure 7-24, respectively.

Number of DALYs for morbidity due to lung cancer caused by 14 carcinogenic pesticides (inhalation pathway) used in energy crops for scenario BAU 2030 at EMEP grid and at 100x100m spatial resolution are presented in Figure 7-25, respectively.

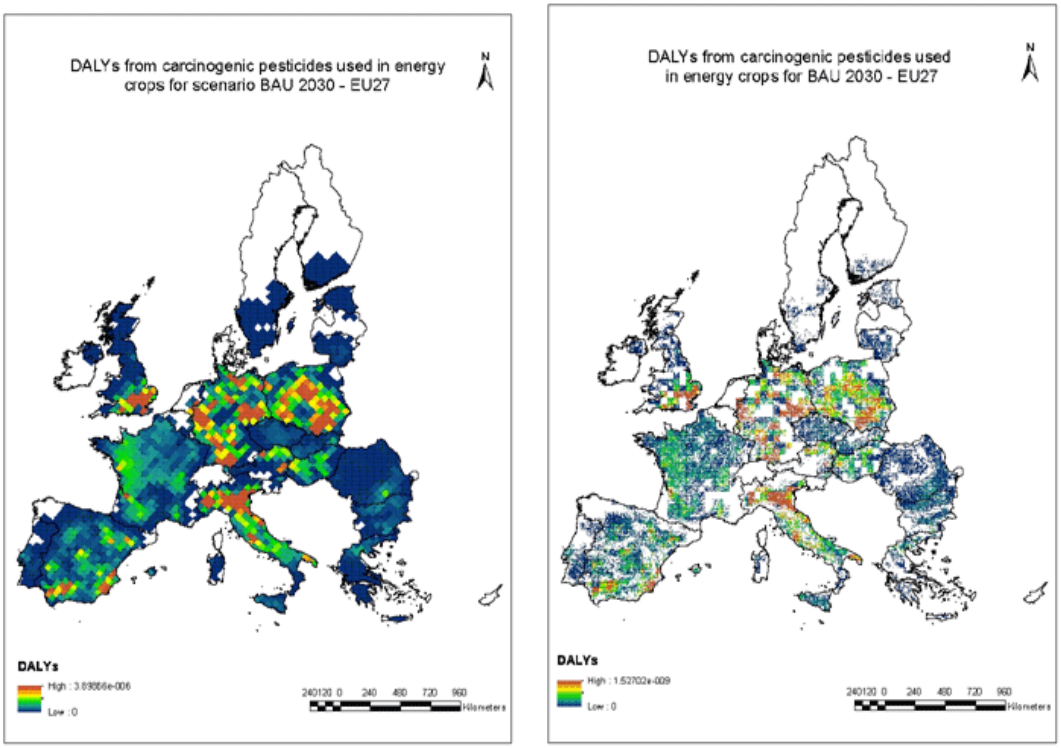

(a) (b)

Figure 7-25: Number of DALYs for morbidity due to lung cancer for 14 carcinogenic pesticides used in energy crops a) EMEP grid and b) 100x100m spatial resolution for scenario BAU 2030 – EU27.

Number of DALYs for morbidity due to lung cancer caused by carcinogenic pesticides via inhalation for baseline and scenarios per country are presented in Figure 7-26. Cyprus and Malta are excluded because of their small values.

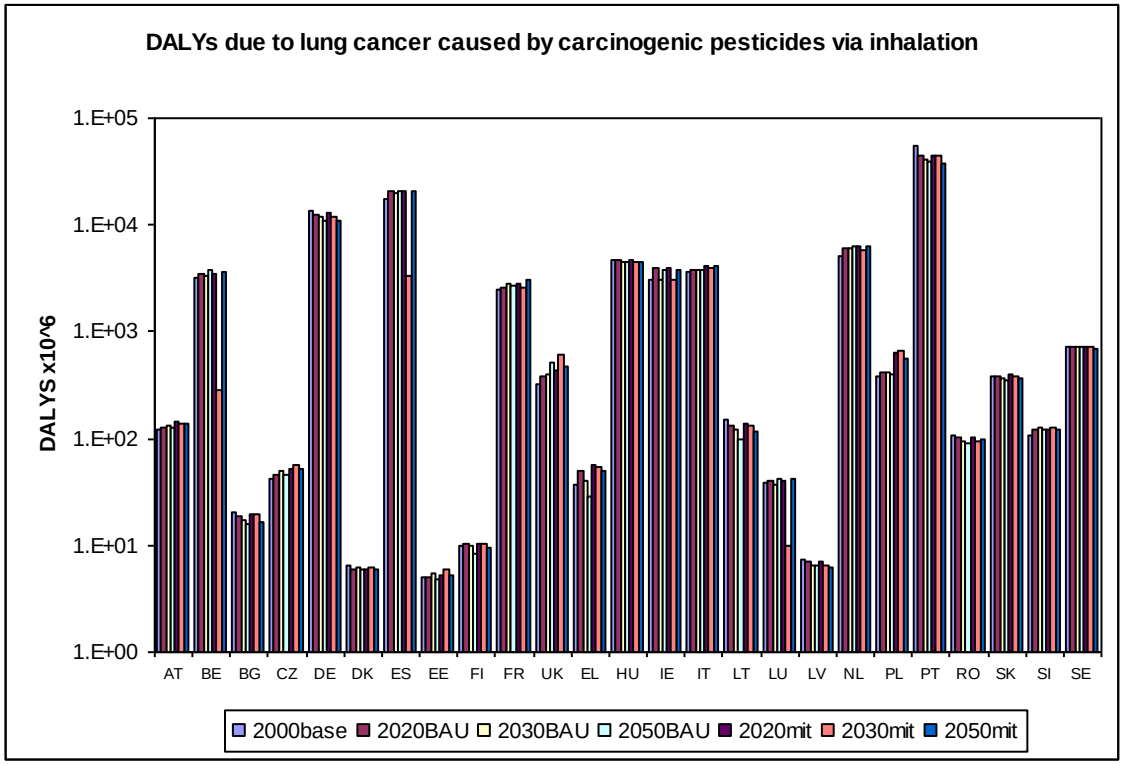

Figure 7-26: Number of DALYs for morbidity due to lung cancer caused by carcinogenic pesticides via inhalation for baseline and scenarios – EU25 (Cyprus and Malta are excluded).

7.1.9 DALYs due to heat

It is currently unclear what role mortality displacement, i.e. the so-called harvesting effect, has in heat exposure induced mortality (Basu 2009). Mortality displacement refers to a phenomenon where the environmental exposure advances the deaths of ill people by only a few days. Nevertheless, an attempt was made to quantify the health impacts also in DALYs and monetary costs (Table 7-10). Life years lost due to a heat attributable death was defined as a uniform probability distribution with a lower boundary of three months and upper boundary of ten years. Because of this, and the uncertainty in the number of the attributable deaths, the uncertainty range in the DALY and monetary cost estimates is very wide. However, if mortality displacement is considered as an important factor in heat related mortality, then the lower boundary estimates should be considered as more representative. Monetary costs were calculated by assuming a uniform distribution for the value of a life year with a lower boundary of 60 000 and upper boundary of 89 715 euros.

Table 7-10: DALYs (mean and 95% confidence limit) due to heat related mortality and the impact of UHI mitigation policies on these (total for North-Continental and Mediterranean regions).

		Climate scenario A1B		Climate scenario B1	
Year	Reference / UHI mitigation scenario	DALYs	DALYs prevented by UHI mitigation policy	DALYs	DALYs prevented by UHI mitigation policy
2010	Current	74820 (6769-174438)		74820 (6769-174438)	
2020	Reference	128452 (11748-300892)		131545 (11754-315112)	
	Vegetation	123101 (11254-288089)	5350 (494-12254)	125452 (11179-300392)	6093 (563-14083)
	Albedo	114185 (10444-266143)	14266 (1315-32717)	115740 (10240-277967)	15805 (1458-36493)
	Veg+alb	109213 (10001-255143)	19239 (1768-44083)	110326 (9724-265101)	21219 (1958-48842)
2030	Reference 1	210594 (19444-495449)		196191 (18261-457578)	
	Vegetation	201434 (18540-475368)	9160 (842-20931)	187835 (17508-438654)	8356 (767-18907)
	Albedo	186706 (17089-441349)	23888 (2199-54238)	175049 (16323-409016)	21142 (1926-48154)
	Veg+alb	177302 (16168-418725)	33291 (3048-75544)	167779 (15618-392542)	28411 (2583-64616)
2050	Reference 1	399529 (38019-931974)		236972 (20532-582922)	
	Vegetation	383678 (36487-894846)	15851 (1536-36460)	227228 (19640-559907)	9744 (858-23146)
	Albedo	359271 (34147-835784)	40258 (3910-92309)	211851 (18171-523118)	25120 (2219-58727)
	Veg+alb	346110 (32882-804732)	53419 (5185-122606)	202988 (17338-502947)	33984 (3022-79548)

The results of the assessment and the uncertainties related to it are discussed in more detail in Appendix E (Annexes

Heat and Urban Heat Island (UHI) Mitigation).

7.2 VALUATION OF HEALTH EFFECTS

The full-chain approach to health impact assessment allows for the aggregation, in monetary terms, of the disparate health end-points resulting from pollution. Use of the money metric is designed to capture people's personal preferences in relation to the health end-points. Thus, the common measure is of the individual's willingness to pay (WTP) to avoid a specific health condition. Whilst there is a pre-existing body of work – see, for example, Bickel et al. (2005) – the breadth of the coverage of environmental media in HEIMTSA has necessitated both a re-evaluation of existing unit value estimates, and an expansion of the number of end-point unit values required.

Table 7-11 presents a summary of the unit values derived in the course of the HEIMTSA project. These values are the result of both an evaluation of the evidence available in the existing literature and new empirical research undertaken in the project. For each health end-point, the unit values are identified on the basis of an informal meta-analysis of the evidence, accounting for the distribution of available values and

an assessment of the quality and geographical focus of each study. Thus, studies whose results converge on modal values, which use state-of-the-art non-market valuation techniques, and that are undertaken within the EU are given greater weight in determining the range of values for each health end-point.

Table 7-11: Summary of Monetary Values relating to specific health end-points (€, 2010)

Health End-Point	Low	Central	High	Unit (2010) per case
Sleep disturbance	480	1,240	1,570	Euro/year
Hypertension	880	950	1,110	Euro/year
Acute myocardial infarction	4,675	86,200	436,200	Euro
Annoyance and high annoyance	88	88	88	Euro
Increased mortality risk (infants)	1,120,000	2,475,000	11,200,000	Euro
New cases of chronic bronchitis	43,000	60,000	100,000	Euro
Increased mortality risk - Value Of Life Years	60,820	89,715	220,000	Euro
Increased mortality risk - VSLacute	1,121,433	1,121,433	5,607,164	Euro
Increased mortality risk - VPFacute	1,120,000	1,650,000	5,600,000	Euro
Life expectancy reduction - Value of Life Years chronic	37,500	60,000	215,000	Euro
Respiratory hospital admissions	2,990	2,990	8,074	Euro
Cardiac hospital admissions	2,990	2,990	8,074	Euro
Work loss days (WLD)	441	441	441	Euro
Restricted activity days (RADs)	194	194	194	Euro
Minor restricted activity days (MRAD)	57	57	57	Euro
Lower respiratory symptoms	57	57	57	Euro
LRS excluding cough	57	57	57	Euro
Cough days	57	57	57	Euro
Medication use / bronchodilator use	74	80	96	Euro
Lung cancer	69,080	719,212	4,187,879	Euro
Leukaemia	2,045,493	3,974,358	7,114,370	Euro
Neuro-development disorders	4,486	14,952	32,895	Euro
Skin cancer	10,953	13,906	26,765	Euro
Osteoporosis	2,990	5,682	8,074	Euro
Renal dysfunction	22,788	30,406	40,977	Euro
Anaemia	748	748	748	Euro

For the assessment of impacts due to emissions of air pollutants in future years an adjustment of the above presented values according to changes in the willingness to pay for avoiding health impacts becomes necessary. In course of the already mentioned NEEDS project (Preiss et al., 2008) evidence was found, that monetary values for health risks for future years increase with an inter-temporal elasticity to GDP per capita growth of 0.7 to 1.0. An expected growth rate for the European economies of 2% per year has been assumed which is according to the expectations of the European Commission. This growth rate will be combined with an elasticity of 0.85 for the next 30 years. The increases will be applied to disutility costs (WTP) and opportunity costs (productivity losses), but not to medical costs. Furthermore, within NEEDS a declining growth rate for GDP after 2030 has been assumed. For these years a rate of 1% will be applied. The resulting factors for uplifting WTP for future health effects are presented in Table 7-12 below.

Table 7-12: Factors for uplifting WTP for future health effects

Year	Uplift-Factor
2010	1
2020	1.183612462
2030	1.400938461
2050	1.659346599

It is obvious from the values presented in Table 7-11, and specifically the range of values associated with a number of the end-points, that there is considerable uncertainty in health valuation. For example, for valuation of life-years and neuro-developmental disorders, there is a difference between low and high estimates of factors of 5 and 8, respectively. In cases such as for anaemia, there is insufficient evidence even to provide a range. The uncertainty derives from a combination of the paucity of the evidence base, the difficulty that people have with identifying their preferences for (avoidance of) health conditions, and the lack of maturity in the study methods themselves. Thus, in the instance of valuing avoidance of the risks of premature death, methods are only now being developed that successfully communicate to survey respondents the small changes in risk that tighter environmental regulation would result in. For example, computer graphics allow such information to be presented in a variety of ways, often with an accompanying voice-over.

7.2.1 Damage costs due to noise

Damage costs due to noise were estimated based on the values per health effect given in Table 7-11. In contrast to the calculation of DALYs (see Section 7.1.1) where highly annoyed persons, high sleep disturbance and myocardial infarction were added, for the costs annoyed persons, highly annoyed persons and myocardial infarction are added. For DALYs, double counting of high annoyance and sleep disturbance was avoided by considering high annoyance only at daytime and sleep disturbance only at nighttime. However, for costs the monetary values are derived by WTP studies, thus, annoyance also includes sleep disturbance. So to avoid double counting sleep disturbance is left aside in the main approach. As an alternative, sleep disturbance and myocardial infarction are added but leaving aside annoyance and high annoyance. For further approaches see the noise report.

Damage costs due to noise can be found in Table 7-13. The results for BAU and 2degree are also shown in Figure 7-27. In contrast to the DALYs, costs increase in the future due to the upscaling of the monetary values for the future (see Section 7.2), if not upscaled values follow the same pattern as the DALYs.

Table 7-13: Damage costs (Euros $_{2010}$) related to road traffic noise in the urban population in Europe for the BAU and the 2degree scenario.

Scenario/measure	2005	2020	2030	2050
BAU (Euros per year)	8.268 billion	10.677 billion	12.699 billion	14.067 billion
Policy scenario	8.268 billion	10.25 billion	12.056 billion	13.183 billion
Difference: BAU - Policy	-	427 million	642 million	884 million

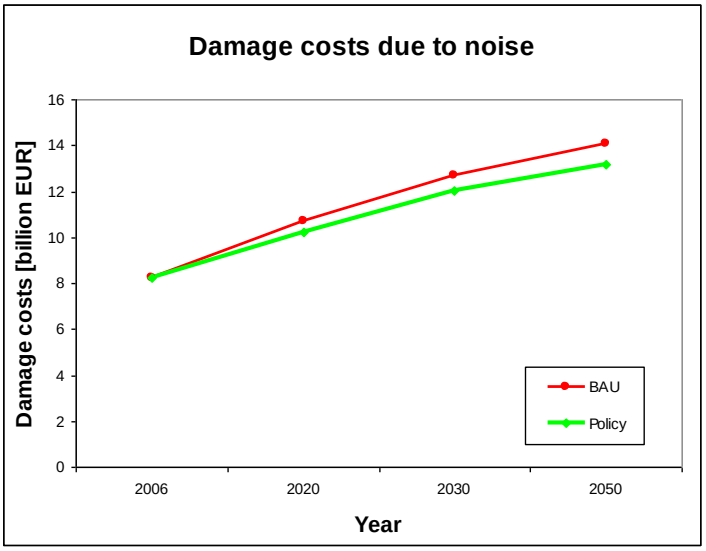

Figure 7-27: Damage costs of noise in the BAU and 450ppm scenarios.

The alternative of valuing sleep disturbance instead of annoyance yields damage costs of about 2.4 times of those with annoyance.

7.2.2 Damage costs due to dampness

The costs of diseases include direct costs of treatment, indirect costs due to loss of productivity (absence from work), and willingness of a person to pay extra to avoid the disease. Because the monetary estimation of impacts was not the main objective in this sub-assessment, we did not go through this laborious path. Instead, we simply assumed that the DALY estimate also provides a reasonable indicator of all monetary costs of the asthma cases. Thus, we multiplied the DALY estimate with an estimate of willingness to pay to avoid a loss of one healthy life year. This has typically been in the order of 30,000 – 60,000 euros per saved life year. This results in a preliminary estimate of monetary impact, which can be used in comparisons in other parts of the Common Case Study and the value of information analysis. More details can be found in HEIMTSA “D 7.1.15: Final report on ‘full chain’ analysis of indoor air pollution: Update based on the Common Case study”.

Table 7-14: Asthma monetary impact (based on DALYs) in Europe due to residential building dampness (mean and 95% confidence interval). Unit: M€ (without United Kingdom, Bulgaria, Hungary, Lithuania, Romania, Slovakia, Slovenia, Malta)

	Year			
Policy	**2010**	**2020**	**2030**	**2050**
BAU	4552 (2065-7861)	5478 (2464-9800)	6105 (2617-11307)	6404 (2622-12279)
All	NA	5491 (2434-9869)	7012 (2981-13005)	7989 (3285-14872)
Insulation	NA	NA	NA	7995 (3244-15283)
Renovation	NA	NA	NA	9059 (3827-16881)

7.2.3 Damage costs due to radon

The costs of diseases include direct costs of treatment, indirect costs due to loss of productivity (absence from work), and willingness of a person to pay extra to avoid the disease. Because the monetary estimation of impacts is not the main objective in this sub-assessment, we do not go through this laborious path. Instead, we simply assume that the DALY estimate also provides a reasonable indicator of all monetary costs of the asthma cases. Thus, we multiply the DALY estimate with an estimate of willingness to pay to avoid a loss of one healthy life year. This has typically been in the order of 30,000 – 60,000 euros per saved life year. This results in a preliminary estimate of monetary impact, which can be used in comparisons in other parts of the Common Case Study. More details can be found in HEIMTSA “D 7.1.15: Final report on ‘full chain’ analysis of indoor air pollution: Update based on the Common Case study”.

Table 7-15: Lung cancer monetary impact (based on DALYs) in Europe due to indoor radon in residences (mean and 95% confidence interval). Unit: M€ (without United Kingdom, Czech Republic, and Slovenia)

	Year			
Policy	**2010**	**2020**	**2030**	**2050**
BAU	16147 (2519-42699)	19250 (3039-53378)	21770 (3121-60868)	23585 (3590-70455)
All	NA	19464 (3009-53226)	25219 (3682-71977)	29715 (3973-94741)
Insulation	NA	NA	NA	29877 (4049-93146)
Renovation	NA	NA	NA	34810 (4748-106804)

7.2.4 Damage costs due to ETS originated VOCs and formaldehyde

Monetary cost was given by multiplying the expected cases to the willingness-to-pay (WTP) cost.

Table 7-16: Monetary cost (under WTP concept) per case in 10^6 Euros

		Medical treatment	Productivity loss	Dis-Utility	Total WTP
Cost per case (10^6 €)	**Lung cancer**	0.011 (0.0046-0.027)	0.07 (0.027-0.273)	0.4 (0.015-2.5)	0.481 (0.046-2.8)
	Leukemia	0.15 (0.06-0.25)	0.008	2.5 (1.3-4.5)	2.66 (1.37-4.76)
	Nasoph. cancer	0.011 (0.0046-0.027)	0.07 (0.027-0.273)	0.4 (0.015-2.5)	0.481 (0.046-2.8)
	Asthma*	*The cost of asthma, was considered equal to 2500 euros per case, corresponding to the average cost of a hospitalization day per year of an asthma crisis			

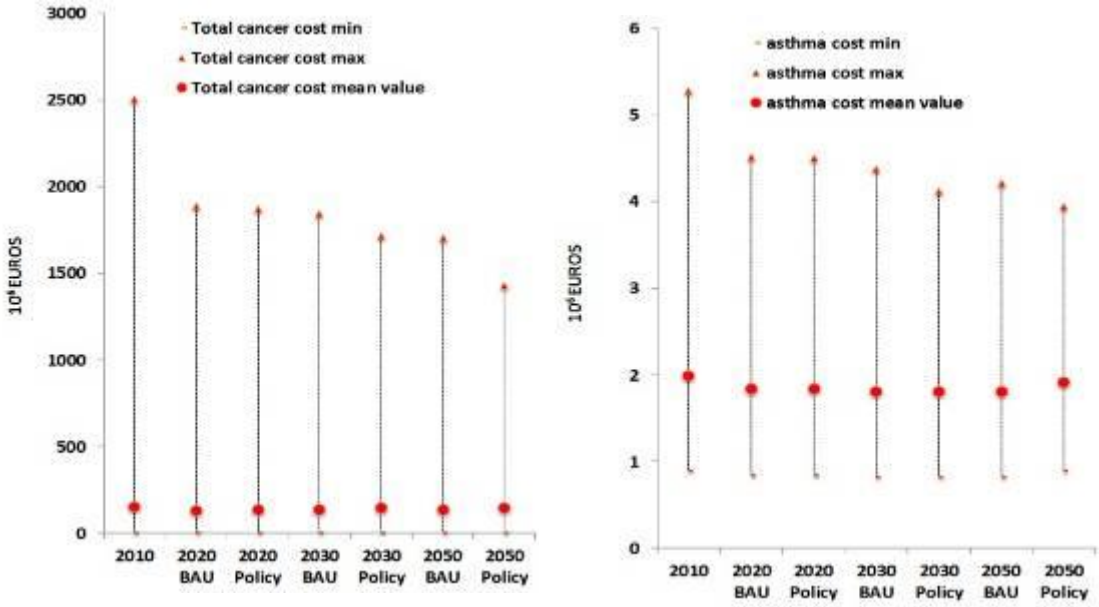

Figure 7-28: Damage costs due to ETS originated VOCs (EU 27)

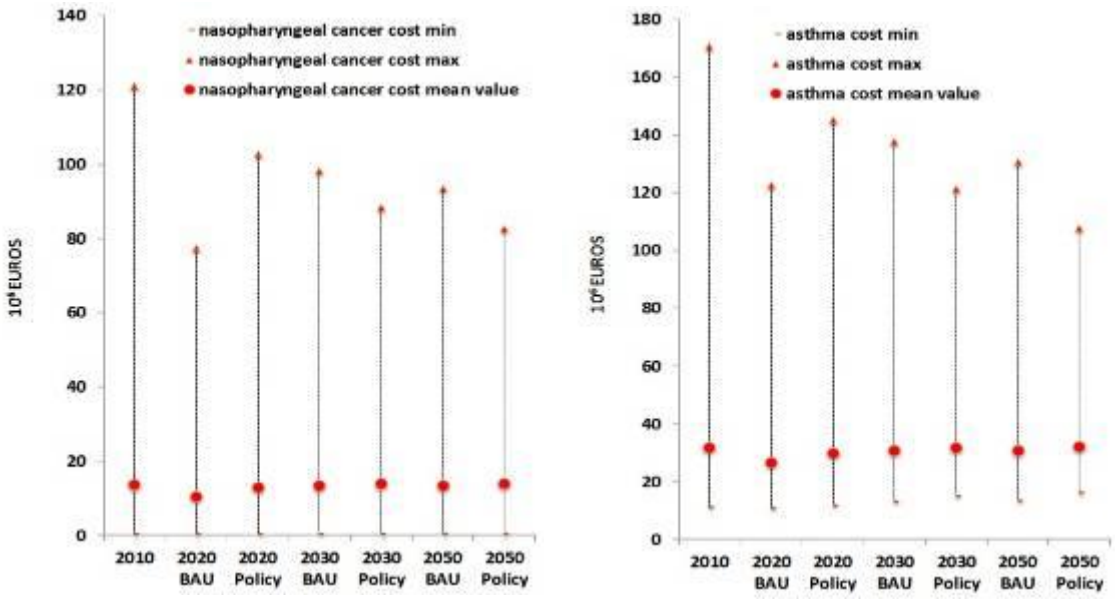

Figure 7-29: Damage costs due to formaldehyde (EU 27)

7.2.5 Damage costs due to air pollutants

Damage costs due to air pollutants in the EU29 in the years 2020, 2030 and 2050 can be found in Table 7-17. For weighing variant 1 (see Section 7.1.6) damage costs are also shown in Figure 7-30.

In contrast to the DALYs, there is an increase in damage costs the further in the future the exposure takes places. This is due to the upscaling of the EUR in future years (see Section 7.2) and means that people will earn more money in the future and, thus, will be able and willing to pay more for avoiding a certain disease.

This trend is not coinciding with the trend in actual health effects (DALYs) as described in 7.1.6. DALYs increase for the BAU scenario from 2020 to 2030 and decrease from 2030 to 2050 under the starting value of 2020. DALYs for the policy scenario decrease from 2020 to 2050.

Damage costs, however, increase for the BAU scenario from 2020 to 2050. For the policy scenario they increase in 2030 and decrease in 2050 again (over the level of 2020). This is due to the aforementioned upscaling of the monetary values and might lead to biases in interpretation if not considered carefully.

Table 7-17: Damage costs due to air pollutants in EU29 in Mio. EUR_{2010}.

Variant 1			Variant 2			Variant 3		
	BAU	Policy		BAU	Policy		BAU	Policy
2020	220,000	230,000	2020	190,000	190,000	2020	160,000	170,000
2030	270,000	250,000	2030	240,000	220,000	2030	210,000	200,000
2050	300,000	240,000	2050	250,000	200,000	2050	220,000	180,000

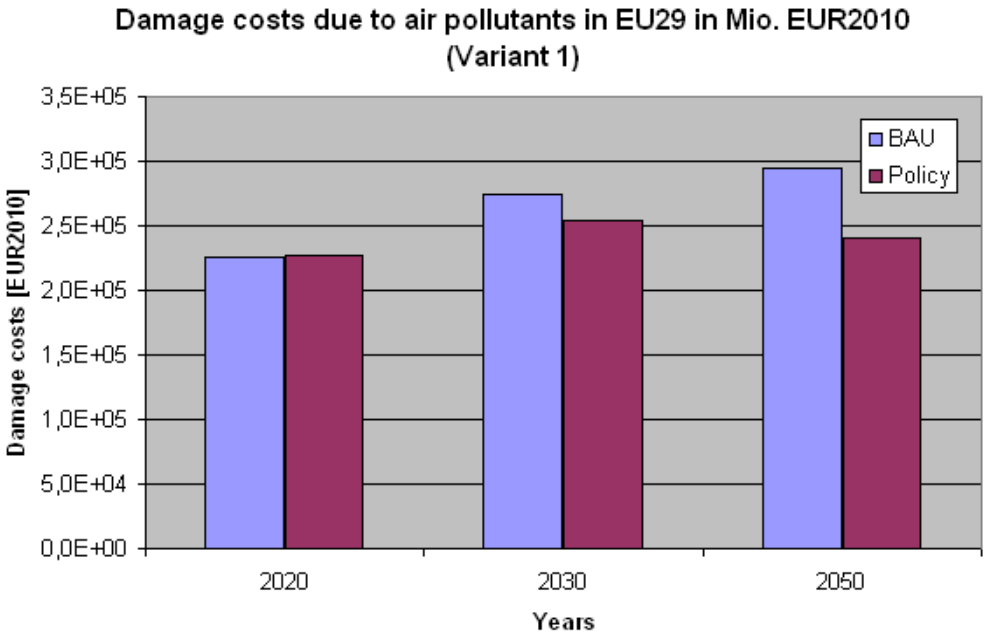

Figure 7-30: Damage costs due to air pollutants in EU29 in Mio. EUR_{2010} (Variant 1).

7.2.6 Damage costs due to personal exposure to PM2.5

Damage costs for all scenarios are shown in Figure 7-31. For the monetary values applied see Section 7.2. Damage costs follow the same trends as the exposure. See Section 4.3.1 for a description and explanation of the trends, and Section 7.1.5 for the DALYs due to exposure to PM.

In contrast to the DALYs, the increase in damage costs is higher the further in the future the exposure takes places. This is due to the upscaling of the EUR in future years (see Section 7.2) and means that people will earn more money in the future and, thus, will be able and willing to pay more for avoiding a certain disease.

a)

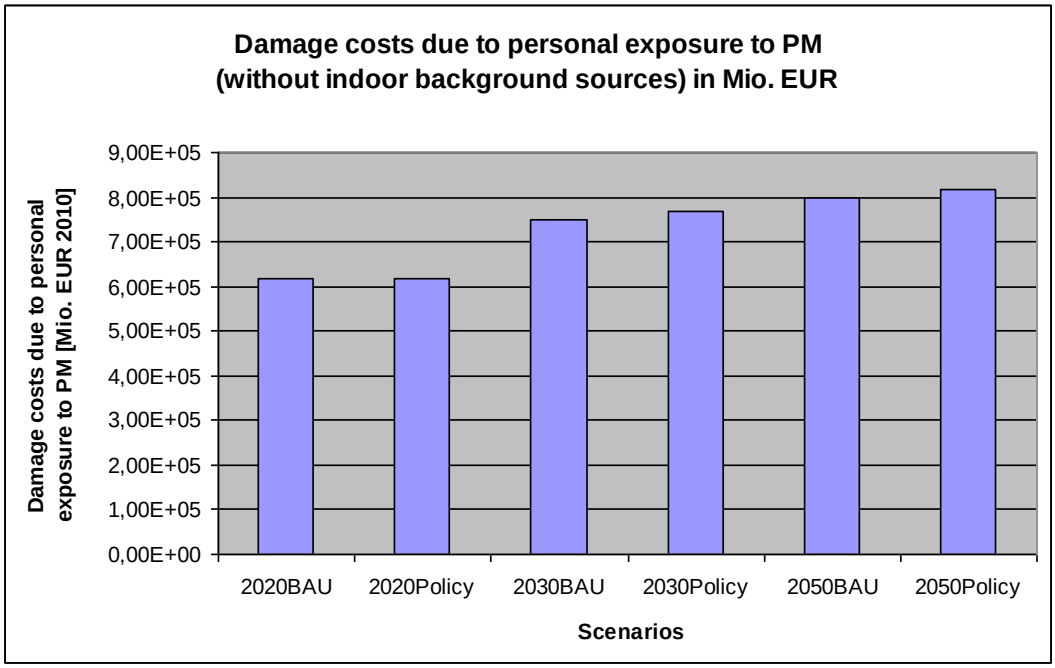

b)

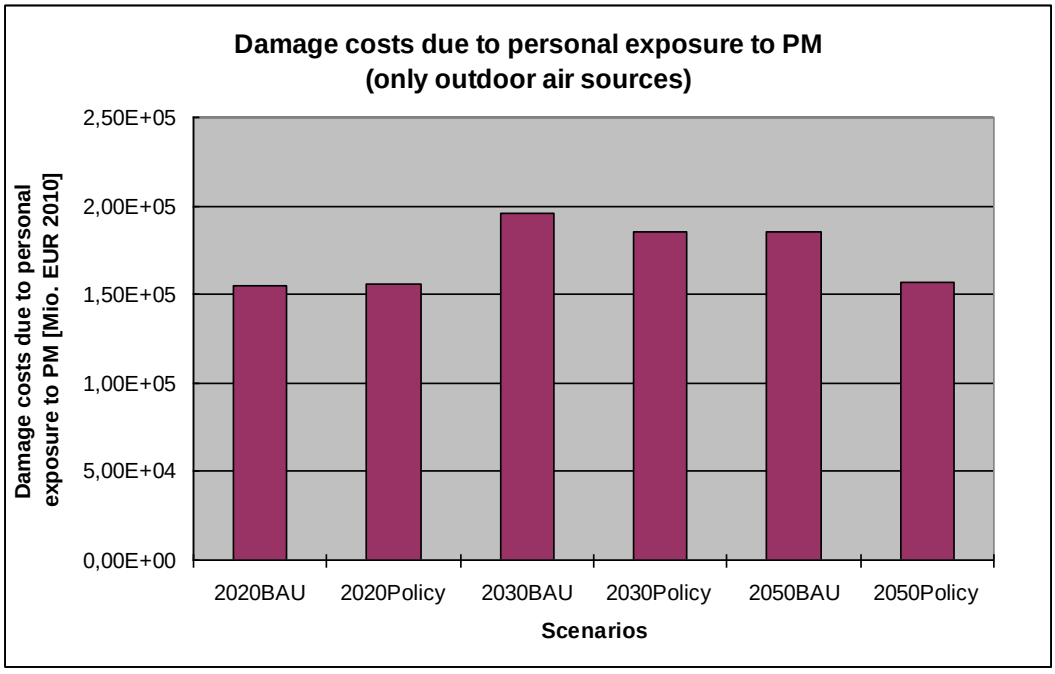

Figure 7-31: Damage costs in Mio. EUR_{2010} (10^6) due to personal exposure to PM in EU30, a) without indoor background sources, b) only with outdoor air sources.

Damage costs due to personal exposure to PM from ETS are estimated as 450,000 million / 430,000 million EUR_{2010} in 2020 (BAU, Policy), 512,000 millon / 536,000 million EUR_{2010} in 2030 (BAU, Policy) and 580,000 million / 630 million EUR_{2010} in 2050 (BAU, Policy). However, theses values are based on mean exposure and do not include uncertainty or variability in the population. Furthermore, as nearly half of all health effects of personal exposure to PM is originating from ETS, and as the exposure thus is very high, we might be overestimating the damage costs due to ETS (see Section 5.2.2).

7.2.7 Damage costs due to POPs

Damage costs per country are derived for all considered European countries as shown in Figure 7-32 for PCB-153 and in Figure 7-34 for 2,3,4,7,8-PeCDF, respectively. Aggregated damage costs for the whole of Europe are shown in Figure 7-33 for PCB-153 and in Figure 7-35 for 2,3,4,7,8-PeCDF, respectively.

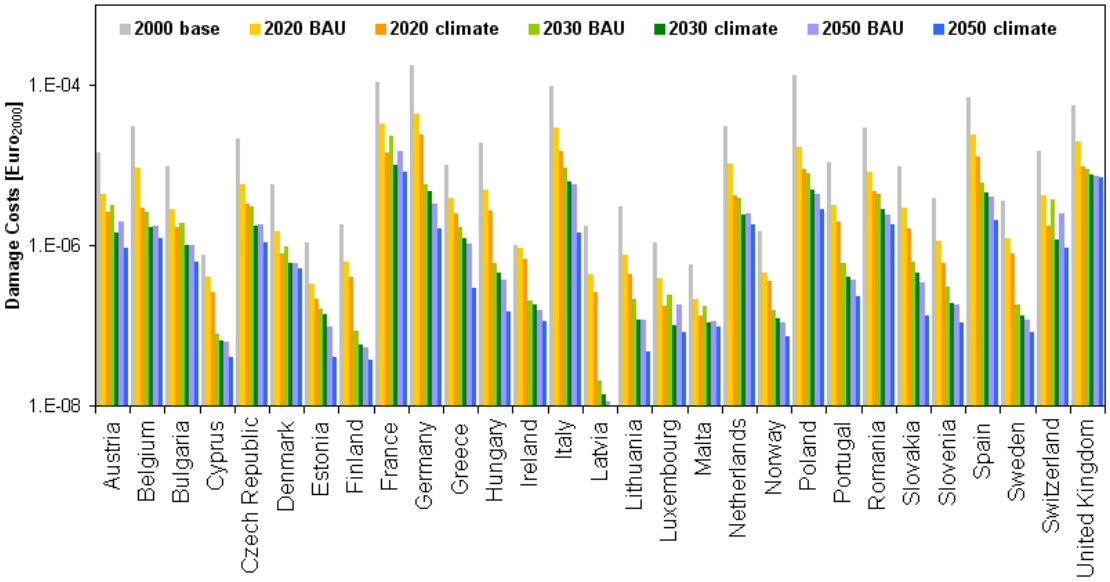

Figure 7-32: Damage costs in European countries due to cancer caused by intake of PCB-153 via inhalation, ingestion of drinking water and ingestion of food crops for all scenarios from years 2000 to 2050.

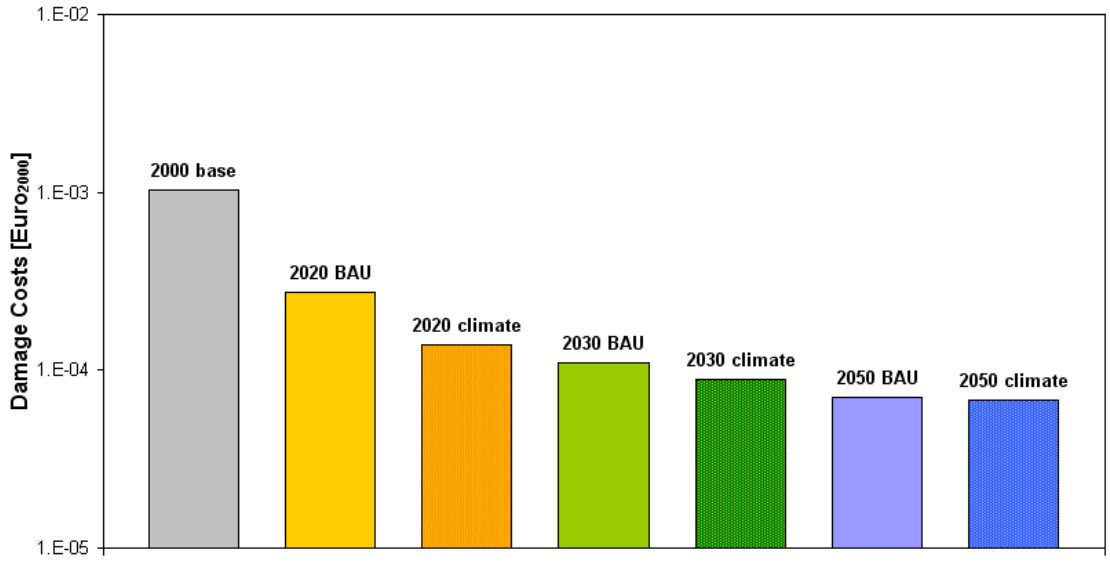

Figure 7-33: Damage costs in Europe due to cancer caused by intake of PCB-153 via inhalation, ingestion of drinking water and ingestion of food crops for all scenarios from years 2000 to 2050.

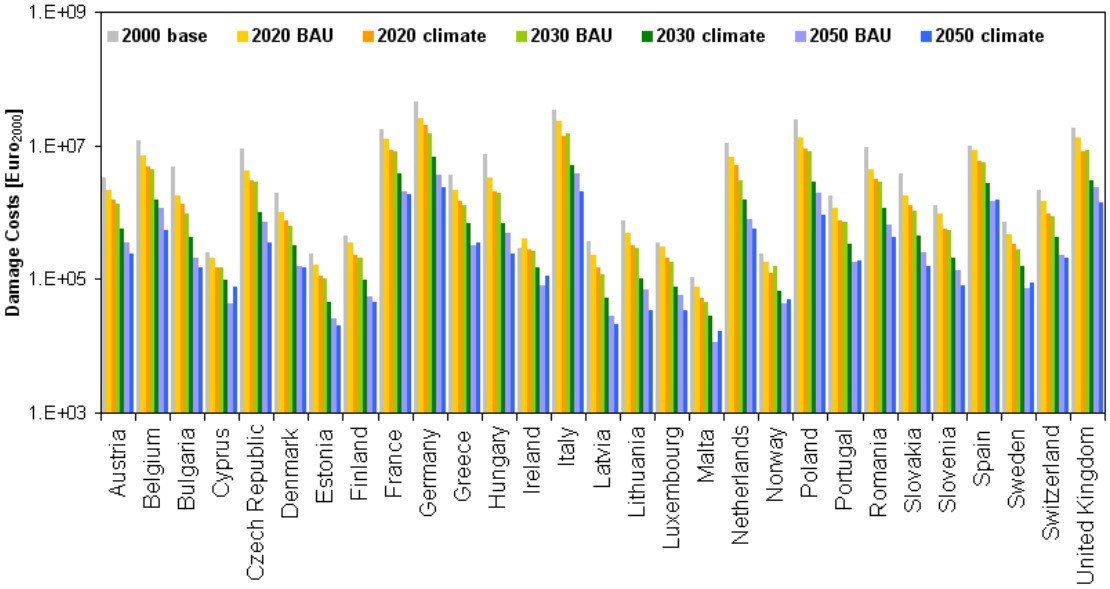

Figure 7-34: Damage costs in European countries due to cancer caused by intake of 2,3,4,7,8-PeCDF via inhalation, ingestion of drinking water and ingestion of food crops for all scenarios from years 2000 to 2050.

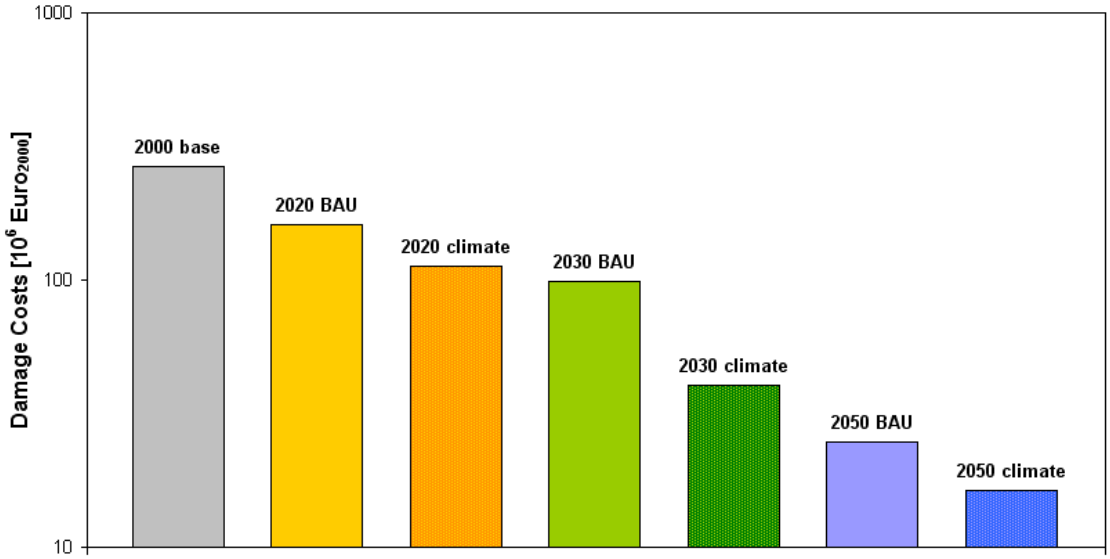

Figure 7-35: Damage costs in Europe due to cancer caused by intake of 2,3,4,7,8-PeCDF via inhalation, ingestion of drinking water and ingestion of food crops for all scenarios from years 2000 to 2050.

7.2.8 Damage costs due to pesticides

Based on the DALY approach applied for selected pesticides with available DRF information, the damage costs per country are derived as shown in Figure 7-36 for northern European countries and in Figure 7-37 for southern European countries, respectively.

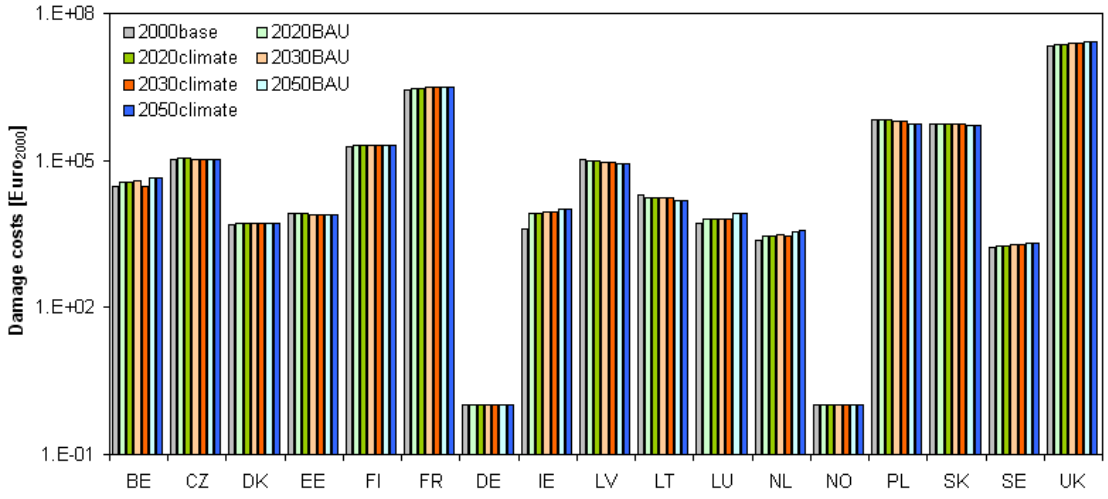

Figure 7-36: Damage costs in northern European countries due to cancer caused by intake of pesticides via ingestion of food crops after direct application for all scenarios from years 2000 to 2050.

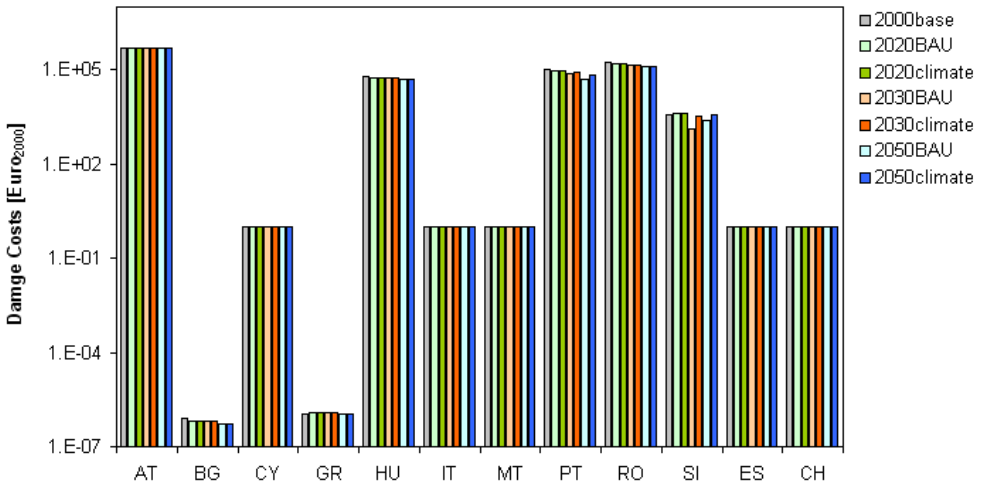

Figure 7-37: Damage costs in southern European countries due to cancer caused by intake of pesticides via ingestion of food crops after direct application for all scenarios from years 2000 to 2050.

The differentiation between northern and southern European countries is mainly due to the predicted future development of climate conditions that have distinct impacts in northern and in southern Europe on e.g. crop yield. In future years, yield is assumed to increase in northern Europe caused by higher temperatures leading to a more moderate climate, while yield is assumed to decrease in southern Europe caused by e.g. the introduction of water shortage that comes along with temperature increase in this region. Crop yield developments are discussed in detain in Section 3.

In northern Europe, the trend towards 2050 is dominated by the effect of increase in area for energy crop production. The highest overall external costs in northern Europe are estimated for UK and France with some ten million Euros of health damage costs caused by the application of carcinogenic pesticides (not necessarily exclusively applied in these countries due to trade of food). Sweden and the Netherlands, in contrast, only show an overall amount of external costs in the range of 1000 Euros (see Figure 7-36). In southern Europe, there are some countries, such as Italy and Portugal, which do not show an increase in costs towards 2050, but instead a slight decrease. This is mainly due to the fact that different effects influence the health damage pattern from 2000 to 2050 antagonistically, i.e. while the trend of increasing energy crop production is causing an increase in the health effects via food crop ingestion (see explanation above), the trend of decreasing food crop yields towards 2050 for southern countries completely outweighs the influence of increasing energy crop production, or even leads to an overall decrease of the health effects and, thus, related external costs, such as in Italy and Portugal. The highest overall external costs in southern Europe are estimated for Romania and Hungary with about 1 million Euros of health damage costs caused by the application of carcinogenic pesticides (again, not necessarily exclusively applied in these countries due to trade of food). Spain, in contrast, only shows an overall amount of external costs in the range of less than one Euro (see Figure 7-37).

Since from available DRFs only information with respect to carcinogenic effects are allowed to be extrapolated from substance to substance based on similar mode of action. This means that for non-carcinogenic effects, which usually add up to the carcinogenic effects, no health impacts and related costs could be estimated due to the lack of any DRFs relating non-carcinogenic effects to at least one of the considered pesticides. Thus, in all figures the external costs are exclusively derived from cancer effect information, which does, however, not mean that other effects do not exist, but are rather as of now not quantifiable. Figure 7-38 finally aggregates all damage costs in Europe over all considered countries for the pesticides with available effect information as well as Figure 7-33 gives the total aggregated damage costs in Europe extrapolated to all considered pesticides.

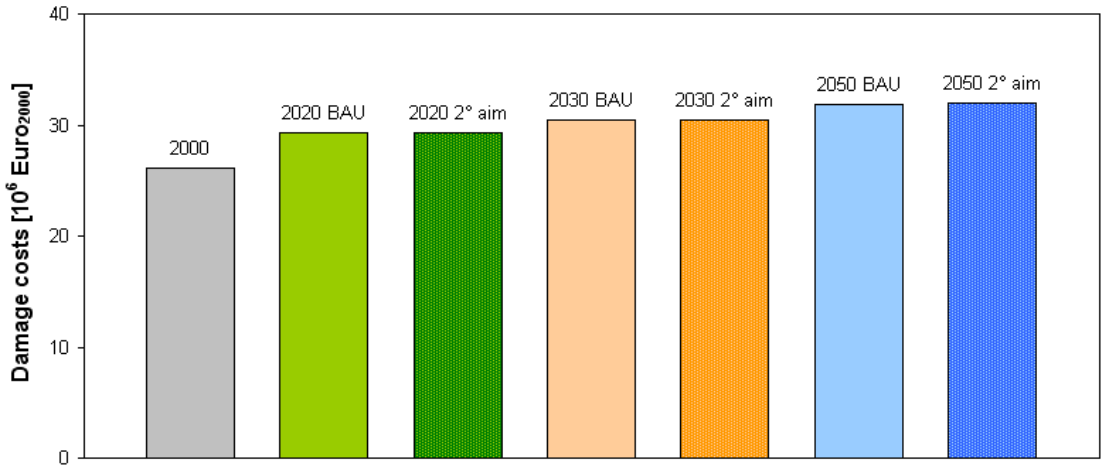

Figure 7-38: Aggregated damage costs in Europe due to cancer caused by intake of pesticides via ingestion of food crops after direct application for all scenarios from years 2000 to 2050 for selected pesticides with available effect information.

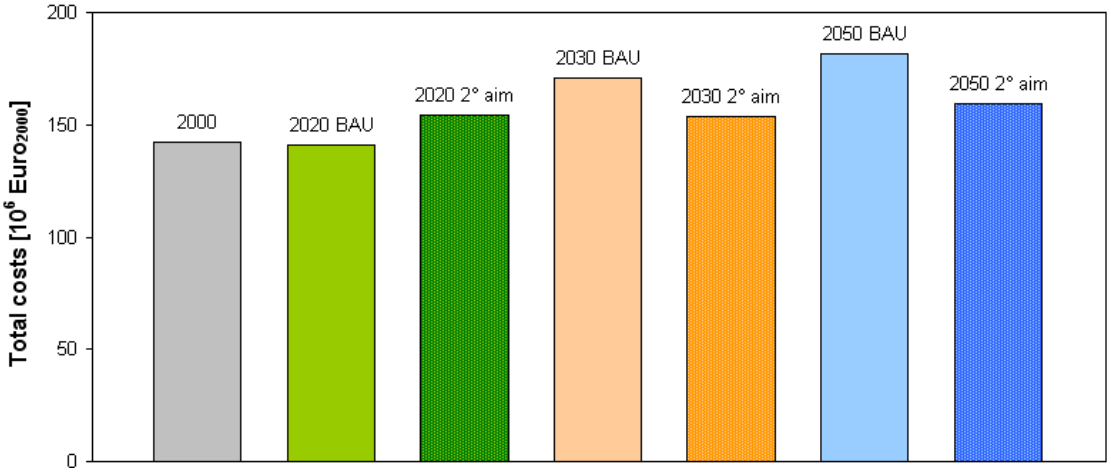

Figure 7-39: Aggregated damage costs in Europe due to cancer caused by intake of pesticides via ingestion of food crops after direct application for all scenarios from years 2000 to 2050 extrapolated to all considered pesticides.

Conclusions – ingestion pathway: Intake fraction of pesticides via ingestion of food crops after direct application varies by three orders of magnitude among European countries. Herbicides show the largest share of intake in most countries, whereas fungicides are dominating in other countries. This is mainly caused by the country-specific climatic and environmental conditions, such as soil moisture. In contrast, insecticides and plant growth regulators contribute only little to the overall intake. Trade of food may re-distribute a large fraction of pesticides contained in food crops. A reduction in health effects between each years 450ppm and BAU scenario is mainly caused by different assumptions behind crop yield in the different countries, predominantly influenced by varying climate conditions, in particular temperature and precipitation pattern. All in all, the reduced crop yield in northern European countries leads to an increase in health impacts by 22 percent between the years 2000 and 2050 (450ppm scenario for the latter).

Damage Costs in Euro for morbidity due to lung cancer caused by carcinogenic pesticides via inhalation for baseline and scenarios per country is presented in Figure 7-40. Cyprus and Malta are excluded because of their small values.

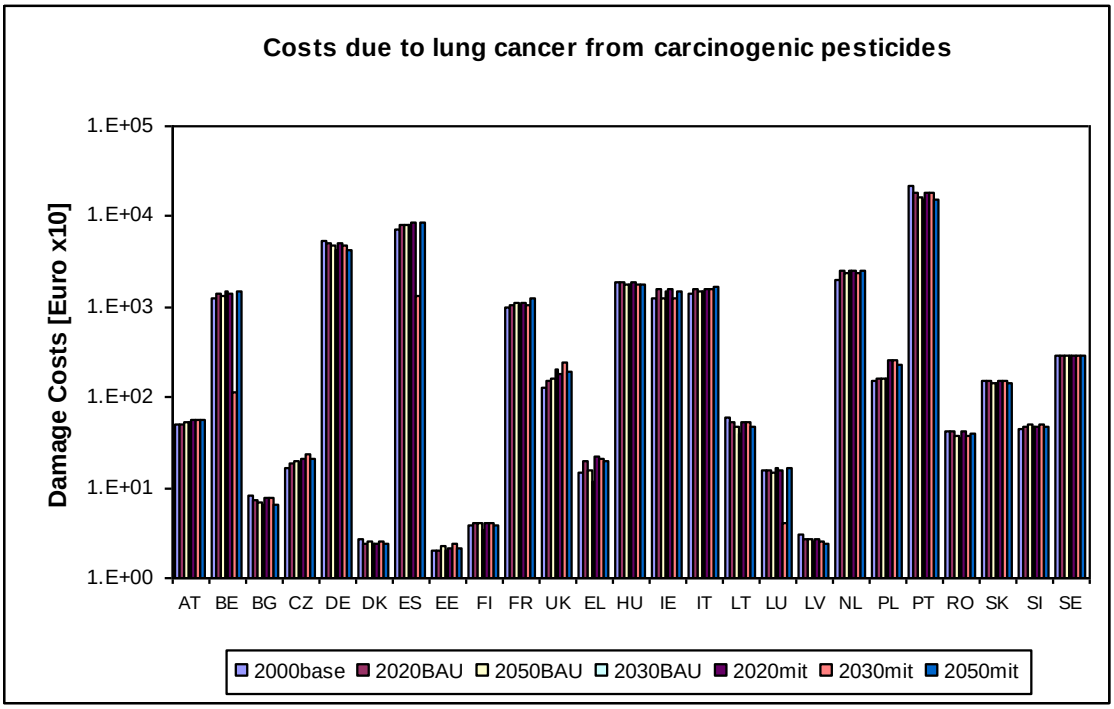

Figure 7-40: Damage Costs in Euro for morbidity due to lung cancer from carcinogenic pesticides for baseline and scenarios – EU25 (Cyprus and Malta are excluded).

For a discussion about uncertainties see Section 6.2.

7.2.9 Damage costs due to heat

Table 7-18: Monetary cost (M€) due to heat related mortality and the impact of UHI mitigation policies (mean + 95% confidence limit, total for North-continental and Mediterr. region cities).

Year	Reference / UHI mitigation scenario	Climate scenario A1B		Climate scenario B1	
		Monetary cost (M€)	Cost prevented by UHI mitigation policy (M€)	Monetary cost (M€)	Cost prevented by UHI mitigation policy (M€)
2010	Current	5580 (528-13482)		5580 (528-13482)	
2020	Reference 1	9582 (892-23336)		9811 (936-24003)	
	Vegetation	9183 (854-22418)	399 (37-948)	9357 (893-22910)	455 (41-1092)
	Albedo	8518 (792-20841)	1064 (99-2543)	8632 (824-21278)	1179 (107-2825)
	Veg+alb	8147 (757-19936)	1435 (133-3437)	8228 (784-20321)	1583 (143-3782)
2030	Reference 1	15710 (1486-38804)		14636 (1382-35890)	
	Vegetation	15026 (1420-37101)	684 (62-1617)	14012 (1322-34360)	624 (57-1466)
	Albedo	13927 (1316-34413)	1783 (164-4224)	13058 (1230-32108)	1578 (145-3774)
	Veg+alb	13226 (1249-32699)	2484 (227-5883)	12516 (1178-30889)	2120 (196-5064)
2050	Reference 1	29814 (2787-72071)		17671 (1600-44000)	
	Vegetation	28631 (2668-69409)	1183 (119-2780)	16944 (1540-42224)	727 (63-1738)
	Albedo	26809 (2492-65419)	3005 (298-7028)	15797 (1432-39485)	1874 (165-4473)
	Veg+alb	25827 (2411-63140)	3987 (394-9311)	15135 (1367-37953)	2535 (225-6019)

The results of the assessment and the uncertainties related to it are discussed in more detail in Appendix D (Annexes

Heat and Urban Heat Island (UHI) Mitigation).

8 SUMMARY OF DALYS AND DAMAGE COSTS INCLUDING DISCUSSION

8.1 MAIN SCENARIOS

In Table 8-1 and Table 8-3 the total DALYs and damage costs due to different stressors and pollutants are listed in the EU29 for the BAU and the policy scenarios.

It can be seen that, independently from BAU and Policy scenarios, a hierarchy of stressors exists: PM from environmental tobacco smoke (ETS) constitutes the main part of the health burden, followed by air pollutants and noise in urban areas. Radon, heat exposure and dampness follow in the midfield, while persistent organic pollutants (POPs), pesticides and formaldehyde account for the smaller parts of the total health effects. (As suggested in Section 5.2.2 it is likely that the DALYs and damage costs of ETS are overestimated. Furthermore, it is the first time to quantify ETS via PM. So we must be cautious with the interpretation. However, it can be concluded that ETS does pose a health problem indoors.) For pesticides only cancer effects were estimated. It is likely that non-cancer effects are more important; thus, pesticides may move to the midfield of importance if those effects are also considered.

Table 8-1: DALYs (in thousand) in EU29 due to different stressors and pollutants.

		Air pollutants	ETS (PM based)[1]	Noise	Radon[1]	Heat	Dampness[1]	POPs	Pesticide (cancer only)[2]	Formaldehyde[1]	Sum
2020	**BAU**	2,486	7,000	777	428	128	122	4	3.3	3.7	11,000
	Policy	2,495	6,700	747	433	132	122	2.8	3.3	4.52	10,600
Policy - BAU		9	-300	-30	5	3	0.1	-1.2	0	0.8	-313
2030	**BAU**	2,574	6,700	781	483	211	136	2.5	3.5	4.6	10,900
	Policy	2,389	7,000	745	563	196	156	1	3.6	4.9	11,000
Policy - BAU		-185	300	-36	80	-14	20	-1.5	-0.01	0.2	163
2050	**BAU**	2,357	6,500	734	524	400	143	0.6	4	4.7	10,700
	Policy	1,929	6,700	693	663	237	178	0.4	3,9	4.9	10,400
Policy - BAU		-428	200	-41	139	-163	35	-0.2	-0.1	0.2	-258

[1] If no additional measures to improve air exchange rate in buildings are implemented.
[2] Only cancer effects were taken into account. Other health endpoints may be more important.

In 2020 biomass is mainly used for residential heating. In the father future biomass is needed to generate biofuels (Fischer-Tropsch process). Thus, in the future PM

emissions from the residential sector decrease leading, amongst all kinds of other effects, to reduced health effects in the future. Effects of the single mitigation measure on the whole scenario can be found in Section 8.2.

Within the contribution of outdoor air pollutants SIA (secondary inorganic aerosols) account for about two thirds of the DALYs, PPM (primary particles) account for about one third of DALYs and SOMO35 (ozone) for about 2 percent (variant 1, see Section 7.1.6 and below). Sensitivity analyses show that if primary particles are weighted higher the fractions change: For variant 2 the fractions are about 40 percent for SIA, about 60 percent for PPM, and about 3 percent for ozone; for variant 3 about one quarter for SIA, about three quarters for PPM, and again about 3 percent for ozone (see Figure 8-1).

Table 8-2: Weighing scheme for different fractions of particulate matter: for sensitivity analysis.

	Variant 1	**Variant 2**	**Variant 3**
PPM2.5	1	* 1.5	* 1.75
nitrates	1	* 0.5	* 0.25
sulphates	1	* 0.6	* 0.25
PPMcoarse	1	* 1	* 1
nitratescoarse	1	* 0.5	* 0.25

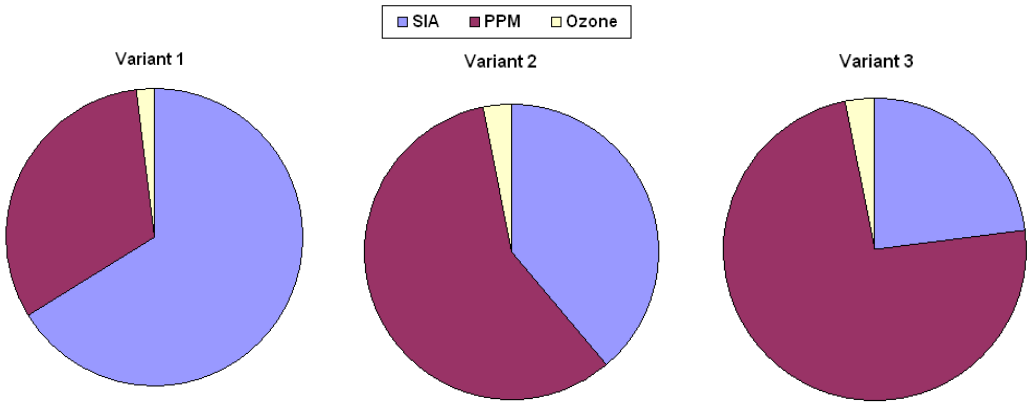

Figure 8-1: DALYs due to outdoor air pollution: Approximate fractions of SIA, PPM and ozone according to different weighing schemes for sensitivity analysis.

Besides the absolute DALYs showing the hierarchy of importance of the stressors, the changes from BAU to Policy scenarios are of major interest: Differences between the policy and the BAU scenarios within each year are very small in 2020 and increase towards 2050 (Table 8-1). This means that in 2030 and 2050 the climate mitigation measures impact more strongly on health effects than in 2020 were the emissions do not differ much yet.

In more detail it can be noticed that a decrease in health effects arises from outdoor air pollutants (SIA, ozone, PPM), noise and heat exposure. However, health effects due to indoor pollutants increase due to tigher building envelopes and, thus, accumulation in residential buildings (Figure 8-3) if no additional measures to improve the air exchange rate in buildings are implemented.

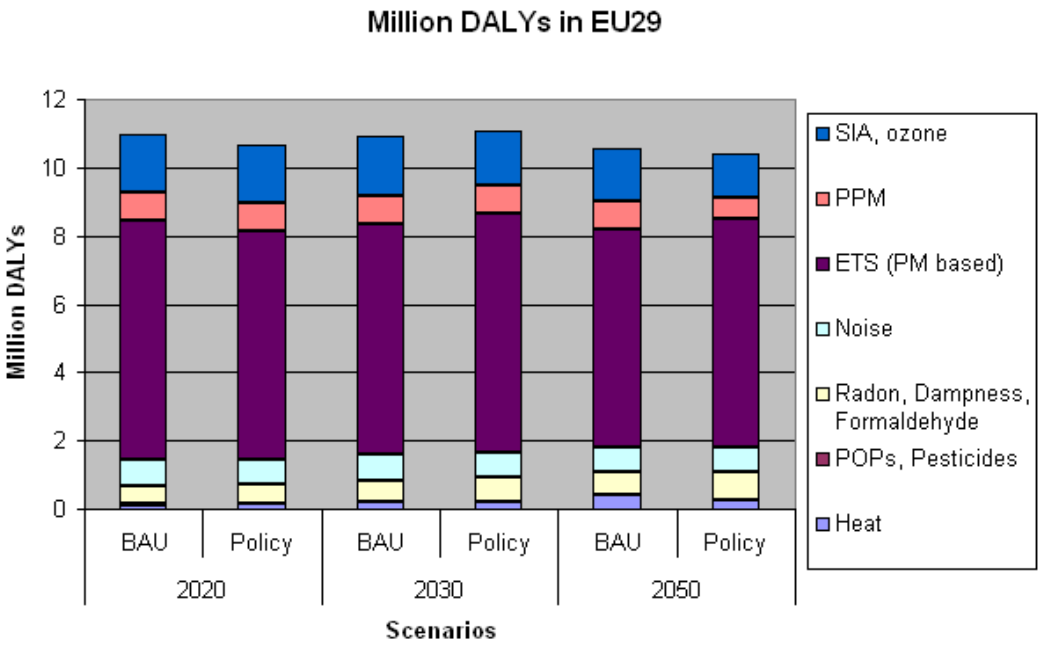

Figure 8-2: DALYs in EU29 due to different pollutant and stressor groups (BAU and policy scenarios for the years 2020, 2030 and 2050).

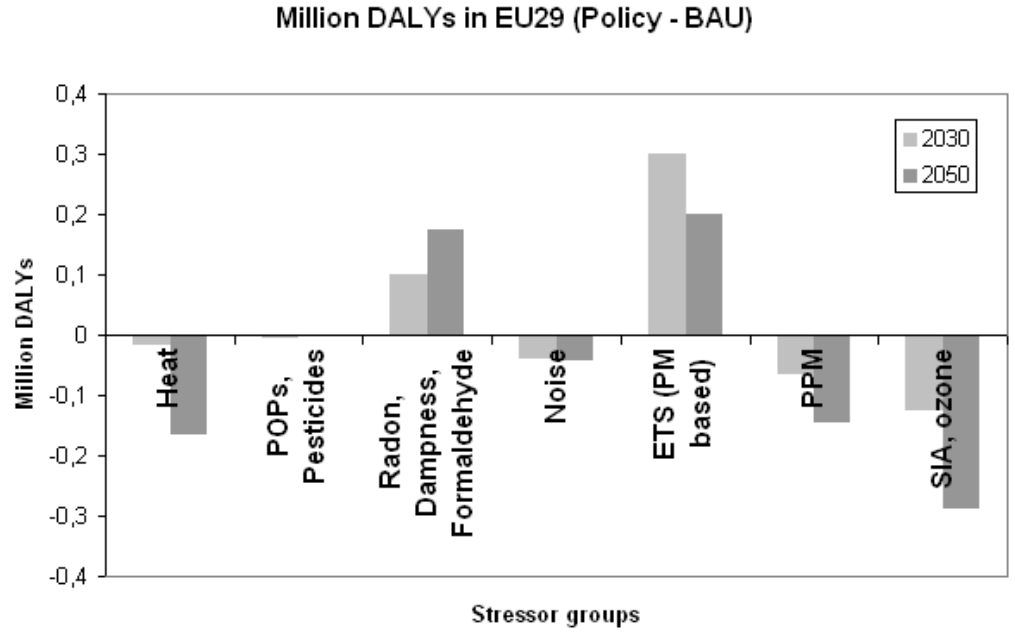

Figure 8-3: DALYs in EU29 due to different pollutant and stressor groups: differences between Policy and BAU scenarios for 2030 and 2050 (negative values means decrease).

Table 8-3: Damage costs in million EUR_{2010} in EU29 due to different stressors and pollutants.

		Air pollutants	ETS (PM based)[1]	Noise	Radon[1]	Heat	Dampness[1]	POPs	Pesticide (cancer only)[2]	Formaldehyde[1]	Sum
2020	**BAU**	226,000	450,000	10,700	19,300	9,600	5,500	160	132	27	721,000
	Policy	227,000	430,000	10,200	19,500	9,800	5,500	110	132	30	702,000
Policy - BAU		1,000	20,000	-500	200	200	0	-50	0	3	-19,000
2030	**BAU**	274,000	512,000	12,700	21,800	15,700	6,100	100	141	31	831,000
	Policy	254,000	536,000	12,100	25,200	14,600	7,000	40	142	32	853,000
Policy - BAU		-20,000	24,000	-600	3,500	-1,100	900	-60	0.5	1	23,000
2050	**BAU**	294,000	580,000	14,100	23,600	29,800	6,400	25	160	31	948,000
	Policy	241,000	630,000	13,200	29,700	17,700	8,000	17	156	32	920,000
Policy - BAU		-53,000	50,000	-900	6,100	-12,100	1,600	-8	-4	1	-28,000

[1] If no additional measures to improve air exchange rate in buildings are implemented.
[2] Only cancer effects were taken into account. Other health endpoints may be more important.

When comparing damage costs instead of DALYs the relation of the stressors to each others differs. This is due to methodological aspects: When using willingsness to pay studies to derive the monetary values per health endpoint this yields another weight compared to when using DALY weights. It is therefore expected that different EUR/DALY values will occur for the different stressors. Indeed EUR/DALY values differ between stressors from about 8.000 to around 100.000 (with most of them being higher than 40.000). This difference in weighing does, however, not change the hierarchy of importanceof the stressors.

The second interesting issue is to compare the avoided damage costs due to avoided health effects to the avoided costs due to avoidance of greenhouse gas emissions (GHG): If including all stressors (knowing that ETS might be overestimated) in 2020 and 2050 a positive ratio can be observed (Table 8-4), for 2030 the ratio is negative. This is due to the high impact of ETS and other indoor stressors that accumulate in tighter buildings if no additional measures to improve air exchange rates are implemented. In 2030 it seems that climate mitigation measures have negative effects on health. However, in 2050 the positive effects (of outdoor air stressors) outweigh the negative effects (of indoor air pollutants). More research is needed to identify the role of ETS.

More realistic seems the picture when only outdoor stressors are considered (Table 8-5): In 2020 the ratio is negative while in 2030 and 2050 the ratio is positive. In 2020 emission scenarios for the Policy and BAU scenario do not differ greatly. Thus, the difference between the scenarios is not so huge.

For 2030 and 2050 the positive ratios range between 0.39 (2020) and 0.23 (2050), i.e. that around 30 % of the positive effects of climate change mitigation measures through their effect on the climate can be reached in addition by their effect on human health! The ratio decreases from 2030 to 2050 as the costs for each ton CO_2-equ. emissions increases (from 39 in 2030 to 87 EUR in 2050). If in 2050 the same price as in 2030 had been used the effect of the measures on human health would even be half of the effect on the climate!

Table 8-4: Avoided damage costs of health effects compared to avoided costs due to green house gas emissions in EU29 for the Policy scenario compared to the BAU scenario in the years 2020, 2030 and 2050 (all sources).

	Damage costs (Policy - BAU)	**Tons CO2-equ. (Policy - BAU)**	**EUR/t CO_2-equ.**	**Damage Costs due to GHG emissions (Policy - BAU)**	**Ratio: health damage costs / GHG damage costs**
2020	-19,000,000,000	-622,378,000	33	-20,538,500,000	0.93
2030	22,600,000,000	-1,437,841,000	39	-56,075,800,000	-0.4
2050	-28,300,000,000	-3,360,330,000	87	-292,348,700,000	0.10

Table 8-5: Avoided damage costs of health effects compared to avoided costs due to green house gas emissions in EU29 for the Policy scenario compared to the BAU scenario in the years 2020, 2030 and 2050 (excluding indoor sources).

	Damage costs (Policy - BAU)	**Tons CO2-equ. (Policy - BAU)**	**EUR/t CO_2-equ.**	**Costs due to GHG emissions (Policy - BAU)**	**Ratio: damage costs / GHG costs**
2020	750,000,000	-622,378,000	33	-20,538,500,000	-0.04
2030	-21,800,000,000	-1,437,841,000	39	-56,075,800,000	0.39
2050	-66,000,000,000	-3,360,330,000	87	-292,348,700,000	0.23

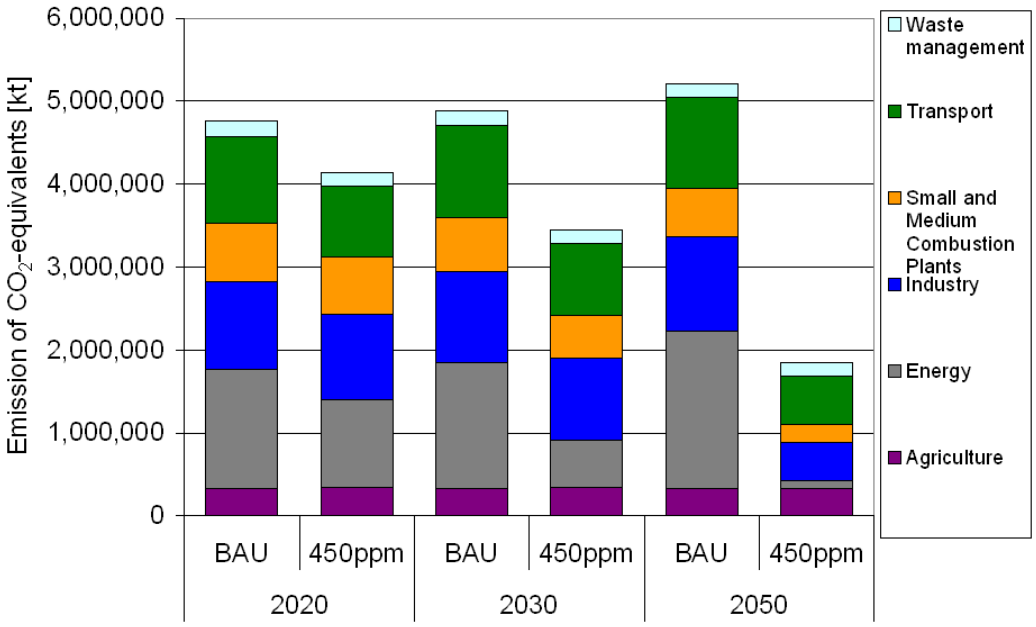

Figure 8-4: Emissions of CO_2-equ. in EU29 for the BAU and policy scenarios.

8.2 SINGLE MEASURES

In Section 3 the changes of emissions of pollutants as well as of greenhouse gases have been estimated for single policy-measure combinations. For selected policies the changes in emissions have been converted into changes in health effects and furtheron in changes in DALYs and damage costs. Results are presented in the following.

Table 8-6: Resulting changes of health impacts in DALYs and damage costs, if renewable energies are used for electricity generation, per ton of CO2eq avoided, in 2020 in [mDALY avoided per t CO2eq] and [Euro per t CO2eq]; negative values indicate increased health impacts

	mDALY per t CO2eq	**Euro per t CO2eq**
	Benefits to human health LCA & Operation [DALY]	Benefits to human health LCA & Operation [million Euro2010]
Solid biomass & renewable waste	-0.127	-12
Biogas/Biofuels	-1.378	-119
Hydro power	0.203	18
Wind on-shore	0.125	12
Wind off-shore	0.182	16
Solar - Photovoltaic	0.173	15
Solar - Thermal	0.092	8

Table 8-6 shows the results of changes in electricity production. The generation of electricity with solid biofuels (wood) and biogas leads to negative health impacts, as wood is burnt in smaller units with higher specific NO_x and PM emissions as the alternative large power plants and biogas is used in combustion engines with higher NO_x emissions. Of course the result is strongly depending on the technology used for the abatement of NOx and PM emissions. With additional effort put into reducing emission factors beyond those of current legislation, the negative health effects could be further reduced.

The use of water, wind and solar energy leads to large reductions of health impacts per t of CO2 avoided.

Table 8-7 shows the effect of burning more wood in smaller firings. Such firings have much higher NMVOC, CO and PM emissions than e.g. oil or gas firings, thus leading to much larger health effects. This means, that the negative effects of burning wood in

small heating plants are so high, that they may even outweigh the positive effects of the reduced greenhouse gas emissions.

Table 8-7: Resulting total changes of health impacts expressed in DALYs avoided and damage costs avoided per t of CO2eq avoided, if more wood is burnt for residential heating, in [mDALY per t CO2eq] and [Euro per t CO2eq].

mDALY per t CO2eq	**Euro per t CO2eq**
Benefits to human health LCA & Operation [DALY]	Benefits to human health LCA & Operation [million Euro2010]
-0.38	-39.64

Of course, the results depend on the technologies used. If for instance, wood firings would be equipped with an efficient dust filter (e.g. using an electrostatic precipitator), health impacts could be reduced drastically.

Table 8-7 shows the results of assessing a number of policies in the transport sector. The final indicators for the direction and importance of health effect used here are avoided DALYs per kt of $CO_{2equivalent}$ avoided and health damage costs per kt of CO_2equivalent avoided. As can be seen, allmeasures have a positive impact on reducing health risks. The measures with the highest reductions of health risks are city tolls and speed limits. Thus estimating health impacts avoided helps to strengthen the argument for implementing these policies.

Table 8-7: DALYs, damage costs and CO_2-equ. emissions (kilotons) for measures in the transport sector.

		CO2-equivalent savings	Unit	DALY urban	DALY rural	DALY noise	DALY-Total	Damage urban	Damage rural	Damage noise	Damage-Total [€]	DALY/CO2-equivalent	Unit	Damage/CO2-equivalent	Unit
Electric Vehicles	2020	-2957.073655	kt	-80	-154	-1,216	-1450	-7,496,903	-14,602,594	-19,446,027	-41,545,524	0.49	DALY / kt-CO_2	14.05	€ / t-CO_2
	2030	-18024.35546	kt	-474	-943	-4,096	-5513	-51,484,154	-103,966,100	-73,245,994	-228,696,247	0.31	DALY / kt-CO_2	12.69	€ / t-CO_2
	2050	-79525.02966	kt	-1826	-4308	-13,380	-19514	-232,043,171	-551,625,101	-284,483,501	-1,068,151,774	0.25	DALY / kt-CO_2	13.43	€ / t-CO_2
		CO2-equivalent savings	**Unit**	**DALY urban**	**DALY rural**	**DALY noise**	**DALY-Total**	**Damage urban**	**Damage rural**	**Damage noise**	**Damage-Total [€]**	**DALY/CO2-equivalent**	**Unit**	**Damage/CO2-equivalent**	**Unit**
Cycling in Cities	2020	-6189.697823	kt	-764	0	-7,333	-8097	-70,753,876	0	-102,025,422	-172,779,298	1.31	DALY/kt	27.91	€ / t-CO_2
	2030	-6213.363082	kt	-564	0	-6,926	-7490	-61,411,785	0	-120,530,917	-181,942,702	1.21	DALY/kt	29.28	€ / t-CO_2
	2050	-6159.717993	kt	-530	0	-5,790	-6320	-67,914,468	0	-125,397,268	-193,311,735	1.03	DALY/kt	31.38	€ / t-CO_2
		CO2-equivalent savings	**Unit**	**DALY urban**	**DALY rural**	**DALY noise**	**DALY-Total**	**Damage urban**	**Damage rural**	**Damage noise**	**Damage-Total**	**DALY/CO2-equivalent**	**Unit**	**Damage/CO2-equivalent**	**Unit**
Economic driving	2020	-29343.80216	kt	-361	-3371		-3731	-33,270,109	-311,194,252		-344,464,362	0.13	DALY/kt	11.74	€ / t-CO_2
	2030	-30977.92553	kt	-270	-2901		-3171	-29,169,457	-314,126,174		-343,295,631	0.10	DALY/kt	11.08	€ / t-CO_2
	2050	-30989.22047	kt	-260	-2861		-3121	-33,153,356	-364,925,130		-398,078,486	0.10	DALY/kt	12.85	€ / t-CO_2
		CO2-equivalent savings	**Unit**	**DALY urban**	**DALY rural**	**DALY noise**	**DALY-Total**	**Damage urban**	**Damage rural**	**Damage noise**	**Damage-Total**	**DALY/CO2-equivalent**	**Unit**	**Damage/CO2-equivalent**	**Unit**
Fuel Tax	2020	-16408.76479	kt	-550	-1269	-5,692	-7512	-50,921,197	-116,854,559	-80,661,280	-248,437,036	0.46	DALY/kt	15.14	€ / t-CO_2
	2030	-33384.66789	kt	-809	-1875	-10,625	-13310	-88,081,498	-202,640,319	-183,114,985	-473,836,802	0.40	DALY/kt	14.19	€ / t-CO_2
	2050	-33292.28256	kt	-764	-1877	-9,576	-12216	-97,856,935	-238,425,754	-204,361,090	-540,643,780	0.37	DALY/kt	16.24	€ / t-CO_2
		CO2-equivalent savings	**Unit**	**DALY urban**	**DALY rural**	**DALY noise**	**DALY-Total**	**Damage urban**	**Damage rural**	**Damage noise**	**Damage-Total**	**DALY/CO2-equivalent**	**Unit**	**Damage/CO2-equivalent**	**Unit**
Green wave	2020	-6062.126284	kt	-822	0		-822	-76,680,787	0		-76,680,787	0.14	DALY/kt	12.65	€ / t-CO_2
	2030	-18018.8251	kt	-1830	0		-1830	-199,522,761	0		-199,522,761	0.10	DALY/kt	11.07	€ / t-CO_2
	2050	-17865.60634	kt	-1758	0		-1758	-226,169,482	0		-226,169,482	0.10	DALY/kt	12.66	€ / t-CO_2

		CO2-equivalent savings	Unit	DALY urban	DALY rural	DALY noise	DALY-Total	Damage urban	Damaga rural	Damage noise	Damage-Total	DALY/CO2-equivalent	Unit	Damage/CO2-equivalent	Unit
City Toll	2020	-951.6338832	kt	-102.3	0	-1,216	-1318	-9,585,214	0	-19,446,027	-29,031,241	1.39	DALY/kt	30.51	€ / t-CO_2
	2030	-977.5672015	kt	-80	0	-1,223	-1302	-8,741,822	0	-23,642,462	-32,384,284	1.33	DALY/kt	33.13	€ / t-CO_2
	2050	-988.4209702	kt	-80	0	-1,159	-1238	-10,257,810	0	-27,479,863	-37,737,673	1.25	DALY/kt	38.18	€ / t-CO_2
		CO2-equivalent savings	Unit	DALY urban	DALY rural	DALY noise	DALY-Total	Damage urban	Damaga rural	Damage noise	Damage-Total	DALY/CO2-equivalent	Unit	Damage/CO2-equivalent	Unit
PC Toll	2020	-40893.27128	kt	-1332	-3134	-14,198	-18664	-123,347,331	-288,443,787	-200,214,613	-612,005,731	0.46	DALY/kt	14.97	€ / t-CO_2
	2030	-41605.06973	kt	-974	-2311	-13,455	-16740	-106,077,047	-249,676,856	-230,399,908	-586,153,811	0.40	DALY/kt	14.09	€ / t-CO_2
	2050	-41493.24449	kt	-920	-2315	-11,524	-14759	-117,883,814	-294,125,263	-247,318,768	-659,327,845	0.36	DALY/kt	15.89	€ / t-CO_2
		CO2-equivalent savings	Unit	DALY urban	DALY rural	DALY noise	DALY-Total	Damage urban	Damaga rural	Damage noise	Damage-Total	DALY/CO2-equivalent	Unit	Damage/CO2-equivalent	Unit
Tyre pressure monitoring systems	2020	-1395.49295	kt	-12	-237		-248	-1,066,208	-21,850,449		-22,916,658	0.18	DALY/kt	16.42	€ / t-CO_2
	2030	-2370.42535	kt	-23	-382		-405	-2,530,917	-41,529,313		-44,060,230	0.17	DALY/kt	18.59	€ / t-CO_2
	2050	-2389.061624	kt	-386	-386		-772	-49,512,975	-49,512,975		-99,025,951	0.32	DALY/kt	41.45	€ / t-CO_2
		CO2-equivalent savings	Unit	DALY urban	DALY rural	DALY noise	DALY-Total	Damage urban	Damaga rural	Damage noise	Damage-Total	DALY/CO2-equivalent	Unit	Damage/CO2-equivalent	Unit
Gear shift indicator	2020	-4261.731779	kt	-45	-310		-355	-4,178,183	-28,680,393		-32,858,576	0.08	DALY/kt	7.71	€ / t-CO_2
	2030	-9269.131245	kt	-109	-601		-710	-11,795,191	-65,443,608		-77,238,800	0.08	DALY/kt	8.33	€ / t-CO_2
	2050	-10061.44495	kt	-112	-629		-741	-14,250,901	-80,781,786		-95,032,687	0.07	DALY/kt	9.45	€ / t-CO_2
		CO2-equivalent savings	Unit	DALY urban	DALY rural	DALY noise	DALY-Total	Damage urban	Damaga rural	Damage noise	Damage-Total	DALY/CO2-equivalent	Unit	Damage/CO2-equivalent	Unit
Speed limit on motorways	2020	-6344.061422	kt	0	-2539		-2539	0	-233,295,530		-233,295,530	0.40	DALY/kt	36.77	€ / t-CO_2
	2030	-6775.153601	kt	0	-2190		-2190	0	-234,997,193		-234,997,193	0.32	DALY/kt	34.69	€ / t-CO_2
	2050	-6751.570609	kt	0	-2132		-2132	0	-269,526,723		-269,526,723	0.32	DALY/kt	39.92	€ / t-CO_2

The following is another example for a negative impact of a climate policy on health. Table 8-9 shows the health impacts of an increased insulation of buildings under certain assumptions.

Table 8-9: DALYs, damage costs and CO_2-equ. emissions for insulation and renovation of residential buildings.

Stressor	**DALYs**	**Damage costs (mio. EUR_{2010})**	**Emissions of CO_2-equ (tons)**	**DALYs / kt CO_2-equ.**	**Damage costs EUR / t CO_2-equ.**
PM from ETS	≈ 200,000 to 300,000	≈ 24,000 to 50,000			
Radon	≈ 140,000 to 250,000	≈ 6,310 to 11,270			
Dampness	≈ 35,000 to 60,000	≈ 1,580 to 2,700			
Sum	≈ 560,000	≈ 12,000	-70,000,000	≈ 8	≈ 170

About 8 additional DALYs per kt avoided CO_2-equ. or about 170 additional EUR_{2010} per t avoided CO_2-equ. occur for the measure insulation and renovation as average over the years from indoor sources (though note that health effects from ETS might be overestimated, see Section 5.2.2) if no additional measures to improve the air exchange rate of renovated buildings are implemented.

Exposure to PM from ETS, radon and dampness increases in general when houses are newly built or renovated and, thus, tighter. This is due to a smaller air exchange rate which leads to an accumulation of pollutants. On the other hand, insulation leads to fewer emissions of the heating systems, thus together with a more effective filtering of the incoming air the contribution of the outdoor concentration to the indoor concentration decreases. However, this effect is not enough to fully compensate the increases of indoor concentrations due to indoor sources.

Table 8-10 shows the results of the implementation of the two measures for reducing heat stress in cities.

In the Vegetation scenario**,** urban vegetation is increased by planting trees on open grassy areas and street curbsides. In the Albedo scenario, the albedo of the city is increased by replacing impervious roof and street surfaces (sidewalks and roadways) by light coloured surfaces. The Veg+alb scenario combines both the vegetation and albedo scenario.

As these are adaptation measures, they do not avoid CO2-emissions. Thus the avoided DALYs and health damage costs are given as indicator. As we assume that the temperature is higher in the BAU (A1B) scenario, the avoided health impacts are higher in this scenario than in the 450ppm (B1) scenario.

Table 8-8: DALYs and damage costs due to adaptation measures in urban development.

Climate scenario & year	UHI mitigation scenario	Policy impact	
		DALYs prevented	Cost prevented (M€)
A1B			
2020			
	Vegetation	5350 (494-12254)	399 (37-948)
	Albedo	14266 (1315-32717)	1064 (99-2543)
	Veg+alb	19239 (1768-44083)	1435 (133-3437)
2030			
	Vegetation	9160 (842-20931)	684 (62-1617)
	Albedo	23888 (2199-54238)	1783 (164-4224)
	Veg+alb	33291 (3048-75544)	2484 (227-5883)
2050			
	Vegetation	15851 (1536-36460)	1183 (119-2780)
	Albedo	40258 (3910-92309)	3005 (298-7028)
	Veg+alb	53419 (5185-122606)	3987 (394-9311)
B1			
2020			
	Vegetation	6093 (563-14083)	455 (41-1092)
	Albedo	15805 (1458-36493)	1179 (107-2825)
	Veg+alb	21219 (1958-48842)	1583 (143-3782)
2030			
	Vegetation	8356 (767-18907)	624 (57-1466)
	Albedo	21142 (1926-48154)	1578 (145-3774)
	Veg+alb	28411 (2583-64616)	2120 (196-5064)
2050			
	Vegetation	9744 (858-23146)	727 (63-1738)
	Albedo	25120 (2219-58727)	1874 (165-4473)
	Veg+alb	33984 (3022-79548)	2535 (225-6019)

Reduced cattle scenario

A reduction in cattle protein consumption in favour of pork and poultry has been considered as a reasonable climate change mitigation measure. The change in human diets leads to a reduction in CH_4 and N_2O emissions. In the year 2020, a reduction of about 10,500 kt CO_2eq will be achieved, in 2030 around 13,000 kt CO_2eq and in 2050 about 21,000 kt CO_2eq, compared to the policy scenario.

However, the reduction in greenhouse gases and damages due to climate change is counteracted by an increase in NH_3, PM_{10} and $PM_{2.5}$ emissions and thus in health damages. Compared to the policy scenario, health damage costs increase by 2,000 million EUR in 2020, by 6,000 million EUR in 2030 and by 10,000 million EUR in 2050 (in EUR_{2010} respectively) in the reduced cattle scenario (see Section 3.1.2).

Table 8-9: Damage costs in million EUR2010 in EU29 due to air pollutants

Year	Scenarios	Damage costs due to air pollutants
2020	**Policy**	227,000
	Reduced Cattle	229,000
	Reduced Cattle - Policy	+2,000
2030	**Policy**	254,000
	Reduced Cattle	260,000
	Reduced Cattle - Policy	+6,000
2050	**Policy**	241,000
	Reduced Cattle	251,000
	Reduced Cattle - Policy	+10,000

Relating the health damage costs to the reduction in CO_2eq which have been achieved with this measure, the damage costs are about **190 EUR/t CO_2eq** in the year 2020, about **460 EUR/t CO_2eq** in 2030 and about **480 EUR/t CO_2eq** in the year 2050.

It can be concluded that a change from cattle protein to pork and poultry consumption leads to an increase in damage costs and is not considered a reasonable measure.

9 OVERALL UNCERTAINTIES

In principle, uncertainty analysis is quite a simple process. Characterisation of uncertainty can include either qualitative or quantitative evaluations, or a combination of both. The approach can also be tiered, that is, the analysis can begin with a simple qualitative uncertainty characterisation and subsequently progress to semi-quantitative and finally a complex quantitative assessment. The latter could follow when a lower tier analysis indicates a high degree of uncertainty for certain identified sources, the sources are highly influential to final result(s), and sufficient information and resources are available to conduct quantitative uncertainty assessment. This is not to suggest that quantitative uncertainty analyses should always be performed in all environmental health impact assessments. The decision regarding the type of uncertainty characterisation performed depends on the scope and purpose of the assessment, on whether the selected analysis will provide additional information to the overall health impact assessment, whether sufficient data are available to conduct a complex quantitative analysis, and if time and resources are available for higher tier characterisations. In the context of the joint HEIMTSA-INTARESE case study on climate change adaptation and mitigation policies health impact assessment qualitative assessment of uncertainty should be done in all sectorial applications (across the board implementation), while quantitative assessment would be done in selected sectors, depending on the availability and quality of the necessary data.

Qualitative uncertainty

In the frame of the HEIMTSA/INTARESE CCS uncertainty was assessed qualitatively across all sectoral applications of the full chain environmental health impact assessment methodology. Namely, qualitative uncertainty assessment was done in the HAI calculations related to ambient air pollution, pesticides and other (e.g. PM2.5) stressors from agriculture, emissions from all industrial and otherwise man-made activities, environmental fate and human exposure to POPs. The methodology followed is described in a brief guidance document that outlines the qualitative dimensions of uncertainty in risk and impact assessment as follows:

Qualitative uncertainty assessment is organised in three distinct steps:

i. Identification of all uncertainty sources;

ii. Qualitative characterisation of uncertainty comprising three dimensions:

   - Assessing the direction and magnitude of the influence of the uncertainty source on the result(s)
   - Assessing the knowledge base of the uncertainty source;
   - Assessing the subjectivity of the choice of uncertainty sources

iii. Qualitative uncertainty reporting

The direction and the magnitude of uncertainty are qualified (direction is determined according to whether the particular source of uncertainty would be expected to induce over- or under-estimation of the correct result in that particular step of the calculation chain; magnitude can be high, medium or low, depending on the estimate of how much that particular source of information would affect the final answer of this calculation step).

The robustness of the knowledge base upon which we base the EHIA is assessed by checking how much the information used as input to the HIA models and our current understanding of the interactions between human health and the environment are well established in the respective relevant scientific community.

The subjectivity introduced in the choices made is assessed in terms of which processes are critical to be described mathematically in detail, which shortcuts can be taken in the full chain calculation to simplify the overall estimation without affecting adversely its outcome, which assumptions made in the calculation are a matter of subjective opinion or could they be widely acceptable, etc.

Organisational coherence is a crucial issue. The steps described in this guidance must be performed by the same analysts and facilitator(s) who performed the full chain of environmental health impact assessment under the overview of the full chain coordinator. Coherence prevents inconsistencies in the assessment scores when different modules and several teams of analysts are involved. Inconsistency can arise from different identification of uncertainty sources among the different modules composing the full chain, or even from a different focus in the uncertainty assessment.

In all applications of the qualitative assessment methodology as employed in the HEIMTSA/INTARESE Common Case Study the following main sources of uncertainty were evaluated:

i. Scenario uncertainty: refers to the description of the context (scenario setting) as a prerequisite for either modelling or measuring experimental data. It includes descriptive errors, aggregation errors, errors in selection of the assessment tier and errors due to incomplete analysis. It often includes the purpose of the environmental health impact assessment and consistency between the scenario definition and the scope and purpose of the assessment.

ii. Model uncertainty: reflects the limited ability of mathematical models to represent the real world accurately and may also reflect lack of sufficient knowledge. It is principally associated to model boundaries, extrapolation limits, modelling errors and correlation (dependency) errors. It also includes errors due to the implementation of tools and software.

iii. Parameter uncertainty: refers to data values that are not known with precision due to measurement error or limited observations (sampling error). Sometimes it consists of variability as an inherent property of the heterogeneity or diversity in the parameter, such as parameters expressed as a function of the entire population. Usually, variability cannot be reducible through further

investigation. It is also possible for the uncertainty and variability of parameters to be combined.

The results were summarized in the following table for each of the sectorial applications of the full chain IEHIA methodology as applied in the CCS:

Sources of uncertainty	Dimensions of uncertainty			
	Direction of uncertainty	Level of uncertainty	Appraisal of knowledge base	Justification text
Policy scenario	O/U (if *not known*, then leave blank)	L/M/H	L/M/H	Textual description giving arguments to justify the selection
Conceptual model	O/U	L/M/H	L/M/H	
Mathematical model	O/U	L/M/H	L/M/H	
Parameters	O/U	L/M/H	L/M/H	

O: source of uncertainty leading to over-estimation of the final result; U: source of uncertainty leading to under-estimation of the final result; L: low impact of the particular uncertainty source on the final result; M: moderate impact on the final result; H: high impact on the final result

Applying the above reporting matrix methodology in the following table the overall qualitative assessment of the level of uncertainty in the various steps of the full chain, or rather the complex network of cause-and-effect relationships creating the full chain assessment in the CCS, is summarized:

Table 9-2: Overall qualitative assessment of uncertainty level associated with each part of the integrated health impact assessment chain as applied in the CCS.

	Emissions	*Ambient air*	*Indoor air*	*Pesticide use*	*POPs*	*Personal Exposure*	*Health Impact*	*Tot-al*
Policy scenario	N/A	L	L	M	N/A	L	L	L
Conceptual model	N/A	L	L	L	M	M	L	M
Mathematical model	N/A	L	L	L	L	L	L	L
Parameters	M/H	L	L	M	M	M	M	M

Analogously, the following table sums up the effect of the different uncertainty sources on the over- or under-estimation of the actual result for each step in the integrated environmental health impact assessment methodology as applied in the CCS.

Table 9-3: Overall qualitative assessment of the direction of uncertainty associated with each part of the integrated health impact assessment chain as applied in the CCS.

	Emissions	*Ambient air*	*Indoor air*	*Pesticide use*	*POPs*	*Personal Exposure*	*Health Impact*	*Tot-al*
Policy scenario	N/A	N	O	N/A	N/A	O	N/A	O
Conceptual model	N/A	N	O	O	O	O	U	O
Mathematical model	N/A	O	U	O	O	U	N	N
Parameters	N	O	N	O	O	N	N	O

(O: the uncertainty source in the respective part of the calculation would tend to overestimate the actual result; U: the uncertainty source would tend to underestimate the actual result; N: the effect of the uncertainty source on the actual result is neutral; N/A: non applicable)

The final qualitative estimation of uncertainty concerns the robustness of the knowledge base upon which this study was based. The results are summarized in table 9-4 for each step of the overall methodology.

Table 9-4: Overall qualitative assessment regarding the robustness of the knowledge base associated with each part of the integrated health impact assessment chain as applied in the CCS.

	Emissions	*Ambient air*	*Indoor air*	*Pesticide use*	*POPs*	*Personal Exposure*	*Health Impact*	*Tot-al*
Policy scenario	L	L	N/A	H	N/A	N/A	M	M
Conceptual model	L	L	L	M	M	L	M	M
Mathematical model	L	L	L	L	L	L	H	L
Parameters	M	M	M	M	M	M	M	M

In summary the overall assessment of the health impact and valuation estimates of the CCS tends to be characterized by low to moderate uncertainty levels. The estimates tend to over-estimate the final health impact and are thus conservative. Finally, the overall knowledge base of this study has a moderate uncertainty when all parts of the integrated assessment chain are taken into account.

Quantitative uncertainty assessment in the common case study.

One of the aims of the common case study (CCS) within the INTERASE and HEIMTSA projects is to provide predictions of the effects of human activity on the environment and how these may affect human health. We wish to make informed choices concerning future activities and as such, together with estimating the outcome of different scenarios, an assessment of the uncertainty in such estimates is required.

Within the projects, a number of different approaches and techniques for dealing with uncertainty have been explored. Such approaches can be described as falling in two complementary groups, broadly speaking of quantitative and qualitative in nature.

Here we give details of a number of quantitative methods for assessing uncertainty that have been implemented within the common case study. Methods for quantitative analysis vary in their levels of complexity but all have the aim of incorporating uncertainty at each stage of the ‘full chain’ and allowing it to be propagated throughout the chain. Techniques include sensitivity analyses, Taylor series expansion and Monte

Carlo simulation. What follows are examples of the use of these techniques within components of the common case study.

Sensitivity analysis

This aims to assess how changes in model inputs, either one at a time or in combination, can affect outputs from a model. It allows parameters that have large (or small) effects to be identified. Within the common case study, these techniques were used in modelling the uptake of toxic chemicals into plants. In this part of the CCS, a dynamic model was developed in which the system was described by a set of interconnected compartments that, by utilizing differential equations, is transformed into a mass balance problem. The model is complex in its structure and involves a large number of input variables and model coefficients. The sensitivity analysis was used in order to assess the relative sensitivity of model output to changes in the various inputs in order to decide which would be suitable candidates for the application of Taylor series expansions, a technique which aims to identify a distribution for the uncertainty of the model output.

The identification of variables that may have a substantial effect on model output is an important step in any analysis of uncertainty as it is these variables which are liable to contribute most to the final uncertainty. This is especially important when the models are complex and computationally expensive to run, as is the case with the plant uptake model, as it may be infeasible to fully incorporate full uncertainty modelling for every variable.

Taylor Series expansion

This is a mathematical technique that approximates the underlying distribution which characterizes uncertainty in a process. Once such an approximation is found, it can provide a computationally inexpensive way of characterising the uncertainty in model output and so is useful when dealing with large and complex models for which simulation based methods may prove to be infeasible. In the study of agricultural health impact via ingestion of pesticide residues in food, a set of important input variables were identified using sensitivity analysis by performing model runs with a set of pre-defined values of all the candidate variables and computing a coefficient indicating their relative sensitivity (RS). The final distribution of uncertainty, based on a log-normal distribution, is constructed by combining the uncertainties from each of the variables weighted by their RS. It is important to note that in identifying dominant sources of uncertainty for a model output, it is the combination of the sensitivity and uncertainty of the parameters that is important and they cannot be considered in isolation, unless in the unlikely case that they can all be considered independent. In the example of plant uptake, these methods were incorporated within the main model and implemented using bespoke code written in Matlab.

Monte Carlo sampling

This replaces single values of input variables for a model with repeated samples from probability distributions. This results in uncertainty being propagated through the model resulting in a distribution for the output. This distribution gives a value for the most likely value (the mean or median) together with a measure of its uncertainty, often represented by quantiles of the distribution. This is a very useful technique where models are highly non-linear, with many input variables, although it can be computationally expensive especially in cases where models are large and incorporate large amounts of data.

Monte Carlo sampling (MC) was used extensively through the CCS and here we give details of two specific examples; the first continues the work on uncertainty in the plant uptake study and the second in assessing the effect of changes in land use on the use of pesticides and subsequent possible effects on human health. An important step in performing any MC analysis is the definition of the distributions for the input parameters as the variability will feed through the model, combining with that from the other parameter to produce the final distribution for the output.

In the plant uptake model, the distributions were chosen to be normal (with suitable constraints) in order to preserve the additive structure of the system equations. The distributions were centred around the values that were used for the original runs of the model (without uncertainty) that were chosen based on a review of the relevant literature. The choices of standard deviations for the Normal distributions, which represent the uncertainty in the input parameters were determined by expert opinion based on the relevant literature. MC was then performed by running the model 100,000 times using input values simulated from the distributions for each of the input parameters resulting in a detailed probability distribution for the model output.

A slightly different approach was used in the agricultural study where data was available which could be used to inform the choice of distributions for the input parameters. For example, in assigning distributions to parameters that determine land use as either being arable and fallow, data from CORINE was used to calculate empirical estimates for possible probability distributions. In this case, both log-Normal and Gamma distributions were considered, with both distributions fulfilling the requirement of being skewed and non-negative. As part of this analysis, a comparison was made between the two in terms of which provided the best fit to both the available data and what would be desirable based on expert opinion. At this stage of the model, the Gamma distribution was found to offer a more flexible and stable alternative to the log-Normal. In further stages of the model, truncated Normal distributions was also used when the distributions were considered to be symmetrical but had to be non-negative.

The agricultural study comprised a series of models each (or groups) of which represented a stage in the full chain. One of the initial stages was to disaggregate large-scale land use data to either arable, pasture or fallow land and then to further disaggregate the arable land to cereal, maize, oilseed and other crops. A key aspect of the use of MC in this project was the ability to use the output distributions from one

stage of the model as input distributions for the next. This could be done in one of two ways, either by fitting a particular distribution to the samples of the output and estimating the parameters of that distribution or by using the samples of the output (empirical) distribution directly as inputs for the next stage. This latter approach is particularly computationally demanding, as it requires the individual samples from each stage to be stored simultaneously.

In both examples, of plant uptake and agricultural land use, the MC sampling was performed using bespoke code written in Matlab and the statistical package R.

In the following sections an example of the implementation of the overall uncertainty assessment according to the HEIMTSA/INTARESE methodology is given for the case of the assessment of the health impact attributed to agricultural practices in Europe under the assumption of different climate change mitigation and adaptation policy scenarios. Similar uncertainty assessments were made in other areas of this report; we choose to exemplify the agricultural case study because it was the one study that employed all of the methodological tools available to or developed by the HEIMTSA and INTARESE teams for qualitative and quantitative uncertainty assessment.

9.1 QUALITATIVE UNCERTAINTY FOR THE AGRICULTURAL STUDY

Uncertainty introduced for the agriculture case study, is identified in several locations according to the flow chart seen in Figure 9-1. A qualitative assessment for all the locations (appear in green) are presented in Table 9-1.

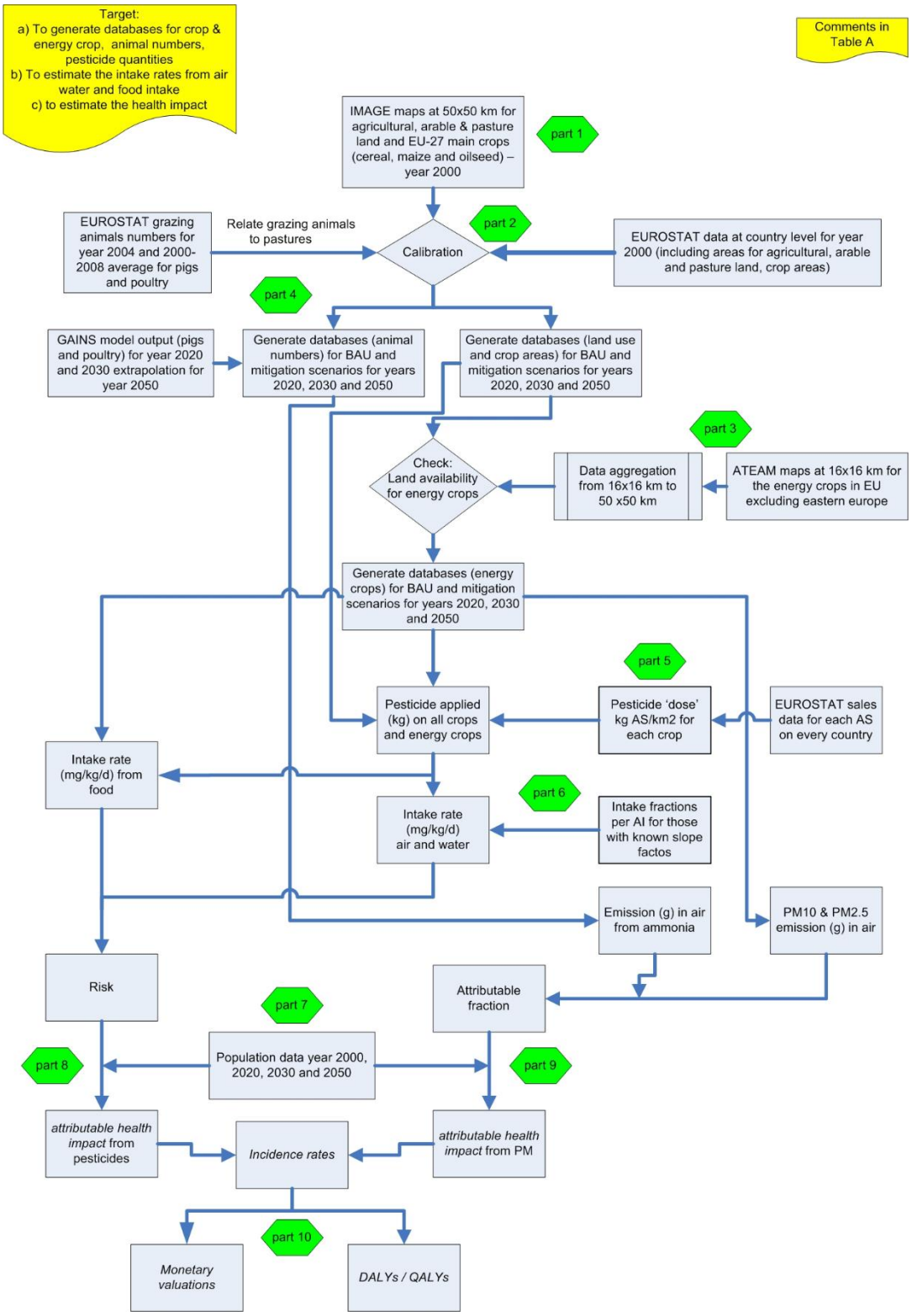

Figure 9-1: Identification of all sources of uncertainty for the agricultural sector

Table 9-1: Agricultural Sector of Common Case Study – activities and modeling step related to uncertainty

				Dimensions of uncertainty		
Section	**Output Data**	**Method used**	**Source of Uncertainty**	**Direction of uncertainty**	**Level of Uncertainty**	**Appraisal of knowledge base**
Part 1 in flowchart	Agricultural, arable and pasture land across Europe (EU-27): *IMAGE model output, at 50x50 km, for years 2020, 2030 and 2050*	Re-allocation of land use data to the EMEP grid: proportional allocation	Uncertainty is introduced from the IMAGE model; no information is available regarding the level of uncertainty	**Underestimation**	***High***	***Low***
Part 2 in flowchart	Main crops : cereals, maize and oil seed *IMAGE model output at 50x50 km*	Re-allocation of land use data to the EMEP grid: proportional allocation	IMAGE maps: no information is available regarding the level of uncertainty	**Underestimation**	***Low***	***Low***
Part 3 in flowchart	Energy crops: mischanthus, sunflower, maize, oil seeds, cardoon, sorghum and poplar: *ATEAM estimates at 16x16 km for Western Europe only*	ATEAM energy crop estimates are aggregated from 16x16 km to 50x50 on the basis of the available agricultural, arable and abandoned land. The % contribution of energy crops to land is based on yield, climatic conditions and regional energy requirements.	A medium level of uncertainty is introduced due to the aggregation algorithm, the spatial allocation of energy crops on land and the selection of energy crops.	**Underestimation**	***Medium***	***Low***
Part 4 in flowchart	Animals : a) grazing animals b) pigs and poultry *a) Changes in pasture area (present and*	a) At country level, changes in pasture area (between present and future) are used to scale animal numbers regardless of	Medium uncertainty is introduced due to: a) projections of pasture area (IMAGE model output assumptions) and the use of a single factor	**Underestimation**	***Medium***	***Low***

				Dimensions of uncertainty		
Section	**Output Data**	**Method used**	**Source of Uncertainty**	**Direction of uncertainty**	**Level of Uncertainty**	**Appraisal of knowledge base**
	future) from IMAGE model *b) GAINS model animal projections at country level until 2030. Liner projection for the year 2050*	the spatial distribution b) Projections of animal numbers from GAINS model, at country level, are used to estimate variation in animal numbers at 50x50 km	(from GAINS model) per country to reflect spatial changes to pasture land b) Animal number projection per country introduce variability, especially when disaggregated to the 50x50km grid.			
Part 5 in flowchart	Quantity of Pesticides used per crop *Estimate quantity from IMAGE crop area (km2) and the pesticide intensity of use (kg/km^2)*	For every active substance the same pesticide 'dose' is utilized regardless the year per country	The utilization of the 'dose' depends on the total sales data as recorded by Eurostat. Sales data introduce low uncertainty and may not reflect actual usage.	**Underestimation**	***Low***	**Medium**
Part 6 in flowchart	Intake rates	Intake fraction are assumed to be constant between people	No adequate data to establish an individual exposure profile	**Underestimation**	***High***	**Medium**
Part 7 in flowchart	Population data: projections 2020, 2030, 2050 including age stratifications and profession	Population data are estimated on the basis of dasymetric modelling of small-area population distribution using land cover and light emissions data	Low uncertainty is introduced via the dasymetric modeling algorithm, the allocation of rural population fraction and the allocation profession to the population data	**Overestimation**	***Low***	**Medium**
Part 8 in flowchart	Risk estimates	Formula used to estimate	Variability to the intake	**Underestimation**	***Medium***	**Low**

				Dimensions of uncertainty		
Section	**Output Data**	**Method used**	**Source of Uncertainty**	**Direction of uncertainty**	**Level of Uncertainty**	**Appraisal of knowledge base**
		risk from intake rate and reference dose	rates, the dose response and the body weight			
Part 9 in flowchart	Attributable health impact from PM/Pesticides	Based on the adjusted relative risk and estimates of concentration (PM/ endotoxins) and the relation of risk to population (pesticides)	Variability in calculation to the concentration estimates, the relative risk and the background rate of disease	**-**	***Low***	**Low**
Part 10 in flowchart	Monetary valuation DALYs / QALYs	DALY & QALY formula	Variability introduced from the severity weight etc	**Overestimation**	***Medium***	***Medium***

9.2 QUANTITATIVE ASSESSMENT OF THE UNCERTAINTY FOR THE AGRICULTURAL CASE STUDY

Quantitative assessment of the uncertainty in the agriculture case study is computed in all the stages of the assessment.

a) area variability for arable and pasture land, edible and energy crops
b) variability in yield for energy crops
c) variability in dosage for the active substances used on edible and energy crops in arable land and for permanent crop.
d) variability in emission rates
e) variability in body weight and population distribution
f) variability in health impact
g) variability in monetary values

A summary of all the distributions used in the agricultural case study for the Monte Carlo simulation are presented in Table 9-2.

Table 9-2: Summary of all distribution used for the Monte Carlo Simulations

N/N	Code	Variable Name	Type of distribution selected	Scenarios 2020 2030 2050	Added noise	Comments
		Land Allocation				
1	1	Arable land	Gamma / Lognormal	Keep parameters for uncertainty propagation	None	-
2	2	Pasture land	Gamma / Lognormal	Same as above	None	-
3	3	Other land use	Nonparametric	Same as above	5% for baseline and scenarios	The added noise is from the IMAGE limitations (no data are available)
4	3_a	Vineyards	Nonparametric	Same as above	-	
5	3_b	Permanent crops	Nonparametric	Same as above	-	It is assumed that the distribution doesn't change over the years
6	3_c	Fallow land	Truncated Gaussian	Same as above	2.5% uniform	a truncated Gaussian is the obvious choice here as it CAP dependent
7	3_d	Other types of land	Nonparametric	Same as above	-	-
8	1_a	Cereal	multinomial distribution	Same as above	2.5% uniform	An extra 2.5% is added to the multinomial distribution in order to compensate any mismatches between IMAGE, CORINE and other variants
9	1_b	Maize	multinomial distribution	Same as above	2.5% uniform	Same as above
10	1_c	Oilseed	multinomial distribution	Same as above	2.5% uniform	Same as above
11	1_d	Other Crops	multinomial distribution	Same as above	2.5% uniform	Same as above

N/N	Code	Variable Name	Type of distribution selected	Scenarios 2020 2030 2050	Added noise	Comments
		Energy Crops				
12	1_3_a	Maize4energy	multinomial distribution	Same as above	2.5% Uniform for BAU and mitigation scenarios	We are not certain about the spatial allocation of the energy crops
13	1_3_b	Sorghum4energy	multinomial distribution	Same as above	Same as above	Same as above
14	1_3_c	Cardoon4energy	multinomial distribution	Same as above	Same as above	Same as above
15	1_3_d	Sunflower4energy	multinomial distribution	Same as above	Same as above	Same as above
16	1_3_e	Poplar4energy	multinomial distribution	Same as above	Same as above	Same as above
17		Mischanthus	The result from a subtraction between distributions..	-	-	Same as above
		Yield from Energy Crops				
18	1_3_a	Maize yield	Normal distribution	Same as above	20% uniform for BAU and Mitigation scenarios	Subjective, into the future, yield may become more uncertain
19	1_3_b	Sorghum yield	Normal distribution	Same as above	Same as above	Same as above
20	1_3_c	Cardoon yield	Normal distribution	Same as above	Same as above	Same as above
21	1_3_d	Sunflower yield	Normal distribution	Same as above	Same as above	Same as above
22	1_3_e	Poplar yield	Normal distribution	Same as above	Same as above	Same as above
		Pesticide Quantities				
23	1a_i	Dosage Cereals	Truncated Gaussian	Same as above	20% variabiltiy for BAU and Mitigation scenarios	Large error introduced via the use of EUROSTAT data for quantity, and IMAGE estimates for crop area. This error in the scenarios should increase
24	1a_ii	Dosage Maize	Truncated Gaussian	Same as above	Same as above	Same as above
25	1a_iii	Dosage Oilseed	Truncated Gaussian	Same as above	Same as above	Same as above

N/N	Code	Variable Name	Type of distribution selected	Scenarios 2020 2030 2050	Added noise	Comments
26	1_3d_iv	Dosage Sunflower	Truncated Gaussian	Same as above	Same as above	Same as above
27	3a_i	Dosage Vineyards	Truncated Gaussian	Same as above	Same as above	Same as above
28	3b_ii	Dosage Fruit trees	Truncated Gaussian	Same as above	Same as above	Same as above
		Pesticide Emission				
29	4	'a' parameter on arable land	Truncated Gaussian	Same as above	2% around mean	-
30	5	'a' parameter on permanent land	Truncated Gaussian	Same as above	2% around mean	-
		Exposure				
31	6	Body Weight	Normal Distribution	N/A	5% around mean	Variation in mean between countries
32	7	Population Rural	Non parametric	Same as above	2.5% baseline and scenarios	Noise is introduced from the assignment of rural population to arable land
		Health Impact				
33	8	Severity Weight on morbidity	Normal Distribution	N/A	none	-
34	9	Severity Weight on mortality	Normal Distribution	N/A	none	-
		Monetary Values				
35	10	Cost of Daly	Normal Distribution	N/A	none	-
36	11	Medical Treatment Cost	Lognormal Distribution	N/A	none	-
37	12	Productivity loss	Lognormal Distribution	N/A	none	-

10 CONCLUSIONS

Results show that the impact of most climate change mitigation policies on environmental human health is about as important as the climate change effects themselves. It is, thus, obvious that any decision support in the field of climate protection should be accompanied by an integrated health impact assessment. The methodology developed in INTARESE and HEIMTSA should be applied, as it is an integrated approach that is capable of taking all relevant aspects of a question into account and uses information and methods according to the current state of knowledge.

Quite some climate protection policies have important positive effects, i.e. they reduce health effects considerably (e.g. the use of wind or solar energy replacing oil and coal). However some policies, especially biomass burning and reducing air exchange rates in houses, cause quite high additional health impacts. Thus, a recommendation here would be to use wood in small furnaces only when equipped with an appropriate filter or to install mechanical venting systems in all new buildings.

The analysis also allows a ranking of stressors in environmental media with regard to overall health impacts in the EU:

The highest overall damage stems from primary and secondary fine particles, followed by noise and radon. Less damage is caused by ozone, then mould followed by dioxins and heat waves. Pesticides and especially PCBs cause relatively low health impacts if only cancer endpoints are considered. This hierarchy does not change if different indicators like DALYs or monetary values are applied. Sensitivity analyses furthermore show that the pattern of importance does not change, either, if different toxicity of PM components is assumed. This information is useful to identify priorities when planning health protection policies.

- The climate and energy package of the EU does not only lead to less green house gas emissions but also affects public health.
- For outdoor air pollutants the posivite effects on health account for about 20 to 40 % of the climate mitigation effects (i.e. avoided damage costs are 20 to 40 % of the costs saved due to reducing green house gases).
- If residential buildings are insulated to save energy demand for heating purposes, and if now further attention is paid to ensure a sufficient air exchange rate for renovated buildings, indoor pollutants like environmental tobacco smoke (ETS), radon and dampness accumulate leading to adverse health effects.

A general conclusion is that taking relevant ‘environmental health effects’ into account will change policy recommendations in many fields substantially.

Some experiences learned while conducting the study are:

a) The use of scoping diagrams for aiding the scoping process is helpful for structuring the thoughts of the analyst; but it is too complex to be used for discussions. For that a disaggregation into impact pathways that are linked with each other is necessary.

b) To motivate stakeholders to be actively involved (which is an important building block of the INTARESE/HEIMTSA methodology) it has to be clearly demonstrated, that the interests of the stakeholder might be considerably affected by the study results.

c) When estimating the effort for executing the study, enough time and effort should be allocated to the screening and scoping process and especially the development of scenarios.

REFERENCES

Abbey DE, Hwang BL, Burchette RJ, Vancuren T, Mills PK. (1995). Estimated long-term ambient concentrations of PM10 and development of respiratory symptoms in a non-smoking population. Arch Env Health; 50: 139-152.

Airbase. (2010). "Airbase, European air quality database". Last accessed: August 2010.

Albatross, 2008: http://www.airport-information.com/data

Alcamo, J. A., D. P. Van Vuuren and W. Cramer (2006). Changes in Provisioning and Regulating Ecosystem Goods and Services and their Drivers Across the Scenarios. Millennium Ecosystem Assessment - Scenarios Assessment. S. Carpenter and P. Pingali. Washington DC, Island Press.

Amann, M., Cofala, J., Gzella, A., Heyes, C., Klimont, Z., Schöpp, W. (2007) Estimating concentrations of fine particulate matter in urban background air of European cities . January 2007. IIASA IR-07-001. http://www.iiasa.ac.at/rains/reports.html

APHEIS (Air Pollution and Health: A European Information System). (2004). Health impact assessment of air pollution and communication: Third Year Report, 2002-2003 (Apheis-3). Available at: http://www.apheis.org/ApheisNewCityReports1.PDF/index.html

Atkinson RW, Anderson HR, Median S, Iñiguez C, Forsberg B, Segerstedt B, Artazcoz L, Paldy A, Zorrilla B, Lefranc A, Michelozzi P. (2005). New E-R function for respiratory hospital admissions. In: Medina S, Boldo E, Saklad M, Niciu EM, Krzyzanowski M, Frank F, Cambra K, Muecke HG, Zorilla B, Atkinson R, Le Tertre A, Forsberg B. and the contribution members of the APHEIS group. APHEIS Health Impact Assessment of Air Pollution and Communications Strategy. Third year report. Institut de Veille Sanitaire, Saint-Maurice. June 2005.

Baccini, M., Biggeri, A., Accetta, G., Kosatsky, T., Katsouyanni, K., Analitis, A., Anderson, H. R., Bisanti, L., D'Ippoliti, D., Danova, J., Forsberg, B., Medina, S., Paldy A., Rabczenko, D., Schindler, C. & Michelozzi, P. (2008) Heat effects on mortality in 15 European cities. Epidemiology, 19, 711-719.

Bacher, J., Pöge, A., and Wenzig, K. (2010). Clusteranalyse: anwendungsorientierte Einführung in Klassifikationsverfahren, Oldenbourg, Munich.

Basu, R. (2009). High ambient temperature and mortality: a review of epidemiological studies from 2001 to 2008. Environmental Health, 8:40.

Bennett, D.H., McKone, T.E., Evans, J.S., Nazaroff, W.W., Margni, M.D., Jolliet, O., Smith, K.R., 2002. Defining Intake Fraction. Environmental Science and Technology 36, 207A-211A.

Bickel P. and R. Friedrich eds. (2005) ExternE Externalities of Energy. Methodology 2005 Update. http://dx.doi.org/10.18419/opus-11923.

Birkved, M., Hauschild, M.Z. (2006) PestLCI - A model for estimating field emissions of pesticides in agricultural LCA, Ecological Modelling 198:433–451.

Blesl et al. 2010: Blesl, M., T. Kober, D. Bruchof, R. Kuder, Effects of climate and energy policy related measures and targets on the future structure of the European energy system in 2020 and beyond. Energy Policy, 38, 6278-6292.

Blesl et al. 2011: Blesl, M., T. Kober, D. Bruchof, R. Kuder, Energy model runs with TIMES PanEU for the Common Case Study, Scenario analysis of the 2°C target with and without external costs, Institute of Energy Economics and the Rational Use of Energy, Department of Energy Economics and Systems Analysis (ESA), University of Stuttgart, February 2011

BLMP Bundesamt für Seeschifffahrt und Hydrographie, 2005. Messprogramm Meeresumwelt, 2005: Zustandsbericht 1999-2002 für Nordsee und Ostsee. Messprogramm Meeresumwelt. Bundesamt für Seeschifffahrt und Hydrographie, Hamburg, p. 301.

Boylan, J., and Russell, A. (2006). "PM and light extinction model performance metrics, goals and, criteria for three-dimensional air quality models." Atmospheric Environment, 40(26), 4946-4959.

Breivik et al. (2007). Breivik K., Sweetman A., Pacyna J.M. and Jones K.C. Towards a global historical emission inventory for selected PCB congeners - a mass balance approach. 3. An update. Science of the Total Environment. vol. 377, No. 2-3, pp. 296-307.

Breivik et al. (2002a). Breivik K, A Sweetman, JM Pacyna and KC Jones Towards a global historical emission inventory for selected PCB congeners – a mass balance approach. 1. Global production and consumption. Science of the Total Environment. vol. 290, pp. 181-198.

Breivik et al. (2002b). Breivik K., Sweetman A., Pacyna J.M., Jones K.C. Towards a global historical emission inventory for selected PCB congeners – a mass balance approach. 2. Emissions. Science of the Total Environment, v.290, pp.199-224.

Briggs (2008). David Briggs: "A framework for integrated environmental health impact assessment of systemic risks." Environmental Health 7(61).

Briggs D. J., Fecht D., Gulliver J., and Vienneau D. 2007 Dasymetric modelling of small-area population distribution using land cover and light emissions data. Remote Sensing of Environment 108:451-466.

Capros, P., Mantzos, L., Papandreou, V. and N. Tasios (2008): Model based analysis of the 2008 EU Policy Package on Climate Change and Renewables. Appendix 1: Baseline scenario. Primes Model – E3MLab/NTUA, Results of end January 2008.

Charles, R., 2004. Modelling Pesticides Residues. Institut des Sciences et Technologies de L'environment. Lausanne, Ecóle Polytechnique Fédérale de Lausanne, Switzerland.

Charron, A., Harrison, R., and Quincey, P. (2006). "What are the sources and conditions responsible for exceedences of the 24 h PM10 limit value (50 µg m-3) at a heavily trafficked London site?" Atmospheric Environment, 41(9), 1960-1975.

CIESIN. 2004. Gridded Population of the World (GWP), Version 3. Center for International Earth Science Information Network (CIESIN), Columbia University, and Centro Internacional de Agricultura Tropical (CIAT). Palisades, NY, Columbia University.

COM (2008). Communication from the Commission to the European Parliament, the Council, the European Economic and Social Committee and the Committee of the Regions. 20 20 by 2020 - Europe's climate change opportunity. COM(2008) 30 final.

COMEAP (Committee on the Medical Effects of Air Pollutants). (1998). The quantification of the effects of air pollution on health in the United Kingdom. London: HMSO.

Contreras, W.A., Ginestar, D., Paraíba, L.C., Bru, R., 2008. Modelling the pesticide concentration in a rice field by a level IV fugacity model coupled with a dispersion-advection equation. Computers & Mathematics with Applications 56(3): 657-669.

De Leeuw, F., van Zantvoort, E., Sluyter, R., and van Pul, W. (2002). "Urban Air Quality Assessment Model: UAQAM." Environmental Modelling and Assessment, 7(4), 43-258.

DG TREN, 2003: European Energy and Transport. Trends to 2030, European Commission, Directorate-General for Energy and Transport, http://ec.europa.eu/dgs/energy_transport/figures/trends_2030/appendix2_en.pdf

Doran, M. (2008), “Contribution of energy crops in displacing fossil fuels in the EU”, Integrating Generations, FIG Working Week 2008, Stockholm, Sweden 14-19 June 2008

Drogue, S., DeMaria, F., 2010. Do different regulations in Maximum Residue Levels of pesticides affect trade competitiveness? The case of apples and pears. ETSG 2010 Lausanne Twelfh Annual Conference, 9-11 September 2010, Faculty of Business and Economics, University of Lausanne, p. 19.

DTU 2010: Part of Deliverable 5.1.1 - A baseline scenario for a business-as-usual development of all relevant activities –and Deliverable Part 5.1.3 – Policy scenario, Waste management activities - Estimation of emissions from landfills, Thomas Højlund Christensen, Christiane Oros, Technical University of Denmark, DTU Environment

EC (2008). Impact Assessment - Document accompanying the Package of Implementation measures for the EU's objectives on climate change and renewable energy for 2020. Commission Staff working document, SEC(2008) 85/3, January 23, 2008, Brussels.

EC European Commission, 1991. Council Directive 91/414/EEC of 15 July 1991 concerning the placing of plant protection products on the market. In: EC (Ed.). Commission of the European Communities, Brussels, p. 290.

EC European Commission, 2005. Regulation (EC) No 396/2005 of the European Parliament and of the Council of 23 February 2005 on maximum residue levels of pesticides in or on food and feed of plant and animal origin and amending Council Directive 91/414/EEC. Commission of the European Communities, Brussels.

EC European Commission, 2009. Regulation (EC) No 1107/2009 of the European Parliament and of the Council of 21 October 2009 concerning the placing of plant protection products on the market and repealing Council Directives 79/117/EEC and 91/414/EEC. In: EC (Ed.). Commission of the European Communities, Brussels, p. 50.

European Commission (EC), Eurostat Labour market statistics. Available at: http://epp.eurostat.ec.europa.eu/; accessed January 2011.

EEA (2006), “How much bioenergy can Europe produce without harming the environment?”, EEA Report No 7/2006, ISSN 1725-9177, TH-AL-06-005-EN-C

EEA (2007), “Estimating the environmentally compatible bioenergy potential from agriculture” EEA Report No 12/2007, ISSN 1725–2237, TH-AK-07-015-EN-N.

EEA. (2006). "Urban Sprawl in Europe." 2006-4, European Environment Agency.

EEA, http://www.eea.europa.eu/de

EEA (2007b): Corine land cover 2000 (CLC2000). 250 m – version 8/2007(http://dataservice.eea.europa.eu/dataservice/..%5Cdataservice%5Cdefault.asp)

EPER, 2008: http://eper.eea.europa.eu/eper/

ESRI, 2008: http://www.esri.com/

ETHZ, 2009a: HEIMTSA-D 5.1.2 - Selected alternative scenarios taking into account different regimes of environmental policies and Global Change, Chapter 3.3, Waste(ETH), Annette Koehler, Dominik Saner, Swiss Federal Institute of Technology, ETH Zurich

ETHZ, 2009b: HEIMTSA-D 5.1.1 – A baseline scenario for a business-as-usual development of all relevant activities, Annette Koehler, Dominik Saner, Swiss Federal Institute of Technology, ETH Zurich

EU 2009: Directive 2009/28/EC of the European Parliament and of the Council of 23 April 2009 on the promotion of the use of energy from renewable sources and amending and subsequently repealing Directives 2001/77/EC and 2003/30/EC. Brussels 2009

EuropaBio (2007)- European Association for Bioindustries- “Biofuels in Europe”, position paper, June 2007

European detailed mortality database (DMDB). Copenhagen, WHO Regional Office for Europe, [2010].

Eurostat (2008), Eurostat pocket-books 2008.

Eurostat, European Commission, “Food: from farm to fork” (Survey on the structure of agricultural holdings, EF_OV_LUFT and EF_OV_KVAAESU), Edition 2008.

Eurostat, European Commission, “The use of plant protection products in the European Union. Data 1992-2003”. Statistical Books. Edition 2007.

Fagerli, H., Simpson, D., and Tsyro, S. (2004). Unified EMEP model: Updates. In: Transboundary Acidification, Eutrophication and Ground Level Ozone in Europe. EMEP/MSC-W Status report 1/2004. Norwegian Meteorological Institute, Oslo, Norway. http://www.emep.int.

Flowerdew R., and Green M. 1994. Areal interpolation and types of data. In S. Fotheringham, and P. Rogerson (Eds.), Spatial analysis and GIS (pp. 121−145). London: Taylor and Francis.

Gallego F.J. 2010. A population density grid of the European Union, Population and Environment. 31: 460-473.

GCD, 2008: Global cement directory 2007-2008, Pro Publications International Limited

Gehrig, R., and Buchmann, B. (2003). "Characterising seasonal variations and spatial distribution of ambient PM10 and PM2.5 concentrations based on long-term Swiss monitoring data." Atmospheric Environment, 37(19), 2571-2580.

GFK, 2008: http://www.gfk-geomarketing.de/

Goodchild MF., and Lam NS-N. 1980. Spatial interpolation methods, a review. American Cartographer, 10, 129−149.

Graff, A. "Comparison of urban and rural PM2.5 measurements in Germany." Conference Cost-effective control of urban air pollution - November 16-17 2006, Laxenburg, Austria.

Gryparis A, Forsberg B, Katsouyanni K, Analitis A, Touloumi G, Schwartz J, Samoli E, Medina S, Anderson HR, Niciu EM, Whichmann HE, Kriz B, Kosnik M, Skorkovsky J, Vonk JM, Dörtbudak Z. (2004). Acute effects of ozone on mortality from the “Air Pollution and Health: A European Approach” project. Am J Respir Crit Care Med; 170: 1080-1087.

Gusev, A., E. Mantseva, O. Rozovskaya, V. Shatalov, B. Strukov, N. Vulykh, W. Aas, K. Breivik [2006] Persistent Organic Pollutants in the Environment. EMEP Status report 3/2006.

Gusev, A., E. Mantseva, V. Shatalov, B. Strukov [2005] Regional Multicompartment Model MSCE-POP. EMEP/MSC-E Technical report 5/2005.

Harris RJ., and Longley PA. 2000. New data and approaches for urban analysis, modelling residential densities. Transactions in GIS, 4(3), 217−234.

Haugen, J. E. and Haakenstad, H. (2006). The development of HERHAM version 2 with 50km and 25km resolution. RegClim General Technical Report, 9, 159-173.

Haugen, J. E. and Iversen, T. (2008). Response in extremes of daily precipitation and wind from a downscaled multi-model ensemble of anthropogenic global climate change scenarios. Tellus A, 60(3), 411-426.

Hong, J., Shaked, S., Rosenbaum, R.K., Jolliet, O., 2010. Analytical uncertainty propagation in life cycle inventory and impact assessment: application to an automobile front panel. The International Journal of Life Cycle Assessment 15, 499-510.

Humbert, S., Margni, M.D., Charles, R., Salazar, O.M.T., Quirós, A.L., Jolliet, O., 2007. Toxicity assessment of the main pesticides used in Costa Rica. Agriculture, Ecosystems and Environment 118, 183-190.

Hurley F, Hunt A, Cowie H, Holland M, Miller B, Pye S, Watkiss P. (2005). Service contract for carrying out cost-benefit analysis of air quality related issues, in particular in the Clean Air for Europe (CAFE) Programme. Methodology for the cost-benefit analysis for CAFE: Volume 2: Health impact assessment. Web published: AEA Technology Environment. Available at: http://europa.eu.int/comm/environment/air/cafe/activities/cba.htm

IEA, 2006: Energy Technology Perspectives 2006. Scenarios & Strategies to 2050, OECD/International Energy Agency, Paris

Ilyina, T.P., 2007. The fate of persistent organic pollutants in the north sea: Multiple year model simulations of a-HCH, y-HCH and PCB 153. Springer Verlag, Heidelberg.

Imbeault-Tétreault, H., Rosenbaum, R.K., Jolliet, O., Deschênes, L., 2010. Analytical Propagation of Uncertainty in LCA Using Matrix Formulation. The International Journal of Life Cycle Assessment.

IPCC, 2007: IPCC Fourth Assessment Report, Working Group III Report "Mitigation of Climate Change 2007", Cambridge, http://www.ipcc.ch/pdf/assessment-report/ar4/wg3/ar4-wg3-chapter7.pdf

J. B. H. Nielsen and P. Oleskowicz (2008), “The future of biogas in Europe: Visions and targets until 2020”, paper presented at AEBIOM Workshop: Biogas – a promising renewable energy source for Europe, European Parliament, Brussels, December 11, 2008

Jacob, D. (2001). "A note to the simulation of the annual and inter-annual variability of the water budget over the Baltic Sea drainage basin." Meteorology and Atmospheric Physics, Springer Wien, 61-73.

Jacob, D., and Podzun, R. (1997). "Sensitivity studies with the Regional Climate Model REMO." Meteorology and Atmospheric Physics, 63, 119-129.

Jacob, D., Van der Hurk, J., Andrae, U., Elgered, G., Fortelius, C., Grahams, L. P., Jackson, S. D., Karstens, U., Köpken, C., Lindau, R., Podzun, R., Rockel, B., Rubel, F., Sass, B. H.,

Jungclaus, J. H., Keenlyside, N., Botzet, M., Haak, H., Luo, J., Latif, M., Marotzke, J., Mikolajewicz, U., and Roeckner, E. (2006). "Ocean circulation and tropical variability in the coupled model ECHAM5/MPI-OM." Journal of Climate, 19, 3952-3972.

Jantunen MJ, Hänninen O, Katsouyanni K, Knöppel H, Künzli N, Lebret E, et al. Air pollution exposure in European cities: the “Expolis”-study. J Exp Anal Environ Epidemiol 1998;8:495–518.

Juraske, R., Castells, F., Vijay, A., Muñoz, P., Antón, A., 2009a. Uptake and persistence of pesticides in plants: Measurements and model estimates for imidacloprid after foliar and soil application. Journal of Hazardous Materials 165, 683-689.

Juraske, R., Mutel, C.L., Stoessel, F., Hellweg, S., 2009b. Life cycle human toxicity assessment of pesticides: Comparing fruit and vegetable diets in Switzerland and the United States. Chemosphere 77, 939-945.

Karabelas, A.J., Plakas, K.V., Solomou, E.S., Drossou, V., Sarigiannis, D.A., ‘Impact of European legislation on marketed pesticides – A view from the standpoint of health impact assessment studies’, Environment International, 35 (2009), pp. 1096–1107.

Klecka, G., Boethling, B., Franklin, J., Grady, L., Graham, D., Howard, P., Kannan, K., Larson, R., Mackay, D., Muir, D., van de Meent, D., 2000. Evaluation of Persistence and Long-Range Transport of Organic Chemicals in the Environment. SETAC Press, Pensacola, Florida, USA.

Knol, A., Petersen, A.C., Sluijs, J.P. van der, Lebret, E.. Dealing with uncertainties in environmental burden of disease assessment. Environmental Health 2009, 8:21 doi:10.1186/1476-069X-8-21. 2009.

Kupiainen, K. and Z. Klimont (2007). Primary Emissions of Fine Carbonaceous Particles in Europe. Atmos. Environ., 41, 2156-2170. doi:10.1016/j.atmosenv.2006.10.066.

Lammel, G., Klöpffer, W., Semeena, V.S., Schmidt, E., Leip, A., 2007. Multicompartmental fate of persistent substances : Comparison of predictions from multi-media box models and a multicompartment chemistry-atmospheric transport model. Environmental Science and Pollution Research 14, 153-165.

Linden van der, A.M.A, Luttik, R., Groenwold, J.G., Kruijne, R. and Merkelbach, RC.M. 2008 Dutch environmental indicator for plant protection products, Version 2. Input, calculation and aggregation procedures, RIVM report 607600002/2008.

Margni, M.D., Rossier, D., Crettaz, P., Jolliet, O., 2002. Life cycle impact assessment of pesticides on human health and ecosystems. Agriculture, Ecosystems and Environment 93, 379-392.

Meijer, S.N., Ockenden, W.A., Sweetman, A., Breivik, K., Grimalt, J.O., Jones, K.C., 2003. Global Distribution and Budget of PCBs and HCB in Background Surface Soils: Implications for Sources and Environmental Processes. Environmental Science and Technology 37, 667-672.

Mennis J. 2003. Generating surface models of population using dasymetric mapping. Professional Geographer, 55, 31−42.

Michelozzi, P., Kirchmayer, U., Katsouyanni, K., Biggeri, A., McGregor, G. R., Menne, B., Kassomenos, P., Anderson, H. R., Baccini, M., Accetta, G., Analitis, A. & Kosatsky, T. (2007) Assessment and prevention of acute health effects of weather conditions in Europe: The PHEWE project - background, objectives, design. Environmental Health, 6.

Milego, R. (2007). "Urban morphological zones 2000 version F1v0 - Definition and procedural steps." European Environment Agency, Barcelona.

Miller BG, Hurley JF. (2003). Life table methods for quantitative impact assessments in chronic mortality. Journal of Epidemiology and Community Health; 57: 200-206.

Motelay-Massei, A., Ollivon, D., Garban, B., Teil, M.J., Blanchard, M., Chevreuil, M., 2004. Distribution and spatial trends of PAHs and PCBs in soils in the Seine River basin, France. Chemosphere 55, 555-565.

Nakicenovic, N., Alcamo, J., Davis, G., De Vries, B., Fenhann, J., Gaffin, S., Gregory, K., Grübler, A., and Jung, T. (2000). " Summary for Policymakers - Emissions Scenarios. A Special Report of Working Group III of the Intergovernmental Panel on Climate Change." IPCC, Geneve, Switzerland.

Nyíri, A., Gauss, M., Tsyro, S., Wind, P., and Hougen, J. E. (2010). Future air quality, including climate change. In: Transboundary acidification, eutrophication and ground level ozone in Europe in 2008, EMEP Status Report 1/2010, Norwegian Meteorological Institute, Oslo, Norway, 2010, http://www.emep.int.

NYSERDA 2006. Mitigating New York City's Heat Island with Urban Forestry, Living Roofs, and Light Surfaces. New York City Regional Heat Island Initiative, Final Report. New York State Energy Research and Development Authority.

ORNL/REF (1994) Estimating Externalities of the Coal Fuel Cycle. Report 3 on the external costs and benefits of fuel cycles. A study by the US Department of Energy and the Commission of the European Communities. Prepared by Oak Ridge National Laboratory and Resources for the Future. McGraw Hill.

Ostro BD. (1987). Air pollution and morbidity revisited: A specification test. J Environ Econ Manage; 14: 87-98.

Özkaynak, H, Xue, J, Weker, R, Butler, D, Koutrakis, P, Spengler, J, The particle TEAM (PTEAM) study: analysis of the data. Technical report. U.S. Environmental Protection Agency: Research Triangle Park, NC, 1996;Vol. III

Panasiuk D. et al. , 2006: Scenarios for heavy metals, dioxins/furans and PCBs emissions to air in Europe for years 2010 and 2020, DROPS D1.2 Report, Katowice

Pebesma, E. J., de Jong, K. & Briggs, D. J. (2007). Interactive visualisation of uncertain spatial and spatio-temporal data under different scenarios: an air quality example. International Journal of Geographical Information Science, 21(5), 515–527.

Pistocchi, A., Vizcaino, P., Hauck, M., A GIS model-based screening of potential contamination of soil and water by pyrethroids in Europe, Journal of Environmental Management 90 (2009) 3410–3421.

Platts, 2008: http://www.platts.com/

PUBLIC NOTICE: INITIATION OF RISK ASSESSMENTS FOR CHEMICALS IN DRINKING WATER, 2001, Office of Environmental Health Hazard Assessment, Pesticide and Environmental Toxicology Section.

Renken, A. (2009). "Analyse der REMO-Simulationsdaten zum Klimawandel in Schleswig-Holstein und Anwendung der Klimaszenarien auf das Kielstaueinzugsgebiet mit dem öko-hydrologischen Model SWAT - In German," Diplom, Kiel University, Kiel, Germany.

Rosegrant et al., 2002 M.W. Rosegrant, X. Cai and S.A. Cline, World Water and Food to 2025: Dealing With Scarcity, International Food Policy Research Institute, Washington, DC (2002).

Rowland, J. 2006 Chemicals Evaluated for Carcinogenic Potential, Office of Pesticide Programs, US EPA.

Russ, P., Wiesenthal, T., van Regenmorter, D. and J.C. Ciscar (2007): Global Climate Policy Scenario for 2030 and beyond. JRC Reference Reports, Institute for Prospective Technological Studies (IPTS), Seville, Spain.

Scheringer, M., Jones, K.C., Matthies, M., Simonich, S., van de Meent, D., 2009. Multimedia Partitioning, Overall Persistence, and Long-Range Transport Potential in the Context of POPs and PBT Chemical Assessments, Special Series: Science-Based Guidance and Framework for the Evaluation and Identification of PBTs and POPs. Integrated Environmental Assessment and Management 5, 557-576.

Scheringer, M., Wania, F., 2003. Multimedia Models of Global Transport and Fate of Persistent Organic Pollutants. The Handbook of Environmental Chemistry 30, 237-269.

Schindler C, Keidel D, Gerbase MW, Zemp E, Bettschart R, Brändli O, Brutsche MH, Burdet L, Karrer W, Knöpfli B, Pons M, Rapp R, Bayer-Oglesby L, Künzli N, Schwartz J, Liu L-JS, Ackermann-Liebrich U, Rochat T and the SAPALIDA Team. (2009). Improvements in PM10 exposure and reduced rates of respiratory symptoms in a cohort of Swiss adults (SAPALDIA). Am J Respir Crit Care Med; 179: 589-587.

Schuhmacher, M., Jones, K.C., Domingo, J.L., 2006. Air-vegetation transfer of PCDD/PCDFs: An assessment of field data and implications for modeling. Environmental Pollution 142, 143-150.

Seike, N., Kashiwagi, N., Otani, T., 2007. PCDD/F Contamination over Time in Japanese Paddy Soils. Environmental Science and Technology 41, 2210-2215.

Sharma, M., McBean, E., Gowing, A., 2007. Bioconcentration of Dioxins and Furans in Vegetation. Water, Air and Soil Pollution 179, 117-124.

Simpson, D., Fagerli, H., Jonson, J. E., Tsyro, S., Wind, P., and Tuovinen, J.-P. (2003). Transboundary Acidification, Eutrophication and Ground Level Ozone in Europe. Part I. Unified EMEP Model Description. EMEP/MSC-W Status report 1/2003 Part I. Norwegian Meteorological Institute, Oslo, Norway. http://emep.int/UniDoc/report.html

Simpson, D., Guenther, A., Hewitt, C.N., and Steinbrecher, R. (1995). Biogenic emissions in Europe: 1. Estimates and uncertainties, J. Geophys. Res., 100, 22875-22890.

Simpson, D., Yttri K.E., Klimont, Z., Kupiainen, K., Kaseiro, A., Gelencser, F., Pio, C., Puxbaum, H., and M. Legrand (2007). Modelling carbonaceous aerosol over Europe. Analysis of the CARBOSOL and EMEP EC/OC campaigns, J. Geophys. Res., 112, D23S14, doi:10.1029/2006JD008158.

Smith, R. N. B., and Yang, X. (2001). "A comprehensive model inter-comparison study investigating the water budget during the BALTEX-PIDCAP period." Meteorology and Atmospheric Physics, 77, 19-43.

Stedman, J., and Derwent, R. (2007). "On the relationship between PM2.5 concentrations and regional-scale primary PM emissions for the United Kingdom: an issue of subsidiarity." Environmental Science and Policy, 11(3), 217-226.

Stieb DM, Smith-Doiron M, Brook JR, Burnett RT, Dann T, Mamedov A, Chen Y. (2002). Air pollution and disability days in Toronto: Results from the National Population Health Survey.

Strzelecka-Jastrzab E. et al., 2007: Emission projections for the years 2010 and 2020 and assessment of the emission reduction scenario implementation costs, DROPS D1.3 Report, Katowice

Swiss Cohort Study on Air Pollution and Lung Disease in Adults (SAPALDIA). (2008). Available at: www.sapaldia.net/en/; Accessed January 2011.

Torras Ortiz, S. (2010). "A hybrid dispersion modelling approach for quantifying and assessing air quality in Germany with focus on urban background and kerbside concentrations," submitted Doctoral Thesis, University of Stuttgart, Stuttgart.

Tsyro, S. (2008). Regional Model for Formation, Dynamics, and Long-range Transport of Atmospheric Aerosol. Russian Meteorology and Hydrology, ISSN 1068-3739, Vol. 33, 2, 82-90.

Tsyro, S., Berge, H., Benedictow, A., and M. Gauss.: Studying the effect of meteorological input on Unified EMEP model results. In: Transboundary acidification, eutrophication and ground level ozone in Europe in 2008, EMEP Status Report 1/2010, Norwegian Meteorological Institute, Oslo, Norway, 2010, http://www.emep.int.

Tsyro, S., Simpson, D., Tarrason, L., Klimont, Z., Kupiainen, K., Pio, C., and K.E. Yttri (2007). Modelling of elemental carbon over Europe, J. Geophys. Res., 112, D23S19, doi:10.1029/2006JD008164.

van der Werf, G. R., Randerson, J. T., Giglio, L., Collatz, G. J., Mu, M., Kasibhatla, P. S., Morton, D. C., DeFries, R. S., Jin, Y., and van Leeuwen, T. T.: Global fire emissions and the contribution of deforestation, savanna, forest, agricultural, and peat fires (1997–2009), Atmos. Chem. Phys., 10, 11707-11735, doi:10.5194/acp-10-11707-2010, 2010.

Van Dingenen, R., Raes, F., Putaud, J.-P., Baltensperger, U., Charron, A., Facchini, M.-C., Decesari, S., Fuzzi, S., Gehrig, R., Hansson, H.-C., Harrison, R. M., Hüglin, C., Jones, A. M., Laj, P., Lorbeer, G., Maenhaut, W., Palmgren, F., Querol, X., Rodriguez, S., Schneider, J., Brink, H. t., Tunved, P., Tørseth, K., Wehner, B., Weingartner, E., Wiedensohler, A., and Wåhlin, P. (2004). "A European aerosol phenomenology--1: physical characteristics of particulate matter at kerbside, urban, rural and background sites in Europe." Atmospheric Environment, 38(16), 2561-2577.

Vulykh, N., O. Rozovskaya, V. Shatalov (2009) Model assessment of potential for long-range transboundary atmospheric transport and persistence of Trifluralin. EMEP/MSC-E Information Note 5/2009.

Vulykh et al. (2001). N. Vulykh, V. Shatalov, investigation of dioxin/furan composition in emissions and in environmental media. Selection of congeners for modelling, EMEP MSC-East,. Technical Note 6/2001 June 2001

Wannaz, C. 2010. PANGEA development handbook. University of Michigan, Ann Arbor, Michigan, United States. (unpublished).

Watkiss P, Pye S, Holland M. (2005). CAFE CBA: Baseline Analysis 2000 to 2020. European Commission DG Environment. Prepared by: AEA Technology plc, Oxon, United Kingdom.

Weitzman, M.L. (2001): Gamma Discounting. The American Economic Review, March 2001; 91, 1; 260-271

WHO: “IPCS Risk Assessment Terminology. Part 1: IPCS/OECD KEY GENERIC TERMS USED IN CHEMICAL HAZARD/RISK ASSESSMENT Part 2: IPCS GLOSSARY OF KEY EXPOSURE ASSESSMENT TERMINOLOGY” IPCS Inter-Organization Programme for the Sound Management of Chemicals, Geneva. 2004.

WHO (2004); prepared by Anderson HR, Atkinson RW, Peacock JL, Marston L, Konstantinou K. Meta-analysis of time-series studies and panel studies of particulate matter (PM) and ozone (O3). Report of a WHO task group. World Health Organization. (http://www.euro.who.int/document/e82792.pdf).

World Health Organization (2010) Effects of Air Pollution on Health. Report from the WHO/Convention Task Force on the Health Aspects of Air Pollution workshop. Geneva, Switzerland 22-24 September 2010. Available at: http://www.unece.org/env/documents/2010/eb/wge/ece.eb.air.wg.1.2010.11.pdf

UNSCEAR 2000 Report Vol. 1 Sources and effects of ionizing radiation. United Nations Scientific Committee on the Effects of Atomic Radiation , 2000.

UNECE, 2008: The 2000 Census of Motor Traffic on Main International Traffic Arteries, http://www.unece.org/trans/main/wp6/transstatcensus.html

Yin, J., Allen, A., Harrison, R., Jennings, S., Wright, E., Fitzpatrick, M., Healy, T., Barry, E., Ceburnis, D., and McCusker, D. (2005). "Major component composition of urban PM10 and PM2.5 in Ireland." Atmospheric Research, 78(3-4), 149-165.

A ANNEXES

A.1 Heat and Urban Heat Island (UHI) Mitigation

Heat exposure assessment – results

Table A 1 provides indicators on how the heat exposure in large European cities will change in the future in the reference scenarios and in case different UHI mitigation policies would be implemented. Heat sum is an indicator derived by adding up the temperature threshold exceedance from all days between April and September. The range in the estimates is based on the 95% confidence limits for the sub-region specific temperature thresholds.

Table A 1: Average daily maximum apparent temperature, no. of days when temperature threshold is exceeded, the average exceedance on these days, and the heat sum (95% confidence limits) in April-September averaged over all large cities. The temperature thresholds: North-continental region 23.3°C (22.5-24.0), Mediterranean region 29.4°C (95% CI 25.7-32.4).

		North-continental cities				Mediterranean cities			
Climate scenario & year	Reference / UHI mitigation scenario	Averge daily max AT (°C)	No. days above threshold	Average threshold exceedance	Heat sum (°C)	Averge daily max AT (°C)	No. days above threshold	Average threshold exceedance	Heat sum (°C)
2010	Current	16.9	27 (23-32)	4.0 (4.0-4.2)	107 (90-130)	24.2	51 (29-79)	4.5 (3.5-5.8)	222 (103-458)
A1B									
2020	Reference 1	17.7	31 (27-34)	4.8 (4.7-5.1)	147 (127-172)	24.4	50 (31-80)	4.6 (3.6-5.8)	227 (109-465)
	Vegetation	17.5	30 (27-33)	4.8 (4.6-5.0)	141 (121-166)	24.2	49 (30-78)	4.6 (3.5-5.7)	218 (104-449)
	Albedo	17.1	28 (25-32)	4.7 (4.5-4.9)	131 (113-155)	23.9	46 (28-76)	4.5 (3.4-5.6)	202 (94-424)
	Veg+alb	16.9	27 (24-31)	4.6 (4.4-4.9)	126 (108-149)	23.7	45 (27-74)	4.4 (3.3-5.6)	194 (89-409)
2030	Reference 1	19.2	43 (38-49)	4.6 (4.4-4.7)	194 (166-230)	25.7	72 (43-101)	4.5 (3.4-6.3)	312 (145-631)
	Vegetation	19.0	42 (36-48)	4.5 (4.4-4.7)	186 (159-221)	25.5	70 (41-99)	4.4 (3.3-6.2)	299 (136-612)
	Albedo	18.7	39 (34-45)	4.5 (4.4-4.6)	173 (147-206)	25.1	66 (38-97)	4.3 (3.2-6.0)	277 (123-579)
	Veg+alb	18.5	38 (33-44)	4.4 (4.3-4.6)	165 (141-197)	25.0	64 (37-96)	4.2 (3.1-5.9)	264 (116-560)
2050	Reference 1	20.5	63 (57-70)	5.2 (5.0-5.4)	323 (281-375)	26.5	75 (48-103)	5.1 (3.9-6.8)	373 (191-702)
	Vegetation	20.3	61 (55-68)	5.1 (4.9-5.4)	311 (270-362)	26.3	74 (47-101)	5.0 (3.9-6.8)	359 (181-682)
	Albedo	19.9	59 (52-65)	5.0 (4.9-5.3)	291 (252-340)	26.0	71 (44-99)	4.8 (3.8-6.6)	336 (166-648)
	Veg+alb	19.8	57 (51-63)	5.0 (4.8-5.2)	280 (242-327)	25.8	69 (42-98)	4.8 (3.7-6.5)	322 (158-629)
B1									
2020	Reference 2	17.9	32 (28-37)	4.6 (4.5-4.7)	146 (126-174)	25.1	58 (33-88)	4.2 (3.2-5.7)	238 (106-505)
	Vegetation	17.7	31 (27-35)	4.6 (4.5-4.7)	140 (121-167)	24.9	56 (31-86)	4.2 (3.1-5.7)	228 (100-488)
	Albedo	17.3	29 (25-33)	4.6 (4.4-4.7)	131 (112-155)	24.5	53 (29-83)	4.1 (3.1-5.5)	210 (89-459)
	Veg+alb	17.1	28 (25-32)	4.5 (4.3-4.6)	125 (107-149)	24.3	51 (27-81)	4.0 (3.0-5.5)	200 (84-443)
2030	Reference 2	17.5	35 (32-40)	5.2 (5.1-5.4)	182 (159-212)	25.3	65 (39-94)	4.6 (3.5-6.2)	288 (136-580)
	Vegetation	17.3	34 (30-38)	5.2 (5.0-5.3)	175 (153-204)	25.1	63 (38-92)	4.5 (3.4-6.1)	276 (129-562)
	Albedo	17.0	33 (29-37)	5.1 (5.0-5.3)	164 (143-192)	24.8	60 (36-90)	4.4 (3.3-5.9)	256 (117-531)
	Veg+alb	16.8	32 (28-36)	5.1 (4.9-5.2)	158 (137-185)	24.6	58 (34-88)	4.3 (3.2-5.8)	245 (110-514)
2050	Reference 2	18.1	27 (23-32)	4.5 (4.5-4.5)	120 (102-143)	25.8	66 (44-92)	5.2 (4.1-6.8)	340 (177-630)
	Vegetation	17.9	26 (22-31)	4.5 (4.4-4.5)	115 (98-137)	25.6	65 (42-91)	5.2 (4.0-6.7)	327 (169-612)
	Albedo	17.5	24 (21-29)	4.5 (4.4-4.5)	106 (91-127)	25.3	62 (40-88)	5.0 (3.8-6.6)	306 (155-582)
	Veg+alb	17.3	23 (20-27)	4.4 (4.4-4.5)	102 (87-122)	25.1	60 (39-87)	5.0 (3.8-6.5)	295 (147-565)

In the reference scenario 1, heat exposure increases in both sub-regions over the years. By 2050, the average exposure in the North-continental cities is estimated to be 200% and in Mediterranean cities 68% higher than in the current climate conditions. In the reference scenario 2, the exposure in the North-continental cities first increases, but then begins to diminish by 2050. In the Mediterranean region, the exposure levels in A1B and B1 climate scenarios are more similar but somewhat lower in the later years in the B1. Increasing both urban vegetation and surface albedo would result in

approximately 14% reduction in the average exposure, while increasing albedo alone would decrease exposure by 11% and increasing vegetation by 4%. The effects of UHI mitigation policies are similar across both IPCC climate scenarios and sub-regions.

When averaged over different sub-regions, the overall trends of heat exposure in the reference scenarios appear reasonable. However, on a country level the trends become more obscure, and there are substantial differences between countries in the way the exposure changes over time and in different climate scenarios (

Table A 2). While the impacts of climate change on local and regional weather conditions are likely to vary, it is questionable whether the level of spatial differences that the temperature data indicates is plausible. Another observation is that, at least for some countries, the data seems to give unrealistically low daily maximum temperatures (Table A 3, data for the year 2005 was used to represent weather conditions in 2010). To find out if this is a systematic feature in the data concerning all regions of Europe or more of a localised peculiarity would require extensive country and city level comparisons of the modelled data and weather observations, which are not feasible in the time and resource frame of the assessment. One factor that also contributes to unrealistically low heat exposure estimates is that the data may underestimate temperatures in coastline cities. This is especially the case for those cities (or parts of larger cities), which are located in grid cells where greater part of the cell area consists of sea. Taking all these issues under consideration, there are concerns about how well the temperature data used in the assessment is actually suited for realistic evaluation of daily maximum apparent temperatures, especially on a city level.

What also needs to be considered is whether the reductions in the heat exposure measure caused by the different UHI mitigation policies realistically reflect the impact these policies would have on the actual heat exposure of the inhabitants. Urban areas contain numerous microclimates, and the heat exposure experienced by the people depends on the microclimatic conditions in which they spend their time. It is unclear how changes in the urban surface energy budget and average urban heat island intensity relate to changes in temperatures in the microclimates where people spend the majority of their time. It is also assumed in the assessment that the absolute air humidity stays the same regardless of the implementation of UHI mitigation measures. This may not be realistic. For example, increasing urban vegetation would likely increase air humidity through higher evapotranspiration. This would subsequently be reflected in the level of discomfort related to a given level of air temperature. However, it is unclear if this could lead to significant bias in the results.

It should also be remembered, that weather conditions and heat exposure vary widely on annual basis. However, no information was available on uncertainty or variability in the temperature estimates. Therefore, it is unknown if the data represents high or low range estimates of annual heat exposure.

Table A 2: Average heat sum (°C) in large cities (April-September) in different European sub-regions (NC = North-continental, Med = Mediterranean) and countries.

Region/ Country		A1B			B1		
	2005	2020	2030	2050	2020	2030	2050
NC	107.3	146.6	193.9	322.6	146.5	182.0	119.7
Med	221.6	227.3	312.2	373.5	238.4	288.4	339.5
AT	279.3	327.6	542.2	465.4	409.2	364.4	258.3
BE	73.9	151.8	173.9	363.1	84.1	176.5	95.2
CZ	160.4	200.2	308.6	308.8	284.3	241.5	117.6
DK	0.0	0.0	0.0	14.1	0.0	0.0	0.3
EE	NAN	NAN	NAN	NAN	NAN	NAN	NAN
FI	6.1	0.3	0.0	7.9	16.6	4.6	0.7
FR	242.9	301.7	458.9	611.9	281.8	417.9	349.0
DE	114.0	160.1	207.5	342.8	178.0	213.9	119.7
GR	475.1	417.4	614.9	506.0	449.4	482.6	610.3
HU	412.0	482.1	842.1	549.2	577.3	564.8	372.1
IE	4.1	30.4	11.0	201.9	0.0	2.1	17.8
IT	160.4	154.5	258.0	295.3	164.3	245.8	242.5
LT	153.9	60.2	115.8	114.7	242.1	136.1	38.2
LU	NAN	NAN	NAN	NAN	NAN	NAN	NAN
MT	NAN	NAN	NAN	NAN	NAN	NAN	NAN
NL	29.6	62.8	69.4	197.5	42.3	77.4	44.7
PL	181.5	172.8	238.0	242.4	273.7	211.6	99.9
PT	3.7	0.1	44.9	63.7	2.7	1.8	7.4
SK	363.5	417.4	694.1	566.2	520.2	459.4	300.1
SI	NAN	NAN	NAN	NAN	NAN	NAN	NAN
ES	341.7	378.2	422.8	558.4	390.7	396.5	544.6
SE	3.9	0.7	0.4	52.6	7.5	10.1	11.9
UK	20.2	58.3	39.9	234.6	7.4	38.8	40.5

Table A 3: Average daily max apparent temperature (°C) in large cities (grid cells defined to be large cities in 2010) in different IPCC climate scenarios in June-August.

Country		A1B			B1		
	2005	2020	2030	2050	2020	2030	2050
AT	24.2	23.4	26.1	25.5	24.7	24.6	22.8
BE	20.0	21.0	22.5	25.7	20.6	22.3	20.2
CZ	21.4	21.4	23.1	23.5	22.7	22.7	20.0
DK	15.7	15.1	17.0	18.4	17.1	15.5	17.6
EE	NAN	NAN	NAN	NAN	NAN	NAN	NAN
FI	14.2	13.3	15.4	15.3	16.7	14.9	15.5
FR	22.5	23.4	25.4	27.8	23.3	25.4	23.6
DE	20.5	20.6	22.2	25.0	21.6	22.5	20.3
GR	33.2	32.4	34.5	33.1	32.7	33.7	34.5
HU	26.8	26.2	29.6	27.2	27.6	27.5	25.4
IE	16.1	17.2	17.5	23.3	16.1	16.4	17.0
IT	27.3	27.5	29.3	30.0	27.6	29.6	28.2
LT	21.1	18.6	20.6	20.4	23.0	21.3	19.4
LU	NAN	NAN	NAN	NAN	NAN	NAN	NAN
MT	NAN	NAN	NAN	NAN	NAN	NAN	NAN
NL	18.6	19.1	20.6	23.3	19.5	19.8	19.3
PL	22.6	21.0	22.6	22.4	23.0	22.4	20.8
PT	23.0	22.2	25.7	26.7	23.7	23.7	23.4
SK	26.0	25.3	27.9	27.1	26.8	26.0	24.2
SI	NAN	NAN	NAN	NAN	NAN	NAN	NAN
ES	29.5	30.1	30.8	32.4	30.8	31.1	31.5
SE	16.6	15.7	17.4	19.3	17.6	17.3	17.7
UK	17.5	18.5	19.1	23.8	17.3	18.2	18.1

Based on the assessment, nearly half of the population in the countries included in the assessment live in densely populated metropolitan areas (Table A 4). However, there are substantial differences among countries, as the fraction of the population living in large cities ranges from 0 to 77%. It is evident, that there are problems in the methodology for identifying large cities. Densely populated but somewhat smaller cities in terms of population number can be excluded from the assessment if the total population density in the grid cell does not surpass 200/km^2. This could also happen in cases where the city is located in between two or more grid cells in a way that the population of any one of the grid cells does not surpass the critical density. This could also lead to underestimation of the population in identified cities if the city is dispersed over several cells, but the cells on the outer edges do not surpass the critical density. Nevertheless, it is reasonable to assume that the methodology has the power to identify majority of the densely populated metropolitan areas similar to those cities for which the PHEWE exposure-response functions were derived for.

Another factor that causes uncertainty in the estimates for exposed population is that the data for the fraction of urban population in each grid cell represents year 2001. These fractions have probably changed to some extent during the past ten years and are likely to keep changing in the time frame of the assessment.

Table A 4: Fraction of total population living in large cities in different European sub-regions and countries.

	Year			
	2010	2020	2030	2050
North-continental	0.45	0.46	0.46	0.46
Mediterranean	0.40	0.41	0.41	0.39
AT	0.26	0.26	0.31	0.26
BE	0.77	0.77	0.77	0.77
CZ	0.18	0.18	0.18	0.18
DK	0.19	0.19	0.19	0.19
EE	0.00	0.00	0.00	0.00
FI	0.20	0.20	0.20	0.20
FR	0.34	0.36	0.38	0.38
DE	0.53	0.53	0.52	0.49
GR	0.35	0.35	0.35	0.34
HU	0.22	0.22	0.22	0.23
IE	0.29	0.29	0.29	0.29
IT	0.42	0.42	0.42	0.38
LT	0.16	0.15	0.00	0.00
LU	0.00	0.00	0.00	0.69
MT	0.00	0.00	0.00	0.00
NL	0.66	0.66	0.68	0.68
PL	0.28	0.28	0.28	0.23
PT	0.42	0.41	0.41	0.40
SK	0.08	0.08	0.08	0.00
SI	0.00	0.00	0.00	0.00
ES	0.41	0.43	0.43	0.43
SE	0.16	0.16	0.21	0.25
UK	0.71	0.73	0.74	0.75

Methodology for modelling health impacts of heat exposure

For each city (i.e. grid cell representing a large city), the number of days when the region-specific AT threshold was exceeded was determined for different scenarios. These days were then classified into different exposure classes based on the level of threshold exceedance on 1°C accuracy.

Mortality caused by heat exposure in 2010

Adjusted relative risk (RR') and population attributable fraction (PAF) for each exposure class (ec) and age-category were calculated as follows:

$$\mathbf{RR'_{ec} = \exp(\beta * E_{ec})}$$

where

β = Percent change in mortality associated with a 1°C increase in maximum apparent temperature above the region specific threshold in different age categories

E_{ec} = AT threshold exceedance in a given exposure class (0, 1, 2, … , 20 ºC)

$$\mathbf{PAF_{ec} = (RR'_{ec} - 1)/ RR'_{ec}}$$

Annual number of deaths attributable to heat exposure was calculated as follows:

$$\mathbf{Attributable\ deaths = PAF_{ec} * MR * Pop * N_{ec}}$$

where

MR = Daily risk of mortality from natural causes in different countries and age-categories

Pop = Number of population in a city in a given age-category in 2010

N_{ec} = Number of days in a given exposure class in 2010

Country-specific current daily mortality risk levels (all non-accidental causes) were derived from the most recent annual mortality data available for each country in the WHO mortality database and the corresponding population data. Used datasets were for most countries from the years 2005-2006. However, somewhat older datasets were used for Belgium (1997), Denmark (2001), Italy and Portugal (2003). The daily mortality risk was assumed stay on the same level throughout the year. This may lead to slight overestimation of the impacts, as population mortality is known to vary between seasons and to be usually higher in winter than summer.

Attributable deaths were summed over different cities to derive the number of deaths on a country or region level.

Mortality caused by heat exposure in reference and policy scenarios in 2020-2050

For each country, the daily risk of natural mortality in the absence of heat exposure (MR_{bg}) was calculated as follows:

$$\mathbf{MR_{bg} = MR - (M_{heat}/Pop/183)}$$

where

MR = Daily risk of mortality from natural causes in different countries and age-categories

M_{heat} = Total number of deaths attributable to heat exposure in a given age-category in 2010

Pop = Number of population in a city in a given age-category in 2010

183 = Number of days in April-September

The background mortality risk was assumed to stay similar in the future. This may slightly overestimate the impacts, as the risk of mortality due to natural causes is likely to decrease to some extent in the future.

Annual number of deaths attributable to heat exposure was calculated as follows:

$$\mathbf{Attributable\ deaths = MR_{bg} * (RR'_{ec} - 1) * Pop * N_{ec}}$$

where

RR'_{ec} = Adjusted relative risk for a given exposure class (see above)

MR_{bg} = Daily risk of mortality from natural causes in different age- categories in the absence of heat exposure

Pop = Number of population in a city in a given age-category and year

N_{ec} = Number of days in a given exposure class in a given year

Attributable deaths were summed over different cities to derive the number of deaths on a country or region level.

Probabilistic modelling (Monte Carlo simulation, 1000 iterations) was conducted to quantitatively estimate uncertainty in the assessment results. Temperature thresholds

and ERFs were defined as probability distributions. Triangular distributions were assumed for all probabilistic inputs. Minimum and maximum values for distributions were based on the lower and upper 95% confidence limits and mode value on the central estimate.

Health impacts of heat exposure and UHI mitigation policies - results

Currently, almost 15000 deaths are attributable to summertime heat exposure annually in the densely populated European metropolitan areas within the countries included in the assessment (Table A 5 and Table A 6). Over 70% of these deaths occur in those aged 75 or older. The number of heat related deaths is likely to increase drastically during the following 40 years as the climate becomes warmer and the population ages. In the reference scenario 1 the attributable deaths increase over 400% by 2050. In the reference scenario 2 the increase in deaths by 2050 is lower, approximately 200%, which is mainly due to the declining trend in heat exposure in the North-continental region cities towards the later years of the assessment time frame. Table 7 provides estimates on the heat related deaths in different countries in the two reference scenarios. However, country level comparisons should be approached with caution due to the uncertainties related to the representativity of the temperature data of local level weather conditions and the methodology used in defining large cities.

Table A 5: Annual deaths (mean and 95% confidence limits) attributable to heat exposure in large cities in the North-continental region.

Climate scenario & year	Reference / UHI mitigation scenario	North-continental cities Age 15-64	65-74	>75	Total
2010	Current	939 (-322-2158)	1181 (-14-2379)	4985 (1607-8491)	7104 (3252-11186)
A1B					
2020	Reference 1	1430 (-403-3485)	2329 (-29-5012)	9988 (2854-17834)	13760 (5544-22968)
	Vegetation	1374 (-387-3352)	2238 (-28-4811)	9595 (2742-17156)	13220 (5326-22101)
	Albedo	1280 (-361-3124)	2082 (-26-4468)	8927 (2552-15962)	12301 (4957-20607)
	Veg+alb	1231 (-348-3002)	2001 (-25-4297)	8569 (2451-15307)	11813 (4763-19808)
2030	Reference 1	1845 (-508-4481)	3485 (-44-7363)	16371 (4780-29728)	21701 (8722-36913)
	Vegetation	1768 (-487-4289)	3337 (-42-7062)	15669 (4574-28500)	20774 (8347-35396)
	Albedo	1646 (-454-3988)	3102 (-39-6569)	14559 (4253-26501)	19307 (7758-32865)
	Veg+alb	1572 (-434-3804)	2956 (-37-6265)	13875 (4055-25270)	18403 (7395-31303)
2050	BAU	2754 (-748-6748)	5202 (-63-11152)	36912 (10695-67314)	44867 (17406-77214)
	Vegetation	2646 (-719-6479)	4998 (-61-10705)	35467 (10277-64622)	43110 (16720-74134)
	Albedo	2487 (-676-6083)	4698 (-57-10053)	33335 (9659-60673)	40520 (15712-69611)
	Veg+alb	2403 (-653-5874)	4533 (-55-9694)	32183 (9322-58592)	39119 (15161-67230)
B1					
2020	Reference 2	1403 (-388-3402)	2294 (-29-4837)	9369 (2740-17000)	13066 (5331-21844)
	Vegetation	1343 (-371-3253)	2195 (-27-4623)	8951 (2618-16263)	12489 (5098-20867)
	Albedo	1244 (-344-3007)	2033 (-26-4286)	8276 (2422-15059)	11553 (4718-19330)
	Veg+alb	1193 (-330-2881)	1949 (-25-4115)	7924 (2319-14444)	11066 (4520-18544)
2030	Reference 2	1679 (-460-4094)	3245 (-39-6928)	15401 (4488-27958)	20325 (8137-34303)
	Vegetation	1611 (-442-3926)	3117 (-38-6647)	14792 (4312-26821)	19521 (7812-32932)
	Albedo	1513 (-415-3682)	2926 (-36-6231)	13880 (4049-25133)	18318 (7332-30917)
	Veg+alb	1457 (-400-3543)	2815 (-34-5991)	13356 (3898-24198)	17629 (7057-29776)
2050	Reference 2	996 (-274-4094)	1881 (-24-6928)	13182 (3841-27958)	16059 (6242-27807)
	Vegetation	956 (-263-3926)	1803 (-23-6647)	12658 (3690-26821)	15417 (5995-26692)
	Albedo	889 (-245-3682)	1674 (-21-6231)	11760 (3431-25133)	14323 (5573-24797)
	Veg+alb	849 (-234-3543)	1598 (-20-5991)	11234 (3279-24198)	13681 (5326-23689)

Table A 6: Annual deaths (mean and 95% confidence limits) attributable to heat exposure in large cities in the Mediterranean region.

Climate scenario & year	Reference / UHI mitigation scenario	Mediterranean cities Age 15-64	65-74	≥75	Total
2010	Current	307 (-266-1064)	759 (54-1897)	6449 (2328-12884)	7516 (2893-15323)
A1B					
2020	Reference 1	355 (-286-1241)	1068 (72-2667)	9890 (3435-21363)	11412 (4192-23547)
	Vegetation	339 (-274-1189)	1021 (69-2557)	9448 (3272-20433)	10904 (3988-22600)
	Albedo	315 (-255-1114)	945 (65-2389)	8726 (2989-18934)	10075 (3653-21034)
	Veg+alb	300 (-244-1070)	900 (62-2292)	8303 (2832-18131)	9589 (3456-20176)
2030	Reference 1	494 (-399-1744)	1888 (119-4768)	17170 (5852-37226)	19552 (7142-40453)
	Vegetation	473 (-381-1682)	1805 (114-4579)	16407 (5580-35848)	18685 (6781-38819)
	Albedo	438 (-352-1577)	1669 (107-4264)	15161 (5128-33420)	17267 (6144-36286)
	Veg+alb	414 (-332-1510)	1578 (102-4057)	14336 (4786-31866)	16329 (5722-34685)
2050	BAU	492 (-398-1664)	2387 (148-5798)	30610 (10830-63792)	33489 (12507-66637)
	Vegetation	472 (-382-1605)	2292 (141-5593)	29373 (10373-61462)	32138 (11980-64412)
	Albedo	441 (-355-1517)	2139 (133-5251)	27363 (9586-57565)	29943 (11081-60713)
	Veg+alb	423 (-340-1468)	2054 (128-5066)	26286 (9134-55649)	28763 (10536-58739)
B1					
2020	Reference 2	395 (-318-1410)	1190 (76-3022)	11110 (3763-24381)	12695 (4571-26552)
	Vegetation	377 (-303-1352)	1133 (72-2887)	10569 (3573-23324)	12078 (4322-25392)
	Albedo	348 (-279-1264)	1043 (67-2674)	9721 (3251-21730)	11112 (3931-23679)
	Veg+alb	330 (-265-1214)	990 (64-2551)	9218 (3064-20702)	10539 (3673-22668)
2030	Reference 2	451 (-361-1585)	1737 (108-4342)	15934 (5453-34236)	18121 (6640-37088)
	Vegetation	430 (-345-1516)	1658 (104-4165)	15199 (5174-32828)	17287 (6313-35682)
	Albedo	399 (-321-1414)	1534 (97-3882)	14051 (4761-30733)	15984 (5808-33241)
	Veg+alb	381 (-306-1364)	1465 (93-3725)	13404 (4530-29470)	15250 (5520-31990)
2050	Reference 2	442 (-358-1489)	2159 (141-5176)	27682 (9879-57297)	30282 (11515-59608)
	Vegetation	424 (-344-1430)	2071 (133-4991)	26523 (9462-55031)	29019 (11016-57430)
	Albedo	398 (-321-1343)	1938 (122-4700)	24768 (8809-51675)	27103 (10129-54246)
	Veg+alb	383 (-309-1300)	1863 (116-4563)	23766 (8381-49735)	26011 (9670-52433)

Table A 7: Annual deaths (mean, 95% confidence limits) attributable to heat exposure in different countries in the reference scenarios (no implementation of UHI mitigation policies)

Country		A1B		B1	
	2010	2030	2050	2030	2050
AT	253 (113-394)	875 (346-1459)	974 (374-1687)	596 (236-991)	527 (200-922)
BE	346 (144-620)	1250 (494-2205)	3452 (1319-6033)	1329 (523-2286)	892 (343-1557)
CZ	146 (67-228)	480 (195-804)	612 (240-1035)	383 (156-642)	225 (89-385)
DK	-	-	12 (4-35)	-	<1 (0-3)
EE	-	-	-	-	-
FI	2 (1-4)	-	4 (2-9)	2 (1-6)	<1 (0-1)
FR	1626 (725-2595)	6234 (2531-10482)	10488 (4014-17794)	5761 (2336-9714)	5841 (2266-9939)
DE	2506 (1086-4145)	6896 (2753-11822)	13675 (5201-23961)	7182 (2802-12248)	4634 (1763-8114)
GR	910 (345-1729)	1954 (694-3882)	2474 (906-4916)	1814 (696-3516)	2898 (1102-5678)
HU	573 (261-876)	1655 (705-2689)	1216 (504-1989)	1111 (474-1794)	802 (331-1328)
IE	2 (1-3)	8 (3-17)	249 (98-433)	2 (1-4)	20 (8-40)
IT	3152 (1223-6332)	9176 (3154-19915)	12703 (4417-27204)	8686 (3059-18601)	9989 (3445-21580)
LT	38 (17-59)	-	-	-	-
LU	-	-	-	-	-
MT	-	-	-	-	-
NL	111 (46-207)	516 (203-938)	1998 (749-3546)	598 (239-1034)	429 (160-788)
PL	946 (427-1476)	2062 (864-3397)	2002 (818-3342)	1811 (752-2965)	869 (358-1482)
PT	26 (0-118)	328 (48-1099)	587 (89-1775)	31 (0-165)	92 (7-381)
SK	78 (36-120)	268 (110-437)	-	178 (73-289)	-
SI	-	-	-	-	-
ES	3448 (1403-6523)	8103 (3121-15810)	17749 (7079-33571)	7591 (2898-14954)	17307 (6940-32684)
SE	2 (1-8)	1 (0-5)	78 (30-149)	10 (4-23)	13 (5-32)
UK	473 (201-857)	1456 (574-2654)	10107 (3863-17565)	1360 (537-2409)	1806 (708-3219)

Thousands of heat exposure related deaths could be averted annually by implementing the evaluated urban heat island mitigation policies (Figure A 1 and Figure A 2). The benefits from the policies increase substantially in the future and are higher in the IPCC climate scenario A1B, which represents stronger climate change and warming and seems, at the moment, to be the more realistic one of the evaluated climate scenarios.

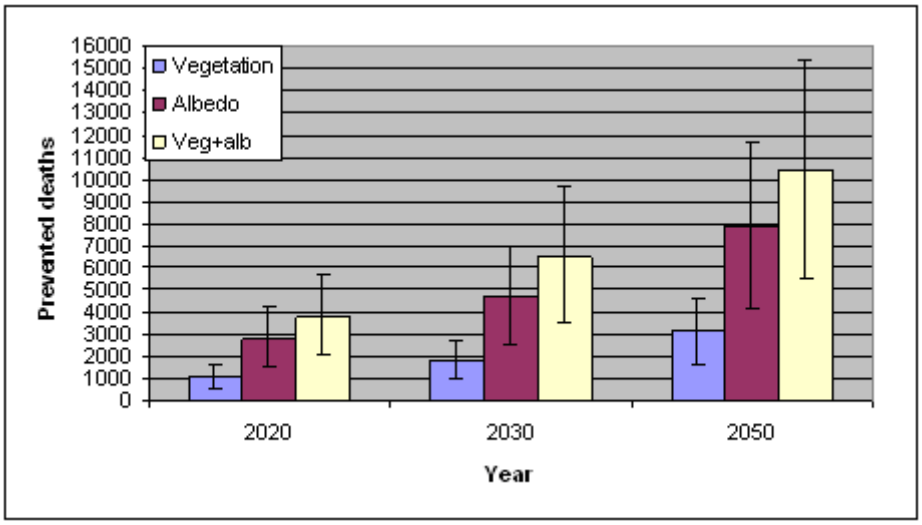

Figure A 1: Heat exposure related deaths prevented annually in IPCC climate scenario A1B if different UHI mitigation policies are implemented.

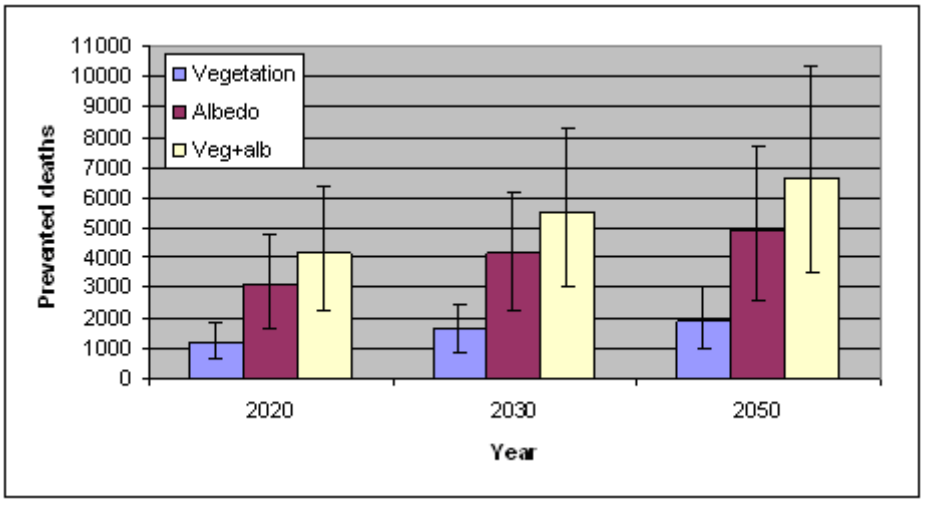

Figure A 2**:** Heat exposure related deaths prevented annually in IPCC climate scenario B1 if different UHI mitigation policies are implemented.

It is currently unclear what role mortality displacement, i.e. the so-called harvesting effect, has in heat exposure induced mortality (Basu 2009). Mortality displacement refers to a phenomenon where the environmental exposure advances the deaths of ill people by only a few days. Nevertheless, an attempt was made to quantify the health

impacts also in DALYs and monetary costs (table 8). Life years lost due to a heat attributable death was defined as a uniform probability distribution with a lower boundary of three months and upper boundary of ten years. Lower boundary was based on an assumed life expectancy for a person with a critical cardiovascular health condition. The upper boundary was based on the notion that majority of heat induced deaths occur in people aged 75 and above. Because of this, and the uncertainty in the number of the attributable deaths, the uncertainty range in the DALY and monetary cost estimates is very wide. However, if mortality displacement is considered as an important factor in heat related mortality, then the lower boundary estimates should be considered as more representative. Monetary costs were calculated by assuming a uniform distribution for the value of a life year with a lower boundary of 60 000 and upper boundary of 89715 euros.

Attributable deaths is an inaccurate indicator for measuring mortality impacts of environmental exposures. This is because everyone dies eventually, and, therefore, deaths can not be prevented but merely postponed. It would be more informative to evaluate mortality impacts by modelling the loss of life years caused by the exposure or the number of life years that could be gained by implementing the different policies aimed at mitigating the exposure. However, it is currently unclear what role mortality displacement, i.e. the so-called harvesting effect, has in heat exposure induced mortality (Basu 2009). Harvesting refers to a phenomenon where the environmental exposure advances the deaths of ill people by only a few days. Therefore, the estimation of life years lost or gained would have substantial uncertainties and was not attempted in this assessment.

Table A 8: DALYs and monetary cost (mean and 95% confidence limit) due to heat related mortality and the impact of UHI mitigation policies on these (total for North-Continental and Mediterranean regions).

Climate scenario & year	Reference / UHI mitigation			Policy impact	
		DALYs	Monetary cost (M€)	DALYs prevented	Cost prevented (M€)
2010	Current	74820 (6769-174438)	5580 (528-13482)		
A1B					
2020	Reference 1	128452 (11748-300892)	9582 (892-23336)		
	Vegetation	123101 (11254-288089)	9183 (854-22418)	5350 (494-12254)	399 (37-948)
	Albedo	114185 (10444-266143)	8518 (792-20841)	14266 (1315-32717)	1064 (99-2543)
	Veg+alb	109213 (10001-255143)	8147 (757-19936)	19239 (1768-44083)	1435 (133-3437)
2030	Reference 1	210594 (19444-495449)	15710 (1486-38804)		
	Vegetation	201434 (18540-475368)	15026 (1420-37101)	9160 (842-20931)	684 (62-1617)
	Albedo	186706 (17089-441349)	13927 (1316-34413)	23888 (2199-54238)	1783 (164-4224)
	Veg+alb	177302 (16168-418725)	13226 (1249-32699)	33291 (3048-75544)	2484 (227-5883)
2050	Reference 1	399529 (38019-931974)	29814 (2787-72071)		
	Vegetation	383678 (36487-894346)	28631 (2668-69499)	15851 (1536-36460)	1183 (119-2780)
	Albedo	359271 (34147-835784)	26809 (2492-65419)	40258 (3910-92309)	3005 (298-7028)
	Veg+alb	346110 (32882-804732)	25827 (2411-63140)	53419 (5185-122606)	3987 (394-9311)
B1					
2020	Reference 2	131545 (11754-315112)	9811 (936-24003)		
	Vegetation	125452 (11179-300392)	9357 (893-22910)	6093 (563-14083)	455 (41-1092)
	Albedo	115740 (10240-277967)	8632 (824-21278)	15805 (1458-36493)	1179 (107-2825)
	Veg+alb	110326 (9724-265101)	8228 (784-20321)	21219 (1958-48842)	1583 (143-3782)
2030	Reference 2	196191 (18261-457578)	14636 (1382-35890)		
	Vegetation	187835 (17508-438654)	14012 (1322-34360)	8356 (767-18907)	624 (57-1466)
	Albedo	175049 (16323-409016)	13058 (1230-32108)	21142 (1926-48154)	1578 (145-3774)
	Veg+alb	167779 (15618-392542)	12516 (1178-30889)	28411 (2583-64616)	2120 (196-5064)
2050	Reference 2	236972 (20532-582922)	17671 (1600-44000)		
	Vegetation	227228 (19640-559907)	16944 (1540-42224)	9744 (858-23146)	727 (63-1738)
	Albedo	211851 (18171-523118)	15797 (1432-39485)	25120 (2219-58727)	1874 (165-4473)
	Veg+alb	202988 (17338-502947)	15135 (1367-37953)	33984 (3022-79548)	2535 (225-6019)

In attributable death estimation, the quantitative uncertainty assessment took into consideration only the uncertainty in the exposure-response functions and exposure thresholds related to them. These two factors alone cause a high range of uncertainty in the results. However, there are also several other sources of uncertainty, the impact of which could not be quantified. These relate to the reliability of the temperature data, the basic assumptions in the UHI mitigation policies and the effect of the policies on temperatures and heat exposure within cities, the methodology used in defining the large cities and population living within them, as well as the assumptions on the background mortality risk in different countries in the future. All these issues have been discussed in more detail in the previous chapters. As a summary, it can be concluded that the issues related to the temperature data and estimation of exposed population are more likely to lead to underestimation of the mortality impacts, while the data used to evaluate background mortality risk is more likely to overestimate the future impacts.

Another important source of uncertainty relates to the suitability of the exposure-response functions to assess mortality impacts of UHI mitigation policies, because the impact of heat island phenomenon is actually embedded in the functions. Thus, in reality the cooling effect of the mitigation measures would be reflected in the ERFs describing the association between background ambient temperature and mortality risk in a city, not in the applied exposure measure. When using these functions to

evaluate future impacts we are also automatically assuming that cities and people's behaviour will not change in the course of the assessment time frame. In reality, the urban infrastructure is likely to change to some extent. People are also likely to adapt to warming weather conditions, both physiologically and behaviourally. For example, the use of air conditioning will probably increase, which would lead to less severe heat exposure even when ambient temperatures rise.

When conducting an assessment on the scale of the whole Europe, it is necessary to make many simplifying assumptions. It is also evident, that there is a lack of simple modelling tools for this type and scale of assessment. The majority of the studies that are conducted on urban heat island mitigation are more local in their nature and make use of complex regional climate models. This kind of approach is not feasible in the time and budget frame of this particular assessment. Given these constraints, the validation of the used methodology is also difficult, as it would require comparisons with more sophisticated modelling approaches. Nevertheless, despite the various sources of uncertainty, the simple methodology used in this assessment can provide valuable insight into the magnitude of health impacts caused by heat exposure in Europe, as well as the potential and relative effectiveness of different policy options in mitigating urban heat island effect and heat exposure in cities.

A.2 Development of a scaling factor to adapt CR functions for outdoor air into ER functions

BACKGROUND AND PURPOSE

Context

There are many well-established relationships linking measurements of particulate matter (PM), from air pollution monitors outdoors, with health effects in the populations living nearby. Typically these monitors are situated at some distance from air pollution sources, and so they measure background concentrations of PM. The associated concentration-response functions (CRFs) have been widely used in assessing the burden of disease from outdoor air pollution and the health impacts of policies that affect concentrations of air pollutants outdoors; and they are used again in HEIMTSA and INTARESE in assessing the health impacts of outdoor air pollution from traffic, from fossil fuel power stations, and other sources.

While the use of such CRFs has proved tremendously powerful in predicting the public health impacts of policies and measures that affect background concentrations of air pollution outdoors, we have extended the available methodology to take into account (i) how policies and measures affect personal exposures (PEs) to PM; and (ii) how changes in the population distribution of PE affect public health. There are two main reasons for doing this.

- First, some policies affecting outdoor air pollution affect PEs in ways other than, or additional to, their effect on background concentrations outdoors. For example, policies and measures that change the mode of transport that people use may affect background concentrations, but they also affect the time spent by people in

or close to traffic; and for at least some of the population, these changes in time-activity patterns and associated changes in PE may be more important than any changes in background concentrations.

- Secondly, many people are exposed from time to time to PM from combustion sources indoors, notably from environmental tobacco smoke (ETS) and from burning biomass fuels (e.g. coal, wood, peat) for heating and/or for cooking; and it is of interest to estimate the burden of disease from these sources, and the health impacts of policies that affect them. Estimating the associated PEs, and resultant health effects, is one way of doing so.

Health Impact Assessment of PM experienced indoors

Note that, here and elsewhere, in thinking about PM experienced indoors, we distinguish between (i) PM from indoor (combustion) sources, as described above; and (ii) the infiltration indoors of PM from outdoor sources. We take the point of view that the CRFs for outdoor air pollution capture (albeit imperfectly) the effects of outdoor air on health, regardless of whether the associated exposures are experienced outdoors, or in traffic, or indoors. It may be possible and indeed in some circumstances useful to estimate separately the health effects of that portion of outdoor PM that has infiltrated homes and buildings; but if this is done, the resulting health effects should not be added to those from the outdoor CRFs. To do so would involve some double-counting of the health effects of outdoor PM.

The situation is different with PM from indoor combustion sources, however. In general we do not expect that PM indoors, from indoor combustion sources, is correlated with measurements of background concentrations of PM outdoors. Consequently we judge that the CRFs for outdoor air pollution do <u>not</u> capture the health impacts of PM from indoor sources. There is a need to estimate these separately, and their health impacts can be added to those of PM from outdoor sources, regardless of whether the latter is estimated via CRFs or via personal exposures.

The problem and underlying idea for a solution

To date there is not a reliable, comprehensive set of estimates of risk coefficients for the effects of particulate matter (PM) based on PEs or on indoor concentrations. Some studies have been done but the scale and scope of these studies, and the range of health outcomes investigated, fall far short of those available for providing CRFs from outdoor air pollution, where a very wide range of health outcomes and associated CRFs is available and used. In particular, there are no reliable estimates, from studies of PM from indoor combustion sources, of the relationship between risk of mortality and long-term exposure to $PM_{2.5}$ from indoor sources. (It is well-established that in Health Impact Assessment of outdoor air pollution, the dominant health impact is via the CRF linking mortality risks in adults with changes in long-term exposure to outdoor air pollution, represented by annual average $PM_{2.5}$.)

However if PEs to outdoor air pollution (wherever that air pollution is experienced, e.g. outdoors or in traffic or in homes or wherever) are statistically correlated with background concentrations, then the concentration-response functions (CRFs) based

on background concentrations could be scaled to give exposure-response functions (ERFs) linking personal exposures to these same health outcomes (Ashmore and Terry, 2009). This indirect approach would then give access to a much wider set of exposure-response functions (ERFs) based on personal exposures to PM than could be found from studies of personal exposures and health directly.

In seeking to establish such a scaling factor we have focused on $PM_{2.5}$ rather than, say, PM_{10} because (i) as noted above, the most important PM-health relationship for outdoor air pollution is in PM expressed as $PM_{2.5}$ and (ii) because of its smaller size, $PM_{2.5}$ is more evenly spread spatially than PM_{10}; this improves the chances that the distribution of personal exposures from outdoor sources is correlated with background concentrations as measured outdoors.

OBJECTIVE

The objective of the work reported here was to establish a relationship between background concentrations of $PM_{2.5}$ as measured outdoors, and the distribution of PEs to $PM_{2.5}$ from outdoor sources in the population resident nearby.

METHODS

General approach

PE attributable to ambient particles can be expressed as a function of the fraction of time a subject spent in each microenvironment and the exposure concentration in each microenvironment attributable to ambient particles, i.e. the background concentration multiplied by a contribution factor specific to each microenvironment (Wilson et al 2000). This contribution fraction represents the contribution of ambient particles to each microenvironment (Formula 1).

$$PE_{amb} = \sum_{i=1}^{n} t_i \times CF_i \times C_{bg} \qquad \sum_{i=1}^{n} t_i = 1 \qquad \text{Formula 1}$$

Where, PE_{amb} is the time-averaged component of personal exposure attributable to ambient particles (μg/m^3); t_i is the fraction of time a person spends in each microenvironment (dimensionless); CF_i is the contribution factor for each microenvironment in relation to the background concentration (dimensionless); C_{bg} is the background concentration (μg /m^3).

Therefore, the scaling factor between personal exposure attributable to ambient particles and background concentrations can be expressed as:

$$\frac{PE_{amb}}{C_{bg}} = \sum_{i=1}^{n} t_i \times CF_i \qquad \text{Formula 2}$$

Specific application and input data

We consider three microenvironments:

1) Outdoors exposed to background concentrations (referred in the text as 'out-bg').
2) Outdoors in traffic or exposed to concentrations near traffic sources (referred in the text as 'out-tr').
3) Indoors (referred in the text as 'in').

Based on Formula 2, the conversion factor, in terms of the three microenvironments considered can be expressed as:

$$\frac{PE_{amb}}{C_{bg}} = CF_{out\text{-}bg} \times t_{out\text{-}bg} + \times CF_{out\text{-}tr} \times t_{out\text{-}tr} + CF_{in} \times (1\text{-}t_{out})$$

Formula 3

Table A.9 shows the input data used to calculate the conversion factor.

- The contribution factor while being exposed to ambient background concentrations equals one, by definition.
- For exposures in the vicinity of traffic sources the contribution factor was calculated as the ratio between the PE when in transport (car, bus, bike and walking) and the ambient background concentration (the estimate was carried out as part of the LAMA methodology).

Table A.9 Input data used to calculate the conversion factor

Microenvironment	Contribution factor (CF_i)	Time fraction (t_i)
Outdoors exposed to background concentrations	1	2/24
Outdoors exposed to concentrations near traffic sources	2	1/24
Indoors	0.6	21/24

- In indoor microenvironments we considered that the contribution factor is given by the infiltration factor (F_{INF}: the fraction of ambient particles that have been infiltrated indoors and remain airborne (Wilson et al. 2000)). F_{INF} depends on the air exchange rate, the penetration factor and the decay rate of particles. The value of the F_{INF} was obtained from the estimates published by Hänninen et al. (2010), based on six European studies involving 10 EU cities (Gothenburg, Stockholm, Helsinki, Amsterdam, Basle, Birmingham, Prague, Athens, Florence

and Rome).The averaged F_{INF} was 0.55 (95% CI: 0.52-0.58), which we have rounded up to 0.6.

Time spent outdoors (exposed to background concentrations and in traffic) and indoors was estimated from the results of the HETUS study (HETUS, 2007): an EU survey on time activity data in 15 EU countries (Belgium, Bulgaria, Estonia, Finland, France, Germany, Italy, Latvia, Lithuania, Norway, Poland, Slovenia, Spain, Sweden and the UK) carried out during 2005-2007. Our estimates were similar to those calculated as part of the LAMA methodology.

Results

By applying the parameters specified in Table 1 to Formula 2 the resulting scaling factor was:

$$\frac{PE_{amb}}{C_{bg}} = 0.7$$

Sensitivity analysis

The sensitivity of the estimated time spent in different microenvironments is shown in two simple examples. Changes in the conversion factor are independent of the background concentration; to illustrate how the scaling factor changed, we assumed a background $PM_{2.5}$ concentration of 20 µg/m^3 based on data published by WHO (WHO, 2006) from 119 $PM_{2.5}$ monitoring stations across EU ($PM_{2.5}$ in urban locations ranged from 15-20 µg/m^3). We consider this is a conservative estimate and has only been chosen with the purpose of showing how the scaling factor is used.

Example 1

Microen-vironment	Ambient background concentration (µg/m^3)	Contri-bution factor	Adjusted concentration (µg/m^3)	Time spent in each micro-environ-ment (hrs)	Exposure (µg/m^3)
Outdoor	20	1	20	2	2/24*20=1.67
Traffic	20	2	40	1	1/24*40=1.67
Indoor	20	0.6	12	21	21/24*12=10.50
Total					13.83

The total exposure is 13.83 which is 13.83/20 = 0.69 times the ambient background concentration. Thus the scaling factor in this example is **0.69 ≈0.7**

If we do not take consideration on the number of hours spent near traffic ($t_{out\text{-}tr}$:=0) the effect on the scaling factor is negligible (Example 2):

Example 2

Microenvironment	Ambient background concentration (µg/m^3)	Contri-bution factor	Adjusted concen-tration (µg/m^3)	Time spent in each microenvironment (hrs)	Exposure (µg/m^3)
Outdoor	20	1	20	3	3/24*20=2.50
Indoor	20	0.6	12	21	21/24*12=10.50
Total					13.00

The total exposure is 13.00 which is 13.00/20 = 0.65 times the ambient background concentration. Thus the scaling factor in this example is **0.65 ≈0.7**

Discussion

We have used a deterministic approach to estimate the value of the scaling factor. We have demonstrated that the uncertainty introduced due to changes in time spent in different outdoors microenvironments is small, as the total time spent outdoors is insignificant compared to the time spent indoors. The scaling factor is driven by time spent indoors and the value of the infiltration factor.

We identified two studies that estimated the contribution of ambient $PM_{2.5}$ (Sarnat al. 2001) and ambient PM_{10} (Ashmore et al. 2009) to PE, based on the relationship of 24-hrs measured or modelled ambient personal exposure vs. 24- hrs measured background concentrations. The slope of this relationship is equivalent to the scaling factor. Ashmore et al. (2009) found a slope of 0.5 in winter and 0.8 in summer. PEs were calculated using the Population Exposure Frequency Model (PEFM) which combines factors from indoor and outdoor exposure models (INDAIR and EXPAIR models). Indoor generated PM_{10} were set to zero and only infiltrated ambient PM_{10} concentrations were considered in indoor microenvironments. The averaged slope for both of the seasons was 0.65, similar to our scaling factor of 0.7.

Sarnat et al. (2001) examined the longitudinal association between the personal exposure to $PM_{2.5}$ attributable to ambient particles and $PM_{2.5}$ background concentrations in a group of 50 subjects (20 adults, 15 children and 15 subjects diagnose with COPD) in Baltimore. The slopes were 0.34 and 0.39 for summer and winter, respectively. The $PM_{2.5}$ component of the personal exposure attributable to ambient sources was estimated by multiplying ambient background $PM_{2.5}$

concentrations by an F_{INF} calculated from the ratio of sulphate found in the PEs to sulphate in background $PM_{2.5}$ concentrations (sulphate is substance randomly present in indoor air, therefore the total concentration in PE is assumed to come from outdoor sources). This methodology does not account for personal exposure whilst outdoors, which might explain the lower slopes compared to those found in Ashmore's study.

We consider our estimate of the F_{INF} (0.6) to represent well the overall infiltration factors in EU households as it was calculated with data from cities across all climate regions (Northern, Central and Southern EU cities). Similar averaged values have been reported in other studies (0.46-0.72) in the US. The RIOPA study (Relationship of Indoor, Outdoor and Personal Air) estimated an F_{INF} of 0.46 calculated from data on air exchange rates and penetration rates from homes and a decay rate for $PM_{2.5}$ of 0.79 h^{-1} (Meng et al. 2005). Infiltration factors for different $PM_{2.5}$ sources were 0.51, 0.78, and 0.04 for $PM_{2.5}$ associated with primary combustion, secondary formation (excluding nitrate), and mechanical generation, respectively (mechanical generated particles are mostly coarse (> 2.5 µm). Liu et al. (2003) estimates of F_{INF} based on measured data in 55 homes ranged from 0.07 to 1.0 with a mean F_{INF}=0.57 and median 0.64. Williams et al. (2005) estimates of the F_{INF} for 37 homes (based on measured data) ranged from 0.26 to 0.87 with a median of 0.56. In Canada, Clark et al. (2010) reported a mean F_{INF}=0.52 ±0.21. The methods used to estimate the infiltration factors varied across the different studies and therefore it is likely that the differences in the reported F_{INF} values are partly explained by the different methods used.

A source of uncertainty in the infiltration factor is likely to be that we have not considered seasonal differences but an overall annual average. In general infiltration increases over the summer and is lower during the winter period (Hänninen et al. 2010) and therefore indoor exposures due to ambient particles will be higher in summer than in winter. However, time activity patterns are likely to change from winter and summer, with possibly longer periods spent outdoors in summer; and indeed summertime average concentrations of $PM_{2.5}$ are likely to differ from those in winter. Our estimate has not considered these seasonal variations. We have based our estimate on an overall annual infiltration factor and overall annual time spent indoors. We think that any resulting error is likely to be small.

Another possible limitation of the estimated scaling factor is the lack of consideration of the so-called personal cloud. The observation of the personal cloud arises from the fact that personal exposures are higher than the time-weighted averaged of concentrations measured in the various microenvironments the subject spend time in (Wilson et al. 2000). The personal cloud comprises ambient particles, household dust, skin flakes, etc. It is larger when moving due to the re-suspension of dust than when sitting (Brauer et al. 1999, Ferro et al. 2004). However, the size of the cloud and the relative composition of the different elements to the personal cloud are not well characterized. Although, it seems to consist mostly from coarse (>2.5 µm) indoor generated particles and as such, it is mostly not relevant to the relationship between outdoor background concentrations and PEs from outdoor sources.

A short review of the literature on 'personal clouds' supported this conclusion.

- Özkaynak et al. (1997) estimated that the contribution of skin flakes to the personal exposure of PM_{10} was approximately 10%. The authors attributed the sources of the personal cloud to in-house activities (dusting, vacuuming, cooking and exposure to cigarette smoke). Long et al. (2000) and Ferro et al. (2004) reported that the major differences between personal and indoor concentrations were for activities involving re-suspension of dust from textiles (dancing/walking on a carpet) rather than similar activities on wood or linoleum. If we assume ambient generated particles will be approximately evenly distributed on all indoor surfaces, these results suggest the personal cloud consists mostly of indoor generated particles (from textiles) rather than outdoor infiltrated particles. An alternative argument to consider the personal cloud consisted entirely of indoor generated particles is that its temporal variation will be determined by indoor activities rather than by the ambient $PM_{2.5}$ concentration (Wilson et al. 2000).
- The size of the personal cloud is difficult to measure, as it depends on the particle size (Ferro et al. 2004) and the distance between the fixed monitor and the individual carrying the personal sampler (Brauer et al. 1999, Ferro et al. 2004). It requires information on the time-averaged concentration in all the microenvironments the individual is in. If a microenvironment is not measured it would be captured as personal cloud. Williams et al. (2003) estimated personal clouds of $PM_{2.5}$ between -98 and 101 $\mu g/m^3$. The negative personal clouds were attributed to failure in monitoring in all microenvironments that the individual was present.
- Ferro et al. (2004) reported that larger distances between the fixed monitor and the subject resulted in larger personal clouds. Personal exposures (whilst indoors) to particles between 1-5 μm were found to be approximately 1.3 times higher than indoor concentrations (measured at 5 m of the subject) in two studies (Brauer et al. 1999, Ferro et al. 2004).
- Özkaynak et al. (1997) and Ferro et al. (2004) showed that the size of the personal cloud increases with increasing particle sizes and that it is mostly dominated by coarse particles (>2.5 μm).
- In Ashmore et al.'s study on the relationship of PE to PM_{10} from ambient origin and background concentrations, the intercepts of the relationship indicate the contribution of the personal cloud from ambient particles. These were 0.8 $\mu g\ m^{-3}$ and 0.4 $\mu g.m^{-3}$ for summer and winter, respectively. Assuming that 50% of the PM_{10} concentrations in Ashmore's study are $PM_{2.5}$, the contribution of $PM_{2.5}$ to the personal cloud would be 0.3 $\mu g.m^{-3}$ (averaged for both seasons). This contribution is too small to change significantly our estimate of the scaling factor.

REFERENCES

Ashmore M, Terry A. (2009) Quantification of health impacts of airborne particulates comparing estimates based on personal exposure and outdoor concentrations. University of York.http://www.cranfield.ac.uk/health/researchareas/environmenthealth/ieh/mike%20ashmore.pdf Last accessed 7th Dec 2010.

Bickel, P. and R. Friedrich (2005). ExternE Externalities of Energy Methodology 2005 Update. http://dx.doi.org/10.18419/opus-11923.

Blesl, M. (2008a). EU 20-20 policy implications on the energy system of Germany – an analysis with TIMES PanEU, in: Maizi, N., Hourcade, J.C. (2008): Carbone et prospectivees, Presses des Mines

Blesl, M., Kober, T., Bruchof, D. and Kuder, R. (2008b). Beitrag von technologischen und strukturellen Veränderungen im Energiesystem der EU-27 zur Erreichung ambitionierter Klimaschutzziele, Zeitschrift für Energiewirtschaft, issue 4/2008, pp. 219-229

Blesl, M., Kober, T., Bruchof, D. and Kuder, R. (2010). Effects of climate and energy policy related measures and targets on the future structure of the European energy system in 2020 and beyond, Energy Policy, 38(2010), pp. 6278-6292

Brauer M, Hirtle RD, Haill AC, Yip TR. (1999) Monitoring personal fine particle exposure with a particle counter. Journal of Exposure Analysis and Environmental Monitoring, 9:228-236

Clark NA, Allen RW, Hystad P, Wallace L, Dell SD, Foty R, Dabek-Zlotorzynska E, Evans G Wheeler AJ. (2010) Exploring Variation and Predictors of Residential Fine Particulate Matter Infiltration. International Journal of Environmental Research and Public Health,7: 3211-3224

Dones, R., Bauer, C. and Röder, A. (2007). Kohle – Data v2.0 (2007). ecoinvent report No. 6-VI, Paul Scherrer Institut, Villingen, December 2007

Faist-Emmenegger, M., Heck, T., Jungbluth, N. and Tuchschmid, M. (2007). Erdgas – Data v2.0 (2007). ecoinvent report No. 6-V; Villingen, December 2007

Ferro AR, Kopperud RJ, Hildemann LM. (2004) Elevated personal exposure to particulate matter from human activities in a residence. Journal of Exposure Analysis and Environmental Epidemiology, 14: S34-S40

Hänninen OO, Hoek G, Mallone S, Chellini E, Katsouyanni K, Gariazzo C, Cattani G, Marconi A, Molnár P, Bellander T, Jantunen M. (2010) Seasonal patterns of outdoor PM infiltration into indoor environments: review and meta-analysis of available studies from different climatologically zones in Europe. Air Quality Atmosphere and Health.

HETUS (2007) Harmonised European Time Use Survey. [online database version 2.0]. Created 2005-2007 by Statistics Finland and Statistics Sweden. [reference date 2007-10-01].
http://www.tus.scb.se (last accessed 25th Jan 2011)

Jungbluth, N., Spielmann, M., Dones, R., Heck, T., Faist-Emmenegger, M. and Frischknecht, R. (2007). Erdöl. ecoinvent report No. 6-IV, Swiss Centre for Life Cycle Inventories, Dübendorf, CH.

Lyoi PJ, Waldman JM, Buckley T, Bullet J, Pietarinen C. (1990) The personal, Indoor and outdoor Cocnentration fo PM_{10} Measured in an Industrial Community During the Winter

Sarnat JA, Brown W, Schwartz J, Coull BA, Koutrakis P, (2005) Ambient Gas Concentrations and Personal Particulate Matter Exposures: Implications for Studying the Health Effects of Particles, Epidemiology, 16: 385-395

Meng QY, Turpin BJ, Korn L, Weisel CP, Morandi M, Colome S, et al. (2005). Influence of ambient (outdoor) sources on residential indoor and personal PM2.5 concentrations: analyses of RIOPA data. Exposure Analysis and Environmental Epidemiology, 15:17–28.

Özkaynak H, Xue J, Weker R, Butler D, Koutrakis K, Spengler J. The Particle Team (PTEAM) study: Analysis of the data. EPA Project Summary, EPA/600/SR-95/098, U.S. EPA: Research Triangle Park, NC, 1996.

Sarnat JA, Schwartz J, Catalano PJ, Suh HH. (2001) Gaseous Pollutants in particulate Matter Epidemiology: Confounders or Surrogates? Environmental Health Perspectives, 109:10

UBA (2009). Emissionsbilanz erneuerbarer Energieträger – Durch Einsatz erneuerbarer Energien vermiedene Emissionen im Jahr 2009. Aktualisierte Anhänge 2 und 4 der Veröffentlichung „Climate Change 12/2009“, September 2010

Wilson WE, Mage DT, Grant LD. (2000) Estimating Separately Personal Exposure to Ambient and Nonambient Particulate Matter for Epidemiology and Risk Assessment: Why and How. Journal of the Air and Waste Management Association, 50:1167-1183

Williams R, Suggs J, Rea A, Leovic K, Vetter A, Croghan C, Sheldon L, Rodes C, Thornburg J, Ejire A, Herbst M, Sanders Jr. W. (2003) The Research Triangel Park particulate matter panel study: PM mass concentration relationships. Atmospheric Environment, 37:5349-5363

B LIST OF AUTHORS

Authors	Contribution to Chapters
Friedrich, Rainer (USTUTT)	Co-ordinator of the case study, all chapters, editor
Kuhn, Alexandra (USTUTT)	1.1, 1.2, 1.3, 1.4, 1.5, 2.1, 3.4, 4.1, 4.2, 4.3, 5.2, 7.1, 7.2, 8.1, editor
Bessagnet, Bertrand (INERIS)	4.2
Blesl, Markus (USTUTT)	2.2
Bruchof, David (USTUTT)	2.2
Cowie, Hilary (IOM)	5.1
Fantke, Peter (USTUTT)	1.3, 1.5, 4.5, 4.6, 6.1, 6.2, 7.1, 7.2
Gerharz, Lydia	4.3, 5.2, 7.1, 7.2
Grellier, James (IC)	1.5
Gusev, Alexey (MSC-E)	4.5, 4.6
Haverinen-Shaughnessy, Ulla (THL)	4.3, 5.1, 5.2, 7.1, 7.2
Hout, Dick van den (TNO)	4.4, 5.2
Hurley, Fintan (IOM)	5.1, 7.1, 7.2
Huynen, Maud (UM-ICIS)	4.7, 5.1
Kampffmeyer, Tatjana (USTUTT)	2.1, 2.2
Karabelas, Anastasios (CERTH)	2.2.4, 4.6, 6.2, 7.1, 7.2, 9.1, 9.2
Karakitsios, Spyros (JRC)	4.3, 5.1, 5.2, 7.1, 7.2
Knol, Anne (RIVM)	7.1
Kober, Tom (USTUTT)	2.2
Kollanus, Virpi (THL)	3.5, 4.7, 5.1, 5.2
Kontoroupis, Periklis (CERTH)	2.2.4, 4.6, 6.2, 7.1, 7.2, 9.1, 9.2
Kuder, Ralf (USTUTT)	2.2
Kugler, Ulrike (USTUTT)	1.5, 2.1, 2.2, 3.3
Loh, Miranda (THL)	4.3, 5.2, 7.1, 7.2
Meleux, Frederik (INERIS)	4.2
Miller, Brian (IOM)	5.1
Müller, Wolf (USTUTT)	3.2, 7.2, 8.2

Nikolaki, Spyridoula (CERTH)	2.2.4, 4.6, 6.2, 7.1, 7.2, 9.1, 9.2
Panasiuk, Damian (NILU Polska)	2.2
Preiss, Philipp (USTUTT)	3.2, 8.2
Rintala, Teemu (THL)	4.3, 5.2, 7.1, 7.2
Roos, Joachim (USTUTT)	4.2, 5.2, 7.1, 7.2, 8.1, 8.2
Roustan, Yelva (ENPC)	4.1, 4.2
Salomons, Erik (TNO)	4.4, 5.2
Sánchez Jiménez, Araceli (IOM)	5.1
Sarigiannis, Denis (JRC, AUTH)	4.3, 4.6, 5.1, 5.2, 7.1, 7.2
Schenk, Konstantin (USTUTT)	3.3, 8.2
Shafrir, Amy (IOM)	5.1
Shatalov, Victor (MSC-E)	4.5, 4.6
Solomou, Ermioni (CERTH)	2.2.4, 4.6, 6.2, 7.1, 7.2, 9.1, 9.2
Theloke, Jochen (USTUTT)	2.1, 2.2
Thiruchittampalam, Balendra (USTUTT)	2.1
Torras Ortiz, Sandra (USTUTT)	4.1, 4.2
Travnikov, Oleg (MSC-E)	4.5, 4.6
Tsyro, Svetlana (Met.no)	4.2
Tuomisto, Jouni (THL)	4.3, 5.1, 5.2, 7.1, 7.2
Vinneau, Danielle (IC)	4.1
Wagner, Susanne (USTUTT)	2.2.4
Yang, Aileen (NILU)	4.3, 5.2, 7.1, 7.2